Characterization of Stem Cell Genes in Solid Tumors

Dissertation

der Mathematisch-Naturwissenschaftlichen Fakultät

der Eberhard Karls Universität Tübingen

zur Erlangung des Grades eines

Doktors der Naturwissenschaften

(Dr. rer. nat.)

vorgelegt von

Hui Wang

aus Shandong, China

Tübingen

2017

Gedruckt mit Genehmigung der Mathematisch-Naturwissenschaftlichen Fakultät der Eberhard Karls Universität Tübingen

Tag der mündlichen Prüfung: 19.07.2018

Dekan: Prof. Dr. Wolfgang Rosenstiel

1. Berichterstatter: Prof. Dr. med. Claudia Lengerke
2. Berichterstatter: Prof. Dr. Klaus Schulze-Osthoff

Acknowledgements

The present work has been carried out at the Department of Hematology and Oncology, University Hospital of Tübingen, Germany, in the period of February 2011 to July 2013, and at the Department of Biomedicine, University Hospital of Basel, Switzerland, since August 2013. The funding of this work by the Baden-Württemberg Stiftung is greatly acknowledged.

I wish to thank my supervisor Prof. Dr. med. Claudia Lengerke who made me interested in the cancer stem cell research and gave me the opportunity to work and finish my Ph.D. in her lab. She always had time to discuss the scientific work of this project and shared with me a lot of her expertise and research insight. She has contributed to my papers and my thesis with a major impact. Moreover she has provided me the opportunity to participate at different Research Conferences in Germany and the USA. I gladly acknowledge these chances to expand my knowledge in the field of cancer stem cell research and of meeting so many great people there.

Special thanks go to Prof. Dr. Klaus Schulze-Osthoff for helped us developing new ideas and concepts and being my Ph.D. supervisor.

I would like to say ‘thank you’ to the following people who cooperated with us and provided assistance in patient sample analysis: Prof. Dr. Sven Perner, Dr. Angela Queisser, Dr. Martin Braun and Dr. Zsuzsanna Varga. I would also like to thank here Dr. Oliver C. Rothfuß and Dr. Frank Essmann for helping us to develop new ideas and providing useful discussions.

I am grateful to the following people: Petra for giving me an introduction into the cancer stem cell project and sharing her knowledge; Martina who gave me a lot of new ideas and practical instructions and introduced me to the zebrafish as an experimental model. Without her, everything would have been much more difficult. Thanks to Thorsten for walking with me along the SOX2-way, and for providing useful discussions. Thanks also to Anna for helping me with the mouse

experiments.

I wish to extend my thanks to the whole present and past staff at the Division of Hematology and Oncology: Sarah, Matthias, Selina, Haijiao, Perihan, Rebekka and at the Department of Biomedicine: Joëlle, Tamara, Elisa, Anja, Loïc, Silvia, Pauline, Marcelle and Christoph for all the emotional support, encouragement and for providing a fun environment in the lab. Special thanks go to Martina and Thorsten for the proofreading.

I especially thank my mom, my dad, and my husband. They have supported me all my life.

Abbreviations

ABC Transporters: ATP-binding cassette Transporters

ABCA5: ATP-binding cassette sub-family A member 5

ABCB5: ATP-binding cassette sub-family B member 5

ABCG2: ATP-binding cassette sub-family G member 2

AKAP12: A-kinase anchor protein 12

AKT: RAC-alpha serine/threonine-protein kinase

ALDH1: aldehyde dehydrogenase1

AML: acute myeloid leukemia

APC: Adenomatous polyposis coli-Protein

ATRA: all-trans retinoic acid

BCL2: B-cell lymphoma 2

CARM1: co-activator associated arginine methyltransferase 1

CBP: CREB-Binding Protein

CBX3: Chromobox protein homolog 3

CCND3: cyclinD3

CCR1: chemokine (C-C motif) receptor 1

CK1: Casein kinase 1

CLL-1: C-type lectin-like molecule-1;

CML: chronic myeloid leukemia

CRPC: Castration-resistant prostate cancer

CSC: cancer stem cell

CSL: CBF1/Suppressor of Hairless/LAG-1

CtBP: C-terminal-binding protein

CXCR4: C-X-C chemokine receptor type 4

Egf: epidermal growth factor

Egfr: epidermal growth factor

EMT: epithelial-mesenchymal transition

EpCAM: epithelial cell adhesion molecule

ER: estrogen receptor

ESA, epithelial surface antigen

ESC: embryonic stem cell

ESZ: embryonalen Stammzellen

EVI1: ecotropic virus integration site 1 protein homolog

FACS: Fluorescence Activated Cell Sorting

FOG2: Friend of GATA 2

FZD: Frizzled

GSK3: Glycogen Synthase Kinase-3

HDACs: histone deacetylases

HER2: human epidermal growth factor receptor 2

HH: Hedgehog

HMG: high-mobility-group

HNSCC, head and neck squamous cell carcinoma

HPV: human papillomaviruses

HSP DNAJB8: heat shock protein DnaJ (Hsp40) homolog subfamily B member 8

ICM: inner cell mass

JNK: c-Jun N-terminal kinase

LGR5: Leucine-rich repeat-containing G-protein coupled receptor 5

LRP: Lipoprotein receptor-related protein

LSC: leukemic stem cell

MAPK: mitogen-activated protein kinase

MDR: multidrug resistance

MDS: Myelodysplastic syndrome

MECOM: MDS1 and EVI1 complex locus protein EVI1

MM: multiple myeloma

MMTV: mouse mammary tumor virus

mNPCs: murine neural pluripotent cells

Napb: NSF Attachment Protein Beta

NICD: Notch intracellular domain

NPC: neural precursor cell

NSCLC: non-small-cell lung cancer

NSG mice: NOD/SCID/IL-2Rγnull mice

P/CAF: P300/CBP-associated factor

PLZF: Promyelocytic Leukemia Zinc Finger

PR domain: PRD1-BF1/BLIMPI-RIZ homology domain

PSC: pluripotent stem cell

RFP: red fluorescent protein

RhoJ: ras homolog family member J

RMST: rhabdomyosarcoma 2-associated transcript

ROCK: Rho-associated protein kinase

Shh: Sonic hedgehog

SMO: smoothened

SOX2: SRY (sex determining region Y)-box 2

SRR1/2: SOX2 regulatory region 1/2

TE: trophectoderm

TGFβ: Transforming growth factor beta

THY1: Thy-1 Cell Surface Antigen

TIE1: Tyrosine kinase with immunoglobulin-like and EGF-like domains 1

TIM3, T cell immunoglobulin and mucin domain-containing-3

TNF: tumor necrosis factor

TNM: tumor/node/metastasis

TSC: trophoblast stem cell

TSZ: Tumorstammzell

UV: ultraviolet

Summary

Stemness genes regulate the maintenance of pluripotency and self-renewal in human embryonic stem cells (ESCs) and allow reprogramming of adult somatic cells into an ESC-like state. Accumulating evidence reveals that these genes are also abnormally expressed in cancers and play important roles in tumorigenicity, metastasis and chemoresistance. Understanding the role and expression pattern of stemness genes might be of utmost importance in different tumor cell types.

SOX2 is one of the most prominent stemness factors in pluripotent stem cells, which subsequently was also reported as being involved in reprogramming and, as shown by us and other groups, found to express in different types of cancer (Bareiss, Paczulla et al. 2013, Schrock, Bode et al. 2014, Schaefer, Wang et al. 2015). In this work, we firstly describe a functional dependence of the Sex determining region Y-box 2 (*SOX2*) gene in regard to the expression and stability on the Ser/Thr-kinase AKT (Schaefer, Wang et al. 2015). In breast carcinoma, SOX2 expression has been linked to cancer stem cells (CSCs) and associated with poor clinical outcome. Here, we show that overexpression of *AKT* raises SOX2 levels, whereas knockdown or inhibition with specific inhibitors of AKT kinase depletes SOX2. *Vice versa*, *SOX2* knockdown has no effect on AKT levels and phosphorylation status, indicating that AKT is upstream of SOX2. This functional dependence was confirmed in *in vitro* spheres and *in vivo* tumorgenicity assays, where either lentivirally mediated depletion of *SOX2* or alternatively AKT-inhibition via treatment with various inhibitors could reduce sphere outgrowth and respectively tumor induction in a dose-dependent manner. Taken together, our results suggest that AKT-inhibitors efficiently target SOX2 and therefore may have the capability to eradicate tumor-initiating breast CSCs.

Interestingly, we also found that the transcriptional activity of SOX2 is linked to CSC character in other cancer types. We constructed a lentiviral reporter vector, in which red fluorescent protein (RFP) is driven under the control of the SOX2 regulatory regions (either SRR1 or SRR2). These reporter-positive cells showed enhanced tumor spheres formation, whereas reporter negative cells generated

fewer and smaller spheres in ovarian as well as breast carcinoma (Bareiss, Paczulla et al. 2013, Wang, Paczulla et al. 2015). Moreover, expression of stemness-related (*NANOG, OCT4* and *LIN28)* and EMT genes (*N-CADHERIN*, *TWIST*, *SNAIL*) were enriched in reporter-positive versus -negative cells. Treatment with chemotherapeutic agents enhanced the percentage of reporter-positive cells. Interestingly, treatment with AKT inhibitors specifically decreased reporter positive cells(Schaefer, Wang et al. 2015). These facts indicate that SRR1/2 activity has the capability to identify CSCs in different tumor types.

Next, we explored the importance of EVI1, a stem cell protein reported to regulate healthy and malignant blood stem cells, for its roles in solid tumor CSCs. We found that EVI1 is also aberrantly expressed in both breast and prostate carcinoma samples (Queisser, Hagedorn et al. 2017, Wang, Schaefer et al. 2017). Although EVI1 expresses in a majority of breast carcinoma samples independent of their ER status, it selectively impacts the biology of estrogen receptor (ER)-negative tumors, where it regulates cell growth via MAPK activity and metastatic behavior via KISS1 (Wang, Schaefer et al. 2017). Interestingly, EVI1 did not selectively mark breast CSCs since homogeneous expression was detected among all tumor cells. However, EVI1 appears to be co-expressed in and to co-regulate this compartment thus suggesting that targeted therapies against EVI1 will also eradicate this subpopulation. In healthy prostatic tissue, EVI1 expression was confined to reside within the prostate stem cell compartment located at the basal layer, as identified by stem cell marker CD44. In a prostate cancer progression cohort, EVI1 staining strongly increased with tumor progression. Functionally, *EVI1* knockdown inhibited proliferation and cell cycle progression of the prostate cancer cell line PC3, as well as migratory capacity and anchorage independent growth of human prostate cancer cells. Moreover, *EVI1* expression was induced in experimentally derived docetaxel-resistant prostate cancer cells (Queisser, Hagedorn et al. 2017). In summary, these data indicate *EVI1* as a novel gene involved in breast and prostate cancer progression that may control carcinogenesis in part at the stem cell level.

Zusammenfassung

Die Expression von Stammzell-Genen führt zur Aufrechterhaltung von Pluripotenz und Selbsterneuerungskapazität in menschlichen embryonalen Stammzellen (ESZ), und hat die Fähigkeit, adulte somatische Zellen in einen ESZ-ähnlichen Zustand umzuwandeln. Immer mehr Arbeiten weisen darauf hin, dass Stammzellfaktoren auch in Krebserkrankungen abnormal exprimiert werden und Tumorigenität, Metastasierung und Chemoresistenz beeinflussen. Es erscheint daher unerlässlich, Expressionsmuster und Rollen dieser Faktoren in verschiedenen Tumorzelltypen zu untersuchen.

In dieser Arbeit beschreiben wir zunächst eine funktionelle Abhängigkeit des Sex determining region Y-box 2 (*SOX2*) Gens bezüglich Expression und Stabilität von der Ser/Thr-Kinase AKT (Schaefer, Wang et al. 2015). SOX2 ist ein Stammzellfaktor in pluripotenten Stammzellen und wird in Zellen verschiedener Krebstypen exprimiert (Bareiss, Paczulla et al. 2013, Schrock, Bode et al. 2014, Schaefer, Wang et al. 2015). Im Mammakarzinom wurde SOX2 mit Tumorstammzell-Status (TSZ) verknüpft, und eine erhöhte SOX2 Expression wurde mit einer schlechten klinischen Prognose assoziiert. Allerdings bleiben die regulatorischen Mechanismen, die der Expression von SOX2 im Brustkrebs zugrunde liegen noch weitgehend unklar. Wir haben gezeigt, dass die Überexpression von *AKT* die SOX2-Expression erhöht, während ein Knockdown der AKT-Kinase oder ihre Inhibition mit spezifischen Hemmstoffen SOX2 herunterreguliert. Umgekehrt zeigt ein *SOX2*-Knockdown keine Auswirkung auf Ebene von AKT und dessen Phosphorylierungsstatus, was darauf hinweist, dass AKT funktionell oberhalb von SOX2 anzusiedeln ist. Diese funktionale Abhängigkeit wurde auch in Tumor Sphären-Assays bestätigt, wo die Zahl und der Durchmesser der Sphären bei AKT-Inhibitoren in einer dosisabhängigen Weise abnahmen. Zusammengenommen zeigen unsere Ergebnisse, dass AKT-Inhibitoren effizient die Expression von SOX2 herabsetzen und darüber Brustkrebs-Stammzellen gezielt beseitigen können. Dies suggeriert, dass AKT-Inhibitoren aussichtsreiche Mittel in der Brustkarzinom-Therapie sein könnten.

Interessanterweise haben wir darüber hinaus festgestellt, dass die Transkriptionsaktivität am *SOX2 Genlocus* indikativ für TSZ in mehreren Tumorarten ist. Wir konstruierten einen lentiviralen Reportervektor, in dem ein rot fluoreszierendes Protein unter der Kontrolle der SOX2-regulatorischen Regionen SRR1 oder SRR2 exprimiert wird (Bareiss, Paczulla et al. 2013, Wang, Paczulla et al. 2015). RFP-positive Zellen zeigten eine robuste Sphärenbildung, während negative Zellen kaum Sphären bildeten. Darüber hinaus wurde die Expression von Stammzell- (*NANOG*, *OCT4* und *LIN28*) und EMT-Genen (*N-CADHERIN*, *TWIST*, *SNAIL*) in Reporter-positiven gegenüber negativer Zellen angereichert. Eine Behandlung mit Chemotherapeutika erhöhte zudem den Prozentsatz der RFP-positiven Zellen, während die Behandlung mit AKT-Inhibitoren auch diese Subpopulation eliminieren konnte (Schaefer, Wang et al. 2015). Diese Ergebnisse zeigen, dass die SRR1/2-Aktivität die potentielle Fähigkeit hat, TSZ zu identifizieren.

Als nächstes erforschten wir die Rollen von EVI1 sowohl in der Karzinogenese des Mamma- als auch des Prostatakarzinoms. EVI1 ist primär als hämatopoetischer Stammzellmarker bekannt, wird aber auch in Brust- und Prostatakarzinomproben exprimiert (Queisser, Hagedorn et al. 2017, Wang, Schaefer et al. 2017). In Brustkrebs wird EVI1 unabhängig vom Östrogenrezeptor-Status exprimiert, wirkt sich aber selektiv auf die Biologie von Östrogenrezeptor-negativen Tumoren aus, wo es das Zellwachstum über Regulation der MAPK-Aktivität und das metastatische Verhalten über die Regulation der Expression von KISS1 reguliert (Wang, Schaefer et al. 2017). Obwohl man Brustkrebs-Stammzellen anhand von EVI1 Expression nicht selektiv identifizieren kann, scheint EVI1 dieses Kompartiment dennoch mitzuregulieren. In der Prostata hingegen ist die EVI1-Expression auf das CD44 exprimierende Prostata-Stammzell-Kompartiment an der Basalschicht beschränkt. In einer Prostatakarzinom-Progressionskohorte stieg die Höhe der EVI1-Proteinexpression in Abhängigkeit zur Tumor-Progression. Auf funktioneller Ebene hemmt die Herrunterregulation von EVI1 die Proliferation und Zellzyklusprogression, die Migrationskapazität und das verankerungs-

unabhängige Wachstum menschlicher Prostatakarzinomzellen. Darüber hinaus konnte eine Expression von EVI1 in experimentell gewonnenen Docetaxel-resistenten Prostatakrebszellen induziert werden (Queisser, Hagedorn et al. 2017). Zusammenfassend konnten wir zeigen, dass die EVI1 Expression als ein neuartiger Faktor die Tumorprogression bei Brust- und Prostatakrebs beeinflusst, und die Karzinogenese auf Stammzell-Ebene kontrollieren kann.

Table of Contents

Chapter 1.

List of publications

1.1. First author publications (attached):

1.1.1. Evaluation of stem cell properties in human ovarian carcinoma cells using multi and single cell-based spheres assays

Wang H, Paczulla A, Lengerke C. J Vis Exp. 2015 Jan 3;(95):e52259. doi: 10.3791/52259.

1.1.2. Molecular and functional interactions between AKT and SOX2 in breast carcinoma

Schaefer T*, Wang H*, Mir P, Konantz M, Pereboom TC, Paczulla AM, Merz B, Fehm T, Perner S, Rothfuss OC, Kanz L, Schulze-Osthoff K, Lengerke C. Oncotarget. 2015 Dec 22;6(41):43540-56. doi:10.18632/oncotarget.6183.

1.1.3. Prominent Oncogenic Roles of EVI1 in Breast Carcinoma

Wang H, Schaefer T, Konantz M, Braun M, Varga Z, Paczulla AM, Reich S, Jacob F, Perner S, Moch H, Fehm TN, Kanz L, Schulze-Osthoff K, Lengerke C. Cancer Res. 2017 Apr 15;77(8):2148-2160. doi: 10.1158/0008-5472.CAN-16-0593. Epub 2017 Feb 16.

1.1.4. Ecotropic viral integration site 1, a novel oncogene in prostate cancer

Queisser A*, Hagedorn S*, Wang H*, Schaefer T, Konantz M, Alavi S, Deng M, Vogel W, von Mässenhausen A, Kristiansen G, Duensing S, Kirfel J, Lengerke C, Perner S. Oncogene. 2017 Mar;36(11):1573-1584. doi: 10.1038/onc.2016.325. Epub 2016 Sep 12.

1.1.5. In Vitro Tumorigenic Assay: The Tumor Spheres Assay

Wang H, Paczulla AM, Konantz M, Lengerke C. Methods Mol Biol. 2018;1692:77-87. doi: 10.1007/978-1-4939-7401-6_7.

1.2. Publications as co-author (not attached):

1.2.1. Expression and role of the embryonic protein SOX2 in head and neck squamous cell carcinoma

Schröck A, Bode M, Göke FJ, Bareiss PM, Schairer R, Wang H, Weichert W, Franzen A, Kirsten R, van Bremen T, Queisser A, Kristiansen G, Heasley L, Bootz F, Lengerke C, Perner S. Carcinogenesis. 2014 Jul;35(7):1636-42. doi: 10.1093/carcin/bgu094. Epub 2014 Apr 17.

1.2.2. SOX2 expression associates with stem cell state in human ovarian carcinoma

Bareiss PM, Paczulla A, Wang H, Schairer R, Wiehr S, Kohlhofer U, Rothfuss OC, Fischer A, Perner S, Staebler A, Wallwiener D, Fend F, Fehm T, Pichler B, Kanz L, Quintanilla-Martinez L, Schulze-Osthoff K, Essmann F, Lengerke C. Cancer Res. 2013 Sep 1;73(17):5544-55. doi: 10.1158/0008-5472.CAN-12-4177. Epub 2013 Jul 18.

1.2.3. EVI-1 modulates leukemogenic potential and apoptosis sensitivity in human acute lymphoblastic leukemia

Konantz M, André MC, Ebinger M, Grauer M, Wang H, Grzywna S, Rothfuss OC, Lehle S, Kustikova OS, Salih HR, Handgretinger R, Fend F, Baum C, Kanz L, Quintanilla-Martinez L, Schulze-Osthoff K, Essmann F, Lengerke C. Leukemia. 2013 Jan;27(1):56-65. doi: 10.1038/leu.2012.211. Epub 2012 Jul 25.

Chapter 2.

Contribution to publications

“Evaluation of stem cell properties in human ovarian carcinoma cells using multi and single cell-based spheres assays”

In this publication all experiments were performed by me. I analysed the data with the help of A.M. Paczulla and C. Lengerke and wrote the manuscript under the supervision of C. Lengerke. A.M. Paczulla helped in proofreading the manuscript. C. Lengerke, A.M. Paczulla and I were involved in the conception and design of the study as well as the development of methodology.

“Molecular and functional interactions between AKT and SOX2 in breast carcinoma”

I have constructed the plasmids for the SOX2 reporter and overexpression constructs, tested the vectors, characterized the transduced cells (qRT-PCR, Western Blot, spheres assay etc.) and took the confocal microscopy images. T. Schaefer performed all other *in vitro* experiments. M. Konantz performed the *in vivo* zebrafish experiments. I helped in analysis and interpretation of the data, and in proofreading of the manuscript.

“Prominent Oncogenic Roles of EVI1 in Breast Carcinoma”

All experiments were performed by me, except patient sample analysis and animal experiments. Patient analyses were kindly performed by M. Braun and Z. Varga. Zebrafish experiments were performed by M. Konantz. The mouse experiment was performed by A.M. Paczulla. T. Schaefer, M. Konantz, M. Braun, Z. Varga, A.M. Paczulla, S. Reich, S. Perner, H. Moch, T.N. Fehm, L. Kanz, C. Lengerke helped in the acquisition of the data by providing animals, acquired and managed patients, provided facilities, etc. T. Schaefer, M. Konantz, M. Braun, Z. Varga, A.M. Paczulla, F. Jacob, S. Perner, T.N. Fehm, K. Schulze-Osthoff, C. Lengerke further helped in analysis and interpretation of the data. I wrote the manuscript under the supervision of C. Lengerke. T. Schaefer, M. Braun, F. Jacob, S. Perner, H. Moch, T.N. Fehm, K. Schulze-Osthoff helped in proofreading and revision of the manuscript. C. Lengerke, T. Schaefer and I were involved in

the conception and design of the study as well as the development of methodology. M. Konantz further contributed to the development of methodology.

“Ecotropic viral integration site 1, a novel oncogene in prostate cancer”

I have performed cell cycle analysis (EdU staining, qRT-PCR, Western Blot etc.), apoptosis analysis (FACS, qRT-PCR, Western Blot etc.), stem cell property tests (spheres assay, qRT-PCR) and the migration qRT-PCR array. A. Queisser, S. Hagedorn and T. Schaefer performed the other *in vitro* experiments. W. Vogel performed the immunohistochemistry stains. M. Konantz performed the *in vivo* zebrafish experiments. S. Alavi generated the docetaxelresistant cell lines. S. Hagedorn performed the statistics. M. Deng performed the cBioPortal analysis. I helped in analysis and interpretation of the data, and in proofreading of the manuscript.

“In Vitro Tumorigenic Assay: The Tumor Spheres Assay”

I wrote the manuscript under the supervision of C. Lengerke. A.M. Paczulla and M. Konantz helped in proofreading the manuscript.

Chapter 3.

Introduction

3.1. Cancer Stem Cells (CSCs)

The mass and architecture of several human tissues, which undergo rapid and continuous cell turnover, are sustained by stem cells, a small minority of long-lived cells with extraordinary self-renewal and expansion potential. They are defined by two fundamental properties: the capability to undergo self-renewal and to differentiate. Healthy tissues as well as tumors are however not only composed of stem cells, but rather display a heterogeneous composition of cells that differ in their apparent state of differentiation. It might be reasonable to regard tumors as abnormal organs, which are maintained by a diseased cancer stem cell population with the capability for self-renewal and aberrant differentiation (Sell and Pierce 1994).

The concept of cancer stem cells (CSCs) was first proposed by Hamburger and Salmon in 1977 (Hamburger and Salmon 1977). With the advent of flow cytometry, allowing the separation of phenotypically distinct subpopulations of live cancer cells to compare their tumorigenic potential, and the development of *in vivo* self-renewal assays, this concept has been further verified and expanded. First evidence confirming the existence of CSCs came from a study in a leukemia model, which showed that $CD34^+$ but not $CD34^-$ leukemic cells can induce leukemia *in vivo* and share healthy hematopoietic stem cell characteristics (Lapidot, Sirard et al. 1994, Bonnet and Dick 1997). After this, the CSC model has being gradually extended to other tumor entities. Here, CSCs were firstly established in breast cancer as $CD44^+CD24^{-/low}Lin^-$ cells (Al-Hajj, Wicha et al. 2003). Subsequently, they have also been identified in other common cancer types, including colon cancer (Dalerba, Dylla et al. 2007, O'Brien, Pollett et al. 2007, Ricci-Vitiani, Lombardi et al. 2007), pancreatic cancer (Li, Heidt et al. 2007), brain tumors (Singh, Hawkins et al. 2004, Bao, Wu et al. 2006, Piccirillo, Reynolds et al. 2006) and ovarian cancer (Zhang, Balch et al. 2008, Alvero, Chen et al. 2009, Curley, Therrien et al. 2009, Stewart, Shaw et al. 2011).

Tumorigenic CSCs are able to ‘‘differentiate’’ into non-tumorigenic cancer cells that have limited proliferative potential, although they retain the oncogenic muta-

tions of their malignant progenitors, and create a hierarchical organization (Reya, Morrison et al. 2001, Dick 2008, Shackleton, Quintana et al. 2009). The origin of CSCs remains largely elusive. Although the hypothesis that cancer results from accumulation of numerous genetic mutations in a single target cell supports the origin of CSCs from transformed tissue stem cells, since stem cells are the only long-lived cells in various tissues, these evidences are not enough to exclude other possibilities, such as tumors arising from differentiated cells that can acquire the ability to self-renew as a result of oncogenic mutations. Over the last years, the clinical relevance of CSCs was also addressed by many studies, which demonstrated that CSCs are resistant to conventional chemotherapy and radiation treatment and are indeed the origin of cancer relapse and metastasis. As such, while therapies often lead to tumor shrinkage, they are not curative because they fail to eliminate CSCs. Consequently, targeting CSC holds hopes for healing cancer patients by inhibition of tumor relapse and metastasis (Klonisch, Wiechec et al. 2008).

3.1.1. Methods to Study CSCs

3.1.1.1. Isolation of CSCs

Similar to normal stem cells, CSCs are commonly identified and enriched using immunomagnetic bead or cytometry-based technologies with antibodies directed at prospectively defined cell surface ‘‘markers’’, or by the use of functional approaches including side population assay or Aldefluor assay. It is also possible to identify CSCs by efflux of incorporated Hoechst dyes via multidrug resistance and ATP-binding cassette transporters. However, identification and isolation of CSCs is still challenging, because of the great heterogeneity with respect to markers depending on the type of tumor. At present expression of cell surface markers such as CD44, CD24, CD29, CD90, CD133, epithelial specific antigen (ESA), and the aldehyde dehydrogenase1 (ALDH1) assay are commonly used for isolating and enriching CSCs from different tumor entities however in part with controversial results (Al-Hajj, Wicha et al. 2003, Singh, Clarke et al. 2003, Ginestier, Hur et al. 2007).

3.1.1.2. *In vivo* characterization of CSCs

Self-renewal is considered the key biological feature distinguishing stem from corresponding non-stem populations. Therefore, the gold standard for the characterization of a stem cell is to measure the maintenance of long term clonal growth in functional repopulation assays, including transplantation into serial recipients and/or *in situ* tracking. As far as CSCs are concerned, the main criterion is tumorigenic capacity upon transplantation into immunodeficient mice. In 1994, based on cell surface marker expression, a study of human acute myeloid leukemia (AML) firstly identified an AML-initiating cell population ($CD34^+CD38^-$) from AML patients by transplantation into immunodeficient mice (Lapidot, Sirard et al. 1994, Bonnet and Dick 1997). In 2003, human CSCs were firstly identified in solid tumors, including breast (Al-Hajj, Wicha et al. 2003) and brain cancer (Singh, Clarke et al. 2003).

3.1.1.3. *In vitro* characterization of CSCs

Since the process of *in vivo* repopulation and respectively cancer initiation can take a long time, *in vitro* culture systems have also been developed to study stem cells and respectively CSCs. For example, individual healthy neural stem cells are typically investigated *in vitro* under non-adherent conditions as spheres or in three-dimensional matrices. Since in theory they allow investigation of both self-renewal and differentiation at the single-cell level, sphere-forming assays have been increasingly adapted for studies on stem cells from other tissues and CSCs. For example, Dontu and colleagues have confirmed the suitability of such assays in healthy and malignant breast tissues (Dontu, Al-Hajj et al. 2003, Shaw, Harrison et al. 2012). Furthermore, less differentiated CSCs were shown to proliferate in suspension and clonally expand to form tumor spheres, when cultured with low nutrients but specific growth factor exposure and in suspension environment, while non-CSCs undergo programmed cell death because they lack substrates (Kruyt and Schuringa 2010). Thus, tumor spheres assays promise to be a useful tool for the analysis of self-renewal potential and CSC enrichment from bulk cancer cells.

3.1.2. CSCs in solid tumors

Solid tumors of epithelial origin can arise in different tissues including breast, lung, colon, prostate and ovary, and account for approximately 80% of all cancers. Although the cellular origin of most solid tumors is largely unknown, it has been considered that different subtypes have distinct cells of origin. In addition, cells within the tumor population itself often exhibit significant functional and morphologic heterogeneity. There is increasing evidence that indicates that several solid tumors are hierarchically arranged with a small subset of CSCs or tumor-initiating cells lying at the apex of the hierarchy. Although these cells often account for only a small percentage of the overall tumor population, they appear to be the only cells that initiate the tumor and drive its growth (Visvader and Lindeman 2008).

Markers specific for healthy stem cells are frequently used to isolate CSCs of the same organ. Al-Hajj et al. described a $CD44^{+}CD24^{-/low}$ cell population that possessed tumor-initiating capacity in breast cancer (Al-Hajj, Wicha et al. 2003). This study was the first to demonstrate that a functional hierarchy reminiscent of stem cell systems exists in a solid tumor. Subsequently, several other studies have been published investigating the existence of CSCs in a wide range of solid malignancies. It was e.g. found that CD133 – a marker of normal neural stem cells in both human (Uchida, Buck et al. 2000) and mouse (Lee, Kessler et al. 2005) – is also able to mark CSCs in different types of brain tumors, such as paediatric medulloblastoma, glioblastoma multiforme and ependymomas (Singh, Hawkins et al. 2004, Taylor, Poppleton et al. 2005, Bao, Wu et al. 2006, Bao, Wu et al. 2006, Piccirillo, Reynolds et al. 2006, Beier, Hau et al. 2007). Additionally, CD133 has been instrumental as a marker of the CSC population in colon (O'Brien, Pollett et al. 2007, Ricci-Vitiani, Lombardi et al. 2007), pancreas (Hermann, Huber et al. 2007), and lung cancer (Eramo, Lotti et al. 2008). The CSC model has been also extended to prostate cancer, in which the expression of α2β1 integrin, CD133 and CD44 (Collins, Berry et al. 2005, Patrawala, Calhoun et al. 2006) has been indicated to identify progenitor/tumorigenic sub-

populations. Table 1 shows a summary of the key features of CSC populations prospectively isolated from solid tumors.

Human tumor	Markers	References
Breast	$CD44^+/CD24^{-/low}$, $ALDH1^+$	(Al-Hajj, Wicha et al. 2003, Ginestier, Hur et al. 2007)
Prostate	$CD44^+/CD24^-$, $ALDH1^+$, $CD133^+$, $\alpha2\beta1^{high}$	(Collins, Berry et al. 2005, Sharpe, Beresford et al. 2013)
Ovarian	$CD44^+$, $CD133^+$, $CD24^+$, $CD117^+$, $EpCAM^+$, $ALDH^+$	(Zhan, Wang et al. 2013)
HNSCC	$CD44^+$, $CD133^+$, $ALDH^+$	(Krishnamurthy and Nor 2012)
Lung	$CD44^+$, $CD133^+$, $CD166^+$, $ALDH1^+$	(Lundin and Driscoll 2013)
Colon	$CD44^+$, $CD133^+$, $CD166^+$, $CD24^+$, $EpCAM^+$, ESA^+, $ALDH1^+$, $LGR5^+$	(Kemper, Sprick et al. 2010, Botchkina 2013, Tseng, Yang et al. 2015)
Esophagus	$CD44^+$, $CD24^+$, $CD133^+$, $ABCG2^+$, $CXCR4^+$, $ALDH1^+$	(Qian, Tan et al. 2016)
Stomach	$CD44^+$, $CD44V8\text{-}10^+$, $CD133^+$, $CD24^+$, $CD54^+$, $CD90^+$, $CD49f^+$, $CD71^+$, $EpCAM^+$, $ALDH1^+$	(Brungs, Aghmesheh et al. 2016)
Pancreas	$CD44^+/CD24^+$, $CD133^+$, ESA^+, $ALHD1^+$	(Li, Heidt et al. 2007, Zhan, Xu et al. 2015)
Brain	$CD44^+$, $CD133^+$	(Jackson, Hassiotou et al. 2015)
Liver	$CD44^+$, $CD133^+$, $CD90^+$, $CD13^+$, $EpCAM^+$	(Sun, Luo et al. 2016)
Melanoma	$CD20^+$, $CD133^+$, $CD271^+$, $ABCB5^+$	(Lang, Mascarenhas et al. 2013)
Osteosarcoma	$CBX3^+/ABCA5^+$	(Saini, Hose et al. 2012)

Renal cell carcinoma	HSP DNAJB8	(Nishizawa, Hirohashi et al. 2012)
AML	$CD34^+$, $CD38^{-/+}$, $CD90^{-/+}$, $CD123^+$, $CD19^+$, $CD45RA^+$, $CD33^+$, $CD13^+$, $CD44^+$, $CD96^+$, $CD47^+$, $CD32^+$, $CD25^+$, CLL-1^+, $TIM3^+$	(Bonnet and Dick 1997, Horton and Huntly 2012)
MM	$CD138^-$, $CD19^+$, $CD27^+$	(Matsui, Wang et al. 2008)

Table 1: Stem cell markers in solid human tumors. (Modified from Journal of Cellular Physiology) (Abbaszadegan, Bagheri et al. 2017)

Several mouse cancer models have also been used to study CSC biology in epithelial solid tumors, including for example for lung, prostate or breast carcinoma (Kim, Jackson et al. 2005, Xin, Lawson et al. 2005, Cho, Wang et al. 2008). In two different models of mammary tumorigenesis, CSC subsets have been identified using distinct marker combinations. It has e.g. been shown that a $THY1^+CD24^+$ cancer cell population (1–4% of tumor cells) was highly enriched for tumorigenic activity relative to the non-$THY1^+CD24^+$ population in MMTV–Wnt1 mammary tumors (Cho, Wang et al. 2008). In another model for breast tumorigenesis, the $Trp53^{-/-}$ mammary tumor model mimicking the development of breast cancer in li–Fraumeni patients, it was demonstrated that the tip of the β1 $integrin^{hi}CD24^+$ cell population possessed the tumor-initiating capacity (Zhang, Behbod et al. 2008).

The CSC model can also allow novel insights into the biology of metastases. Metastasis is the predominant lethal cause for cancer patients. However, not every disseminated cell from a primary tumor has the ability to form a new tumor in other organs. In the context of the CSC model, only the rare CSCs appear to be able to disseminate and induce metastatic diseases. For epithelial malignancies, a crucial event in the metastatic process is the epithelial-mesenchymal transition (EMT), in which epithelial cell homeostasis is disrupted and tumor cells acquire a migratory mesenchymal phenotype (Thiery 2002). It has been shown in several studies that the induction of EMT enhances self-renewal and associates with ac-

quisition of CSC characteristics (Yang, Mani et al. 2004, Ansieau, Bastid et al. 2008, Mani, Guo et al. 2008). It is assumed that these cells could be precursors to metastatic cancer cells, or respectively that EMT enables the formation of metastatic CSCs. CSCs may also be involved in the formation of a specific niche for metastasis. It has e.g. been found that primary tumor cells can recruit hematopoietic progenitor cells to generate a pre-metastatic niche (Kaplan, Riba et al. 2005).

3.1.3. Molecular mechanisms regulating CSCs

Like healthy stem cells, CSCs have the ability to self-renew. It seems therefore reasonable to propose that CSCs utilize the same self-renewal and cell division machinery as normal stem cells. There is evidence that signaling pathways involved in healthy stem cell self-renewal, including Notch, Sonic hedgehog (Shh) and Wnt, also associate with oncogenesis.

Wnt signaling is a critical evolutionarily conserved pathway in regulating developmental programs and stem cell function (Clevers 2006). In the so-called canonical Wnt signaling pathway, Wnt binds to FZD (Frizzled) and LRP receptors, decomposes the β-catenin destruction complex (Axin, GSK3, APC, and CK1), and leads to accumulation and translocation of β-catenin to the nucleus for target gene transcription (Figure 1). Abnormal activation of Wnt signaling is involved in the regulation of a variety of CSC types including colorectal cancer, breast cancer, hematologic cancer, skin cancer, and lung cancer (Reya, Duncan et al. 2003, Malanchi, Peinado et al. 2008, Mukherjee, Mazumdar et al. 2014, Zhang, Lou et al. 2015, Basu, Haase et al. 2016). For example, increased Wnt signaling disrupts the normal growth and differentiation of colonic crypt stem cells, and results in a colorectal CSC phenotype through its target genes such as c-Myc and Cyclin D (MacDonald, Tamai et al. 2009, Medema and Vermeulen 2011). Moreover, a study of squamous cell carcinomas has shown that canonical Wnt signaling activation plays a critical role in tumorigenesis of $CD34^+$ bulge CSCs. Ablation of the β-catenin gene depleted $CD34^+$ CSCs and devoid propagation of secondary tumors whereas expression of a non-degradable β-catenin induced by

tamoxifen in the skin sufficiently expanded the bulge CSC's population (Malanchi, Peinado et al. 2008).

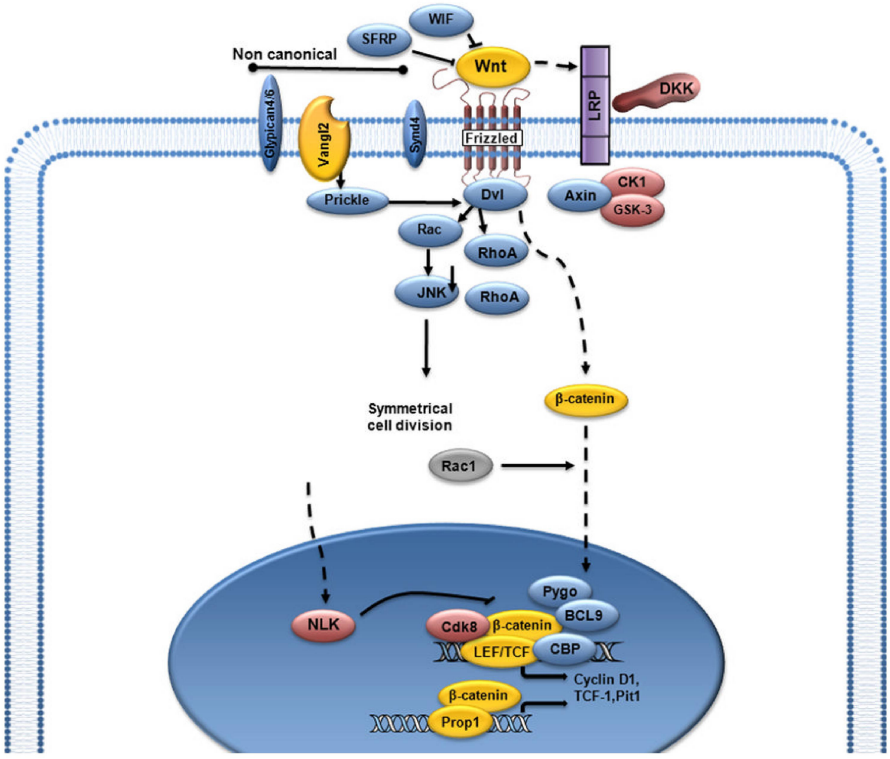

Figure 1: Wnt/β-catenin signaling pathway (adapted from The International Journal of Biochemistry & Cell Biology) (Yu, Pestell et al. 2012)

Canonical Notch signaling is another critical evolutionarily conserved pathway, playing essential roles in regulating development and adult tissue homeostasis (Chen, Li et al. 2011). Notch ligands bind to Notch receptors, which induce proteolytic cleavage and release of the Notch intracellular domain (NICD). Subsequently, NICD translocates to the nucleus and regulates the expression of target genes including those pertinent to CSC self-renewal such as Survivin, Myc, Nanog, Oct-4, and Sox2 through interaction with a CBF1/Suppressor of Hairless/LAG-1 (CSL) family DNA-binding protein (Figure 2). The important role of abnormal activation of Notch signaling has been demonstrated in breast cancer, pancreas and glioblastoma CSCs (Abel, Kim et al. 2014, Seymour, Nowak et al. 2015, Choy, Hagenbeek et al. 2017). In breast CSCs, activation of Notch signaling was for example shown to promote tumorigenesis of Fascin-positive CSCs

(Barnawi, Al-Khaldi et al. 2016). In another study, immunohistochemical analysis of 115 breast tumor tissues from primary lesions showed that Notch expression significantly associated with enhanced expression of the ALDH family member A1 (Zhong, Shen et al. 2016).

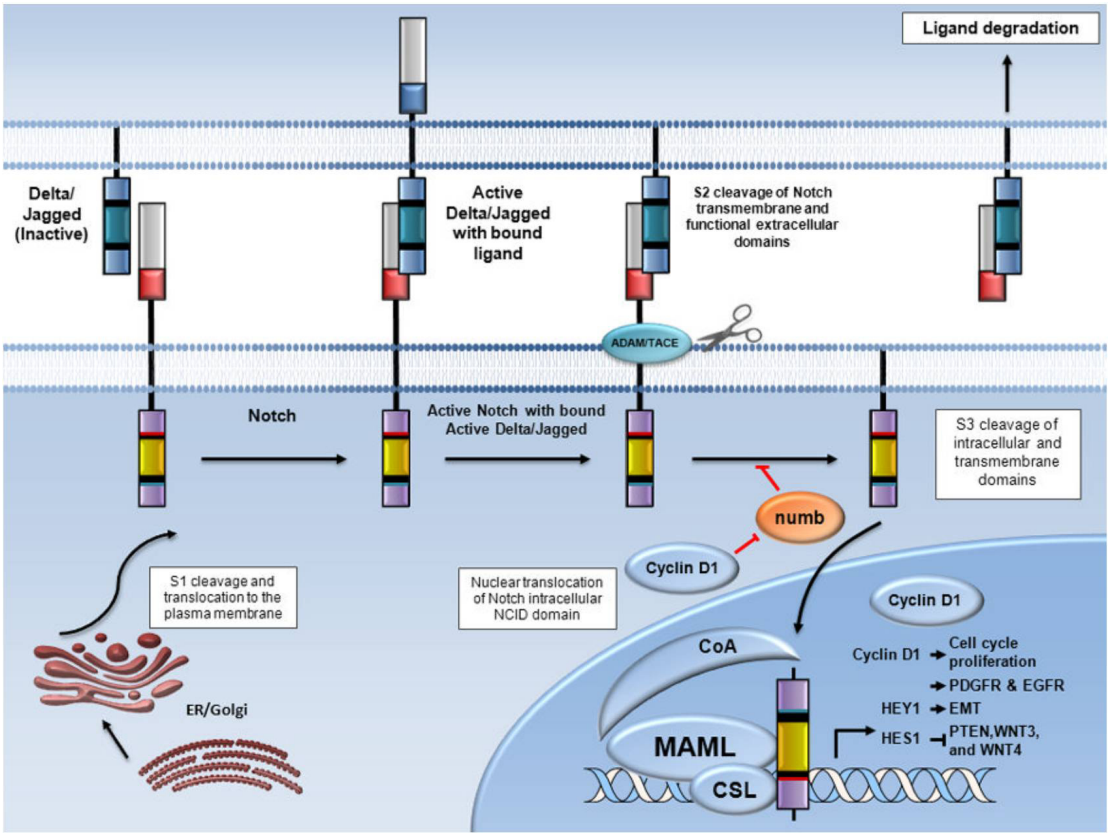

Figure 2: Notch signaling pathway (adapted from The International Journal of Biochemistry & Cell Biology) (Yu, Pestell et al. 2012).

It has been reported that the HH pathway is involved in regulation and maintenance of CSCs and is aberrantly activated in numerous cancer types such as glioblastoma, lung squamous cell carcinoma, breast cancer, pancreatic adenocarcinoma, myeloma, and chronic myeloid leukemia (CML) (Bar, Chaudhry et al. 2007, Clement, Sanchez et al. 2007, Dierks, Beigi et al. 2008, Zhao, Chen et al. 2009, Merchant and Matsui 2010, Justilien, Walsh et al. 2014). For instance, in CSCs of human lung squamous cell carcinoma and glioma, it was shown that activation of HH signaling was higher than that in non-CSCs bulk tumor cells, indicating the critical role of aberrant HH signaling activation for CSC self-renewal

and regulation (Clement, Sanchez et al. 2007, Justilien, Walsh et al. 2014). Consistently, inhibition of HH signaling by the SMO antagonist cyclopamine effectively reduced glioblastoma CSC populations (Bar, Chaudhry et al. 2007). Similar results were observed with colon, pancreatic, prostate and lung CSCs (Watkins, Berman et al. 2003, Huang, Zhuan-Sun et al. 2012, Singh, Chitkara et al. 2012, Batsaikhan, Yoshikawa et al. 2014).

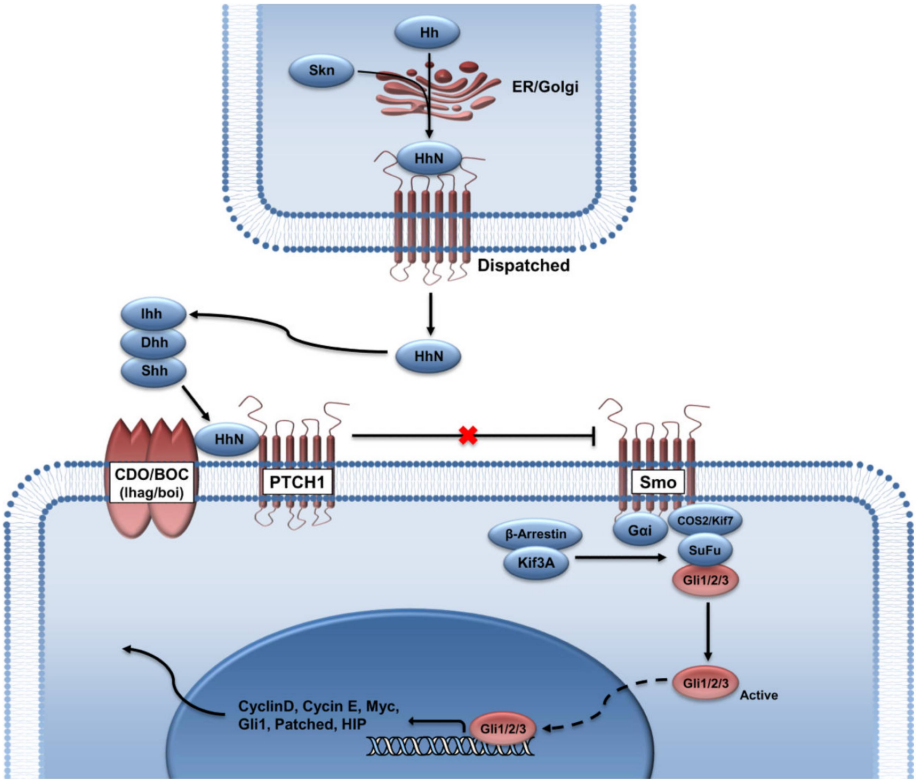

Figure 3: Hedgehog signaling pathway. (adapted from The International Journal of Biochemistry & Cell Biology) (Yu, Pestell et al. 2012)

3.2. SOX2

3.2.1. Biochemical properties and functional roles

SRY (sex determining region Y)-box 2, also known as *SOX2*, locates on chromosome 3 (3q26.33), and belongs to the SRY-related high-mobility-group (HMG)-box (SOX) gene family. It can bind non-B-type DNA and change the conformation and flexibility of chromatin to regulate transcription, replication and DNA repair (Thomas 2001, Stros, Launholt et al. 2007).

SOX2 plays a critical role in the maintenance of self-renewal or pluripotency of undifferentiated embryonic stem cells during embryonic development and in some adult organs. In the pre-implantation development, *SOX2* is initially expressed in both the inner cell mass (ICM) and the trophectoderm (TE), which supports the derivation of ESC from ICM and the derivation of trophoblast stem cells (TSCs) from the TE. Moreover, the cooperation of SOX2 with other transcription factors, such as OCT4 and Nanog maintains the regulatory networks responsible for self-renewal and represses the differentiation programs in embryonic stem cells (ESCs) (Boyer, Lee et al. 2005, Chen, Xu et al. 2008, Kim, Chu et al. 2008, Orkin and Hochedlinger 2011). Furthermore, *SOX2* continues to express in some adult stem and progenitor cells, which were shown to not only require SOX2 during development but also in adult life for tissue homeostasis and repair. In addition, SOX2 has been involved, next to OCT4, as one of the key factors mediating reprogramming of mature terminally differentiated human cells into pluripotent stem cells (PSCs).

Timing of *SOX2* expression and expression levels are precisely controlled in pluripotent and adult stem cells of different tissues by different intracellular cofactors and extracellular signals in different manners. During development of the neural system, SOX2 is directly regulated by STAT3, which leads to ESC commitment to the neural progenitor cell fate (Foshay and Gallicano 2008). Moreover, SOX2 and other pluripotency factors are involved in an auto-regulatory loop to induce their own expression to maintain the undifferentiated state in ESCs (Boyer, Lee et al. 2005). Similarly, in murine neural pluripotent cells (mNPCs), Egf and Shh signaling induce the expression of Sox2, which then binds to Egfr and Shh genes to induce positive feedback loops, which is again important for stem cell maintenance (Hu, Zhang et al. 2010, Engelen, Akinci et al. 2011). In contrast to Egf and Shh signaling, thyroid hormone signaling was reported to inhibit Sox2 expression and induce differentiation of neural progenitors (Lopez-Juarez, Remaud et al. 2012). The hormone-dependent repression is caused by the binding of thyroid receptor-α1 to a negative thyroid hormone response element within the SOX2 enhancer. Julian et al. proved that the cell cycle regulators E2f3a and E2f3b in

the adult brain regulate SOX2 expression and control NPC proliferation (Julian, Vandenbosch et al. 2013). A SOX2 repressor P21 has also been found to bind to a SOX2 enhancer and to directly repress SOX2 expression in neural stem cells (Marques-Torrejon, Porlan et al. 2013). SOX2 expression can also be modulated by extrinsic environmental factors, through which stem cell number or fate is determined. For instance, hypoxia can promote SOX2 expression and lead to induction of CD133 in lung cancer (Iida, Suzuki et al. 2012).

Additionally, post-translational modifications play a critical role in the regulation of SOX2 by influencing protein stability, activity, and cellular distribution. At least three phosphorylation sites, S249, S250 and S251, have been identified in SOX2. In a study of Van Hoof et al., the phosphorylation of SOX2 promotes the sumoylation of SOX2 preventing the binding of SOX2 to DNA (Tsuruzoe, Ishihara et al. 2006, Van Hoof, Munoz et al. 2009). It has been also reported that the acetylation of lysine residues of SOX2 blocks its nuclear export and sustains expression of its target genes under hyper-acetylation or differentiation conditions (Baltus, Kowalski et al. 2009). Moreover, the methylation of SOX2 at arginine 113 by the co-activator associated arginine methyltransferase 1 (CARM1) was reported to induce elevation of the SOX2 self-association and trans-activation in MCF7 human breast cancer cells (Zhao, Zhang et al. 2011).

SOX2 interacts also with other molecules to modulate signaling pathways essential for self-renewal. In ESCs, the cooperation of SOX2 with OCT4 efficiently recruits other factors important for gene activation to bind to DNA. SOX2 loss-of-function phenotypes can be rescued by *OCT4* overexpression indicating that OCT4 and SOX2 can jointly activate targets genes (Masui, Nakatake et al. 2007). During lens development, SOX2 combines with PAX6 to activate the *delta-crystallin* gene, inducing lens placode formation by binding to lens-specific enhancer elements (Kamachi, Uchikawa et al. 2001). It was also reported that interaction of SOX2 with long non-coding RNA rhabdomyosarcoma 2-associated transcript (RMST) can co-regulate a large pool of downstream genes involved in the regulation of neural stem cell fate (Ng, Johnson et al. 2012). Cimadamore et

al. found that SOX2 maintains endogenous levels of LIN28 in NPCs (neural precursor cells), subsequently regulating let-7 miR biogenesis, which globally modulates mRNA splicing (Cimadamore, Amador-Arjona et al. 2013).

In general, SOX2 expression is regulated at genetic, transcriptional, and protein levels with other cofactors and cell-signaling regulators to keep self-renewal and differentiation programs in balance.

3.2.2. SOX2 dysregulation in cancer

In recent years, SOX2 has been increasingly recognized as a powerful oncogene and regulator of CSC identity in various tumors. Accumulating data indicate that *SOX2* is abnormally expressed and promotes tumorigenesis in tissues containing *SOX2* expressing cell-types, e.g. lungs, esophagus, neural cells, and Merkel cells as well as in squamous cell carcinoma of the skin. *SOX2* has been shown to be amplified in human squamous cell carcinomas of the lung (23%), and esophagus (15%), as well as in 27% of human small cell lung cancers, indicating that an increase in copy number is partially responsible for abnormal *SOX2* expression in cancer (Bass, Watanabe et al. 2009, Rudin, Durinck et al. 2012, Schrock, Bode et al. 2014). Although the molecular function of SOX2 in tumorigenesis has not been fully elucidated, recent data suggest especially its pro-survival, anti-differentiation and pro-migration roles. Furthermore, SOX2 expression was linked to cell proliferation: overexpression of *SOX2* in mouse lung tissue (Tompkins, Besnard et al. 2011) and adenocarcinoma (Lu, Futtner et al. 2010) was shown to promote proliferation, whereas *SOX2* knockdown in human oesophagus and small cell lung cancer derived cell lines compromised cell growth (Bass, Watanabe et al. 2009, Rudin, Durinck et al. 2012). In studies focusing on *in vitro* cell lines and *in vivo* transplantation models of human osteosarcoma, SOX2 played a critical role in cancer cell proliferation and differentiation by antagonizing Wnt signaling (Basu-Roy, Seo et al. 2012).

Furthermore, SOX2 is an important regulator of CSC biology. In ovarian carcinoma cells, we have found that induction of *SOX2* expression increases the *in*

vivo tumor initiating capacity by conferring enhanced apoptosis resistance and clonogenicity (Bareiss, Paczulla et al. 2013). Similar results were observed in breast carcinoma, where overexpression of *SOX2* increased mammosphere formation, and vice-versa *SOX2* knockdown reduced mammospheres and delayed tumor induction in xenograft models (Leis, Eguiara et al. 2012). In some tumor types including breast and ovarian carcinoma, *SOX2* was shown to be expressed heterogeneously (Piva, Domenici et al. 2014, Vanner, Remke et al. 2014, Bayo, Jou et al. 2015, Lawson, Bhakta et al. 2015) with only subpopulations of tumor cells showing SOX2 positivity. It was reported that, by using a human SOX2 promoter reporter, SOX2-positive cells isolated from heterogeneous cervical cancer cell populations exhibited a higher frequency of CSCs compared to SOX2-negative cells in limiting cell dilution tumor assays (Liu, Yang et al. 2014). Similar results have also been reported in a study of squamous cell carcinoma of the skin in a mouse model, which indicated that *SOX2* is ectopically expressed in rare stem cell-like populations (Beck, Driessens et al. 2011, Schober and Fuchs 2011). Furthermore, several studies have shown that the rare SOX2-positive cells are members of a quiescent, slowly cycling CSC population capable of repopulating the tumor following drug withdrawal (Vanner, Remke et al. 2014). These observations strongly suggest important roles of ectopic *SOX2* expression in the CSC biology and thus tumor initiation and therapy resistance. It remains unclear whether altered *SOX2* expression in these tumors is intrinsically regulated or ectopically induced by external factors.

Taken together, similar to its multiple roles in development and differentiation, SOX2 seems to function at different levels of carcinogenesis to promote tumor development.

3.3. EVI1

3.3.1. Structure, biochemical properties and expression

The MDS1 and EVI1 complex locus MECOM on chromosome 3 in humans (3q26.2) comprises of several protein isoforms of which one is EVI1 (ecotropic

virus integration site 1 protein homolog) (Wieser 2007). The *EVI1* gene spans 60 kilobases containing 16 exons, and the first in-frame ATG start codon is located on exon 3. The *EVI1* gene is transcribed into an mRNA with several variant 5′-ends (Fears, Mathieu et al. 1996, Vinatzer, Mannhalter et al. 2003, Aytekin, Vinatzer et al. 2005) and several alternative splice forms (Bordereaux, Fichelson et al. 1990, Morishita, Parganas et al. 1990, Bartholomew and Clark 1994, Alzuherri, McGilvray et al. 2006). From these transcript variants at least three different proteins, EVI1, MDS1/EVI1 (also called EVI1c), and EVI1Δ324 (also called EVI1b) can be produced (Figure 4). The major EVI1 form is a 1051 amino acid protein with a molecular weight of 145 kDa (Morishita, Parganas et al. 1990). The MDS1/EVI1 protein contains 188 additional amino acids at its N-terminus encoded by the first two *MDS1* exons, in addition to the entire EVI1 amino acid sequence. The fusion of MDS1 and EVI1 encodes a so-called “PR” domain (PRD1-BF1/BLIMPI-RIZ homology), which prevents oligomerization, and further affects its biochemical functions (Fears, Mathieu et al. 1996, Nitta, Izutsu et al. 2005). This domain has been identified in at least 17 kinds of different proteins, and a large body of evidence suggests that in contrast to the full-length isoform including the PR domain, the PR-absent forms are oncogenic (Jiang and Huang 2000). Truncated EVI1Δ324 has also been described, lacking 324 internal amino acids with a molecular weight of 88-kDa. However, the biological function of EVI1Δ324 is not known so far.

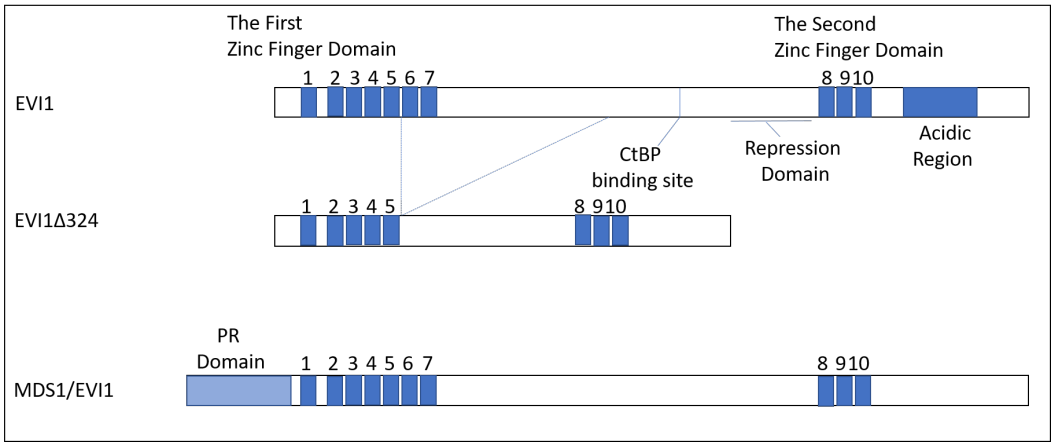

Figure 4: Structure of alternatively spliced forms of EVI1. (Adapted from International Journal of Hematology) (Goyama and Kurokawa 2010)

In mouse, *Evi1* is found in various developing tissues in different spatiotemporal patterns, e.g. the urinary system, limbs and the heart (Perkins, Mercer et al. 1991). In adult human tissues, EVI1 is more or less absent from skeletal muscle and bone marrow, but found at low levels in the small intestine, colon, thymus, spleen, heart, brain, testis, and placenta, and at moderate to high levels in lung, kidney, uterus, prostate, and the stomach (Aytekin, Vinatzer et al. 2005). Furthermore, high expression levels are detected in the rare hematopoietic stem cell subpopulations (Goyama, Yamamoto et al. 2008).

As a transcription factor, EVI1 localizes in the nucleus and associates with its recognition motif (5'-GACAAGATA-3') through either one of its zinc finger domains to regulate the expression of various genes, such as *GATA-2*, *PLZF*, *Map3K14*, *Napb*, and *FOG2* (Takahashi and Licht 2002, Yatsula, Lin et al. 2005, Yuasa, Oike et al. 2005). Moreover, EVI1 can also particularly interact with both transcriptional co-repressors and co-activators to modify the activation of genes in an epigenetic manner. For instance, binding of EVI1 to CtBP through consensus sites in its transcription repression domain (C-terminal-binding protein) recruits histone deacetylases (HDACs) as well as many other co-repressor molecules leading to transcription repression via chromatin remodeling (Chakraborty, Senyuk et al. 2001, Izutsu, Kurokawa et al. 2001, Palmer, Brouillet et al. 2001). EVI1 can also bind to the co-activators CBP and P/CAF. A study from 2001 showed that co-expression of CBP could turn a repressive effect of EVI1 on a reporter gene construct into an activating effect (Chakraborty, Senyuk et al. 2001). Furthermore, EVI1 desensitized a cell to TGFβ signaling not through displacing Smad3 from a gene's promoter but rather through direct interaction with the Smad3 protein, followed by recruitment of co-repressors to make the DNA inaccessible to the transcription machinery.

In addition to its role in transcriptional regulation, EVI1 has been reported to interact with other molecules to modulate signaling pathways, which are essential for cell cycle progression, apoptosis and proliferation. Abnormal cellular proliferation mediated by the TGFβ pathway has frequently been mentioned in EVI1 ex-

pressing cells. EVI1 forms a ternary complex with Smad3 and Smad4 and significantly reduces Smad3/4 DNA binding properties, thus inhibiting TGFβ-mediated transcriptional effects this way ablating TGFβ-induced anti-proliferative effects (Kurokawa, Mitani et al. 1998). Moreover, EVI1 has been shown to repress bone morphogenic protein/Smad1 and activin/Smad2-mediated transactivation of their respective target gene promoters. Additionally, Kurokawa and colleagues demonstrated that EVI1 directly interacts with and inhibits c-Jun N-terminal kinase (JNK) to protect cells from JNK-activated stress-induced cell death (Kurokawa, Mitani et al. 2000).

3.3.2. Functional roles

EVI1 plays a crucial role in the regulation of several developmental processes. Due to its temporally and spatially restricted expression pattern in the mouse, it was first suggested that EVI1 plays essential roles in turning on and off proliferation and differentiation programs during development. Consistently, Evi1 deficiency results in multiple malformations, including widespread hypocellularity and cardiac immaturity with delayed chamber development and defects of peripheral and central neural system during mouse development (Hoyt, Bartholomew et al. 1997). *In vitro* studies confirmed an involvement of EVi1 in neural development by showing that experimental expression of Evi1 was capable to mimic all-trans retinoic acid (ATRA)-induced neuronal differentiation of the murine embryonic carcinoma cell line P19 (Kazama, Kodera et al. 1999). As in the mouse, temporal and spatial specificity of Evi1 expression in Xenopus, chicken, and zebrafish indicate conserved functions of Evi1 in developmental regulation throughout vertebrate evolution (Mead, Parganas et al. 2005, Van Campenhout, Nichane et al. 2006).

In addition to its role in development, EVI1 also influences cell differentiation, proliferation and apoptosis in adult tissues. The function of EVI1 on cell differentiation appears at great extend depending on the cell type. Experiments in human and mouse cell lines have shown that on one side, EVI1 is able to prevent the terminal differentiation of bone marrow progenitor cells to granulocytes and

erythroid cells, on the other hand, it can also favor the differentiation of hematopoietic stem cells to megakaryocytes (Buonamici, Chakraborty et al. 2003). Moreover, ectopic expression of *Evi1* enhanced colony formation of murine bone marrow progenitor cells in soft agar (Buonamici, Li et al. 2004, Buonamici, Li et al. 2005, Jin, Yamazaki et al. 2007), and accelerated the cell cycle of Rat-1 fibroblasts (Bartholomew, Kilbey et al. 1997, Kilbey, Stephens et al. 1999, Palmer, Brouillet et al. 2001), of the murine myeloid cell line 32Dcl3 (Chakraborty, Senyuk et al. 2001, Chi, Senyuk et al. 2003), and of murine ESCs (Sitailo, Sood et al. 1999), indicating that EVI1 is also involved in cell proliferation. Furthermore, it was also described that EVI1 counteracted ultraviolet (UV) light induced apoptosis of 293T human fetal kidney and Jurkat acute T-cell leukemia cells, as well as tumor necrosis factor (TNF)-α induced apoptosis of U937 histiocytic lymphoma cells (Kurokawa, Mitani et al. 2000). These observations support an anti-apoptotic role of EVI1 in various tissues.

3.3.3. EVI1 in cancer

In addition to its crucial functions in development, EVI1 also plays roles in oncogenesis. The *Evi1* gene was first identified due to its transcriptional activation upon retroviral insertion-induced leukemia in a murine model system (Morishita, Parker et al. 1988). Activation of *EVI1* often occurs through translocation and inversion event on chromosome 3, where also the *EVI1* gene is located. The inv(3)(q21q26) and t(3;3)(q21;26) rearrangements can be detected in 7–10 % of MDS/AML cases (Nucifora, Laricchia-Robbio et al. 2006). They are associated with the formation of riboforin I-EVI1 fusion gene, which is controlled by the strong promoter of the riboforin I gene (Suzukawa, Parganas et al. 1994). t(3;21)(q26;q22) chromosome rearrangements are especially associated with *de novo* or therapy-derived MDS/AML and in some cases with blast crisis CML (Nucifora and Rowley 1995, Mitani 2004, Haltrich, Kost-Alimova et al. 2006, Poppe, Dastugue et al. 2006). *EVI1* expression can also be induced in the absence of 3q26 rearrangements, indicating the presence of other mechanisms for *EVI1* activation. In AML patients, high *EVI1* expression, which occurs in approxi-

mately 10% of cases of AML, defines a distinct subtype of AML with particularly poor clinical prognosis (Valk, Verhaak et al. 2004). These AML have a gene expression pattern closest to healthy hematopoietic $CD34^+$ cells, suggesting a stem cell phenotype of EVI1-related leukemia. Indeed, EVI1 expression has been also demonstrated as a feature of healthy hematopoietic and leukemic stem cells (LSCs). Furthermore, enhanced expression of *EVI1* plays also important roles in solid tumor carcinogenesis and progression, such as in ovarian (Brooks, Woodward et al. 1996), colorectal (Liu, Chen et al. 2006) and hepatocellular carcinoma (Yasui, Konishi et al. 2015). It has also been reported that EVI1 induces cell resistance against apoptosis in colorectal carcinoma (Liu, Chen et al. 2006), promotes metastasis of breast cancer cells in a mouse model, and even can predict malignancy in estrogen receptor-negative breast cancer patients, depending on expression level (Patel, Appaiah et al. 2011).

Chapter 4.

Aim of this project

There is more and more evidence that only specific cellular subpopulations, so-called cancer stem or tumor-initiating cells, have the ability to initiate and sustain cancer. These so-called CSC subpopulations are suggested to be resistant to the majority of current cancer treatments and to be the cause of metastases and cancer-related death. The CSC model thus entails significant therapeutic implications by proposing that the design of new cancer therapeutics requires targeting and elimination of CSCs in order to provide cure. Therefore, understanding the molecular mechanisms regulating CSCs is essential. The main focus of my PhD thesis is thus set on CSC biology and the significance of embryonic transcription factors in CSC identification and regulation. Stem cell factors such as SOX2 and OCT4 strongly affect cellular fate and can reprogram differentiated somatic cells to a pluripotent stem cell state. We hypothesized that CSCs may be generated in a similar manner and have indeed identified an oncogenic role of the pluripotency-associated stem cell factor SOX2 in ovarian and breast cancer. Furthermore, the transcriptional regulator EVI1 has also been shown to regulate hematopoietic and leukemic stem cell biology. We have therefore analyzed the expression and roles of EVI1 in breast and prostate cancer and shown that EVI1 plays important oncogenic roles and (co-)-regulates CSC subpopulations in these tumor types.

Chapter 5.

Results and Discussion

5.1. Characterization of CSCs

5.1.1. Isolation of CSCs using a SOX2 reporter

CSCs possess self-renew capability and often retain, or reactivate, molecular regulatory networks active in corresponding healthy tissue stem cells (Bao, Ahmad et al. 2013). Therefore, such mechanisms might be also used to identify CSC identity. Here we investigated whether SOX2 expression can identify tumor cell subsets with CSC identity.

Given the broad expression of SOX2 in stem cells of both embryonic and tissue type, we postulated that SOX2 promoter activity may be technically exploited as an indicator of CSCs. Towards this goal, we constructed a lentiviral reporter system in which a TdTomato fluorescence gene was cloned under the control of a SOX2 regulatory element previously described to have high SOX2 promoter activity in breast cancer (Leis, Eguiara et al. 2012) (Figure 5. A). If transduced with these lentiviral particles, cells of endogenously high SOX2 promoter activity therefore will also express red fluorescent protein, which enables their isolation by FACS. Furthermore, our construct also contains a destabilization domain of the ProteoTuner Shield System (Banaszynski, Chen et al. 2006) in front of the TdTomato fluorescence protein to circumvent accumulation of background signal, thus providing for high signal-to-noise ratio (Figure 5. B).

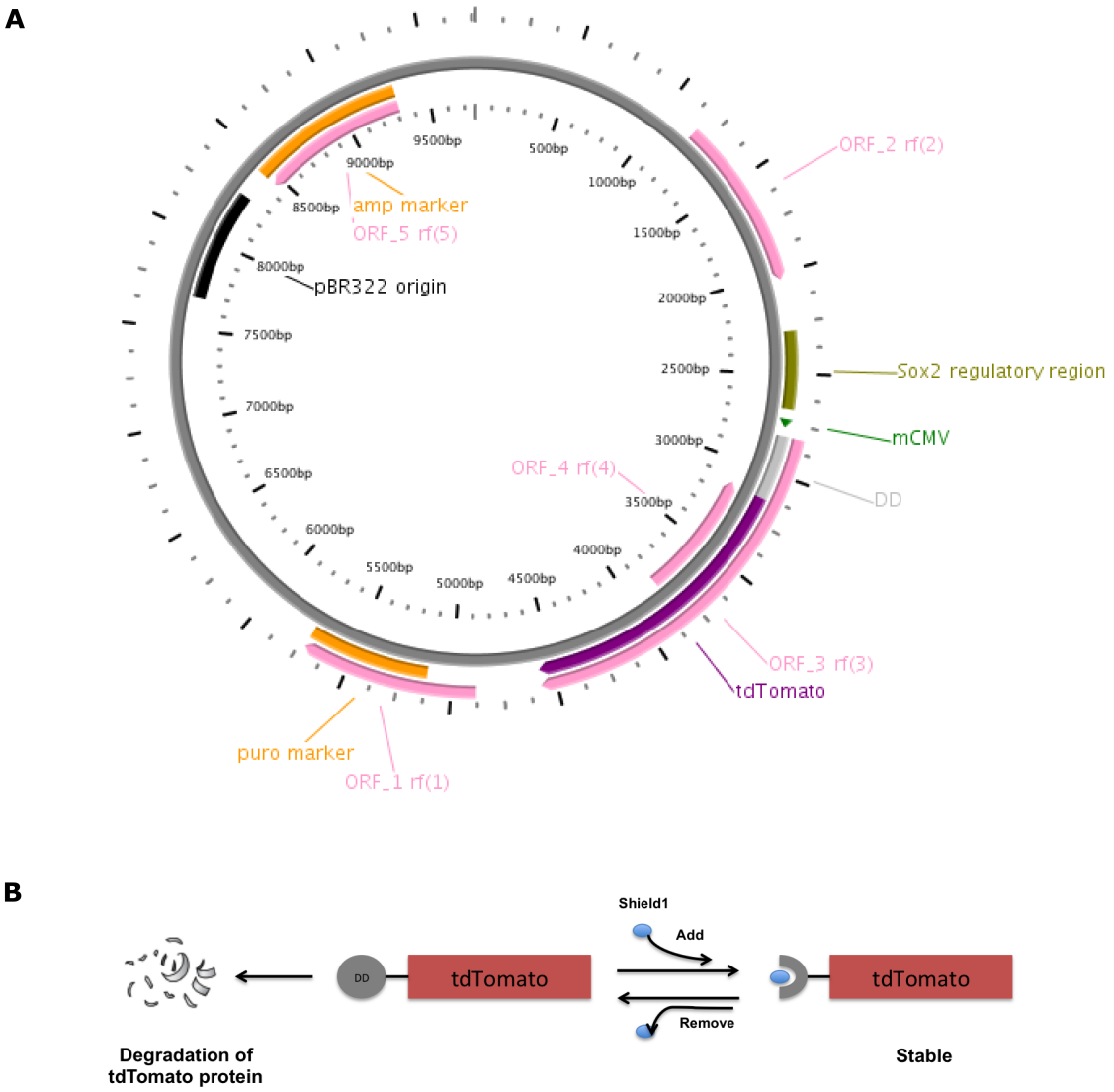

Figure 5. (A) Reporter plasmid information. The TdTomato gene is controlled by the Sox2 regulatory region. (B) A General method to conditionally control protein stability.

MCF7 breast cancer and OVCAR-3 serous ovarian carcinoma (SOC) cell lines were stably transduced with lentiviral particles containing the SOX2-reporter construct described above. To evaluate the capability of the reporter construct to isolate CSC, the sphere-formation assay was used. Our data demonstrated that 2D-cultured MCF7 cells showed 0.4-0.8 % reporter-positive cells. Spheroid cultures enriching for stem cell activity displayed an enhanced frequency of reporter-positive cells of up to 2 %, instead (Figure 6).

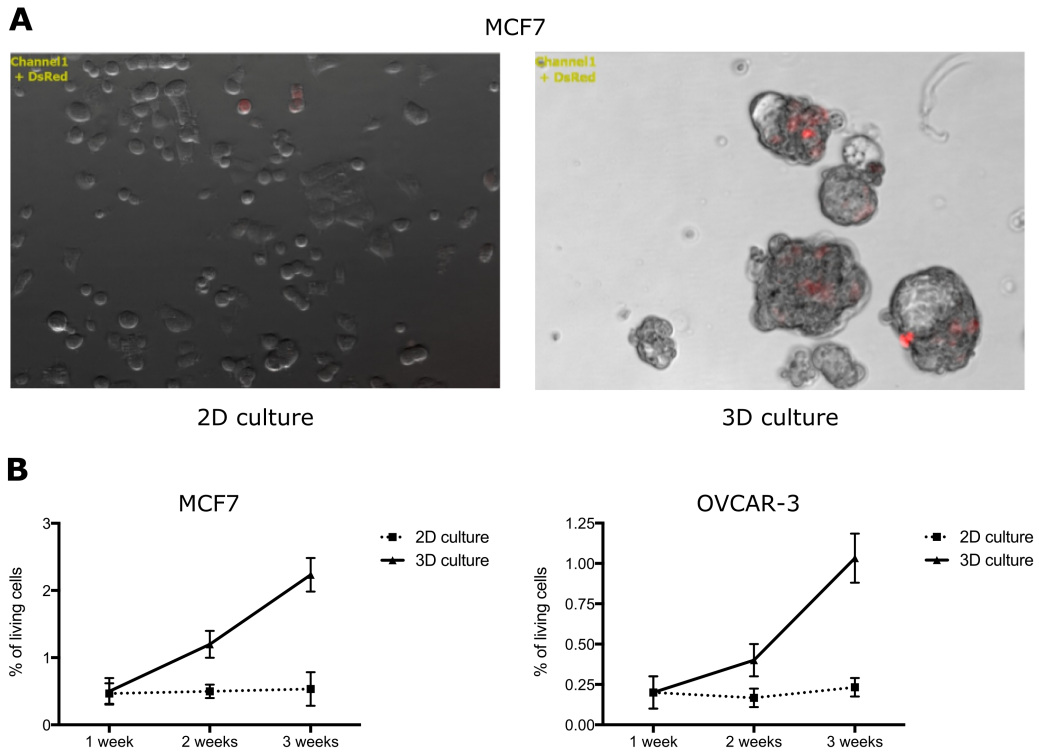

Figure 6. Reporter positive cells were enriched in the sphere culture (3D) condition. (A) Microscopy pictures of cells plated in different cell culture conditions taken one week after plating in RPMI (2D) and spheres culture medium (3D). (B) Quantitative analysis of the red fluorescence signal by flow cytometry in dissociated adherent cells (2D) and spheres (3D).

When isolated by FACS, reporter-positive cells showed significantly enhanced spheres formation, while reporter negative cells generated fewer and smaller spheres (Figure 7).

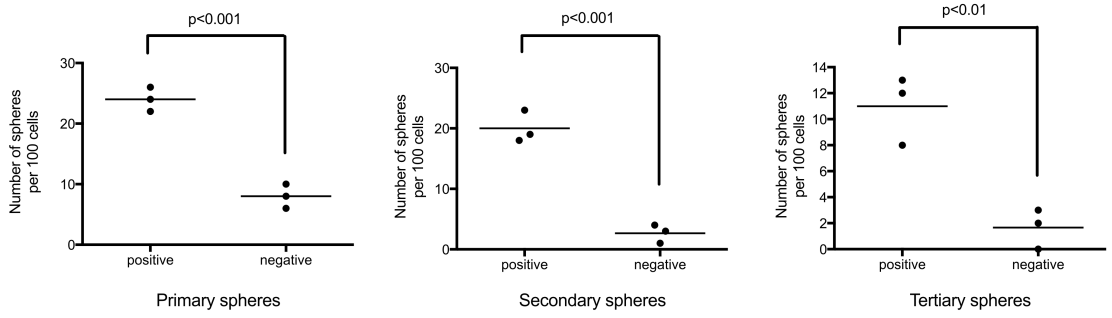

Figure 7. Reporter positive cells have higher sphere-forming potential in breast cancer cells. Reporter positive and negative MCF7 cells isolated by FACS were plated in sphere conditions at

100 cells per well and spheres counted after 7 days. For all replating assays, spheres were pooled, dissociated to single cells, and replated at a density of 100 cells per well.

Comparable results were obtained with OVCAR-3 human ovarian carcinoma cells. Reporter positive OVCAR-3 cells showing red fluorescence were enriched in sphere culture conditions as compared to 2D cultures (Bareiss, Paczulla et al. 2013), and gave rise to more and larger spheres than reporter negative cells. Interestingly, reporter positive OVCAR-3 cells formed more spheres than reporter positive MCF7 cells in the primary sphere assay. In fact, almost every reporter positive OVCAR-3 cell thereby gave rise to an individual tumor sphere, which reflects the cellular inherent difference at tumor initiation (Figure 8).

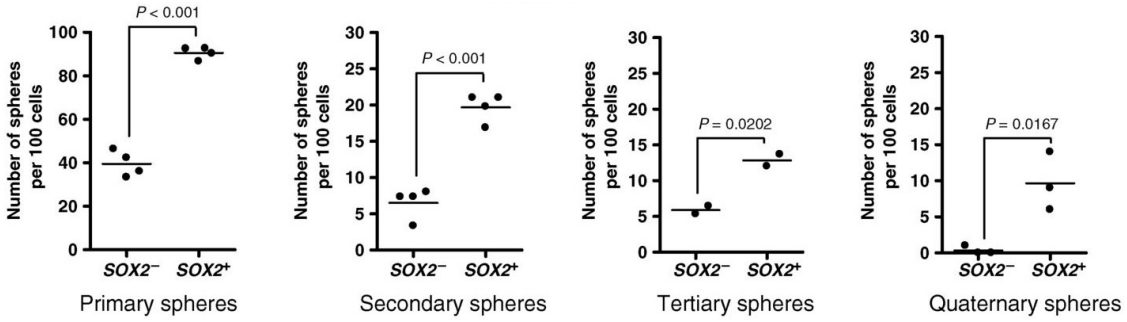

Figure 8. Reporter positive cells have higher sphere-forming potential in an ovarian cancer cell line. Reporter positive and negative OVCAR-3 cells isolated by FACS were plated in sphere conditions at 100 cells per well and spheres counted after 7 days. For all replating assays, spheres were pooled, dissociated to single cells, and replated at a density of 100 cells per well. (Adapted from (Bareiss, Paczulla et al. 2013))

Interestingly we also found that both MCF7 and OVCAR-3 reporter negative cells remained negative and exhausted their sphere forming potential in follow-up serial replating assays, while reporter positive cells formed spheres containing a mixture of reporter positive and negative cells, reflecting the ability for self-renewal, differentiation and maintenance of their sphere forming capacity (Figure 9).

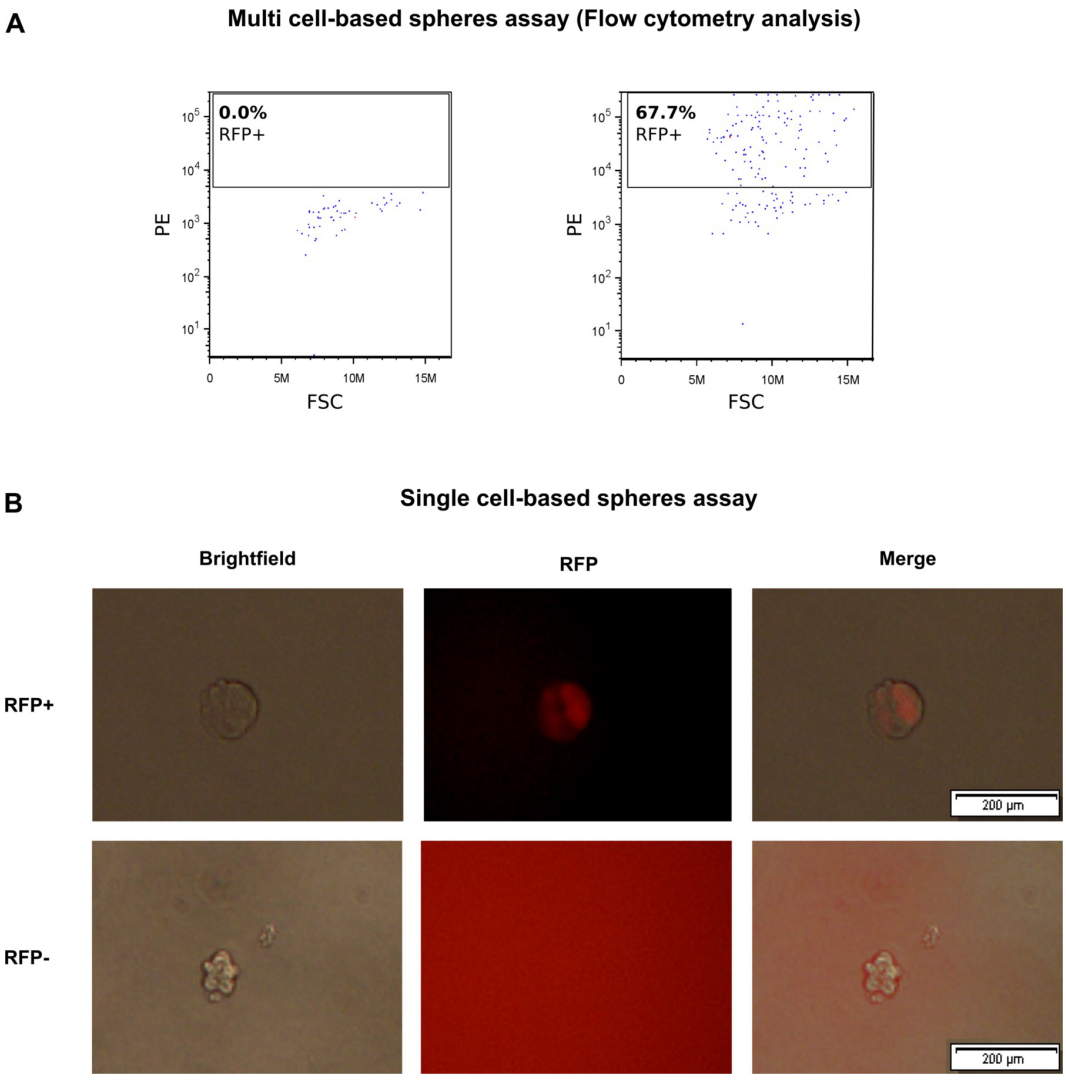

Figure 9. Analysis of the red fluorescence signal in tumor spheres formed from reporter positive and respectively reporter negative OVCAR-3 cells. (A) Flow cytometry analysis for the red fluorescence signal in dissociated spheres derived from reporter positive (right) and negative cells (left) (multi cell-based spheres assay); (B) Microscopy pictures of spheres derived from reporter positive (RFP+) and negative cells (RFP-) (single cell-based spheres assay) reveals heterogeneous fluorescence signal in spheres derived from reporter positive but not from negative cells. Pictures were taken at day 7 for conventional spheres and at day 10 for single cell-based sphere assays. Note the larger size of spheres derived from reporter positive putative CSCs. (Adapted from (Wang, Paczulla et al. 2015))

The expression levels of distinct pluripotency genes coordinate the maintenance of pluripotency in (embryonic) stem cells (ESCs) (Hadjimichael, Chanoumidou et al. 2015). With regards to putative CSCs, we found that *SOX2* overexpression

enhanced *in vitro* tumor sphere formation both in ovarian and breast cancer cells, and induced the expression of stemness-related genes such as *OCT4*, *LIN28* and *NANOG* in ovarian cancer as well (Bareiss, Paczulla et al. 2013, Schaefer, Wang et al. 2015). In line with this, we found that these stemness-related genes were also enriched in reporter-positive MCF7 and OVCAR-3 versus negative cells (Figure 10). These results indicate that the reporter construct not only associates with SOX2 activation, but also links the fact that SOX2 activation associates with a stem cell state further characterized also by expression of other pluripotency genes.

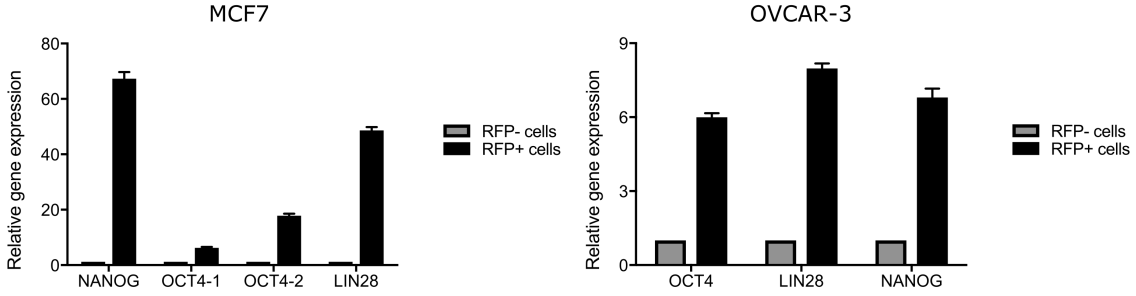

Figure 10. Enhanced gene expression of putative stem cell genes in reporter positive (RFP+) MCF7 and OVCAR-3 cells.

CSCs are also considered able to disseminate and induce metastatic disease. They are supposedly generated by EMT, a process in which epithelial cell homeostasis is disrupted and tumor cells acquire a migratory mesenchymal phenotype (Kalluri and Weinberg 2009). Interestingly, our data show that overexpression of *SOX2* in the breast cancer cell line MDA-MB-468 cells indeed increases cell mobility (Figure 11 A). Furthermore, reporter positive MCF7 and MDA-MB-468 cells enriched expression of EMT genes such as *N-CADHERIN*, *TWIST* and *SNAIL* when compared to reporter negative counterparts (Figure 11 B).

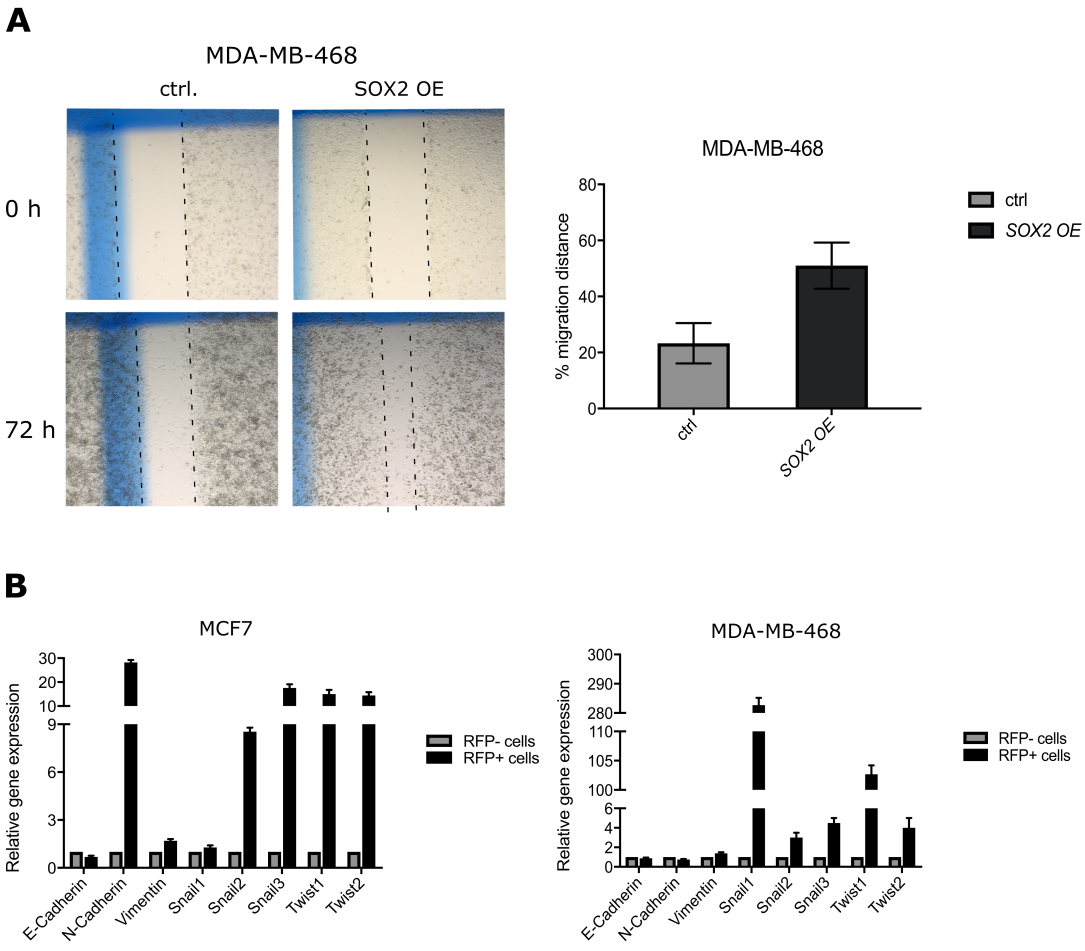

Figure 11. SOX2 regulates breast carcinoma cell migration. (A) *SOX2* overexpression enhanced cell migration in the breast cancer cell line MDA-MB-468. (B) Reporter positive breast cancer MCF7 and MDA-MB-468 cells expressed higher levels of EMT genes compared to reporter negative cells. qRT-PCR analysis was performed on RNA isolated from sorted reporter positive and negative cells.

CSCs are supposed to show enhanced resistance to chemotherapeutic agents. Indeed, treatment of MCF7 cells with cisplatin or paclitaxel reduced overall cell growth, but enhanced the frequency of reporter positive cells in the surviving cell fraction. Interestingly, unlike chemotherapies, treatment with the AKT inhibitor MK-2206 impaired overall cell growth to a similar extend as the reference drugs mentioned above without selecting reporter positive cells (Schaefer, Wang et al. 2015). This is consistent with the fact that stem cells heavily rely on anaerobic glycolysis, and their function is also regulated by bioenergetic signaling and the

AKT–mTOR pathway (Ito and Suda 2014). Therefore, the AKT inhibitor may reduce not only bulk cancer cells but could also be a potential agent inducing the elimination of CSCs.

Taken together, these reporter positive cells fulfilled several evaluation criteria of CSCs suggesting that the designed reporter construct can be a useful tool for the isolation of CSCs in different tumor types. Although in cancer pluripotency genes are perhaps not exclusively expressed by CSCs, and CSCs may possess different patterns of perturbation in pluripotency gene expression, detection especially of subpopulations showing joint expression of several pluripotency factors (as identified by our reporter construct) appears as a useful tool for CSC identification across different tumor subtypes. Of note, this technique is not biased by enzyme digestion, which may indeed introduce technical deviations affecting cell surface marker expression, and furthermore allows the evaluation of microenvironmental effects and cellular plasticity in a time sensitive manner. Collectively, the identification of transactivation of pluripotency genes promises to allow a reliable isolation of CSCs in solid tumors.

5.1.2. The tumor sphere assay as an *in vitro* surrogate assay for CSC detection

The gold standard of assessing human CSC identity are xenotransplantation assays in immune suppressed animal models (mostly mice). Since these experiments are time consuming and expensive, increased efforts have been made to develop surrogate *in vitro* assays. A commonly used method to assess CSC potential *in vitro* is the tumor spheres assay in which cells are plated under non-adherent culture conditions in serum-free medium supplemented with growth factors. In this study, we compared different methods for their ability to score sphere formation from breast and ovarian carcinoma cells (Wang, Paczulla et al. 2015). On the one hand, we assessed a multi cell-based assay format in which tumor cells were plated at different densities. We found that although this method does actually reflect the capability of tumor cells for tumor initiation to some extent, it is also strongly influenced by the density of plated cells. Cell clumping and sphere

fusion or disaggregation can occur modifying sphere numbers and leading to inaccurate results. To achieve more precise results, cell mobility was limited by including 1% methylcellulose or semi-solid material such as collagen or matrigel. Thereby we could reduce cell clumping and aggregation. Limits to this application are the facts that medium refreshment is hardly possible and not all cell types could form spheres in such medium. We thus developed a single cell-based assay in which cells are sorted according to specific characteristics and then seeded and cultured individually in 96 well plates. This method is more laborious but leads to overall more accurate results in the functional assessment of individual cells.

Interestingly, comparison with *in vivo* tumor induction experiments in mice indicated that not every sphere-forming cell of the same source indeed has *in vivo* tumorigenic properties upon transplantation in immunosuppressed NOD/SCID/IL-2Rγnull (NSG) mice (Bareiss, Paczulla et al. 2013). The frequency of sphere-initiating cells was higher than the frequency of tumor-initiating cells measured in mouse model, suggesting that either the tumor spheres assay may lead also to false positive results (e.g. due to co-recognition of more differentiated progenitor cells) or, alternatively, the *in vivo* assay may be inefficient and results in false negative results (perhaps due to technical reasons such as incomplete cross-reactivity between mouse and human proteins and microenvironment insufficiencies). Additionally to murine xenotransplantation studies, we have developed a xenotransplantation assay in zebrafish embryos and used it for side-by-side investigations of *in vivo* tumorigenicity (Konantz, Balci et al. 2012). This model has many obvious benefits. On one side, compared to sphere assays, it mimics the more complicated circumstances accompanying tumor initiation *in vivo*; on the other side, it is faster than the mouse model, allowing highly sensitive detection of tumor formation via *in vivo* microscopy already after five to seven days post-transplantation. The zebrafish xenograft model also revealed higher frequencies of tumor-initiating cells when compared to the murine model, which requires further investigation. Of note, the zebrafish model has its own limitations. Due to higher differences between species, conservation of microenvironmenal mecha-

nisms might be even lower between zebrafish and human. Thus, the model might selectively suppress the outgrowth of tumor types that heavily rely on cytokines or growth factors.

5.2. Oncogenic functions of SOX2

5.2.1. SOX2 plays important roles in CSCs

Enforced acquisition of stem cell factors such as SOX2 and OCT4 profoundly affects cellular fate and can reprogram differentiated somatic cells to pluripotency (Vazquez-Martin, Cufi et al. 2013). Induced cellular reprogramming was further linked to cancer and CSCs hypothesized to arise via related mechanisms (Bernhardt, Galach et al. 2012, Leis, Eguiara et al. 2012, Menendez, Camus et al. 2012).

In accordance with this hypothesis, *SOX2* expression was detected in different tumor types, particularly with a lower degree of differentiation (Ben-Porath, Thomson et al. 2008), in line with our results in breast cancer (Lengerke, Fehm et al. 2011). We have further shown that overexpression of *SOX2* in ovarian or breast carcinoma cells induced the expression of other stemness and/or pluripotency genes such as *OCT4*, *NANOG*, *LIN28* and *ALDH1* (Bareiss, Paczulla et al. 2013) and promoted *in vitro* sphere forming capacity, which is consistent with the notion that SOX2 mediates self-renewal and sustains CSC identity, as also suggested by results emerging from other groups in breast, gastric, prostate cancer, glioma, osteosarcoma, lung adenocarcinoma and non-small-cell lung cancer (NSCLC) (Gangemi, Griffero et al. 2009, Alonso, Diez-Valle et al. 2011, Basu-Roy, Seo et al. 2012, Leis, Eguiara et al. 2012, Singh, Trevino et al. 2012, Tian, Zhang et al. 2012, Rybak and Tang 2013, Xu, Xie et al. 2013).

5.2.2. Molecular mechanisms regulating *SOX2* expression

The mechanisms regulating *SOX2* expression vary among different tumors. In prostate and NSCLC, *SOX2* expression is influenced by EGFR/Src/Akt signaling, whereas in melanoma, *SOX2* is regulated by HH signaling as demonstrated by the binding of GLI1 and GLI2 to the proximal promoter of *SOX2* (Santini,

Pietrobono et al. 2014). Here we employed our SOX2 reporter construct to investigate possible upstream regulators of SOX2 in breast carcinoma. We found that treatment with chemotherapeutics enriched the frequency of SOX2 reporter positive cells, while AKT inhibitors not only impaired overall cell growth but were also able to eliminate this CSC subpopulation (Schaefer, Wang et al. 2015). This indicated that the AKT pathway might play important roles in mammary CSCs. Both AKT signaling and SOX2 expression have been discussed as a regulator of stem cell viability in breast carcinomas before (Shaw and Cantley 2006). More recently, AKT was reported to modulate SOX2 transcriptional activity via p27 and a regulatory circuit involving miR-30a in human nasopharyngeal cancers (Qin, Ji et al. 2015). However, we found no evidence for such molecular interaction in breast carcinoma cells. In contrast, in breast carcinoma cell lines and primary patient samples, pAKT directly phosphorylates the SOX2 protein thereby stabilizing and preserving it from proteasomal degradation. Interestingly, this dependence of SOX2 protein on pAKT was not equally observed in other tumor types (e.g. ovarian or squamous head and neck cell carcinoma lines). Jointly, these data indicate that SOX2 regulation occurs in a highly tissue-specific manner.

5.2.3. SOX2 regulates multiple cellular processes in tumor cells

SOX2 has been shown to promote proliferation (breast, prostate, pancreatic and cervical cancers) (Ji and Zheng 2010, Jia, Li et al. 2011, Stolzenburg, Rots et al. 2012, Herreros-Villanueva, Zhang et al. 2013), to inhibit apoptosis (prostate, ovarian, gastric cancer and NSCLC) (Jia, Li et al. 2011, Bareiss, Paczulla et al. 2013, Chen, Li et al. 2014, Hutz, Mejias-Luque et al. 2014) and to promote invasion, migration and metastasis (melanoma, colorectal, glioma, gastric, ovarian cancer and hepatocellular carcinoma) (Alonso, Diez-Valle et al. 2011, Girouard, Laga et al. 2012, Han, Fang et al. 2012, Lou, Han et al. 2013, Sun, Sun et al. 2013). Cellular proliferation is tightly regulated by SOX2 in many cancer types. In lung and esophageal carcinoma, down-regulation of *SOX2* expression by RNA interference showed that the growth of tumor cells was suppressed (Fukazawa, Guo et al. 2016). In pancreatic cancer cells, knockdown of *SOX2* induced $p21^{Cip1}$

and $p27^{Kip1}$ to induce a cell cycle arrest, whereas overexpression of *SOX2* promoted cyclinD3 (CCND3) transcription and allowed further S-phase entry (Herreros-Villanueva, Zhang et al. 2013).

Thus, we next explored the functional roles of SOX2 in human cancer using the above-described models. In contrast to the above-mentioned effects, we could not observe any correlation between *SOX2* expression level and the degree of cellular proliferation or cell cycle regulation in ovarian carcinoma cells. We also did not find a correlation between *SOX2* expression intensity and Ki67 positivity in patient samples (Bareiss, Paczulla et al. 2013). SOX2 also plays an important role in cell invasion, migration and metastasis and also we observed a correlation between high *SOX2* expression and enhanced metastasis in breast carcinomas (Lengerke, Fehm et al. 2011). However, this finding was not reproduceable in lung carcinoma where SOX2-expressing tumors proved less invasive, smaller, and more differentiated when compared to SOX2-negative tumors (Wilbertz, Wagner et al. 2011). Matching these different functional roles, immunohistochemical analyses have detected different patterns of SOX2 expression in various types of tumors, such as squamous cell carcinoma of the lung, skin, esophagus, lung adenocarcinoma, HPV-negative head and neck tumors, breast and ovarian carcinomas (Lengerke, Fehm et al. 2011, Maier, Wilbertz et al. 2011, Wilbertz, Wagner et al. 2011, Bareiss, Paczulla et al. 2013, Pham, Scheble et al. 2013, Schrock, Bode et al. 2014). In our results, breast and ovarian carcinomas mostly displayed a heterogeneous SOX2 protein expression (with <10% SOX2-expressing tumor cells) while lung tumors and other squamous cell carcinomas appeared more homogeneously stained (Wilbertz, Wagner et al. 2011, Schrock, Bode et al. 2014). Moreover, we also showed that, chromosomal amplifications of the *SOX2* gene locus were detected as the cause for the increased *SOX2* expression only in squamous cell carcinomas, but not in breast and ovarian carcinomas. This strongly suggests that the molecular regulation of SOX2 might highly depend on the tissue of origin, and that SOX2 expression may be a decisive indicator of CSC populations sonly in certain indications (including breast and ovarian but not lung carcinoma).

Furthermore, SOX2 is also important indicator of disease prognosis, relapse and therapy resistance. In breast carcinoma, high *SOX2* expression was associated with larger tumor size and positive lymph node status; corresponding metastatic lymph nodes showed higher *SOX2* expression and were significantly more often SOX2 positive than primary tumors (Lengerke, Fehm et al. 2011). *SOX2* expression was also predominantly a feature of high-grade tumors in ovarian cancer (Pham, Scheble et al. 2013). Additionally, in esophageal squamous cancer, high expression of *SOX2* and *OCT4* was associated with higher histological grade or TNM stage, and high SOX2 levels significant correlated with lower patient survival (Wang, He et al. 2009). Expression of various pluripotency markers like SOX2, OCT4 and NANOG typically led to a decrease in differentiation status and induced drug resistance. In breast carcinoma, knockdown of *SOX2* furthermore restored tamoxifen sensitivity (Piva, Domenici et al. 2014). We also showed that SOX2-expressing cells display enhanced apoptosis resistance in response to conventional chemotherapies and TRAIL in ovarian cancer cells (Bareiss, Paczulla et al. 2013). In HNSCC, we further demonstrated that induction of *SOX2* expression elevates the expression of the anti-apoptotic protein BCL-2 thereby enhancing chemotherapy resistance (Schrock, Bode et al. 2014). Therefore analysis of SOX2 functions in cancer may provide new therapeutic opportunities. Since SOX2 itself does not allow for direct therapeutic intervention, targeting up or downstream signals (e.g. pAKT) might be employed as therapeutic strategy. For example, in NSCLC, SOX2 relies on EGFR signaling and using anti-EGFR drugs, such as gefitinib and erlotinib could inhibit SOX2 positive CSCs self-renewal effects (Singh, Trevino et al. 2012).

Taken together, investigating the oncogenic effects and molecular regulation of SOX2 in cancer might yield important insights and improve prognostication and therapeutic interventions in cancer patients.

5.3. EVI1: oncogenic roles and downstream targets in cancer

EVI1 is particularly known for its expression in early hematopoietic stem cells and myeloid neoplasms. It has been especially studied in acute myeloid leukemia

where it associates with particularly aggressive disease. *EVI1* expression has been also reported in several solid cancers. The relevance of *EVI1* expression in these tumors, and especially in CSCs, is under-investigated.

5.3.1. Dysregulation of *EVI1* expression in breast and prostate carcinoma

Translocation and inversion events affecting chromosome 3 are the most common causes for the aberrant activation of *EVI1* expression in myeloid leukemia (Wieser 2007). In ovarian carcinoma instead, elevated *EVI1* expression is associated with enhanced copy number gains (Nanjundan, Nakayama et al. 2007). Unlike the above-mentioned mechanisms, in our patient cohort of breast and prostate carcinoma, we could neither detect translocation nor amplification of the *EVI1* gene. Other mechanisms of EVI1 activation have also been reported in ~ 30% of acute myeloid leukemia with high EVI1 expression (e.g. regulation via miRNAs) (Patel, Appaiah et al. 2011). In line with potentially conserved mechanisms in other cancers, a common *EVI1* polymorphism (rs6774494 A>G) targeted by miR-206/133b was suggested to predict adverse outcome in postmenopausal breast carcinoma patients (Wang, Huang et al. 2014). After all though, the exact molecular mechanisms underlying EVI1 activation in cancer require further investigation.

5.3.2. Role as a stem cell factor

While EVI1 has been demonstrated to regulate healthy hematopoietic and leukemic stem cells, its association or roles in solid tumor CSCs remains unclear. Several reports indicate that the development of castration-resistant prostate cancer (CRPC) follows CSC models (Chen, Rycaj et al. 2013, Li, Yang et al. 2014). These tumors contain prostate CSCs, which originate from androgen receptor-negative cells of the basal layer of the healthy prostatic gland and androgen deprivation therapy promotes the development of a CSC phenotype by upregulation of stem cell markers such as SOX2 and CD44 (Tu and Lin 2012, Yu, Pestell et al. 2012, Kerr and Hussain 2014). Our study indicates possible roles of EVI1 as a CSC protein, which might be involved in the development of CRPC.

Firstly, we demonstrate that EVI1 is selectively expressed in cells of the androgen negative stem-cell-associated basal layer of healthy prostatic glands, where SOX2 and CD44 expression are detected as well (Kregel, Kiriluk et al. 2013). Secondly, in primary prostate cancer patients, EVI1 is heterogeneously expressed only in a small subset of primary prostate cancer cells and knockdown of *EVI1* resulted in co-suppression of other stem cell factors such as *SOX2* and *PROM1*. Thirdly, long-term treatment of PC3 cells with docetaxel — a chemotherapeutic drug used to treat CRPC patients — induced up-regulation of *EVI1* expression and drug resistance, which in turn could be reverted upon *EVI1* knockdown. Additionally, using both the sphere and a zebrafish xenotransplantation assay, we could show that the self-renewal capacity was diminished after *EVI1* knockdown. Moreover, the soft agar assay also showed reduced *in vitro* colony formation. These results support the hypothesis that EVI1 regulates CSC properties in prostate cancer cells. In contrast, in breast carcinoma, EVI1 rather homogenously marked tumor cells. This is rather controversial to the CSC model in which CSCs usually represent a small subpopulation of the tumor bulk. However, EVI1 knockdown affected the frequency of *in viv*o tumor- as well as *in vitro* mammosphere-initiating breast carcinoma cells. Furthermore, down-regulation of the stem cell factor SOX2 was observed following *EVI1* knockdown in breast carcinoma cells. Hence, these results suggest that *EVI1* expression co-regulates breast CSCs, but however its function is not just limited to CSCs in this tumor.

Taken together, we can conclude that EVI1 is involved in the regulation of CSCs, but due to its multiple roles in different processes, it needs to be studied individually in each tumor type and does not represent a marker identifying the CSC compartment in every tumor.

5.3.3. Role in the regulation of metastasis

It is assumed that CSCs may play a central role for metastasis in solid tumors. The influence of EVI1 on cell migration and metastasis has not been comprehensively investigated to date. However, it is known that down-regulation of *EVI1* suppresses migration in pancreatic cancer cell lines (Tanaka, Suzuki et al. 2014),

and *vice versa* overexpression of *EVI1* in ovarian cancer cell conferred migratory potential (Nanjundan, Nakayama et al. 2007). In line with this, in our prostate carcinoma patient cohort, higher *EVI1* expression was associated with metastases, and the role of EVI1 in prostate carcinoma cell migration was also revealed in *in vitro* scratch assays. By analyzing genes involved in cell motility and metastasis, we identified several candidate genes that potentially mediate these effects, including components of the RHO-ROCK adhesion pathway, CD82, IL1b and matrix metalloproteinases.

In breast carcinoma, a study in a mouse model indicated that high EVI1 expression associated with metastatic disease (Patel, Appaiah et al. 2011). Consistently, we showed that modulation of *EVI1* expression in human breast carcinoma cells influenced cell mobility and expression of several factors implicated in cell communication and cell migration. In addition to established factors, such as CXCR4, CCR1, AKAP12, TIE1, RhoJ (Chan, Yuan et al. 2008, Wilson, Leszczynska et al. 2014, Finger, Castellini et al. 2015, Xu, Zhao et al. 2015, Li, Wu et al. 2016), we identified KISS1 as a novel transcriptional target of EVI1 mediating cell motility. These results suggest that EVI1 serves as a master regulator of both prostate and breast carcinoma cell motility.

5.3.4. Targeting EVI1-driven oncogenic effects

EVI1 plays key roles in the modulation of multiple cellular processes. Especially its regulatory function in CSC biology makes it valuable as a potential target in tumor therapy. In our prostate carcinoma study, long-term treatment with docetaxel induced drug resistance, which is considered to be associated with enrichment of CSCs. Importantly, arsenic trioxide was reported to degrade oncogenic EVI1 protein in leukemic cells inducing differentiation and sensitizing cells to chemotherapy-induced apoptosis (Kustikova, Schwarzer et al. 2013). If these mechanisms are conserved in prostate carcinoma cells, treatment with arsenic trioxide might be an effective option for targeting EVI1-positive prostate carcinoma cancer (stem) cells, which will be the subject of further studies.

Our data also showed that EVI1 strongly modulates prostate and breast carcinoma cell growth. In both tumor entities, *EVI1* knockdown led to a profound delay in cell cycle progression accompanied by deregulated expression of several cell cycle proteins. Mechanistically, these changes might be at least in part mediated by de-repression of SMAD3, a known transcriptional target of EVI1 (Kurokawa, Mitani et al. 1998), followed by consecutive induction of cell cycle inhibitor $p21^{CIP1}$ expression. The suppressed pERK levels observed in *EVI1* knockdown versus control cells might further contribute to the observed growth impairment.

In breast carcinoma, estrogen and HER2 signaling as well as EVI1-mediated transcriptional modulation seemingly merge to stimulate MAPK signaling. This functional convergence identifies EVI1 as a major driver of cell growth acting independently of estrogen signaling. Thus, EVI1 and downstream MAPK activation might represent therapeutic targets in patients resistant to anti-estrogen therapies. Moreover, targeting the newly identified EVI1-GPR54-KISS1 axis, for example by GPR54 inhibitors, may be considered for the treatment of metastasizing ER^- breast carcinoma. Effective targeting of EVI1-induced breast carcinoma cell migration might however require either inhibition of EVI1 itself or joint suppression of additional migratory pathways (e.g., RHO/ROCK signaling).

Additionally, our study confirmed that both in breast and prostate carcinoma, EVI1 was able to confer tumor cell resistance against apoptosis, through inducing a concerted suppression of pro- and induction of anti-apoptotic genes This indicates that direct depression of EVI1 expression might be an effective way to kill tumor cells. Similar results were previously obtained by our group in EVI1 expressing acute lymphoblastic leukemia (Konantz, Andre et al. 2013).

.Taken together, our data identify EVI1 as a potent oncoprotein regulating tumor cell proliferation, apoptosis resistance, and migration in several cancer types. Since EVI1 expression co-regulates CSCs, EVI1 is thus an attractive novel target for anti-tumor therapies.

Chapter 6.

Outlook

In summary, our studies confirm that the stemness related transcription factors SOX2 and EVI1 play important roles in tumor progression, metastasis, apoptosis resistance and probably maintaining the population of CSCs in tumors as well. They confer tumor resistance to various therapeutic agents, and are responsible for the release of resistant tumors. Our newly developed method also strongly supports that we are able to identify CSCs based on different transcriptional activity of SOX2. It provides not only a powerful tool to identify CSCs in real time in complicated tumor microenvironments, but also makes it easier to screen CSC-targeting drugs.

However, due to diversity and plasticity of CSCs, focusing on SOX2 and EVI1 is for sure does not allow to characterize all types of CSCs. More efforts should be invested to identify new candidates involved in maintaining CSCs. Moreover, there is still a strong need to elucidate how stemness transcription factors are regulated under different microenvironments, how they determine tumor cell fates and how they are responsible for the outcome of various therapeutic agents.

Chapter 7.

References

Abbaszadegan, M. R., V. Bagheri, M. S. Razavi, A. A. Momtazi, A. Sahebkar and M. Gholamin (2017). "Isolation, identification, and characterization of cancer stem cells: A review." J Cell Physiol **232**(8): 2008-2018.

Abel, E. V., E. J. Kim, J. Wu, M. Hynes, F. Bednar, E. Proctor, L. Wang, M. L. Dziubinski and D. M. Simeone (2014). "The Notch pathway is important in maintaining the cancer stem cell population in pancreatic cancer." PLoS One **9**(3): e91983.

Al-Hajj, M., M. S. Wicha, A. Benito-Hernandez, S. J. Morrison and M. F. Clarke (2003). "Prospective identification of tumorigenic breast cancer cells." Proc Natl Acad Sci U S A **100**(7): 3983-3988.

Alonso, M. M., R. Diez-Valle, L. Manterola, A. Rubio, D. Liu, N. Cortes-Santiago, L. Urquiza, P. Jauregi, A. Lopez de Munain, N. Sampron, A. Aramburu, S. Tejada-Solis, C. Vicente, M. D. Odero, E. Bandres, J. Garcia-Foncillas, M. A. Idoate, F. F. Lang, J. Fueyo and C. Gomez-Manzano (2011). "Genetic and epigenetic modifications of Sox2 contribute to the invasive phenotype of malignant gliomas." PLoS One **6**(11): e26740.

Alvero, A. B., R. Chen, H. H. Fu, M. Montagna, P. E. Schwartz, T. Rutherford, D. A. Silasi, K. D. Steffensen, M. Waldstrom, I. Visintin and G. Mor (2009). "Molecular phenotyping of human ovarian cancer stem cells unravels the mechanisms for repair and chemoresistance." Cell Cycle **8**(1): 158-166.

Alzuherri, H., R. McGilvray, A. Kilbey and C. Bartholomew (2006). "Conservation and expression of a novel alternatively spliced Evi1 exon." Gene **384**: 154-162.

Ansieau, S., J. Bastid, A. Doreau, A. P. Morel, B. P. Bouchet, C. Thomas, F. Fauvet, I. Puisieux, C. Doglioni, S. Piccinin, R. Maestro, T. Voeltzel, A. Selmi, S. Valsesia-Wittmann, C. Caron de Fromentel and A. Puisieux (2008). "Induction of EMT by twist proteins as a collateral effect of tumor-promoting inactivation of premature senescence." Cancer Cell **14**(1): 79-89.

Aytekin, M., U. Vinatzer, M. Musteanu, S. Raynaud and R. Wieser (2005). "Regulation of the expression of the oncogene EVI1 through the use of alternative mRNA 5'-ends." Gene **356**: 160-168.

Baltus, G. A., M. P. Kowalski, H. Zhai, A. V. Tutter, D. Quinn, D. Wall and S. Kadam (2009). "Acetylation of sox2 induces its nuclear export in embryonic stem cells." Stem Cells **27**(9): 2175-2184.

Banaszynski, L. A., L. C. Chen, L. A. Maynard-Smith, A. G. Ooi and T. J. Wandless (2006). "A rapid, reversible, and tunable method to regulate protein function in living cells using synthetic small molecules." Cell **126**(5): 995-1004.

Bao, B., A. Ahmad, A. S. Azmi, S. Ali and F. H. Sarkar (2013). "Overview of cancer stem cells (CSCs) and mechanisms of their regulation: implications for cancer therapy." Curr Protoc Pharmacol **Chapter 14**: Unit 14 25.

Bao, S., Q. Wu, R. E. McLendon, Y. Hao, Q. Shi, A. B. Hjelmeland, M. W. Dewhirst, D. D. Bigner and J. N. Rich (2006). "Glioma stem cells promote radioresistance by preferential activation of the DNA damage response." Nature **444**(7120): 756-760.

Bao, S., Q. Wu, S. Sathornsumetee, Y. Hao, Z. Li, A. B. Hjelmeland, Q. Shi, R. E. McLendon, D. D. Bigner and J. N. Rich (2006). "Stem cell-like glioma cells promote tumor angiogenesis through vascular endothelial growth factor." Cancer Res **66**(16): 7843-7848.

Bar, E. E., A. Chaudhry, A. Lin, X. Fan, K. Schreck, W. Matsui, S. Piccirillo, A. L. Vescovi, F. DiMeco, A. Olivi and C. G. Eberhart (2007). "Cyclopamine-mediated hedgehog pathway inhibition depletes stem-like cancer cells in glioblastoma." Stem Cells **25**(10): 2524-2533.

Bareiss, P. M., A. Paczulla, H. Wang, R. Schairer, S. Wiehr, U. Kohlhofer, O. C. Rothfuss, A. Fischer, S. Perner, A. Staebler, D. Wallwiener, F. Fend, T. Fehm, B. Pichler, L. Kanz, L. Quintanilla-Martinez, K. Schulze-Osthoff, F. Essmann and C. Lengerke (2013). "SOX2 expression associates with stem cell state in human ovarian carcinoma." Cancer Res **73**(17): 5544-5555.

Barnawi, R., S. Al-Khaldi, G. Majed Sleiman, A. Sarkar, A. Al-Dhfyan, F. Al-Mohanna, H. Ghebeh and M. Al-Alwan (2016). "Fascin Is Critical for the Maintenance of Breast Cancer Stem Cell Pool Predominantly via the Activation of the Notch Self-Renewal Pathway." Stem Cells **34**(12): 2799-2813.

Bartholomew, C. and A. M. Clark (1994). "Induction of two alternatively spliced evi-1 proto-oncogene transcripts by cAMP in kidney cells." Oncogene **9**(3): 939-942.

Bartholomew, C., A. Kilbey, A. M. Clark and M. Walker (1997). "The Evi-1 proto-oncogene encodes a transcriptional repressor activity associated with transformation." Oncogene **14**(5): 569-577.

Bass, A. J., H. Watanabe, C. H. Mermel, S. Yu, S. Perner, R. G. Verhaak, S. Y. Kim, L. Wardwell, P. Tamayo, I. Gat-Viks, A. H. Ramos, M. S. Woo, B. A. Weir, G. Getz, R. Beroukhim, M. O'Kelly, A. Dutt, O. Rozenblatt-Rosen, P. Dziunycz, J. Komisarof, L. R. Chirieac, C. J. Lafargue, V. Scheble, T. Wilbertz, C. Ma, S. Rao, H. Nakagawa, D. B. Stairs, L. Lin, T. J. Giordano, P. Wagner, J. D. Minna, A. F. Gazdar, C. Q. Zhu, M. S. Brose, I. Cecconello, U. Ribeiro, Jr., S. K. Marie, O. Dahl, R. A. Shivdasani, M. S. Tsao, M. A. Rubin, K. K. Wong, A. Regev, W. C. Hahn, D. G. Beer, A. K. Rustgi and M. Meyerson (2009). "SOX2 is an amplified lineage-survival oncogene in lung and esophageal squamous cell carcinomas." Nat Genet **41**(11): 1238-1242.

Basu, S., G. Haase and A. Ben-Ze'ev (2016). "Wnt signaling in cancer stem cells and colon cancer metastasis." F1000Res **5**.

Basu-Roy, U., E. Seo, L. Ramanathapuram, T. B. Rapp, J. A. Perry, S. H. Orkin, A. Mansukhani and C. Basilico (2012). "Sox2 maintains self renewal of tumor-initiating cells in osteosarcomas." Oncogene **31**(18): 2270-2282.

Batsaikhan, B. E., K. Yoshikawa, N. Kurita, T. Iwata, C. Takasu, H. Kashihara and M. Shimada (2014). "Cyclopamine decreased the expression of Sonic Hedgehog and its downstream genes in colon cancer stem cells." Anticancer Res **34**(11): 6339-6344.

Bayo, P., A. Jou, A. Stenzinger, C. Shao, M. Gross, A. Jensen, N. Grabe, C. H. Mende, P. V. Rados, J. Debus, W. Weichert, P. K. Plinkert, P. Lichter, K. Freier and J. Hess (2015). "Loss of SOX2 expression induces cell motility via vimentin up-regulation and is an unfavorable risk factor for survival of head and neck squamous cell carcinoma." Mol Oncol **9**(8): 1704-1719.

Beck, B., G. Driessens, S. Goossens, K. K. Youssef, A. Kuchnio, A. Caauwe, P. A. Sotiropoulou, S. Loges, G. Lapouge, A. Candi, G. Mascre, B. Drogat, S. Dekoninck, J. J. Haigh, P. Carmeliet and C. Blanpain (2011). "A vascular niche and a VEGF-Nrp1 loop regulate the initiation and stemness of skin tumours." Nature **478**(7369): 399-403.

Beier, D., P. Hau, M. Proescholdt, A. Lohmeier, J. Wischhusen, P. J. Oefner, L. Aigner, A. Brawanski, U. Bogdahn and C. P. Beier (2007). "CD133(+) and CD133(-) glioblastoma-derived

cancer stem cells show differential growth characteristics and molecular profiles." Cancer Res **67**(9): 4010-4015.

Ben-Porath, I., M. W. Thomson, V. J. Carey, R. Ge, G. W. Bell, A. Regev and R. A. Weinberg (2008). "An embryonic stem cell-like gene expression signature in poorly differentiated aggressive human tumors." Nat Genet **40**(5): 499-507.

Bernhardt, M., M. Galach, D. Novak and J. Utikal (2012). "Mediators of induced pluripotency and their role in cancer cells - current scientific knowledge and future perspectives." Biotechnol J **7**(6): 810-821.

Bonnet, D. and J. E. Dick (1997). "Human acute myeloid leukemia is organized as a hierarchy that originates from a primitive hematopoietic cell." Nat Med **3**(7): 730-737.

Bordereaux, D., S. Fichelson, P. Tambourin and S. Gisselbrecht (1990). "Alternative splicing of the Evi-1 zinc finger gene generates mRNAs which differ by the number of zinc finger motifs." Oncogene **5**(6): 925-927.

Botchkina, G. (2013). "Colon cancer stem cells--from basic to clinical application." Cancer Lett **338**(1): 127-140.

Boyer, L. A., T. I. Lee, M. F. Cole, S. E. Johnstone, S. S. Levine, J. P. Zucker, M. G. Guenther, R. M. Kumar, H. L. Murray, R. G. Jenner, D. K. Gifford, D. A. Melton, R. Jaenisch and R. A. Young (2005). "Core transcriptional regulatory circuitry in human embryonic stem cells." Cell **122**(6): 947-956.

Brooks, D. J., S. Woodward, F. H. Thompson, B. Dos Santos, M. Russell, J. M. Yang, X. Y. Guan, J. Trent, D. S. Alberts and R. Taetle (1996). "Expression of the zinc finger gene EVI-1 in ovarian and other cancers." Br J Cancer **74**(10): 1518-1525.

Brungs, D., M. Aghmesheh, K. L. Vine, T. M. Becker, M. G. Carolan and M. Ranson (2016). "Gastric cancer stem cells: evidence, potential markers, and clinical implications." J Gastroenterol **51**(4): 313-326.

Buonamici, S., S. Chakraborty, V. Senyuk and G. Nucifora (2003). "The role of EVI1 in normal and leukemic cells." Blood Cells Mol Dis **31**(2): 206-212.

Buonamici, S., D. Li, Y. Chi, R. Zhao, X. Wang, L. Brace, H. Ni, Y. Saunthararajah and G. Nucifora (2004). "EVI1 induces myelodysplastic syndrome in mice." J Clin Invest **114**(5): 713-719.

Buonamici, S., D. Li, F. M. Mikhail, A. Sassano, L. C. Platanias, O. Colamonici, J. Anastasi and G. Nucifora (2005). "EVI1 abrogates interferon-alpha response by selectively blocking PML induction." J Biol Chem **280**(1): 428-436.

Chakraborty, S., V. Senyuk, S. Sitailo, Y. Chi and G. Nucifora (2001). "Interaction of EVI1 with cAMP-responsive element-binding protein-binding protein (CBP) and p300/CBP-associated factor (P/CAF) results in reversible acetylation of EVI1 and in co-localization in nuclear speckles." J Biol Chem **276**(48): 44936-44943.

Chan, B., H. T. Yuan, S. Ananth Karumanchi and V. P. Sukhatme (2008). "Receptor tyrosine kinase Tie-1 overexpression in endothelial cells upregulates adhesion molecules." Biochem Biophys Res Commun **371**(3): 475-479.

Chen, S., X. Li, D. Lu, Y. Xu, W. Mou, L. Wang, Y. Chen, Y. Liu, X. Li, L. Y. Li, L. Liu, D. Stupack, R. A. Reisfeld, R. Xiang and N. Li (2014). "SOX2 regulates apoptosis through MAP4K4-survivin signaling pathway in human lung cancer cells." Carcinogenesis **35**(3): 613-623.

Chen, X., K. Rycaj, X. Liu and D. G. Tang (2013). "New insights into prostate cancer stem cells." Cell Cycle **12**(4): 579-586.

Chen, X., H. Xu, P. Yuan, F. Fang, M. Huss, V. B. Vega, E. Wong, Y. L. Orlov, W. Zhang, J. Jiang, Y. H. Loh, H. C. Yeo, Z. X. Yeo, V. Narang, K. R. Govindarajan, B. Leong, A. Shahab, Y. Ruan, G. Bourque, W. K. Sung, N. D. Clarke, C. L. Wei and H. H. Ng (2008). "Integration of external signaling pathways with the core transcriptional network in embryonic stem cells." Cell **133**(6): 1106-1117.

Chen, Y., D. Li, H. Liu, H. Xu, H. Zheng, F. Qian, W. Li, C. Zhao, Z. Wang and X. Wang (2011). "Notch-1 signaling facilitates survivin expression in human non-small cell lung cancer cells." Cancer Biol Ther **11**(1): 14-21.

Chi, Y., V. Senyuk, S. Chakraborty and G. Nucifora (2003). "EVI1 promotes cell proliferation by interacting with BRG1 and blocking the repression of BRG1 on E2F1 activity." J Biol Chem **278**(50): 49806-49811.

Cho, R. W., X. Wang, M. Diehn, K. Shedden, G. Y. Chen, G. Sherlock, A. Gurney, J. Lewicki and M. F. Clarke (2008). "Isolation and molecular characterization of cancer stem cells in MMTV-Wnt-1 murine breast tumors." Stem Cells **26**(2): 364-371.

Choy, L., T. J. Hagenbeek, M. Solon, D. French, D. Finkle, A. Shelton, R. Venook, M. J. Brauer and C. W. Siebel (2017). "Constitutive NOTCH3 Signaling Promotes the Growth of Basal Breast Cancers." Cancer Res **77**(6): 1439-1452.

Cimadamore, F., A. Amador-Arjona, C. Chen, C. T. Huang and A. V. Terskikh (2013). "SOX2-LIN28/let-7 pathway regulates proliferation and neurogenesis in neural precursors." Proc Natl Acad Sci U S A **110**(32): E3017-3026.

Clement, V., P. Sanchez, N. de Tribolet, I. Radovanovic and A. Ruiz i Altaba (2007). "HEDGEHOG-GLI1 signaling regulates human glioma growth, cancer stem cell self-renewal, and tumorigenicity." Curr Biol **17**(2): 165-172.

Clevers, H. (2006). "Wnt/beta-catenin signaling in development and disease." Cell **127**(3): 469-480.

Collins, A. T., P. A. Berry, C. Hyde, M. J. Stower and N. J. Maitland (2005). "Prospective identification of tumorigenic prostate cancer stem cells." Cancer Res **65**(23): 10946-10951.

Curley, M. D., V. A. Therrien, C. L. Cummings, P. A. Sergent, C. R. Koulouris, A. M. Friel, D. J. Roberts, M. V. Seiden, D. T. Scadden, B. R. Rueda and R. Foster (2009). "CD133 expression defines a tumor initiating cell population in primary human ovarian cancer." Stem Cells **27**(12): 2875-2883.

Dalerba, P., S. J. Dylla, I. K. Park, R. Liu, X. Wang, R. W. Cho, T. Hoey, A. Gurney, E. H. Huang, D. M. Simeone, A. A. Shelton, G. Parmiani, C. Castelli and M. F. Clarke (2007). "Phenotypic characterization of human colorectal cancer stem cells." Proc Natl Acad Sci U S A **104**(24): 10158-10163.

Dick, J. E. (2008). "Stem cell concepts renew cancer research." Blood **112**(13): 4793-4807.

Dierks, C., R. Beigi, G. R. Guo, K. Zirlik, M. R. Stegert, P. Manley, C. Trussell, A. Schmitt-Graeff, K. Landwerlin, H. Veelken and M. Warmuth (2008). "Expansion of Bcr-Abl-positive leukemic stem cells is dependent on Hedgehog pathway activation." Cancer Cell **14**(3): 238-249.

Dontu, G., M. Al-Hajj, W. M. Abdallah, M. F. Clarke and M. S. Wicha (2003). "Stem cells in normal breast development and breast cancer." Cell Prolif **36 Suppl 1**: 59-72.

Engelen, E., U. Akinci, J. C. Bryne, J. Hou, C. Gontan, M. Moen, D. Szumska, C. Kockx, W. van Ijcken, D. H. Dekkers, J. Demmers, E. J. Rijkers, S. Bhattacharya, S. Philipsen, L. H. Pevny, F. G. Grosveld, R. J. Rottier, B. Lenhard and R. A. Poot (2011). "Sox2 cooperates with Chd7 to regulate genes that are mutated in human syndromes." Nat Genet **43**(6): 607-611.

Eramo, A., F. Lotti, G. Sette, E. Pilozzi, M. Biffoni, A. Di Virgilio, C. Conticello, L. Ruco, C. Peschle and R. De Maria (2008). "Identification and expansion of the tumorigenic lung cancer stem cell population." Cell Death Differ **15**(3): 504-514.

Fears, S., C. Mathieu, N. Zeleznik-Le, S. Huang, J. D. Rowley and G. Nucifora (1996). "Intergenic splicing of MDS1 and EVI1 occurs in normal tissues as well as in myeloid leukemia and produces a new member of the PR domain family." Proc Natl Acad Sci U S A **93**(4): 1642-1647.

Finger, E. C., L. Castellini, E. B. Rankin, M. Vilalta, A. J. Krieg, D. Jiang, A. Banh, W. Zundel, M. B. Powell and A. J. Giaccia (2015). "Hypoxic induction of AKAP12 variant 2 shifts PKA-mediated protein phosphorylation to enhance migration and metastasis of melanoma cells." Proc Natl Acad Sci U S A **112**(14): 4441-4446.

Foshay, K. M. and G. I. Gallicano (2008). "Regulation of Sox2 by STAT3 initiates commitment to the neural precursor cell fate." Stem Cells Dev **17**(2): 269-278.

Fukazawa, T., M. Guo, N. Ishida, T. Yamatsuji, M. Takaoka, E. Yokota, M. Haisa, N. Miyake, T. Ikeda, T. Okui, N. Takigawa, Y. Maeda and Y. Naomoto (2016). "SOX2 suppresses CDKN1A to sustain growth of lung squamous cell carcinoma." Sci Rep **6**: 20113.

Gangemi, R. M., F. Griffero, D. Marubbi, M. Perera, M. C. Capra, P. Malatesta, G. L. Ravetti, G. L. Zona, A. Daga and G. Corte (2009). "SOX2 silencing in glioblastoma tumor-initiating cells causes stop of proliferation and loss of tumorigenicity." Stem Cells **27**(1): 40-48.

Ginestier, C., M. H. Hur, E. Charafe-Jauffret, F. Monville, J. Dutcher, M. Brown, J. Jacquemier, P. Viens, C. G. Kleer, S. Liu, A. Schott, D. Hayes, D. Birnbaum, M. S. Wicha and G. Dontu (2007). "ALDH1 is a marker of normal and malignant human mammary stem cells and a predictor of poor clinical outcome." Cell Stem Cell **1**(5): 555-567.

Girouard, S. D., A. C. Laga, M. C. Mihm, R. A. Scolyer, J. F. Thompson, Q. Zhan, H. R. Widlund, C. W. Lee and G. F. Murphy (2012). "SOX2 contributes to melanoma cell invasion." Lab Invest **92**(3): 362-370.

Goyama, S. and M. Kurokawa (2010). "Evi-1 as a critical regulator of leukemic cells." Int J Hematol **91**(5): 753-757.

Goyama, S., G. Yamamoto, M. Shimabe, T. Sato, M. Ichikawa, S. Ogawa, S. Chiba and M. Kurokawa (2008). "Evi-1 is a critical regulator for hematopoietic stem cells and transformed leukemic cells." Cell Stem Cell **3**(2): 207-220.

Hadjimichael, C., K. Chanoumidou, N. Papadopoulou, P. Arampatzi, J. Papamatheakis and A. Kretsovali (2015). "Common stemness regulators of embryonic and cancer stem cells." World J Stem Cells **7**(9): 1150-1184.

Haltrich, I., M. Kost-Alimova, G. Kovacs, G. Klein, G. Fekete and S. Imreh (2006). "Multipoint interphase FISH analysis of chromosome 3 abnormalities in 28 childhood AML patients." Eur J Haematol **76**(2): 124-133.

Hamburger, A. W. and S. E. Salmon (1977). "Primary bioassay of human tumor stem cells." Science **197**(4302): 461-463.

Han, X., X. Fang, X. Lou, D. Hua, W. Ding, G. Foltz, L. Hood, Y. Yuan and B. Lin (2012). "Silencing SOX2 induced mesenchymal-epithelial transition and its expression predicts liver and lymph node metastasis of CRC patients." PLoS One **7**(8): e41335.

Hermann, P. C., S. L. Huber, T. Herrler, A. Aicher, J. W. Ellwart, M. Guba, C. J. Bruns and C. Heeschen (2007). "Distinct populations of cancer stem cells determine tumor growth and metastatic activity in human pancreatic cancer." Cell Stem Cell **1**(3): 313-323.

Herreros-Villanueva, M., J. S. Zhang, A. Koenig, E. V. Abel, T. C. Smyrk, W. R. Bamlet, A. A. de Narvajas, T. S. Gomez, D. M. Simeone, L. Bujanda and D. D. Billadeau (2013). "SOX2 promotes dedifferentiation and imparts stem cell-like features to pancreatic cancer cells." Oncogenesis **2**: e61.

Horton, S. J. and B. J. Huntly (2012). "Recent advances in acute myeloid leukemia stem cell biology." Haematologica **97**(7): 966-974.

Hoyt, P. R., C. Bartholomew, A. J. Davis, K. Yutzey, L. W. Gamer, S. S. Potter, J. N. Ihle and M. L. Mucenski (1997). "The Evi1 proto-oncogene is required at midgestation for neural, heart, and paraxial mesenchyme development." Mech Dev **65**(1-2): 55-70.

Hu, Q., L. Zhang, J. Wen, S. Wang, M. Li, R. Feng, X. Yang and L. Li (2010). "The EGF receptor-sox2-EGF receptor feedback loop positively regulates the self-renewal of neural precursor cells." Stem Cells **28**(2): 279-286.

Huang, F. T., Y. X. Zhuan-Sun, Y. Y. Zhuang, S. L. Wei, J. Tang, W. B. Chen and S. N. Zhang (2012). "Inhibition of hedgehog signaling depresses self-renewal of pancreatic cancer stem cells and reverses chemoresistance." Int J Oncol **41**(5): 1707-1714.

Hutz, K., R. Mejias-Luque, K. Farsakova, M. Ogris, S. Krebs, M. Anton, M. Vieth, U. Schuller, M. R. Schneider, H. Blum, E. Wagner, A. Jung and M. Gerhard (2014). "The stem cell factor SOX2 regulates the tumorigenic potential in human gastric cancer cells." Carcinogenesis **35**(4): 942-950.

Iida, H., M. Suzuki, R. Goitsuka and H. Ueno (2012). "Hypoxia induces CD133 expression in human lung cancer cells by up-regulation of OCT3/4 and SOX2." Int J Oncol **40**(1): 71-79.

Ito, K. and T. Suda (2014). "Metabolic requirements for the maintenance of self-renewing stem cells." Nat Rev Mol Cell Biol **15**(4): 243-256.

Izutsu, K., M. Kurokawa, Y. Imai, K. Maki, K. Mitani and H. Hirai (2001). "The corepressor CtBP interacts with Evi-1 to repress transforming growth factor beta signaling." Blood **97**(9): 2815-2822.

Jackson, M., F. Hassiotou and A. Nowak (2015). "Glioblastoma stem-like cells: at the root of tumor recurrence and a therapeutic target." Carcinogenesis **36**(2): 177-185.

Ji, J. and P. S. Zheng (2010). "Expression of Sox2 in human cervical carcinogenesis." Hum Pathol **41**(10): 1438-1447.

Jia, X., X. Li, Y. Xu, S. Zhang, W. Mou, Y. Liu, Y. Liu, D. Lv, C. H. Liu, X. Tan, R. Xiang and N. Li (2011). "SOX2 promotes tumorigenesis and increases the anti-apoptotic property of human prostate cancer cell." J Mol Cell Biol **3**(4): 230-238.

Jiang, G. L. and S. Huang (2000). "The yin-yang of PR-domain family genes in tumorigenesis." Histol Histopathol **15**(1): 109-117.

Jin, G., Y. Yamazaki, M. Takuwa, T. Takahara, K. Kaneko, T. Kuwata, S. Miyata and T. Nakamura (2007). "Trib1 and Evi1 cooperate with Hoxa and Meis1 in myeloid leukemogenesis." Blood **109**(9): 3998-4005.

Julian, L. M., R. Vandenbosch, C. A. Pakenham, M. G. Andrusiak, A. P. Nguyen, K. A. McClellan, D. S. Svoboda, D. C. Lagace, D. S. Park, G. Leone, A. Blais and R. S. Slack (2013). "Opposing regulation of Sox2 by cell-cycle effectors E2f3a and E2f3b in neural stem cells." Cell Stem Cell **12**(4): 440-452.

Justilien, V., M. P. Walsh, S. A. Ali, E. A. Thompson, N. R. Murray and A. P. Fields (2014). "The PRKCI and SOX2 oncogenes are coamplified and cooperate to activate Hedgehog signaling in lung squamous cell carcinoma." Cancer Cell **25**(2): 139-151.

Kalluri, R. and R. A. Weinberg (2009). "The basics of epithelial-mesenchymal transition." J Clin Invest **119**(6): 1420-1428.

Kamachi, Y., M. Uchikawa, A. Tanouchi, R. Sekido and H. Kondoh (2001). "Pax6 and SOX2 form a co-DNA-binding partner complex that regulates initiation of lens development." Genes Dev **15**(10): 1272-1286.

Kaplan, R. N., R. D. Riba, S. Zacharoulis, A. H. Bramley, L. Vincent, C. Costa, D. D. MacDonald, D. K. Jin, K. Shido, S. A. Kerns, Z. Zhu, D. Hicklin, Y. Wu, J. L. Port, N. Altorki, E. R. Port, D. Ruggero, S. V. Shmelkov, K. K. Jensen, S. Rafii and D. Lyden (2005). "VEGFR1-positive haematopoietic bone marrow progenitors initiate the pre-metastatic niche." Nature **438**(7069): 820-827.

Kazama, H., T. Kodera, S. Shimizu, H. Mizoguchi and K. Morishita (1999). "Ecotropic viral integration site-1 is activated during, and is sufficient for, neuroectodermal P19 cell differentiation." Cell Growth Differ **10**(8): 565-573.

Kemper, K., M. R. Sprick, M. de Bree, A. Scopelliti, L. Vermeulen, M. Hoek, J. Zeilstra, S. T. Pals, H. Mehmet, G. Stassi and J. P. Medema (2010). "The AC133 epitope, but not the CD133 protein, is lost upon cancer stem cell differentiation." Cancer Res **70**(2): 719-729.

Kerr, C. L. and A. Hussain (2014). "Regulators of prostate cancer stem cells." Curr Opin Oncol **26**(3): 328-333.

Kilbey, A., V. Stephens and C. Bartholomew (1999). "Loss of cell cycle control by deregulation of cyclin-dependent kinase 2 kinase activity in Evi-1 transformed fibroblasts." Cell Growth Differ **10**(9): 601-610.

Kim, C. F., E. L. Jackson, A. E. Woolfenden, S. Lawrence, I. Babar, S. Vogel, D. Crowley, R. T. Bronson and T. Jacks (2005). "Identification of bronchioalveolar stem cells in normal lung and lung cancer." Cell **121**(6): 823-835.

Kim, J., J. Chu, X. Shen, J. Wang and S. H. Orkin (2008). "An extended transcriptional network for pluripotency of embryonic stem cells." Cell **132**(6): 1049-1061.

Klonisch, T., E. Wiechec, S. Hombach-Klonisch, S. R. Ande, S. Wesselborg, K. Schulze-Osthoff and M. Los (2008). "Cancer stem cell markers in common cancers - therapeutic implications." Trends Mol Med **14**(10): 450-460.

Konantz, M., M. C. Andre, M. Ebinger, M. Grauer, H. Wang, S. Grzywna, O. C. Rothfuss, S. Lehle, O. S. Kustikova, H. R. Salih, R. Handgretinger, F. Fend, C. Baum, L. Kanz, L. Quintanilla-Martinez, K. Schulze-Osthoff, F. Essmann and C. Lengerke (2013). "EVI-1 modulates leukemogenic potential and apoptosis sensitivity in human acute lymphoblastic leukemia." Leukemia **27**(1): 56-65.

Konantz, M., T. B. Balci, U. F. Hartwig, G. Dellaire, M. C. Andre, J. N. Berman and C. Lengerke (2012). "Zebrafish xenografts as a tool for in vivo studies on human cancer." Ann N Y Acad Sci **1266**: 124-137.

Kregel, S., K. J. Kiriluk, A. M. Rosen, Y. Cai, E. E. Reyes, K. B. Otto, W. Tom, G. P. Paner, R. Z. Szmulewitz and D. J. Vander Griend (2013). "Sox2 is an androgen receptor-repressed gene that promotes castration-resistant prostate cancer." PLoS One **8**(1): e53701.

Krishnamurthy, S. and J. E. Nor (2012). "Head and neck cancer stem cells." J Dent Res **91**(4): 334-340.

Kruyt, F. A. and J. J. Schuringa (2010). "Apoptosis and cancer stem cells: Implications for apoptosis targeted therapy." Biochem Pharmacol **80**(4): 423-430.

Kurokawa, M., K. Mitani, K. Irie, T. Matsuyama, T. Takahashi, S. Chiba, Y. Yazaki, K. Matsumoto and H. Hirai (1998). "The oncoprotein Evi-1 represses TGF-beta signalling by inhibiting Smad3." Nature **394**(6688): 92-96.

Kurokawa, M., K. Mitani, T. Yamagata, T. Takahashi, K. Izutsu, S. Ogawa, T. Moriguchi, E. Nishida, Y. Yazaki and H. Hirai (2000). "The evi-1 oncoprotein inhibits c-Jun N-terminal kinase and prevents stress-induced cell death." EMBO J **19**(12): 2958-2968.

Kustikova, O. S., A. Schwarzer, M. Stahlhut, M. H. Brugman, T. Neumann, M. Yang, Z. Li, A. Schambach, N. Heinz, S. Gerdes, I. Roeder, T. C. Ha, D. Steinemann, B. Schlegelberger and C. Baum (2013). "Activation of Evi1 inhibits cell cycle progression and differentiation of hematopoietic progenitor cells." Leukemia **27**(5): 1127-1138.

Lang, D., J. B. Mascarenhas and C. R. Shea (2013). "Melanocytes, melanocyte stem cells, and melanoma stem cells." Clin Dermatol **31**(2): 166-178.

Lapidot, T., C. Sirard, J. Vormoor, B. Murdoch, T. Hoang, J. Caceres-Cortes, M. Minden, B. Paterson, M. A. Caligiuri and J. E. Dick (1994). "A cell initiating human acute myeloid leukaemia after transplantation into SCID mice." Nature **367**(6464): 645-648.

Lawson, D. A., N. R. Bhakta, K. Kessenbrock, K. D. Prummel, Y. Yu, K. Takai, A. Zhou, H. Eyob, S. Balakrishnan, C. Y. Wang, P. Yaswen, A. Goga and Z. Werb (2015). "Single-cell analysis reveals a stem-cell program in human metastatic breast cancer cells." Nature **526**(7571): 131-135.

Lee, A., J. D. Kessler, T. A. Read, C. Kaiser, D. Corbeil, W. B. Huttner, J. E. Johnson and R. J. Wechsler-Reya (2005). "Isolation of neural stem cells from the postnatal cerebellum." Nat Neurosci **8**(6): 723-729.

Leis, O., A. Eguiara, E. Lopez-Arribillaga, M. J. Alberdi, S. Hernandez-Garcia, K. Elorriaga, A. Pandiella, R. Rezola and A. G. Martin (2012). "Sox2 expression in breast tumours and activation in breast cancer stem cells." Oncogene **31**(11): 1354-1365.

Lengerke, C., T. Fehm, R. Kurth, H. Neubauer, V. Scheble, F. Muller, F. Schneider, K. Petersen, D. Wallwiener, L. Kanz, F. Fend, S. Perner, P. M. Bareiss and A. Staebler (2011). "Expression of the embryonic stem cell marker SOX2 in early-stage breast carcinoma." BMC Cancer **11**: 42.

Li, C., D. G. Heidt, P. Dalerba, C. F. Burant, L. Zhang, V. Adsay, M. Wicha, M. F. Clarke and D. M. Simeone (2007). "Identification of pancreatic cancer stem cells." Cancer Res **67**(3): 1030-1037.

Li, P., R. Yang and W. Q. Gao (2014). "Contributions of epithelial-mesenchymal transition and cancer stem cells to the development of castration resistance of prostate cancer." Mol Cancer **13**: 55.

Li, Y., J. Wu and P. Zhang (2016). "CCL15/CCR1 axis is involved in hepatocellular carcinoma cells migration and invasion." Tumour Biol **37**(4): 4501-4507.

Liu, X. F., W. T. Yang, R. Xu, J. T. Liu and P. S. Zheng (2014). "Cervical cancer cells with positive Sox2 expression exhibit the properties of cancer stem cells." PLoS One **9**(1): e87092.

Liu, Y., L. Chen, T. C. Ko, A. P. Fields and E. A. Thompson (2006). "Evi1 is a survival factor which conveys resistance to both TGFbeta- and taxol-mediated cell death via PI3K/AKT." Oncogene **25**(25): 3565-3575.

Lopez-Juarez, A., S. Remaud, Z. Hassani, P. Jolivet, J. Pierre Simons, T. Sontag, K. Yoshikawa, J. Price, G. Morvan-Dubois and B. A. Demeneix (2012). "Thyroid hormone signaling acts as a neurogenic switch by repressing Sox2 in the adult neural stem cell niche." Cell Stem Cell **10**(5): 531-543.

Lou, X., X. Han, C. Jin, W. Tian, W. Yu, D. Ding, L. Cheng, B. Huang, H. Jiang and B. Lin (2013). "SOX2 targets fibronectin 1 to promote cell migration and invasion in ovarian cancer: new molecular leads for therapeutic intervention." OMICS **17**(10): 510-518.

Lu, Y., C. Futtner, J. R. Rock, X. Xu, W. Whitworth, B. L. Hogan and M. W. Onaitis (2010). "Evidence that SOX2 overexpression is oncogenic in the lung." PLoS One **5**(6): e11022.

Lundin, A. and B. Driscoll (2013). "Lung cancer stem cells: progress and prospects." Cancer Lett **338**(1): 89-93.

MacDonald, B. T., K. Tamai and X. He (2009). "Wnt/beta-catenin signaling: components, mechanisms, and diseases." Dev Cell **17**(1): 9-26.

Maier, S., T. Wilbertz, M. Braun, V. Scheble, M. Reischl, R. Mikut, R. Menon, P. Nikolov, K. Petersen, C. Beschorner, H. Moch, C. Kakies, C. Protzel, J. Bauer, A. Soltermann, F. Fend, A. Staebler, C. Lengerke and S. Perner (2011). "SOX2 amplification is a common event in squamous cell carcinomas of different organ sites." Hum Pathol **42**(8): 1078-1088.

Malanchi, I., H. Peinado, D. Kassen, T. Hussenet, D. Metzger, P. Chambon, M. Huber, D. Hohl, A. Cano, W. Birchmeier and J. Huelsken (2008). "Cutaneous cancer stem cell maintenance is dependent on beta-catenin signalling." Nature **452**(7187): 650-653.

Mani, S. A., W. Guo, M. J. Liao, E. N. Eaton, A. Ayyanan, A. Y. Zhou, M. Brooks, F. Reinhard, C. C. Zhang, M. Shipitsin, L. L. Campbell, K. Polyak, C. Brisken, J. Yang and R. A. Weinberg (2008).

"The epithelial-mesenchymal transition generates cells with properties of stem cells." Cell **133**(4): 704-715.

Marques-Torrejon, M. A., E. Porlan, A. Banito, E. Gomez-Ibarlucea, A. J. Lopez-Contreras, O. Fernandez-Capetillo, A. Vidal, J. Gil, J. Torres and I. Farinas (2013). "Cyclin-dependent kinase inhibitor p21 controls adult neural stem cell expansion by regulating Sox2 gene expression." Cell Stem Cell **12**(1): 88-100.

Masui, S., Y. Nakatake, Y. Toyooka, D. Shimosato, R. Yagi, K. Takahashi, H. Okochi, A. Okuda, R. Matoba, A. A. Sharov, M. S. Ko and H. Niwa (2007). "Pluripotency governed by Sox2 via regulation of Oct3/4 expression in mouse embryonic stem cells." Nat Cell Biol **9**(6): 625-635.

Matsui, W., Q. Wang, J. P. Barber, S. Brennan, B. D. Smith, I. Borrello, I. McNiece, L. Lin, R. F. Ambinder, C. Peacock, D. N. Watkins, C. A. Huff and R. J. Jones (2008). "Clonogenic multiple myeloma progenitors, stem cell properties, and drug resistance." Cancer Res **68**(1): 190-197.

Mead, P. E., E. Parganas, S. Ohtsuka, K. Morishita, L. Gamer, E. Kuliyev, C. V. Wright and J. N. Ihle (2005). "Evi-1 expression in Xenopus." Gene Expr Patterns **5**(5): 601-608.

Medema, J. P. and L. Vermeulen (2011). "Microenvironmental regulation of stem cells in intestinal homeostasis and cancer." Nature **474**(7351): 318-326.

Menendez, S., S. Camus, A. Herreria, I. Paramonov, L. B. Morera, M. Collado, V. Pekarik, I. Maceda, M. Edel, A. Consiglio, A. Sanchez, H. Li, M. Serrano and J. C. Belmonte (2012). "Increased dosage of tumor suppressors limits the tumorigenicity of iPS cells without affecting their pluripotency." Aging Cell **11**(1): 41-50.

Merchant, A. A. and W. Matsui (2010). "Targeting Hedgehog--a cancer stem cell pathway." Clin Cancer Res **16**(12): 3130-3140.

Mitani, K. (2004). "Molecular mechanisms of leukemogenesis by AML1/EVI-1." Oncogene **23**(24): 4263-4269.

Morishita, K., E. Parganas, E. C. Douglass and J. N. Ihle (1990). "Unique expression of the human Evi-1 gene in an endometrial carcinoma cell line: sequence of cDNAs and structure of alternatively spliced transcripts." Oncogene **5**(7): 963-971.

Morishita, K., D. S. Parker, M. L. Mucenski, N. A. Jenkins, N. G. Copeland and J. N. Ihle (1988). "Retroviral activation of a novel gene encoding a zinc finger protein in IL-3-dependent myeloid leukemia cell lines." Cell **54**(6): 831-840.

Mukherjee, S., M. Mazumdar, S. Chakraborty, A. Manna, S. Saha, P. Khan, P. Bhattacharjee, D. Guha, A. Adhikary, S. Mukhjerjee and T. Das (2014). "Curcumin inhibits breast cancer stem cell migration by amplifying the E-cadherin/beta-catenin negative feedback loop." Stem Cell Res Ther **5**(5): 116.

Nanjundan, M., Y. Nakayama, K. W. Cheng, J. Lahad, J. Liu, K. Lu, W. L. Kuo, K. Smith-McCune, D. Fishman, J. W. Gray and G. B. Mills (2007). "Amplification of MDS1/EVI1 and EVI1, located in the 3q26.2 amplicon, is associated with favorable patient prognosis in ovarian cancer." Cancer Res **67**(7): 3074-3084.

Ng, S. Y., R. Johnson and L. W. Stanton (2012). "Human long non-coding RNAs promote pluripotency and neuronal differentiation by association with chromatin modifiers and transcription factors." EMBO J **31**(3): 522-533.

Nishizawa, S., Y. Hirohashi, T. Torigoe, A. Takahashi, Y. Tamura, T. Mori, T. Kanaseki, K. Kamiguchi, H. Asanuma, R. Morita, A. Sokolovskaya, J. Matsuzaki, R. Yamada, R. Fujii, H. H. Kampinga, T. Kondo, T. Hasegawa, I. Hara and N. Sato (2012). "HSP DNAJB8 controls tumor-initiating ability in renal cancer stem-like cells." Cancer Res **72**(11): 2844-2854.

Nitta, E., K. Izutsu, Y. Yamaguchi, Y. Imai, S. Ogawa, S. Chiba, M. Kurokawa and H. Hirai (2005). "Oligomerization of Evi-1 regulated by the PR domain contributes to recruitment of corepressor CtBP." Oncogene **24**(40): 6165-6173.

Nucifora, G., L. Laricchia-Robbio and V. Senyuk (2006). "EVI1 and hematopoietic disorders: history and perspectives." Gene **368**: 1-11.

Nucifora, G. and J. D. Rowley (1995). "AML1 and the 8;21 and 3;21 translocations in acute and chronic myeloid leukemia." Blood **86**(1): 1-14.

O'Brien, C. A., A. Pollett, S. Gallinger and J. E. Dick (2007). "A human colon cancer cell capable of initiating tumour growth in immunodeficient mice." Nature **445**(7123): 106-110.

Orkin, S. H. and K. Hochedlinger (2011). "Chromatin connections to pluripotency and cellular reprogramming." Cell **145**(6): 835-850.

Palmer, S., J. P. Brouillet, A. Kilbey, R. Fulton, M. Walker, M. Crossley and C. Bartholomew (2001). "Evi-1 transforming and repressor activities are mediated by CtBP co-repressor proteins." J Biol Chem **276**(28): 25834-25840.

Patel, J. B., H. N. Appaiah, R. M. Burnett, P. Bhat-Nakshatri, G. Wang, R. Mehta, S. Badve, M. J. Thomson, S. Hammond, P. Steeg, Y. Liu and H. Nakshatri (2011). "Control of EVI-1 oncogene expression in metastatic breast cancer cells through microRNA miR-22." Oncogene **30**(11): 1290-1301.

Patrawala, L., T. Calhoun, R. Schneider-Broussard, H. Li, B. Bhatia, S. Tang, J. G. Reilly, D. Chandra, J. Zhou, K. Claypool, L. Coghlan and D. G. Tang (2006). "Highly purified CD44+ prostate cancer cells from xenograft human tumors are enriched in tumorigenic and metastatic progenitor cells." Oncogene **25**(12): 1696-1708.

Perkins, A. S., J. A. Mercer, N. A. Jenkins and N. G. Copeland (1991). "Patterns of Evi-1 expression in embryonic and adult tissues suggest that Evi-1 plays an important regulatory role in mouse development." Development **111**(2): 479-487.

Pham, D. L., V. Scheble, P. Bareiss, A. Fischer, C. Beschorner, A. Adam, C. Bachmann, H. Neubauer, H. Boesmueller, L. Kanz, D. Wallwiener, F. Fend, C. Lengerke, S. Perner, T. Fehm and A. Staebler (2013). "SOX2 expression and prognostic significance in ovarian carcinoma." Int J Gynecol Pathol **32**(4): 358-367.

Piccirillo, S. G., B. A. Reynolds, N. Zanetti, G. Lamorte, E. Binda, G. Broggi, H. Brem, A. Olivi, F. Dimeco and A. L. Vescovi (2006). "Bone morphogenetic proteins inhibit the tumorigenic potential of human brain tumour-initiating cells." Nature **444**(7120): 761-765.

Piva, M., G. Domenici, O. Iriondo, M. Rabano, B. M. Simoes, V. Comaills, I. Barredo, J. A. Lopez-Ruiz, I. Zabalza, R. Kypta and M. Vivanco (2014). "Sox2 promotes tamoxifen resistance in breast cancer cells." EMBO Mol Med **6**(1): 66-79.

Poppe, B., N. Dastugue, J. Vandesompele, B. Cauwelier, B. De Smet, N. Yigit, A. De Paepe, J. Cervera, C. Recher, V. De Mas, A. Hagemeijer and F. Speleman (2006). "EVI1 is consistently

expressed as principal transcript in common and rare recurrent 3q26 rearrangements." Genes Chromosomes Cancer **45**(4): 349-356.

Qian, X., C. Tan, F. Wang, B. Yang, Y. Ge, Z. Guan and J. Cai (2016). "Esophageal cancer stem cells and implications for future therapeutics." Onco Targets Ther **9**: 2247-2254.

Qin, J., J. Ji, R. Deng, J. Tang, F. Yang, G. K. Feng, W. D. Chen, X. Q. Wu, X. J. Qian, K. Ding and X. F. Zhu (2015). "DC120, a novel AKT inhibitor, preferentially suppresses nasopharyngeal carcinoma cancer stem-like cells by downregulating Sox2." Oncotarget **6**(9): 6944-6958.

Reya, T., A. W. Duncan, L. Ailles, J. Domen, D. C. Scherer, K. Willert, L. Hintz, R. Nusse and I. L. Weissman (2003). "A role for Wnt signalling in self-renewal of haematopoietic stem cells." Nature **423**(6938): 409-414.

Reya, T., S. J. Morrison, M. F. Clarke and I. L. Weissman (2001). "Stem cells, cancer, and cancer stem cells." Nature **414**(6859): 105-111.

Ricci-Vitiani, L., D. G. Lombardi, E. Pilozzi, M. Biffoni, M. Todaro, C. Peschle and R. De Maria (2007). "Identification and expansion of human colon-cancer-initiating cells." Nature **445**(7123): 111-115.

Rudin, C. M., S. Durinck, E. W. Stawiski, J. T. Poirier, Z. Modrusan, D. S. Shames, E. A. Bergbower, Y. Guan, J. Shin, J. Guillory, C. S. Rivers, C. K. Foo, D. Bhatt, J. Stinson, F. Gnad, P. M. Haverty, R. Gentleman, S. Chaudhuri, V. Janakiraman, B. S. Jaiswal, C. Parikh, W. Yuan, Z. Zhang, H. Koeppen, T. D. Wu, H. M. Stern, R. L. Yauch, K. E. Huffman, D. D. Paskulin, P. B. Illei, M. Varella-Garcia, A. F. Gazdar, F. J. de Sauvage, R. Bourgon, J. D. Minna, M. V. Brock and S. Seshagiri (2012). "Comprehensive genomic analysis identifies SOX2 as a frequently amplified gene in small-cell lung cancer." Nat Genet **44**(10): 1111-1116.

Rybak, A. P. and D. Tang (2013). "SOX2 plays a critical role in EGFR-mediated self-renewal of human prostate cancer stem-like cells." Cell Signal **25**(12): 2734-2742.

Saini, V., C. D. Hose, A. Monks, K. Nagashima, B. Han, D. L. Newton, A. Millione, J. Shah, M. G. Hollingshead, K. M. Hite, M. W. Burkett, R. M. Delosh, T. E. Silvers, D. A. Scudiero and R. H. Shoemaker (2012). "Identification of CBX3 and ABCA5 as putative biomarkers for tumor stem cells in osteosarcoma." PLoS One **7**(8): e41401.

Santini, R., S. Pietrobono, S. Pandolfi, V. Montagnani, M. D'Amico, J. Y. Penachioni, M. C. Vinci, L. Borgognoni and B. Stecca (2014). "SOX2 regulates self-renewal and tumorigenicity of human melanoma-initiating cells." Oncogene **33**(38): 4697-4708.

Schaefer, T., H. Wang, P. Mir, M. Konantz, T. C. Pereboom, A. M. Paczulla, B. Merz, T. Fehm, S. Perner, O. C. Rothfuss, L. Kanz, K. Schulze-Osthoff and C. Lengerke (2015). "Molecular and functional interactions between AKT and SOX2 in breast carcinoma." Oncotarget.

Schober, M. and E. Fuchs (2011). "Tumor-initiating stem cells of squamous cell carcinomas and their control by TGF-beta and integrin/focal adhesion kinase (FAK) signaling." Proc Natl Acad Sci U S A **108**(26): 10544-10549.

Schrock, A., M. Bode, F. J. Goke, P. M. Bareiss, R. Schairer, H. Wang, W. Weichert, A. Franzen, R. Kirsten, T. van Bremen, A. Queisser, G. Kristiansen, L. Heasley, F. Bootz, C. Lengerke and S. Perner (2014). "Expression and role of the embryonic protein SOX2 in head and neck squamous cell carcinoma." Carcinogenesis **35**(7): 1636-1642.

Sell, S. and G. B. Pierce (1994). "Maturation arrest of stem cell differentiation is a common pathway for the cellular origin of teratocarcinomas and epithelial cancers." Lab Invest **70**(1): 6-22.

Seymour, T., A. Nowak and F. Kakulas (2015). "Targeting Aggressive Cancer Stem Cells in Glioblastoma." Front Oncol **5**: 159.

Shackleton, M., E. Quintana, E. R. Fearon and S. J. Morrison (2009). "Heterogeneity in cancer: cancer stem cells versus clonal evolution." Cell **138**(5): 822-829.

Sharpe, B., M. Beresford, R. Bowen, J. Mitchard and A. D. Chalmers (2013). "Searching for prostate cancer stem cells: markers and methods." Stem Cell Rev **9**(5): 721-730.

Shaw, F. L., H. Harrison, K. Spence, M. P. Ablett, B. M. Simoes, G. Farnie and R. B. Clarke (2012). "A detailed mammosphere assay protocol for the quantification of breast stem cell activity." J Mammary Gland Biol Neoplasia **17**(2): 111-117.

Shaw, R. J. and L. C. Cantley (2006). "Ras, PI(3)K and mTOR signalling controls tumour cell growth." Nature **441**(7092): 424-430.

Singh, S., D. Chitkara, R. Mehrazin, S. W. Behrman, R. W. Wake and R. I. Mahato (2012). "Chemoresistance in prostate cancer cells is regulated by miRNAs and Hedgehog pathway." PLoS One **7**(6): e40021.

Singh, S., J. Trevino, N. Bora-Singhal, D. Coppola, E. Haura, S. Altiok and S. P. Chellappan (2012). "EGFR/Src/Akt signaling modulates Sox2 expression and self-renewal of stem-like side-population cells in non-small cell lung cancer." Mol Cancer **11**: 73.

Singh, S. K., I. D. Clarke, M. Terasaki, V. E. Bonn, C. Hawkins, J. Squire and P. B. Dirks (2003). "Identification of a cancer stem cell in human brain tumors." Cancer Res **63**(18): 5821-5828.

Singh, S. K., C. Hawkins, I. D. Clarke, J. A. Squire, J. Bayani, T. Hide, R. M. Henkelman, M. D. Cusimano and P. B. Dirks (2004). "Identification of human brain tumour initiating cells." Nature **432**(7015): 396-401.

Sitailo, S., R. Sood, K. Barton and G. Nucifora (1999). "Forced expression of the leukemia-associated gene EVI1 in ES cells: a model for myeloid leukemia with 3q26 rearrangements." Leukemia **13**(11): 1639-1645.

Stewart, J. M., P. A. Shaw, C. Gedye, M. Q. Bernardini, B. G. Neel and L. E. Ailles (2011). "Phenotypic heterogeneity and instability of human ovarian tumor-initiating cells." Proc Natl Acad Sci U S A **108**(16): 6468-6473.

Stolzenburg, S., M. G. Rots, A. S. Beltran, A. G. Rivenbark, X. Yuan, H. Qian, B. D. Strahl and P. Blancafort (2012). "Targeted silencing of the oncogenic transcription factor SOX2 in breast cancer." Nucleic Acids Res **40**(14): 6725-6740.

Stros, M., D. Launholt and K. D. Grasser (2007). "The HMG-box: a versatile protein domain occurring in a wide variety of DNA-binding proteins." Cell Mol Life Sci **64**(19-20): 2590-2606.

Sun, C., L. Sun, Y. Li, X. Kang, S. Zhang and Y. Liu (2013). "Sox2 expression predicts poor survival of hepatocellular carcinoma patients and it promotes liver cancer cell invasion by activating Slug." Med Oncol **30**(2): 503.

Sun, J. H., Q. Luo, L. L. Liu and G. B. Song (2016). "Liver cancer stem cell markers: Progression and therapeutic implications." World J Gastroenterol **22**(13): 3547-3557.

Suzukawa, K., E. Parganas, A. Gajjar, T. Abe, S. Takahashi, K. Tani, S. Asano, H. Asou, N. Kamada, J. Yokota and et al. (1994). "Identification of a breakpoint cluster region 3' of the ribophorin I gene at 3q21 associated with the transcriptional activation of the EVI1 gene in acute myelogenous leukemias with inv(3)(q21q26)." Blood **84**(8): 2681-2688.

Takahashi, S. and J. D. Licht (2002). "The human promyelocytic leukemia zinc finger gene is regulated by the Evi-1 oncoprotein and a novel guanine-rich site binding protein." Leukemia **16**(9): 1755-1762.

Tanaka, M., H. I. Suzuki, J. Shibahara, A. Kunita, T. Isagawa, A. Yoshimi, M. Kurokawa, K. Miyazono, H. Aburatani, S. Ishikawa and M. Fukayama (2014). "EVI1 oncogene promotes KRAS pathway through suppression of microRNA-96 in pancreatic carcinogenesis." Oncogene **33**(19): 2454-2463.

Taylor, M. D., H. Poppleton, C. Fuller, X. Su, Y. Liu, P. Jensen, S. Magdaleno, J. Dalton, C. Calabrese, J. Board, T. Macdonald, J. Rutka, A. Guha, A. Gajjar, T. Curran and R. J. Gilbertson (2005). "Radial glia cells are candidate stem cells of ependymoma." Cancer Cell **8**(4): 323-335.

Thiery, J. P. (2002). "Epithelial-mesenchymal transitions in tumour progression." Nat Rev Cancer **2**(6): 442-454.

Thomas, J. O. (2001). "HMG1 and 2: architectural DNA-binding proteins." Biochem Soc Trans **29**(Pt 4): 395-401.

Tian, T., Y. Zhang, S. Wang, J. Zhou and S. Xu (2012). "Sox2 enhances the tumorigenicity and chemoresistance of cancer stem-like cells derived from gastric cancer." J Biomed Res **26**(5): 336-345.

Tompkins, D. H., V. Besnard, A. W. Lange, A. R. Keiser, S. E. Wert, M. D. Bruno and J. A. Whitsett (2011). "Sox2 activates cell proliferation and differentiation in the respiratory epithelium." Am J Respir Cell Mol Biol **45**(1): 101-110.

Tseng, J. Y., C. Y. Yang, S. H. Yang, J. K. Lin, C. H. Lin and J. K. Jiang (2015). "Circulating CD133(+)/ESA(+) cells in colorectal cancer patients." J Surg Res **199**(2): 362-370.

Tsuruzoe, S., K. Ishihara, Y. Uchimura, S. Watanabe, Y. Sekita, T. Aoto, H. Saitoh, Y. Yuasa, H. Niwa, M. Kawasuji, H. Baba and M. Nakao (2006). "Inhibition of DNA binding of Sox2 by the SUMO conjugation." Biochem Biophys Res Commun **351**(4): 920-926.

Tu, S. M. and S. H. Lin (2012). "Prostate cancer stem cells." Clin Genitourin Cancer **10**(2): 69-76.

Uchida, N., D. W. Buck, D. He, M. J. Reitsma, M. Masek, T. V. Phan, A. S. Tsukamoto, F. H. Gage and I. L. Weissman (2000). "Direct isolation of human central nervous system stem cells." Proc Natl Acad Sci U S A **97**(26): 14720-14725.

Valk, P. J., R. G. Verhaak, M. A. Beijen, C. A. Erpelinck, S. Barjesteh van Waalwijk van Doorn-Khosrovani, J. M. Boer, H. B. Beverloo, M. J. Moorhouse, P. J. van der Spek, B. Lowenberg and R. Delwel (2004). "Prognostically useful gene-expression profiles in acute myeloid leukemia." N Engl J Med **350**(16): 1617-1628.

Van Campenhout, C., M. Nichane, A. Antoniou, H. Pendeville, O. J. Bronchain, J. C. Marine, A. Mazabraud, M. L. Voz and E. J. Bellefroid (2006). "Evi1 is specifically expressed in the distal tubule and duct of the Xenopus pronephros and plays a role in its formation." Dev Biol **294**(1): 203-219.

Van Hoof, D., J. Munoz, S. R. Braam, M. W. Pinkse, R. Linding, A. J. Heck, C. L. Mummery and J. Krijgsveld (2009). "Phosphorylation dynamics during early differentiation of human embryonic stem cells." Cell Stem Cell **5**(2): 214-226.

Vanner, R. J., M. Remke, M. Gallo, H. J. Selvadurai, F. Coutinho, L. Lee, M. Kushida, R. Head, S. Morrissy, X. Zhu, T. Aviv, V. Voisin, I. D. Clarke, Y. Li, A. J. Mungall, R. A. Moore, Y. Ma, S. J. Jones, M. A. Marra, D. Malkin, P. A. Northcott, M. Kool, S. M. Pfister, G. Bader, K. Hochedlinger, A. Korshunov, M. D. Taylor and P. B. Dirks (2014). "Quiescent sox2(+) cells drive hierarchical growth and relapse in sonic hedgehog subgroup medulloblastoma." Cancer Cell **26**(1): 33-47.

Vazquez-Martin, A., S. Cufi, E. Lopez-Bonet, B. Corominas-Faja, E. Cuyas, L. Vellon, J. M. Iglesias, O. Leis, A. G. Martin and J. A. Menendez (2013). "Reprogramming of non-genomic estrogen signaling by the stemness factor SOX2 enhances the tumor-initiating capacity of breast cancer cells." Cell Cycle **12**(22): 3471-3477.

Vinatzer, U., C. Mannhalter, M. Mitterbauer, H. Gruener, H. Greinix, H. H. Schmidt, C. Fonatsch and R. Wieser (2003). "Quantitative comparison of the expression of EVI1 and its presumptive antagonist, MDS1/EVI1, in patients with myeloid leukemia." Genes Chromosomes Cancer **36**(1): 80-89.

Visvader, J. E. and G. J. Lindeman (2008). "Cancer stem cells in solid tumours: accumulating evidence and unresolved questions." Nat Rev Cancer **8**(10): 755-768.

Wang, H., A. Paczulla and C. Lengerke (2015). "Evaluation of stem cell properties in human ovarian carcinoma cells using multi and single cell-based spheres assays." J Vis Exp(95): e52259.

Wang, Q., W. He, C. Lu, Z. Wang, J. Wang, K. E. Giercksky, J. M. Nesland and Z. Suo (2009). "Oct3/4 and Sox2 are significantly associated with an unfavorable clinical outcome in human esophageal squamous cell carcinoma." Anticancer Res **29**(4): 1233-1241.

Wang, T. Y., Y. P. Huang and P. Ma (2014). "Correlations of common polymorphism of EVI-1 gene targeted by miRNA-206/133b with the pathogenesis of breast cancer." Tumour Biol **35**(9): 9255-9262.

Watkins, D. N., D. M. Berman, S. G. Burkholder, B. Wang, P. A. Beachy and S. B. Baylin (2003). "Hedgehog signalling within airway epithelial progenitors and in small-cell lung cancer." Nature **422**(6929): 313-317.

Wieser, R. (2007). "The oncogene and developmental regulator EVI1: expression, biochemical properties, and biological functions." Gene **396**(2): 346-357.

Wilbertz, T., P. Wagner, K. Petersen, A. C. Stiedl, V. J. Scheble, S. Maier, M. Reischl, R. Mikut, N. K. Altorki, H. Moch, F. Fend, A. Staebler, A. J. Bass, M. Meyerson, M. A. Rubin, A. Soltermann, C. Lengerke and S. Perner (2011). "SOX2 gene amplification and protein overexpression are associated with better outcome in squamous cell lung cancer." Mod Pathol **24**(7): 944-953.

Wilson, E., K. Leszczynska, N. S. Poulter, F. Edelmann, V. A. Salisbury, P. J. Noy, A. Bacon, J. Z. Rappoport, J. K. Heath, R. Bicknell and V. L. Heath (2014). "RhoJ interacts with the GIT-PIX complex and regulates focal adhesion disassembly." J Cell Sci **127**(Pt 14): 3039-3051.

Xin, L., D. A. Lawson and O. N. Witte (2005). "The Sca-1 cell surface marker enriches for a prostate-regenerating cell subpopulation that can initiate prostate tumorigenesis." Proc Natl Acad Sci U S A **102**(19): 6942-6947.

Xu, C., D. Xie, S. C. Yu, X. J. Yang, L. R. He, J. Yang, Y. F. Ping, B. Wang, L. Yang, S. L. Xu, W. Cui, Q. L. Wang, W. J. Fu, Q. Liu, C. Qian, Y. H. Cui, J. N. Rich, H. F. Kung, X. Zhang and X. W. Bian (2013). "beta-Catenin/POU5F1/SOX2 transcription factor complex mediates IGF-I receptor signaling and predicts poor prognosis in lung adenocarcinoma." Cancer Res **73**(10): 3181-3189.

Xu, C., H. Zhao, H. Chen and Q. Yao (2015). "CXCR4 in breast cancer: oncogenic role and therapeutic targeting." Drug Des Devel Ther **9**: 4953-4964.

Yang, J., S. A. Mani, J. L. Donaher, S. Ramaswamy, R. A. Itzykson, C. Come, P. Savagner, I. Gitelman, A. Richardson and R. A. Weinberg (2004). "Twist, a master regulator of morphogenesis, plays an essential role in tumor metastasis." Cell **117**(7): 927-939.

Yasui, K., C. Konishi, Y. Gen, M. Endo, O. Dohi, A. Tomie, T. Kitaichi, N. Yamada, N. Iwai, T. Nishikawa, K. Yamaguchi, M. Moriguchi, Y. Sumida, H. Mitsuyoshi, S. Tanaka, S. Arii and Y. Itoh (2015). "EVI1, a target gene for amplification at 3q26, antagonizes transforming growth factor-beta-mediated growth inhibition in hepatocellular carcinoma." Cancer Sci **106**(7): 929-937.

Yatsula, B., S. Lin, A. J. Read, A. Poholek, K. Yates, D. Yue, P. Hui and A. S. Perkins (2005). "Identification of binding sites of EVI1 in mammalian cells." J Biol Chem **280**(35): 30712-30722.

Yu, Z., T. G. Pestell, M. P. Lisanti and R. G. Pestell (2012). "Cancer stem cells." Int J Biochem Cell Biol **44**(12): 2144-2151.

Yuasa, H., Y. Oike, A. Iwama, I. Nishikata, D. Sugiyama, A. Perkins, M. L. Mucenski, T. Suda and K. Morishita (2005). "Oncogenic transcription factor Evi1 regulates hematopoietic stem cell proliferation through GATA-2 expression." EMBO J **24**(11): 1976-1987.

Zhan, H. X., J. W. Xu, D. Wu, T. P. Zhang and S. Y. Hu (2015). "Pancreatic cancer stem cells: new insight into a stubborn disease." Cancer Lett **357**(2): 429-437.

Zhan, Q., C. Wang and S. Ngai (2013). "Ovarian cancer stem cells: a new target for cancer therapy." Biomed Res Int **2013**: 916819.

Zhang, M., F. Behbod, R. L. Atkinson, M. D. Landis, F. Kittrell, D. Edwards, D. Medina, A. Tsimelzon, S. Hilsenbeck, J. E. Green, A. M. Michalowska and J. M. Rosen (2008). "Identification of tumor-initiating cells in a p53-null mouse model of breast cancer." Cancer Res **68**(12): 4674-4682.

Zhang, S., C. Balch, M. W. Chan, H. C. Lai, D. Matei, J. M. Schilder, P. S. Yan, T. H. Huang and K. P. Nephew (2008). "Identification and characterization of ovarian cancer-initiating cells from primary human tumors." Cancer Res **68**(11): 4311-4320.

Zhang, X., Y. Lou, H. Wang, X. Zheng, Q. Dong, J. Sun and B. Han (2015). "Wnt signaling regulates the stemness of lung cancer stem cells and its inhibitors exert anticancer effect on lung cancer SPC-A1 cells." Med Oncol **32**(4): 95.

Zhao, C., A. Chen, C. H. Jamieson, M. Fereshteh, A. Abrahamsson, J. Blum, H. Y. Kwon, J. Kim, J. P. Chute, D. Rizzieri, M. Munchhof, T. VanArsdale, P. A. Beachy and T. Reya (2009). "Hedgehog signalling is essential for maintenance of cancer stem cells in myeloid leukaemia." Nature **458**(7239): 776-779.

Zhao, H. Y., Y. J. Zhang, H. Dai, Y. Zhang and Y. F. Shen (2011). "CARM1 mediates modulation of Sox2." PLoS One **6**(10): e27026.

Zhong, Y., S. Shen, Y. Zhou, F. Mao, Y. Lin, J. Guan, Y. Xu, S. Zhang, X. Liu and Q. Sun (2016). "NOTCH1 is a poor prognostic factor for breast cancer and is associated with breast cancer stem cells." Onco Targets Ther **9**: 6865-6871.

Chapter 8.

Attachments

Paper I

Evaluation of stem cell properties in human ovarian carcinoma cells using multi and single cell-based spheres assays.

Wang H, Paczulla A, Lengerke C.

J Vis Exp. 2015 Jan 3;(95):e52259.

Video Article

Evaluation of Stem Cell Properties in Human Ovarian Carcinoma Cells Using Multi and Single Cell-based Spheres Assays

Hui Wang[1,2], Anna Paczulla[1], Claudia Lengerke[1,2]

[1]Department of Biomedicine, University Hospital Basel

[2]Department of Internal Medicine II, University Hospital Tübingen

Correspondence to: Claudia Lengerke at claudia.lengerke@unibas.ch

URL: http://www.jove.com/video/52259
DOI: doi:10.3791/52259

Keywords: Medicine, Issue 95, Cancer stem cells, spheres assay, ovarian, single cell, SOX2, *in vitro* assay, ovarian carcinoma

Date Published: 1/3/2015

Citation: Wang, H., Paczulla, A., Lengerke, C. Evaluation of Stem Cell Properties in Human Ovarian Carcinoma Cells Using Multi and Single Cell-based Spheres Assays. *J. Vis. Exp.* (95), e52259, doi:10.3791/52259 (2015).

Abstract

Years of research indicates that ovarian cancers harbor a heterogeneous mixture of cells including a subpopulation of so-called “cancer stem cells” (CSCs) responsible for tumor initiation, maintenance and relapse following conventional chemotherapies. Identification of ovarian CSCs is therefore an important goal. A commonly used method to assess CSC potential *in vitro* is the spheres assay in which cells are plated under non-adherent culture conditions in serum-free medium supplemented with growth factors and sphere formation is scored after a few days. Here, we review currently available protocols for human ovarian cancer spheres assays and perform a side-by-side analysis between commonly used multi cell-based assays and a more accurate system based on single cell plating. Our results indicate that both multi cell-based as well as single cell-based spheres assays can be used to investigate sphere formation *in vitro*. The more laborious and expensive single cell-based assays are more suitable for functional assessment of individual cells and lead to overall more accurate results while multi cell-based assays can be strongly influenced by the density of plated cells and require titration experiments upfront. Methylcellulose supplementation to multi cell-based assays can be effectively used to reduce mechanical artifacts.

Video Link

The video component of this article can be found at http://www.jove.com/video/52259/

Introduction

There is increasing evidence that ovarian carcinomas are comprised of heterogeneous mixtures of cells and harbor so-called “cancer stem cells” (CSCs) responsible for disease initiation, maintenance and relapse after conventional cytotoxic therapies[1-3]. Therefore, the development of molecular strategies targeting ovarian CSCs is an important goal and promises to improve the therapy of ovarian cancer patients.

A pre-requisite for the understanding of the molecular features of CSCs is their reliable isolation from the non-CSCs. However, identification of ovarian CSCs appears challenging. While CD133 expression and aldehyde dehydrogenase (ALDH) activity[4,5] have been reported to mark ovarian CSCs, some data indicate that these markers are unstable[6]. Consistently, in ovarian cancer, other than for example in breast carcinoma[7], expression of ALDH1 associates with favorable outcome[8] and expression of the proposed stem cell marker CD44 variant has no prognostic value[9]. More recently, we have shown that expression of the embryonic stem cell protein SOX2 confers stemness to ovarian carcinoma cells[10] and high *SOX2* expression associates with clinically aggressive ovarian and breast carcinomas[11,12]. Therefore, in this report we use a lentiviral reporter construct containing a red fluorescence protein (RFP) whose expression is controlled by a *SOX2* regulatory region, as a method to isolate putative ovarian CSCs.

By definition, CSCs can both self-renew and differentiate, giving rise to all tumor cell types. Putative CSC populations need to be analyzed in functional assays performed *in vivo*. For obvious reasons, in human cells such functional tests are confined to xenograft assays, comprising mostly transplantation of human tumor cells into immuno-compromised mice[10,13].

An alternative *in vitro* method was offered by Brent Reynolds and Sam Weiss who firstly reported the so-called neurosphere assay as a surrogate assay evaluating stem potential in neural cells[14]. Dontu and colleagues later confirmed the use of this assay for evaluation of stem cell potential in breast cells[15,16]. Here, human mammary cells were plated in different numbers in serum-free medium supplemented with epidermal growth factor (EGF), basic fibroblast growth factor (bFGF), B-27 and heparin and cultured under non-adherent conditions for seven to ten days before sphere formation was scored by microscopy. Following this protocol with some adjustments in cell numbers, growth medium and supplements, several groups have explored *in vitro* stem cell potential from several cancer types such as breast[17], brain[18], pancreas[19] and colon[20] tumors. In ovarian carcinoma, we have recently reported feasibility of the spheres assay and compared its results to those collected in *in vivo* murine xenograft models[10]. We found that overexpression of the stem cell protein SOX2 enhanced both *in vitro* sphere formation as well as *in vivo* tumorigenicity of human ovarian carcinoma cells[10]. However, the frequency of sphere-initiating cells was higher than the frequency of

Copyright © 2015 Journal of Visualized Experiments

tumor-initiating cells measured *in vivo*[10] suggesting that either the sphere assay may lead to false positive results due to technical reasons or, alternatively, the *in vivo* assay may be inefficient and result in false negative results.

In this report, we analyze multi cell-based ovarian spheres assays in more detail, review the different protocols available in the literature and compare them to a single cell-based assay. We show that the single cell-based assay provides more accurate and reproducible results than multi cell-based assays, which can be highly influenced by the density of plated cells unless methylcellulose is added to the cultures to immobilize cells. However, also in single cell-based assays, *in vitro* sphere-initiating potential is observed at higher frequency than *in vivo* tumor-initiating potential.

Protocol

1. Generation of OVCAR-3 Human ovarian Carcinoma Cells Stably Transduced with Lentiviruses Containing the *SOX2* Regulatory Region Reporter Construct

1. Generate lentiviral particles by transfecting the HEK 293T-packaging cell line with a reporter construct recognizing a *SOX2* regulatory region as described[10,21].
   NOTE: The reporter construct further contains a destabilization domain of the ProteoTuner Shield System ahead of the tdTomato fluorescence protein. Shield1 binds to the destabilization domain thereby preventing the proteasome to degrade the fluorescence protein[22].
2. Transduce OVCAR-3 cells with lentiviral particles over a time period of 24 hr. Afterwards, remove the viral supernatant and wash the cells with phosphate buffered saline (PBS) and cultured in complete medium (RPMI supplemented with 10% FBS, 100 U/ml penicillin, 100 µg/ml streptomycin).
3. 48 hr later, 10 µg/ml puromycin were added to the cultures and maintained for 5 days to allow selection of properly transduced cells.

2. Preparation of Cell Sorting and Plating

1. Add Shield1 at 1:1,000 dilution 24 hr prior to cell sorting. Use stably transduced OVCAR-3 cells without Shield1 treatment as negative controls (**Figure 1**). Aspirate media from flask, wash cells with 1x PBS and trypsinize cells with 0.05% Trypsin-EDTA for 3 min.
2. Stop trypsin by using complete medium (see above), count cell numbers, centrifuge cells at 300 x g at RT (15 - 25 °C) for 5 min.
3. Decant supernatant and resuspend cells carefully in 0.5 - 1 ml sterile PBS.
4. Use 40 µm cell strainer cap filter to obtain single-cell suspension.
5. Adjust cell count to 5 million cells per ml.
6. Prepare ultra low-attachment 96-well plates with 100 µl spheres medium (MEGM supplemented with growth factors, cytokines, and supplements, B-27, heparine-sodium; or DMEM/F12 supplemented with growth factors, cytokines, and supplements, B-27, heparine-sodium with or without addition of 1% methylcellulose, see also **Table 1**). Optionally add antibiotics to the medium at a concentration of 100 U/ml penicillin and 100 µg/ml streptomycin to minimize the risk of possible contamination.
7. Sort RFP+ and RFP- cells into prepared 96-well plates from above, 1 cell per well (single cell-based spheres assay) and 100 cells per well (multi cell-based spheres assay), respectively. Perform sort on commercially available cell sorter (see **Materials**) using single cell mode, Sort setup: 100 µ nozzle, sheath pressure 20 psi, and yield mask 0, purity mask 32, phase mask 16.
8. Assess plating efficiency by microscopically scoring wells containing cells (for the single cell-based assay) and by counting cell numbers in individual wells (for the multi cell-based assay; **Figure 2**).
9. Incubate cells under standard conditions in spheres medium (for composition see **step 2.6**) at 37 °C and 5% CO_2. Supplement daily bFGF (20 ng/ml) and EGF (20 ng/ml).
10. After one week, count numbers of emerging tumor spheres using a standard microscope with 4X or 10X magnification and a fluorescence microscope to detect fluorescence signal from the integrated reporter system. Count spheres with a diameter exceeding 100 µm as “large” spheres, and spheres with a diameter 50 - 100 µm as “small” spheres (**Figure 3**). Be sure that you count real spheres and not cell clusters.
    NOTE: In single cell-based assays sphere formation is easier to score microscopically after 10 (versus 7) days of culture.
11. Calculate the proportion of sphere-forming cells in RFP+ and respectively RFP- cells in single cell-based assays (one 96-well plate for each individual experiment) or multi cell-based spheres assays (one well for each individual experiment) as presented by Shaw *et al.*[16]
    NOTE: Proportion of sphere forming cells (%) = (number of spheres) / (number of seeded cells) x 100

3. Serial Passaging of Spheres

1. Place the content of each well in an appropriate sterile tube and centrifuge at 300 x g for 10 min at RT. For multi cell-based spheres assays, collect together the spheres from one well. Wash the well 3 - 5 times with PBS and centrifuge 2 min longer. For single cell-based spheres assays, collect individual spheres. Due to the low numbers of cells, use 1.5 ml tubes for centrifugation and washing steps.
2. Remove supernatant and resuspend pellet in 200 µl of 0.05% Trypsin-EDTA.
3. In order to achieve optimal cell separation, incubate the cell suspension at 37 °C for 5 min in a soft shaker. Optimize trypsinization time for your cell line to lower cell death rate: if no large spheres is visible triturate gently using a 100 µl pipette tip. In case large spheres are still present, incubate with trypsin another 3 min and then proceed to the trituration step. In case of single cell-based assays make sure to optimize the time for optimal cell yield of living cells during the trypsinization step.
4. To inactivate the trypsin, add 500 µl complete medium and centrifuge at 300 x g for 10 min, in the case of single cell assays, centrifuge for additional 2 min.
5. Remove supernatant and resuspend cells carefully in spheres medium.
6. Use a 40 µm cell strainer cap filter to obtain a single-cell suspension.
7. In the case of using RFP+ and RFP- cells in multi cell-bassed assays, assess the percentage of fluorescent cells in each well after resuspension via flow cytometer analysis.

Copyright © 2015 Journal of Visualized Experiments

8. For serial replating assays of single cells, seed 1 cell per well into a new ultra low-attachment 96-well plate prepared as detailed above. From one individual sphere, seed approximately 20 individual wells. For replating assays of multi cell-based primary spheres, seed cells obtained from one well of primary spheres into a new 96-well plate and count the cell numbers next day by microscopy.
9. Assess the proportion of sphere-forming cells in secondary spheres assays using the formula described in **step 2.11**.

4. Result Analysis

1. Analyze results from experiments performed in independent triplicates and use two-sided Student's t-Test to analyze normally distributed values and otherwise Mann-Whitney-Tests for statistical analysis.

Representative Results

In conventional spheres assays, nearly 40% of RFP+ OVCAR-3 cells vs. 20% of RFP- cells gave rise to an individual tumor sphere in the primary spheres assay (**Figure 4A**). Moreover, spheres formed by RFP+ cells were larger in size than those formed by RFP- cells.

When plated in single cell-based assays, RFP+ cells also formed more spheres than RFP- cells, confirming the results above. However, there was a tendency towards generation of fewer spheres per plated in the single versus the multi cell-based assay (**Figure 4A,B**), indicating that in this assay sphere formation may be biased through technical artifacts such as mechanical sphere fusion or dissociation in the non-adherent culture medium.

To further explore these aspects, we compared the influence of cell plating density on spheres formation. We plated cells using limiting dilution from 1,000 cells to 1 cell per well in 96-well plates and found that the numbers of emerging spheres were highly dependent on the numbers of initially plated cells. Surprisingly, higher numbers of spheres were counted from lower numbers of plated cells in both MGEM and DMEM/F12-based media, demonstrating that indeed plating modalities highly bias results in this assay (**Figure 5**). In contrast, when cells were immobilized by adding 1% methylcellulose to DMEM/F12-based spheres medium[23,24] the efficiency of sphere formation was mostly independent of cell density.

To explore the influence of spheres culture conditions on CSC properties, we analyzed the percentage of cells expressing red fluorescence signal after 7 days of incubation in the spheres assay. We found that in multi cell-based spheres cultures approximately 35% of the cells from RFP+ spheres lost their red fluorescence signal after seven days of culture (**Figure 6A**), suggesting that they have undergone differentiation, while 65% retained a RFP+ signal suggesting self-renewal capacity. In contrast, cells from spheres generated from initially RFP- cells remained RFP negative (**Figure 6A**), indicating that they cannot re-establish stem cell potential under these conditions.

Fluorescence microscopy performed on spheres generated from single cells confirmed these results showing that single spheres derived RFP+ cells contained both RFP+ and RFP- cells while spheres derived from RFP- cells remained negative for the red signal.

Similar results were observed in replating assays from both conditions.

Copyright © 2015 Journal of Visualized Experiments

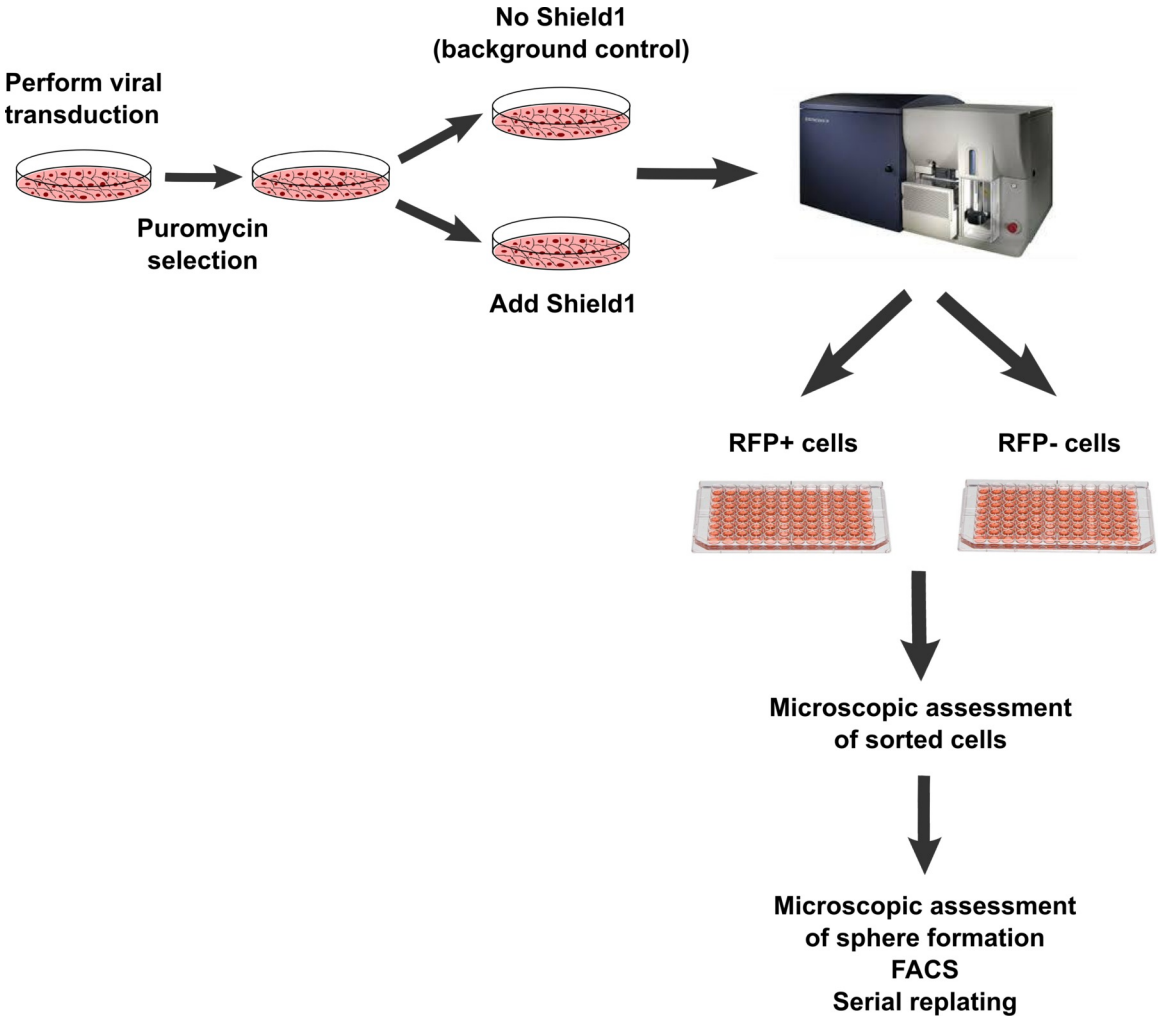

Figure 1. Workflow of lentiviral transduction, selection and sorting of RFP+ and RFP- cells. After lentiviral transduction and positive selection of successfully transduced cells via puromycin exposure, RFP- and RPF+ cells are sorted by FACS into individual wells of a 96-well plate in spheres medium. For multi cell-based spheres assays, 100 cells are placed into one well. Plating efficiency is assessed by microscopy performed after sorting. Spheres were scored by microscopy after seven to ten days, dissociated into single cells, analyzed via flow cytometry and replated into secondary spheres. Please click here to view a larger version of this figure.

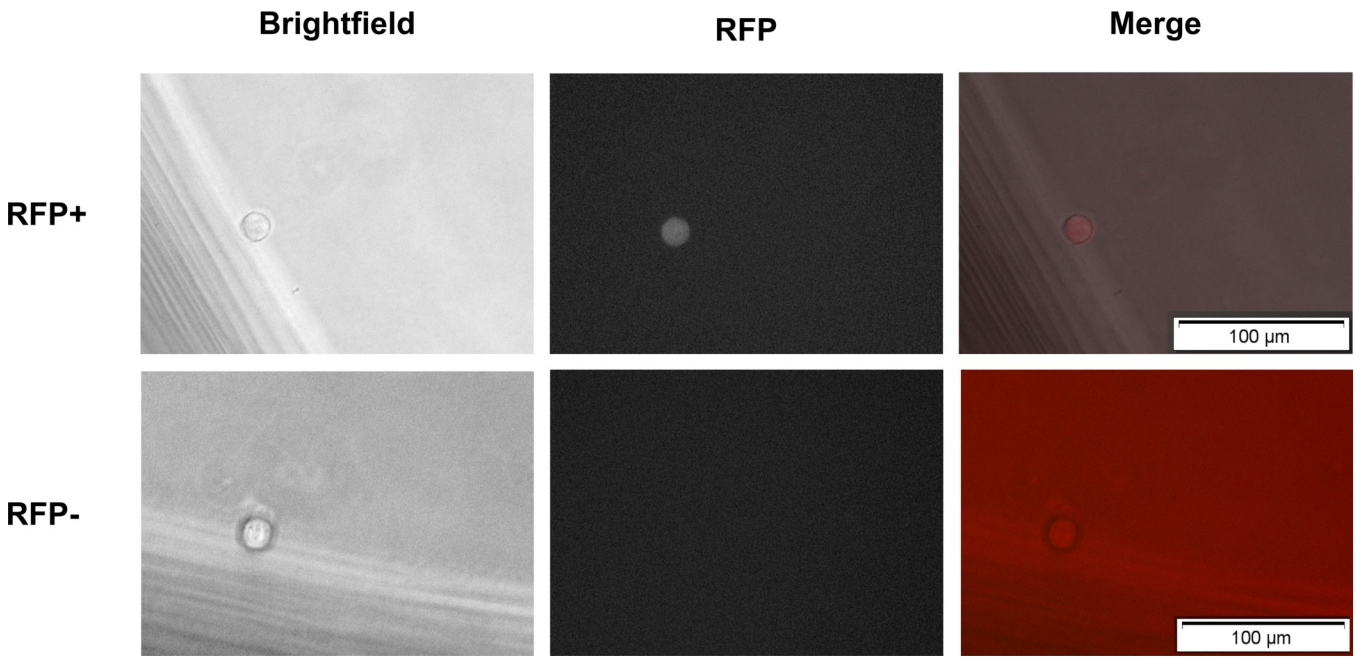

Figure 2. Imaging of sorted RFP+ and RFP- cells after plating. Single RFP+ and RFP- cells sorted into each well of a 96-well plate are analyzed for correct plating by using a (fluorescent) microscope. Please click here to view a larger version of this figure.

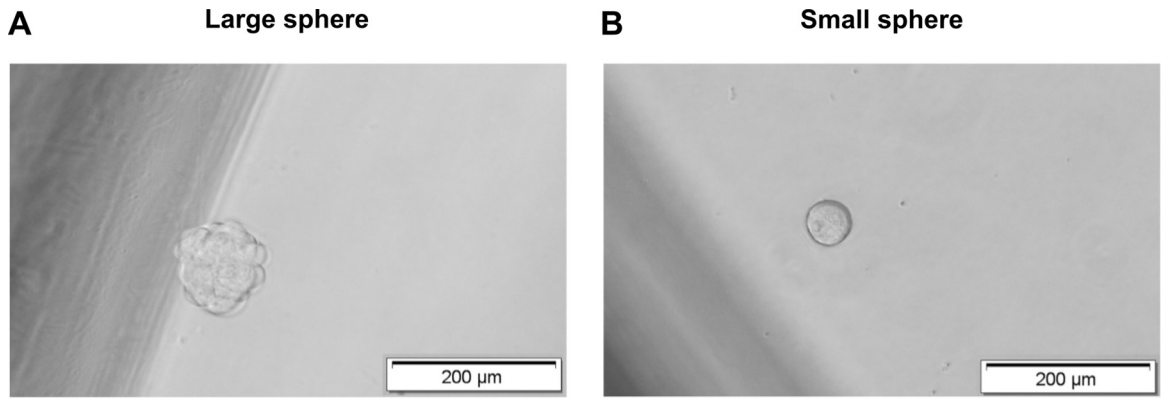

Figure 3. Analysis of spheres formation in single cell-based assays. Spheres formation is analyzed after seven to ten days. (**A**) Large (diameter > 100 µm) and (**B**) small (diameter 50 - 100 µm) spheres are distinguished microscopically based on size. Please click here to view a larger version of this figure.

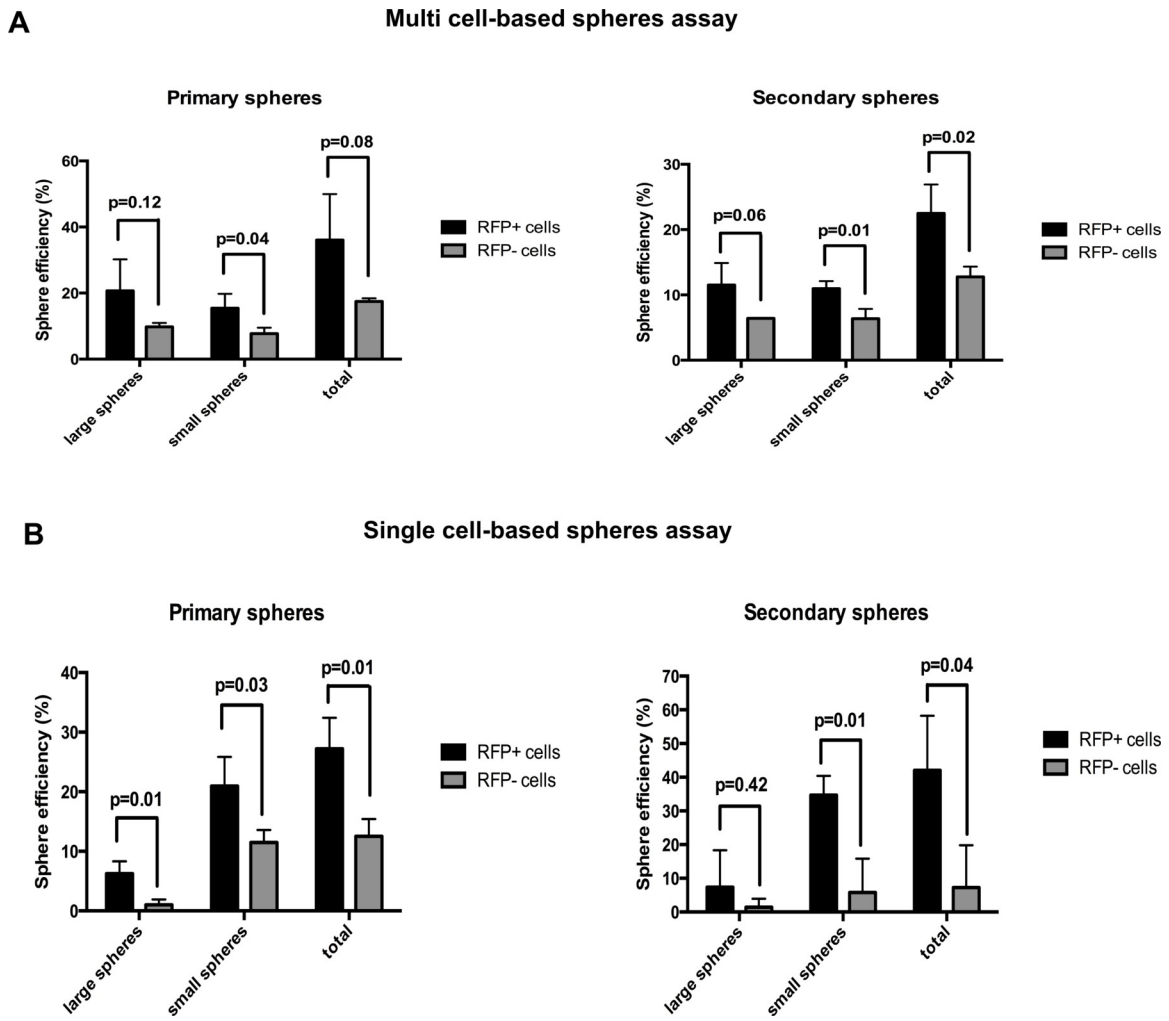

Figure 4. Efficiency of tumor spheres formation from RFP+ and RFP- OVCAR-3 cells in multi versus single-cell based spheres assays. Comparison of primary and secondary sphere efficiency from OVCAR-3 cells as assayed in multi (**A**) versus single cell-based spheres assays (**B**). Please click here to view a larger version of this figure.

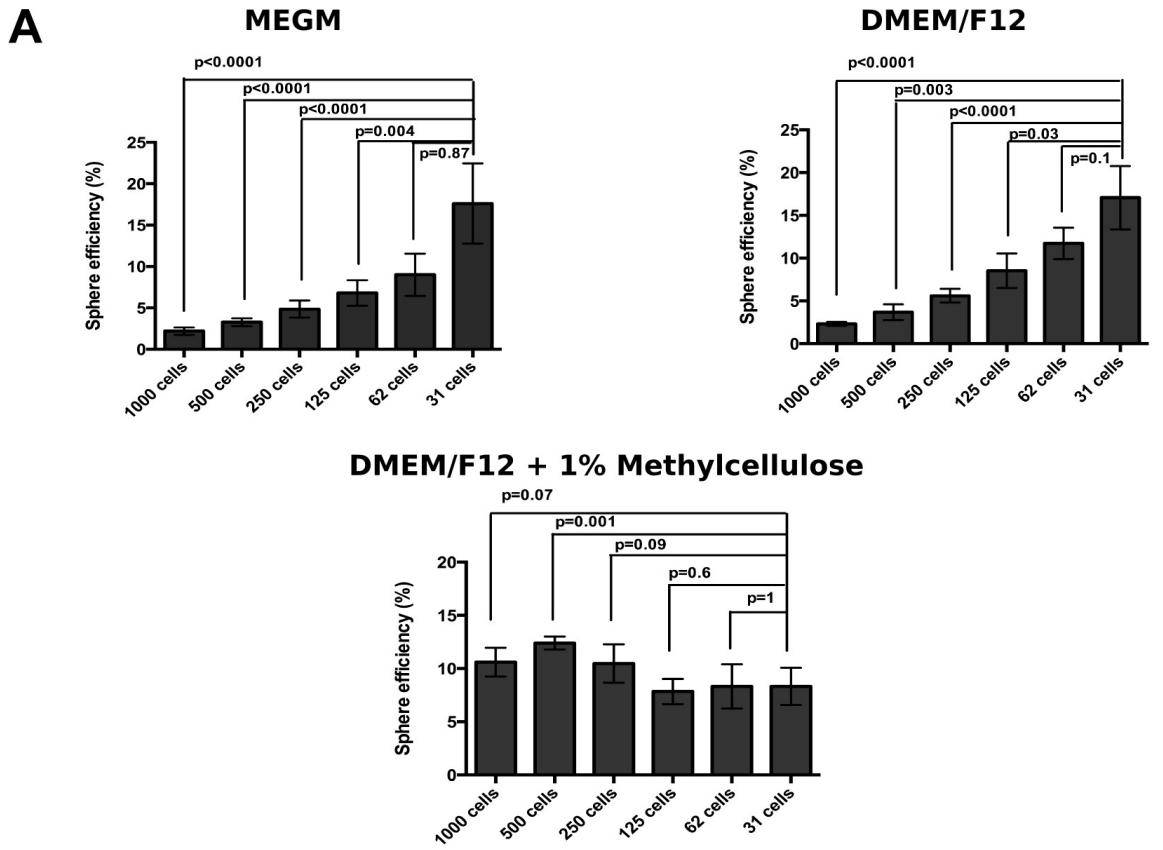

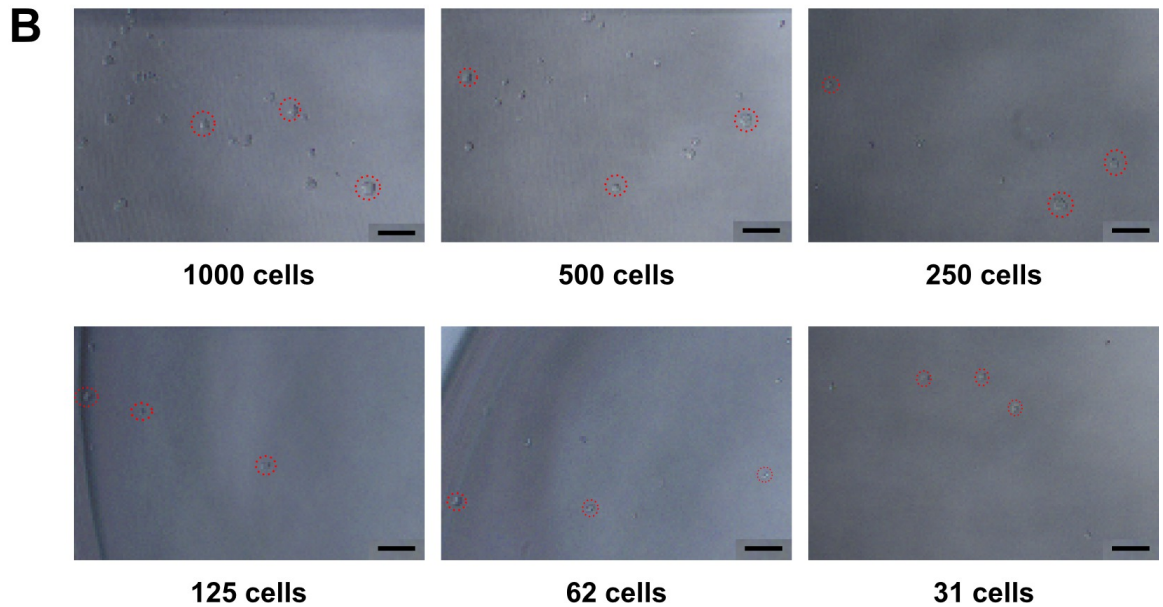

Figure 5. Cell plating density strongly impacts sphere counts from OVCAR-3 cells in the multi cell-based spheres assay performed in liquid but not in methylcellulose supplemented cultures. Use of different cell densities and growth media have been reported in the literature for ovarian cancer spheres assays. To analyze possible biases introduced by these variables, cells are plated at different densities in 200 µl of different spheres culture media (MGEM, DMEM/F12 with all supplements as detailed in the protocol section, or DMEM/F12 with all supplements and containing 1% methylcellulose) and sphere formation is scored after 7 days (**A**). Shown in (**B**) are microscopy pictures of cells plated at different densities taken one day after plating in DMEM/F12 spheres culture medium without methylcellulose. Note the cell clusters emerging at high cellular density as opposed to single cells seen in low density plates. Scale bar for pictures: 50 µm. Please click here to view a larger version of this figure.

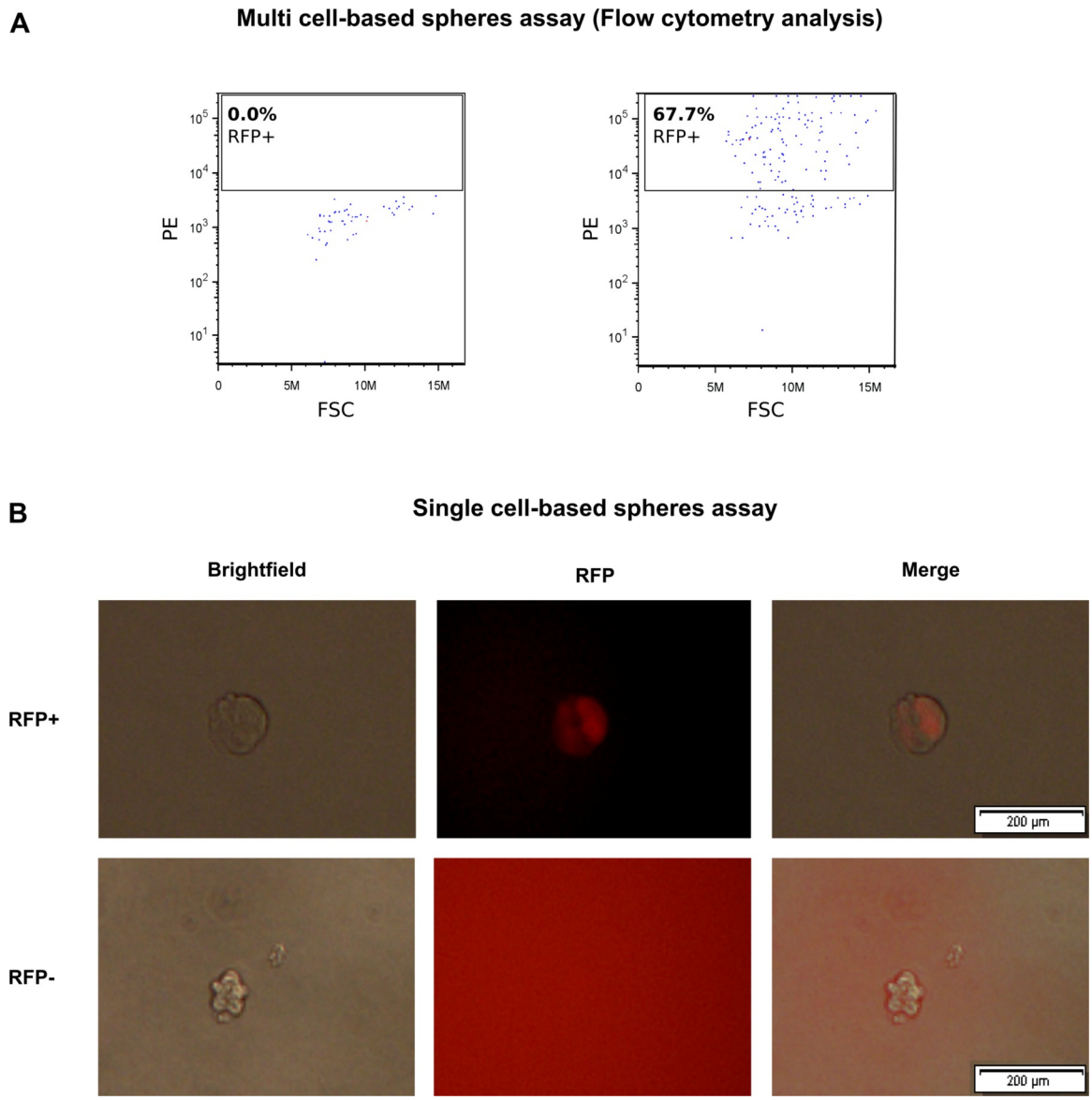

Figure 6. Analysis of RFP signal in tumor spheres formed from RFP+ and respectively RFP- OVCAR-3 cells. (**A**) Flow cytometry analysis for RFP signal in dissociated spheres derived from RFP+ and RFP- cells (multi cell-based spheres assay); (**B**) Microscopy of spheres derived from RFP+ and RFP- cells (single cell-based spheres assay) reveals heterogeneous RFP signal in spheres derived from RFP+ but not from RFP- cells. Pictures were taken at day 7 for conventional spheres and day 10 for single cell-based sphere assays. Note the larger size of spheres derived from RFP+ putative CSCs. Please click here to view a larger version of this figure.

Human ovarian cancer cell source	Basic medium	Supplements	Authors
OVCAR-3, Caov-3, primary material	MEGM	20 ng/ml rEGF, 20 ng/ml bFGF, B-27, 4 µg/ml heparin, hydrocortisone, insulin (SingleQuot kit)	Bareiss *et al.*
SKOV3	DMEM/F12	5 µg/ml insulin, 10 ng/ml rEGF, 10 ng/ml bFGF, 12 ng/ml LIF, 0.3% BSA	Li Ma *et al.*
A2780	DMEM/F12	5 µg/ml insulin, 20 ng/ml rEGF, 2% B-27, 0.4% BSA	Haiwei Wang *et al.*
SKOV3	DMEM/F12	5 µg/ml insulin, 20 ng/ml rEGF, 10 ng/ml bFGF, 2% B-27, 1 ng/ml hydrocortisone	Yong-Rui Du *et al.*
A2780, primary material	DMEM/F12	5 µg/ml insulin, 20 ng/ml rEGF, 10 ng/ml bFGF, 0.4% BSA	T. Xiang *et al.*
Primary material	DMEM/F12	5 µg/ml insulin, 10 ng/ml rEGF, 10 ng/ml bFGF, 12 ng/ml LIF, 0.3% BSA	*Te Liu et al.*
MLS	DMEM/F12	10 ng/ml insulin, 20 ng/ml rEGF, 20 ng/ml bFGF, 2% B-27	Soritau *et al.*
3AO	DMEM/F12	1 mg/ml insulin, 20 ng/ml rEGF, 20 ng/ml bFGF, 2% B-27	M. F. Shi *et al.*
Primary material	DMEM/F12	5 µg/ml insulin, 20 ng/ml rEGF, 10 ng/ml bFGF, 0.4% BSA	Shu Zhang *et al.*
Primary material	EBM-2 or X-VIVO	5 µg/ml insulin, 20 ng/ml rEGF	Ilona Kryczek *et al.*
OVCAR-3	MEGM	20 ng/ml rEGF, 20 ng/ml bFGF, B-27, 4 µg/mL heparin	Dongming Liang *et al.*

Table 1. Examples of different cell sources (cell lines and primary patient-derived tissue), media and supplements used for ovarian spheres assays in previous reports.

Discussion

Spheres cultures are a widely used method to assay cancer stem cell potential and enrich for stem-like cells in a wide range of human tumor cells[15,25,26]. Under these culture conditions, cancer cells that lack self-renewal ability are expected to differentiate and eventually undergo cell death. Although they may initially form cell clusters or even tumor spheres especially in primary assays, they are not able to sustain sphere-forming ability upon serial replating due to lack of self-renewing properties. Spheres assays are used as surrogate assays to identify CSCs and evaluate their frequency in whole tumor cell populations.

However, substantial variability can be observed between spheres assays performed following different published protocols[5,10,27-35] (**Table 1**). In our laboratory, we have previously published sphere formation from human ovarian carcinoma cells using MEGM supplemented with B-27, bFGF, Heparin and SingleQuot™ (containing insulin, rEGF and hydrocortisone). Other labs use whole DMEM/F12 Medium, while some add only B-27 and rEGF. In this report, multi cell-based spheres assay in OVCAR-3 cells were therefore performed using different conditions. Using MEGM or DMEM/F12 with all supplements no significant difference in sphere formation was observed in these cells (**Figure 5A**). In addition, some labs have speculated that EGF and FGF may be quickly degraded and have established protocols adding these growth factors daily to the medium. We therefore compared spheres assays performed in a medium in which EGF and FGF was added only at the beginning of the spheres assays with daily addition of EGF and FGF to the cell culture, and we find these assays to yield equivalent results in OVCAR-3 cells (data not shown), suggesting that the expensive and laborious daily supplementation with EGF and FGF may not always be necessary. Whether these results are applicable to cells from other ovarian cancer cell lines or primary samples, or under different experimental conditions remains to be determined.

However, we observed a substantial bias in the numbers of scored spheres introduced by another tested variable, the cell plating density. Surprisingly, wells seeded with lower numbers of cells showed higher numbers of spheres. Limiting cell mobility by 1% methylcellulose resulted in the same efficiency of sphere formation, independent on the number of initially plated cells. These results suggest that cell clumping and sphere fusion or disaggregation can occur modifying sphere numbers and leading to inaccurate results in multi cell-based spheres assays. When cells are plated at proper density, multi cell-based assays however lead to results rather comparable to data collected in single cell-based sphere assays (**Figure 4**). To further explore these results we compared single and multi cell-based assays using ovarian carcinoma cells sorted into putative CSCs via a recently published lentiviral RFP expressing reporter system for a *SOX2* regulatory region[10]. Indeed, both assays confirmed the enhanced primary and secondary sphere forming capacity of RFP+ versus RFP- cells (**Figure 4A,B**). Importantly, the higher numbers of spheres observed from RFP+ cells were not due to higher proliferative capacity of the *SOX2* expressing cells (data not shown), which is in

line with previous results showing that induction of *SOX2* promotes spheres formation and *in vivo* tumorigenicity without accelerating cell cycle progression[10].

Taken together, single cell-based spheres assays are more laborious and expensive but they result in more accurate data, which also is confirmed by the higher reproducibility of results between experiments. Since plating density highly influences results in multi cell-based suspension spheres assays, upfront titration of adequate plating density is required for each individual tumor cell type before assaying sphere formation using these assays. Alternatively, the more accurate single cell-based assays can be used upfront, or methylcellulose supplementation to improve accuracy of results by reducing mechanical artifacts. If sphere formation is compared between conditions where the genetic modification or drug treatment may severely alter viability of the cells, thereby decreasing cell density, single cell-based sphere assays may be mandatory to avoid false positive results.

In summary, under proper experimental conditions both the multi cell-based spheres assay and the single cell-based spheres assay are able to indicate differences in sphere potential between different cell populations (stem and non-stem cells). However, multi cell-based spheres assays which commonly are performed in liquid cultures are more susceptible to errors introduced by experimental design through plating density. Supplementation of methylcellulose (1%) to multi cell-based assays can limit artifacts related to cell clumping and sphere fusion. Based on these data, we recommend single cell-based spheres assays to be performed unless detailed titration analyses have been performed upfront and negative impact of experimental conditions on cell viability and thereby cell density has been ruled out. However, single cell-based spheres assays are more laborious and more expensive, and might not be required in each experimental setting. Methylcellulose-supplemented multi cell-based spheres assays may represent another alternative in some experimental settings.

Disclosures

The authors have nothing to disclose.

Acknowledgements

This study was supported by a grant from the Baden-Württemberg Stiftung (Adult Stem Cells Program II) awarded to C.L. We thank Dr. Martina Konantz for critical input and review of the manuscript. We thank Emmanuel Traunecker and Toni Krebs from the DBM FACS Facility (University Hospital Basel) for assistance with FACS sorting.

References

1. Pardal, R., Clarke, M. F., & Morrison, S. J. Applying the principles of stem-cell biology to cancer. *Nat Rev Cancer.* **3** (12), 895-902, doi:10.1038/nrc1232, (2003).
2. Reya, T., Morrison, S. J., Clarke, M. F., & Weissman, I. L. Stem cells, cancer, and cancer stem cells. *Nature.* **414** (6859), 105-111, doi:10.1038/35102167, (2001).
3. Ahmed, N., Abubaker, K., & Findlay, J. K. Ovarian cancer stem cells: Molecular concepts and relevance as therapeutic targets. *Mol Aspects Med.* **S0098-2997**(13) 00042-3, doi:10.1016/j.mam.2013.06.002, (2013).
4. Silva, I. A. *et al.* Aldehyde dehydrogenase in combination with CD133 defines angiogenic ovarian cancer stem cells that portend poor patient survival. *Cancer Res.* **71** (11), 3991-4001, doi:10.1158/0008-5472.CAN-10-3175, (2011).
5. Kryczek, I. *et al.* Expression of aldehyde dehydrogenase and CD133 defines ovarian cancer stem cells. *Int J Cancer.* **130** (1), 29-39, doi:10.1002/ijc.25967, (2012).
6. Stewart, J. M. *et al.* Phenotypic heterogeneity and instability of human ovarian tumor-initiating cells. *Proc Natl Acad Sci U S A.* **108** (16), 6468-6473, doi:10.1073/pnas.1005529108, (2011).
7. Ginestier, C. *et al.* ALDH1 is a marker of normal and malignant human mammary stem cells and a predictor of poor clinical outcome. *Cell Stem Cell.* **1** (5), 555-567, doi:10.1016/j.stem.2007.08.014, (2007).
8. Chang, B. *et al.* ALDH1 expression correlates with favorable prognosis in ovarian cancers. *Mod Pathol.* **22** (6), 817-823, doi:10.1038/modpathol.2009.35, (2009).
9. Cannistra, S. A. *et al.* CD44 variant expression is a common feature of epithelial ovarian cancer: lack of association with standard prognostic factors. *J Clin Oncol.* **13** (8), 1912-1921, (1995).
10. Bareiss, P. M. *et al.* SOX2 expression associates with stem cell state in human ovarian carcinoma. *Cancer Res.* **73** (17), 5544-5555, doi:10.1158/0008-5472.CAN-12-4177, (2013).
11. Pham, D. L. *et al.* SOX2 expression and prognostic significance in ovarian carcinoma. *Int J Gynecol Pathol.* **32** (4), 358-367, doi:10.1097/PGP.0b013e31826a642b, (2013).
12. Lengerke, C. *et al.* Expression of the embryonic stem cell marker SOX2 in early-stage breast carcinoma. *BMC Cancer.* **11** 42, doi:10.1186/1471-2407-11-42, (2011).
13. Lapidot, T. *et al.* A cell initiating human acute myeloid leukaemia after transplantation into SCID mice. *Nature.* **367** (6464), 645-648, doi:10.1038/367645a0, (1994).
14. Reynolds, B. A., & Weiss, S. Generation of neurons and astrocytes from isolated cells of the adult mammalian central nervous system. *Science.* **255** (5052), 1707-1710, doi: 10.1126/science.1553558, (1992).
15. Dontu, G. *et al.* In vitro propagation and transcriptional profiling of human mammary stem/progenitor cells. *Genes Dev.* **17** (10), 1253-1270, doi:10.1101/gad.1061803, (2003).
16. Shaw, F. L. *et al.* A detailed mammosphere assay protocol for the quantification of breast stem cell activity. *J Mammary Gland Biol Neoplasia.* **17** (2), 111-117, doi:10.1007/s10911-012-9255-3, (2012).
17. Leis, O. *et al.* Sox2 expression in breast tumours and activation in breast cancer stem cells. *Oncogene.* **31** (11), 1354-1365, doi:10.1038/onc.2011.338, (2012).

Copyright © 2015 Journal of Visualized Experiments

18. Higgins, D. M. *et al.* Brain tumor stem cell multipotency correlates with nanog expression and extent of passaging in human glioblastoma xenografts. *Oncotarget.* **4** (5), 792-801, (2013).
19. Wang, Y. J., Bailey, J. M., Rovira, M., & Leach, S. D. Sphere-forming assays for assessment of benign and malignant pancreatic stem cells. *Methods Mol Biol.* **980** 281-290, doi:10.1007/978-1-62703-287-2_15, (2013).
20. Li, Y. F., Xiao, B., Tu, S. F., Wang, Y. Y., & Zhang, X. L. Cultivation and identification of colon cancer stem cell-derived spheres from the Colo205 cell line. *Braz J Med Biol Res.* **45** (3), 197-204, doi:10.1590/S0100-879X2012007500015, (2012).
21. Wu, F. *et al.* Identification of two novel phenotypically distinct breast cancer cell subsets based on Sox2 transcription activity. *Cell Signal.* **24** (11), 1989-1998, doi:10.1016/j.cellsig.2012.07.008, (2012).
22. Banaszynski, L. A., Chen, L. C., Maynard-Smith, L. A., Ooi, A. G., & Wandless, T. J. A rapid, reversible, and tunable method to regulate protein function in living cells using synthetic small molecules. *Cell.* **126** (5), 995-1004, doi:10.1016/j.cell.2006.07.025, (2006).
23. Kawase, Y., Yanagi, Y., Takato, T., Fujimoto, M., & Okochi, H. Characterization of multipotent adult stem cells from the skin: transforming growth factor-beta (TGF-beta) facilitates cell growth. *Exp Cell Res.* **295** (1), 194-203, doi:10.1016/j.yexcr.2003.12.027, (2004).
24. Walia, V. *et al.* Loss of breast epithelial marker hCLCA2 promotes epithelial-to-mesenchymal transition and indicates higher risk of metastasis. *Oncogene.* **31** (17), 2237-2246, doi:10.1038/onc.2011.392, (2012).
25. Leung, E. L. *et al.* Non-small cell lung cancer cells expressing CD44 are enriched for stem cell-like properties. *PLoS One.* **5** (11), e14062, doi:10.1371/journal.pone.0014062, (2010).
26. Bertolini, G. *et al.* Highly tumorigenic lung cancer CD133+ cells display stem-like features and are spared by cisplatin treatment. *Proc Natl Acad Sci U S A.* **106** (38), 16281-16286, doi:10.1073/pnas.0905653106, (2009).
27. Ma, L., Lai, D., Liu, T., Cheng, W., & Guo, L. Cancer stem-like cells can be isolated with drug selection in human ovarian cancer cell line SKOV3. *Acta Biochim Biophys Sin (Shanghai).* **42** (9), 593-602, doi:10.1093/abbs/gmq067, (2010).
28. Wang, H., Zhang, Y., & Du, Y. Ovarian and breast cancer spheres are similar in transcriptomic features and sensitive to fenretinide. *Biomed Res Int.* **2013** 510905, doi:10.1155/2013/510905, (2013).
29. Du, Y. R. *et al.* Effects and mechanisms of anti-CD44 monoclonal antibody A3D8 on proliferation and apoptosis of sphere-forming cells with stemness from human ovarian cancer. *Int J Gynecol Cancer.* **23** (8), 1367-1375, doi:10.1097/IGC.0b013e3182a1d023, (2013).
30. Xiang, T. *et al.* Interleukin-17 produced by tumor microenvironment promotes self-renewal of CD133 cancer stem-like cells in ovarian cancer. *Oncogene.* doi:10.1038/onc.2013.537, (2013).
31. Liu, T., Cheng, W., Lai, D., Huang, Y., & Guo, L. Characterization of primary ovarian cancer cells in different culture systems. *Oncol Rep.* **23** (5), 1277-1284, doi:10.3892/or_00000761, (2010).
32. Soritau, O. *et al.* Enhanced chemoresistance and tumor sphere formation as a laboratory model for peritoneal micrometastasis in epithelial ovarian cancer. *Rom J Morphol Embryol.* **51** (2), 259-264, (2010).
33. Shi, M. F. *et al.* Identification of cancer stem cell-like cells from human epithelial ovarian carcinoma cell line. *Cell Mol Life Sci.* **67** (22), 3915-3925, doi:10.1007/s00018-010-0420-9, (2010).
34. Zhang, S. *et al.* Identification and characterization of ovarian cancer-initiating cells from primary human tumors. *Cancer Res.* **68** (11), 4311-4320, doi:10.1158/0008-5472.CAN-08-0364, (2008).
35. Liang, D. *et al.* The hypoxic microenvironment upgrades stem-like properties of ovarian cancer cells. *BMC Cancer.* **12** 201, doi:10.1186/1471-2407-12-201, (2012).

Copyright © 2015 Journal of Visualized Experiments

Paper II

Molecular and functional interactions between AKT and SOX2 in breast carcinoma.

Schaefer T*, **Wang H***, Mir P, Konantz M, Pereboom TC, Paczulla AM, Merz B, Fehm T, Perner S, Rothfuss OC, Kanz L, Schulze-Osthoff K, Lengerke C.

Oncotarget. 2015 Dec 22;6(41):43540-56.

Molecular and functional interactions between AKT and SOX2 in breast carcinoma

Thorsten Schaefer[1,*], Hui Wang[1,2,*], Perihan Mir[2], Martina Konantz[1], Tamara C. Pereboom[1], Anna M. Paczulla[1], Britta Merz[3], Tanja Fehm[4], Sven Perner[5], Oliver C. Rothfuss[3], Lothar Kanz[2], Klaus Schulze-Osthoff[3,6], Claudia Lengerke[1,2,7]

[1]Department of Biomedicine, University Hospital Basel, Basel, Switzerland

[2]Department of Internal Medicine II, University Hospital Tuebingen, Tuebingen, Germany

[3]Interfaculty Institute of Biochemistry, University of Tuebingen, Tuebingen, Germany

[4]Women's Hospital, University Hospital Duesseldorf, Duesseldorf, Germany

[5]Institute of Pathology, University of Luebeck, Luebeck, Germany

[6]German Cancer Consortium (DKTK) and German Cancer Research Center (DKFZ), Heidelberg, Germany

[7]Clinic for Hematology, University Hospital Basel, Basel, Switzerland

[*]These authors have contributed equally to this work

Correspondence to: Claudia Lengerke, **e-mail:** claudia.lengerke@unibas.ch

Keywords: *SOX2, AKT, breast carcinoma, cancer stem cells, clonogenicity*

Received: *August 16, 2015* ***Accepted:*** *October 10, 2015* ***Published:*** *October 20, 2015*

ABSTRACT

The transcription factor SOX2 is a key regulator of pluripotency in embryonic stem cells and plays important roles in early organogenesis. Recently, SOX2 expression was documented in various cancers and suggested as a cancer stem cell (CSC) marker. Here we identify the Ser/Thr-kinase AKT as an upstream regulator of SOX2 protein turnover in breast carcinoma (BC). SOX2 and pAKT are co-expressed and co-regulated in breast CSCs and depletion of either reduces clonogenicity. Ectopic SOX2 expression restores clonogenicity and *in vivo* tumorigenicity of AKT-inhibited cells, suggesting that SOX2 acts as a functional downstream AKT target. Mechanistically, we show that AKT physically interacts with the SOX2 protein to modulate its subcellular distribution. AKT kinase inhibition results in enhanced cytoplasmic retention of SOX2, presumably via impaired nuclear import, and in successive cytoplasmic proteasomal degradation of the protein. In line, blockade of either nuclear transport or proteasomal degradation rescues SOX2 expression in AKT-inhibited BC cells. Finally, AKT inhibitors efficiently suppress the growth of SOX2-expressing putative cancer stem cells, whereas conventional chemotherapeutics select for this population. Together, our results suggest the AKT/SOX2 molecular axis as a regulator of BC clonogenicity and AKT inhibitors as promising drugs for the treatment of SOX2-positive BC.

INTRODUCTION

Pluripotency-associated proteins like SOX2 and OCT4 are key regulators of embryonic stem cells and foster the reprogramming of terminally differentiated somatic cells back to a pluripotent stem cell state [1]. SOX2 is furthermore a major regulator of embryonic development and more recently was demonstrated to determine cellular identity in certain adult stem and progenitor cells [2]. Consistent with the notion that stemness and embryonic pathways can play oncogenic roles, SOX2 expression was documented in several cancers, especially of endodermal, epithelial and neural origin [3–13]. In the breast, SOX2 expression has not been reported in healthy tissues but is detectable across different breast carcinoma (BC) subtypes [14] and particularly prominent also in certain BC-derived metastases [15]. Interestingly, SOX2 expression in BC is mostly confined to a minor subset of tumor cells and detectable at early stages of the disease as well as at relapse, suggesting that

it is involved in BC stem cell biology and might represent a genetic driver event [14, 16].

Another major molecular regulator of both embryonic and cancer stem cell self-renewal is the kinase AKT. The canonical PI3K/AKT pathway is known to influence cell metabolism, growth, proliferation and survival and its deregulation is a common determinant in various cancers [17–19]. In healthy mammary epithelial cells, constitutive PI3K/AKT signaling supports the outgrowth of a stem cell population, which can be antagonized by the PI3K/AKT cross-reactive inhibitor perifosine [20]. Furthermore, inhibition of AKT was shown to affect cancer stem cell populations including breast CSCs [21, 22], the underlying molecular details however remain largely unknown.

In the present study we hypothesize that AKT influences BC stem cells by regulating their SOX2 protein levels. We employ the tumor sphere formation assay as a surrogate assay identifying clonogenic tumor cells with CSC-like features in BC cell lines as well as patient-derived cells [23, 24]. We further demonstrate that in BC cells AKT directly interacts with SOX2 and stabilizes the protein by promoting its nuclear localization. Inhibition of AKT kinase activity induces successive proteasomal clearance of SOX2 protein in the cytosol. Underscoring the particular significance of this post-translational regulatory circuit, ectopic overexpression of *SOX2* rescues clonogenicity and *in vivo* tumorigenicity in AKT inhibitor-treated BC cells. Further supporting the notion that disease-initiating breast CSCs are dependent on AKT signaling, treatment with AKT inhibitors suppresses total cell growth, whereas conventional cytostatics impose a selective advantage on BC cells with active *SOX2*-regulatory elements. Therefore, inhibition of the AKT pathway may provide additional benefit for the treatment of SOX2-positive BC patients.

RESULTS

The role of *SOX2* in breast CSCs

We initially investigated *SOX2* mRNA expression in eight human BC cell lines available in the laboratory (Figure 1A and Supplementary Figure 1). Of these, MCF7, BT474 and T47D cells were selected for further analysis to cover a dynamic range of endogenous SOX2 expression levels (Figure 1A). The remaining cell lines showed modest *SOX2* expression under standard cultivation conditions (2D), but a clear induction of *SOX2* mRNA under 3D conditions that favor the outgrowth of stem cells (Supplementary Figure 1). SOX2 expression was additionally examined on mRNA level in a panel of 10 patient-derived primary cells (Figure 1B). Two SOX2-expressing samples (P1 and P2) were selected for reference experiments.

To verify a functional significance of *SOX2* for BC clonogenicity and to assure its relevance in the particular experimental settings used here, we first investigated the effect of *SOX2* knockdown and inducible overexpression on tumor sphere formation *in vitro*. To this end, MCF7 cells displaying a high endogenous SOX2 expression were treated with two specific *SOX2* shRNAs or respective control GFP-lentiviral particles and correctly transduced cells were isolated by flow cytometry. Effective knockdown of *SOX2* expression in GFP-positive cells was verified by qRT-PCR and immunoblotting (Figure 1C and Supplementary Figure 2). Confirming functional relevance for clonogenicity, *SOX2* knockdown cells displayed a significantly reduced sphere formation capacity in comparison to control cells (Figure 1D, Supplementary Figure 2C, and [25]). To monitor a stimulatory effect of SOX2 on sphere formation, the human *SOX2* gene was N-terminally fused to *mCherry*, cloned under the control of a doxycycline-dependent Tet_{ON} induction system, and lentivirally integrated in T47D cells that showed low endogenous *SOX2* expression (see above). Transduced cells were selected via puromycine resistance and efficient induction of *SOX2* expression following doxycycline treatment confirmed by qRT-PCR and immunoblotting (Figure 1E). Indeed, spheres formation was only observed from SOX2-induced T47D cells, whereas mock-treated control cells were only able to associate in irregularly shaped aggregates (Figure 1F and Supplementary Figure 3).

AKT inhibition targets clonogenic BC cells

Activating mutations in the AKT pathway are amongst the most frequent somatic aberrations observed in breast cancer [26]. Furthermore, the PI3K/AKT pathway has been implicated in healthy and malignant breast stem cell biology [20]. Supporting these notions, we could show an induction of functionally active pAKT (i.e. AKT carrying a pSer473 auto-phosphorylation signature) along with enhanced SOX2 expression in 3D- versus 2D-cultured cells, albeit total AKT levels remained largely unchanged (Figure 2A and 2B). We therefore reasoned that AKT activity and SOX2 expression could be functionally linked in BC stem cells.

To validate this assumption and to test whether AKT inhibitors may effectively target SOX2-positive breast CSCs, a SRR (*SOX2* regulatory region 1)-based stem cell reporter was stably introduced into the MCF7 cell line [24, 27]. Treatment with conventional cytostatics (e.g. cisplatin, paclitaxel) clearly reduced overall cell growth (Figure 2C), but enhanced the frequency of reporter-positive CSCs in the surviving cell fraction (Figure 2D). By contrast, the pan-AKT inhibitor MK-2206 impaired overall BC cell growth, but did not allow the selective outgrowth of *SOX2*-positive cells (Figure 2C and 2D).

Next, we performed sphere formation assays in presence or absence of MK-2206. Indeed, AKT inhibition resulted in a dose-dependent reduction of sphere formation throughout all analyzed BC cell lines and primary cells (Figure 2E). Taken together, AKT kinase activity influences CSC functions and is a prerequisite for BC cell clonogenicity.

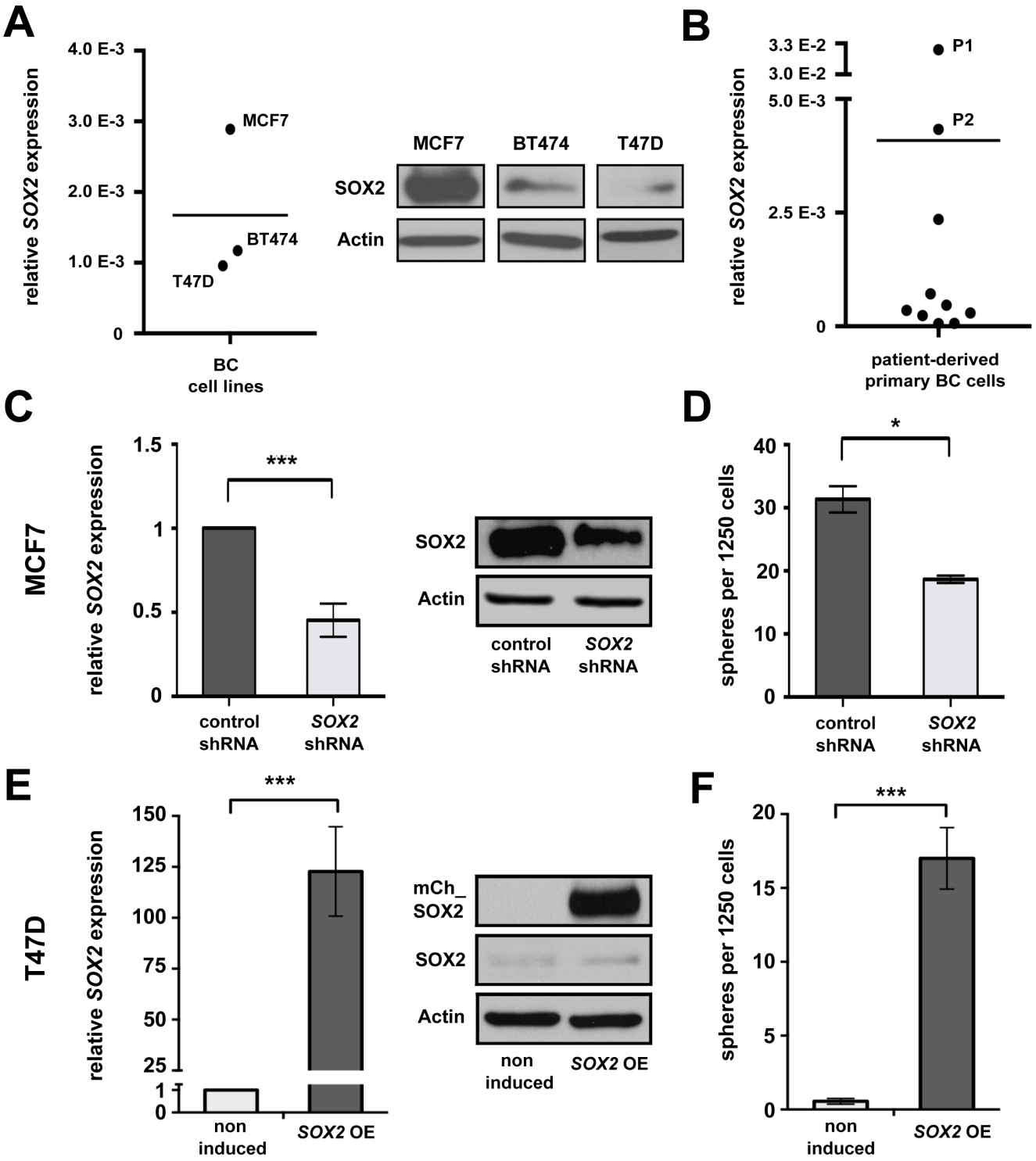

Figure 1: SOX2 is expressed in BC and promotes clonogenicity. **(A)** Endogenous SOX2 mRNA (left) and protein (right) expression in BC cell lines MCF7, BT474, and T47D propagated under standard (2D) cultivation conditions. Indicated are mRNA expression levels relative to *GAPDH*. Midline illustrates average *SOX2* expression in the three cell lines analyzed. Actin is shown as a protein loading control. **(B)** Relative *SOX2 mRNA* expression in 10 primary patient-derived BC samples (P1 and P2: samples showing highest endogenous *SOX2* expression, midline to illustrate average). **(C)** Reduced *SOX2* mRNA and protein expression, and **(D)** impaired sphere formation in MCF7 cells transduced with *SOX2* shRNA vs. control lentiviral particles. **(E)** Inducible *mCherry-SOX2* expression in stably transfected T47D cells at 24 hours of induction with 1 µg/ml of doxycycline, as verified by qRT-PCR (left) and immunoblotting (right). **(F)** Ectopic expression of a *mCherry-SOX2* fusion protein (*SOX2 OE*) induces sphere formation in T47D cells. Samples were incubated in 3D medium in the absence or presence of doxycycline (1 µg/ml) for 5 days.

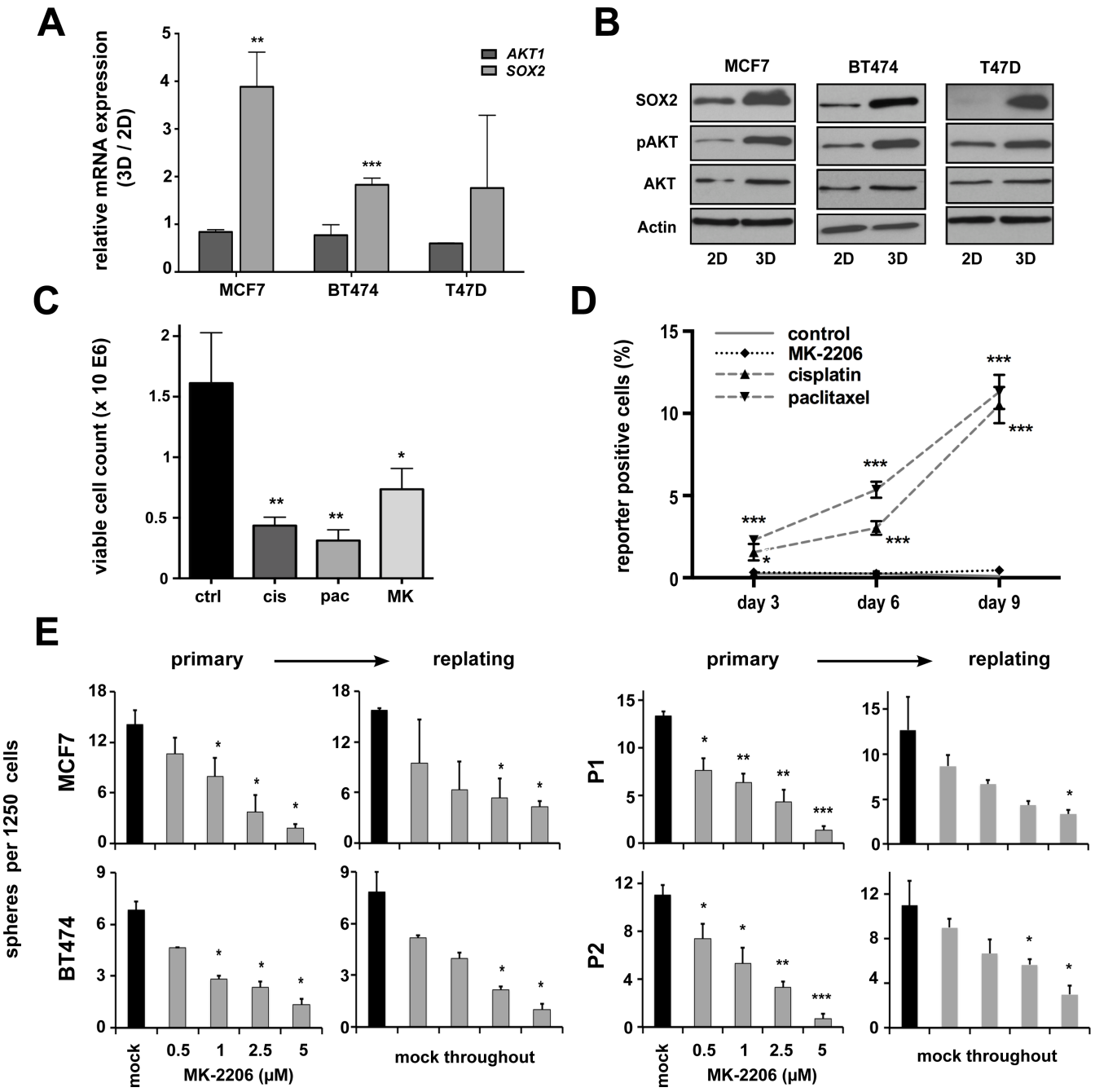

Figure 2: pAKT expression is induced in putative breast CSCs and regulates BC clonogenicity. (A) Induction of *SOX2* but not *AKT1* gene expression in BC cell lines grown under conditions enriching for CSCs (3D) versus conventional cultures (2D). Indicated are fold changes in expression of the indicated target genes (ΔΔCt of either *AKT1* or *SOX2* mRNA relative to *GAPDH*) in cells grown under 3D versus 2D conditions (3D/2D). **(B)** Corresponding immunoblots document co-induction of SOX2 and pAKT proteins in 3D-cultures, whereas total AKT levels remain largely unchanged. **(C)** Treatment with conventional chemotherapeutic drugs (cisplatin, cis, 5 μM; paclitaxel, pac, 5 nM) or the AKT inhibitor MK-2206 (MK, 1 μM) inhibits the growth of MCF7 cells (50.000 cells seeded, 72 hour follow-up). **(D)** Enrichment of SRR1-expressing putative CSCs in cisplatin or paclitaxel but not MK-2206 treated cells. Indicated is the percentage of SRR reporter-positive MCF7 cells in the surviving cell fraction, as detected by flow cytometry at indicated times. Dead cells were eliminated by DAPI staining and analyses performed on the gated live cell population. **(E)** Dose-dependent suppression of sphere formation by MK-2206 in primary and replating sphere assays (black bars: mock-treated cells; grey bars: MK-2206-treated cells). Note that in replating assays sphere formation was impaired despite the removal of inhibitor. BC cell lines (left), patient-derived primary BC cells (right).

pAKT is an upstream regulator of SOX2 protein expression in BC

Since both SOX2 and pAKT proteins regulate BC clonogenicity, and AKT kinase inhibitors effectively target cells with active *SOX2*-regulatory elements (SRR), we hypothesized that pAKT and SOX2 molecularly interact in breast CSCs. To further explore this notion, SOX2 expression was analyzed in BC cells treated with the pan-AKT inhibitor MK-2206. Indeed, profoundly reduced SOX2 protein levels were observed along with pAKT inhibition upon treatment with MK-2206 (Figure 3A and 3B). This inhibitory effect was dose-dependent, commenced successively, and was consistently observed throughout all analyzed cell lines and patient-derived BC samples. Conversely, induction of pAKT upon transfection with a myristoylated *AKT1* construct clearly up-regulated SOX2 protein (Figure 3C). Together, these data suggest that SOX2 is a pAKT downstream target. To further explore this hypothesis and to control for putative off-target effects of MK-2206, the upstream PI3K inhibitors wortmannin and GDC-0941, as well as the alternative AKT inhibitor Akti1/2 were used to block AKT kinase activity. SOX2 protein depletion was uniformly observed in all these conditions (Figure 3D and 3E), confirming a functional dependence of SOX2 protein expression on canonical PI3K/AKT signaling. Importantly, inhibition of the AKT-downstream target mTOR by rapamycin did not suppress SOX2, albeit efficient inhibition of RPS6 phosphorylation confirmed drug efficacy (Figure 3D). We conclude that AKT kinase is an immediate upstream regulator of SOX2 turnover in BC, and that the disappearance of SOX2 protein in AKT-inhibited cells is not primarily explained by altered *de novo* protein synthesis (Figure 3E).

SOX2 expression restores clonogenicity and *in vivo* tumor initiation capacity in anti-AKT treated BC cells

Interestingly, BC cells treated with MK-2206 showed a dose-dependent reduction in sphere formation not only in primary but also in replating sphere assays where MK-2206 was not anymore added to the cultures (Figure 2E, right panels). To further explore whether this effect was due to continuous pAKT suppression in the absence of the inhibitor or due to effects on cell fate established during the brief treatment window, additional serial replating experiments and corresponding immunoblot analyses were performed. Indeed, while effective suppression of both pAKT and SOX2 protein by MK-2206 was confirmed under 3D cultivation conditions (Figure 4A, left), a sequential re-appearance of pAKT and subsequently also of SOX2 protein was noted upon depletion of the inhibitor. Matching these molecular results, a gradual recovery of sphere formation capacity was observed (Figure 4A and 4B).

To more directly investigate the functional relevance of SOX2 as a downstream pAKT target, SOX2 was ectopically expressed in MK-2206 treated BC cells using a conditional lentiviral *mCherry-SOX2* fusion construct. Efficient dose-dependent induction of *mCherry-SOX2* by doxycycline was confirmed by immunoblot analysis and fluorescence microscopy, and had no overt effect on endogenous AKT/pAKT levels (Figure 4C and Supplementary Figure 4). Supporting the notion that SOX2 is a downstream target of AKT, enforced SOX2 expression partially rescued sphere formation in AKT-inhibited cells (Figure 4D). However, SOX2-expressing spheres derived from AKT inhibitor-treated cells displayed a growth disadvantage in comparison to mock-treated controls suggesting that, in contrast to clonogenicity, proliferation-related defects may not be concomitantly rescued by SOX2. This assumption was supported by cell-cycle analyses, revealing a reduced cell proliferation in AKT-inhibited cells that was not rescued by *SOX2* expression. Furthermore, treatment with AKT inhibitors impaired the expression of several cell cycle-regulators (e.g. cyclin D1, cyclin E, and CDK2), which could not be restored by *SOX2* expression (Supplementary Figure 5).

To investigate the relevance of the described AKT/SOX2 molecular axis *in vivo*, we next performed xenotransplantation experiments of human BC cells that were micro-injected into the yolk sac of zebrafish embryos, and quantified tumor formation in dependence of AKT and SOX2. Of note, xenotransplantation into zebrafish has been applied in studies of BC tumorigenicity before [28, 29] and was used here because of its advantages in monitoring *in vivo* tumor induction and drug treatment effects [30]. First, fluorescently labeled control or SOX2-overexpressing T47D cells were administered into the yolk sac of zebrafish embryos at 48 hours post fertilization and tumor formation quantified after 5 days of continuous incubation in the presence of doxycycline (Figure 5A). In line with data from murine studies, SOX2 overexpression enhanced tumor induction also in xenotransplanted fish (Figure 5B). Moreover, treatment with AKT inhibitors was able to fully suppress tumor formation (Figure 5C and 5D) while, in agreement with our *in vitro* findings, induction of *SOX2* expression was able to partially restore tumor formation inspite of AKT inhibition (Figure 5C). Taken together, this series of experiments indicate that AKT regulates BC cell clonogenicity and *in vivo* tumorigenicity via modulation of SOX2 protein levels.

pAKT and SOX2 proteins physically interact in BC cells

Next, we interrogated the molecular basis of the upstream regulatory effect of AKT on SOX2 protein expression. Cell fractionation experiments in different BC lines indicated a nucleo-cytoplasmatic segregation of SOX2 protein at steady-state, and a partial co-fractionation

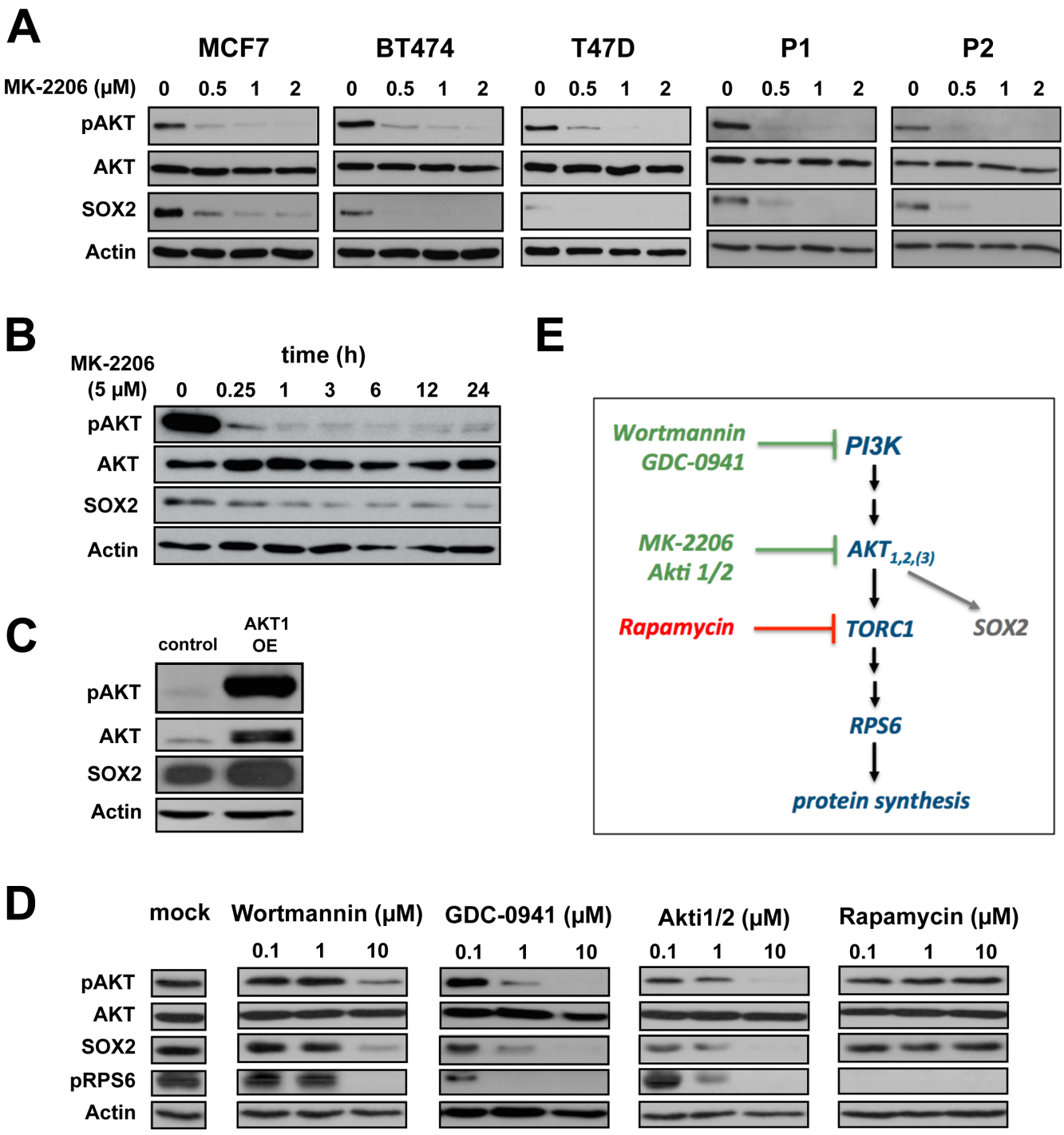

Figure 3: AKT is an upstream regulator of SOX2 protein expression. **(A)** Dose-dependent co-depletion of pAKT and SOX2 proteins following MK-2206 treatment in BC cell lines (MCF7, BT474, T47D) and patient-derived cells (P1, P2) within 48 hours of incubation. Note the grossly unaltered levels of total AKT. Anti-actin staining is shown for reference. **(B)** Temporal resolution of pAKT and SOX2 protein expression in MCF7 cells upon AKT inhibition throughout an observation window of 24 hours. **(C)** Transfection with myristoylated *AKT1* induces both pAKT and SOX2 protein expression in MCF7 cells. **(D)** Confirmation of SOX2 protein depletion by the alternative AKT kinase inhibitor Akti1/2 and upstream PI3K inhibitors (wortmannin and GCD-0941) in MCF7 cells. AKT downstream inhibitor rapamycin has no impact on SOX2 expression, instead. Functional integrity of reagents was verified by uniform depletion of pRPS6. Mock-treated control lanes are shown at the left. **(E)** Schematic illustration of the canonical PI3K/AKT/TORC1 pathway. Green: drugs that impair SOX2 protein expression.

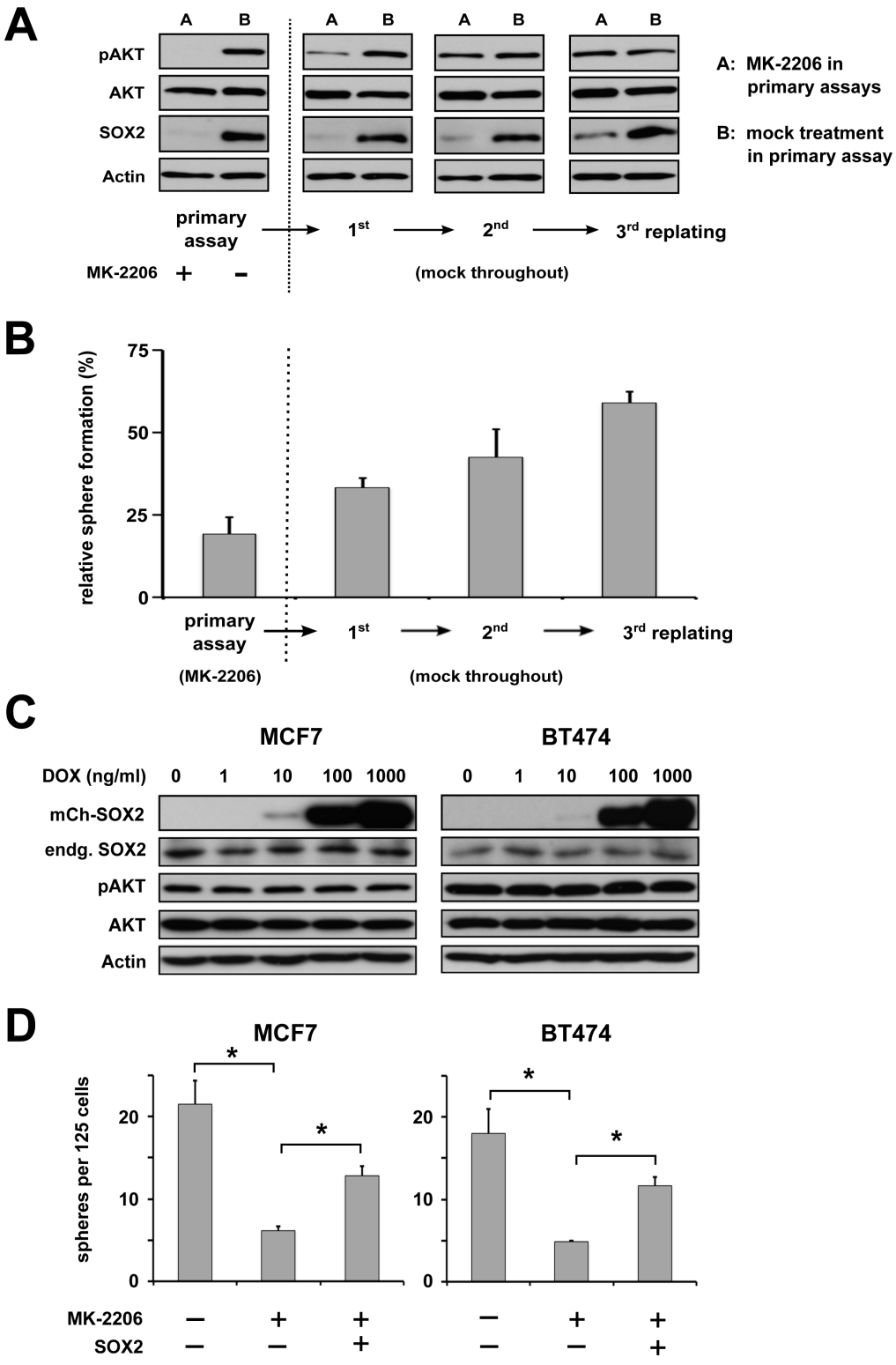

Figure 4: AKT regulates BC clonogenicity via SOX2. **(A)** Primary and serial replating sphere assays document a tight dependence of SOX2 protein expression and **(B)** clonogenicity on pAKT. MK-2206 treatment was ceased after the primary assay cycle. Note a successive recurrence of pAKT and slightly delayed also SOX2 protein in replating assay cycles, which coincides with restoration of sphere formation capacity. Indicated is the percentage of sphere formation relative to replated, mock-treated controls. **(C)** and **(D)** Dose-dependent ectopic induction of a *mCherry-SOX2* fusion protein in the indicated BC cell lines does not affect endogenous SOX2 and pAKT/AKT protein levels (C), but rescues sphere formation in MK-2206-treated cells (D), indicating that SOX2 is as a functional downstream target of pAKT (left: untreated controls, center: 5 μM MK-2206 followed by mock treatment, right: 5 μM MK-2206 and subsequent induction of *mCherry-SOX2*).

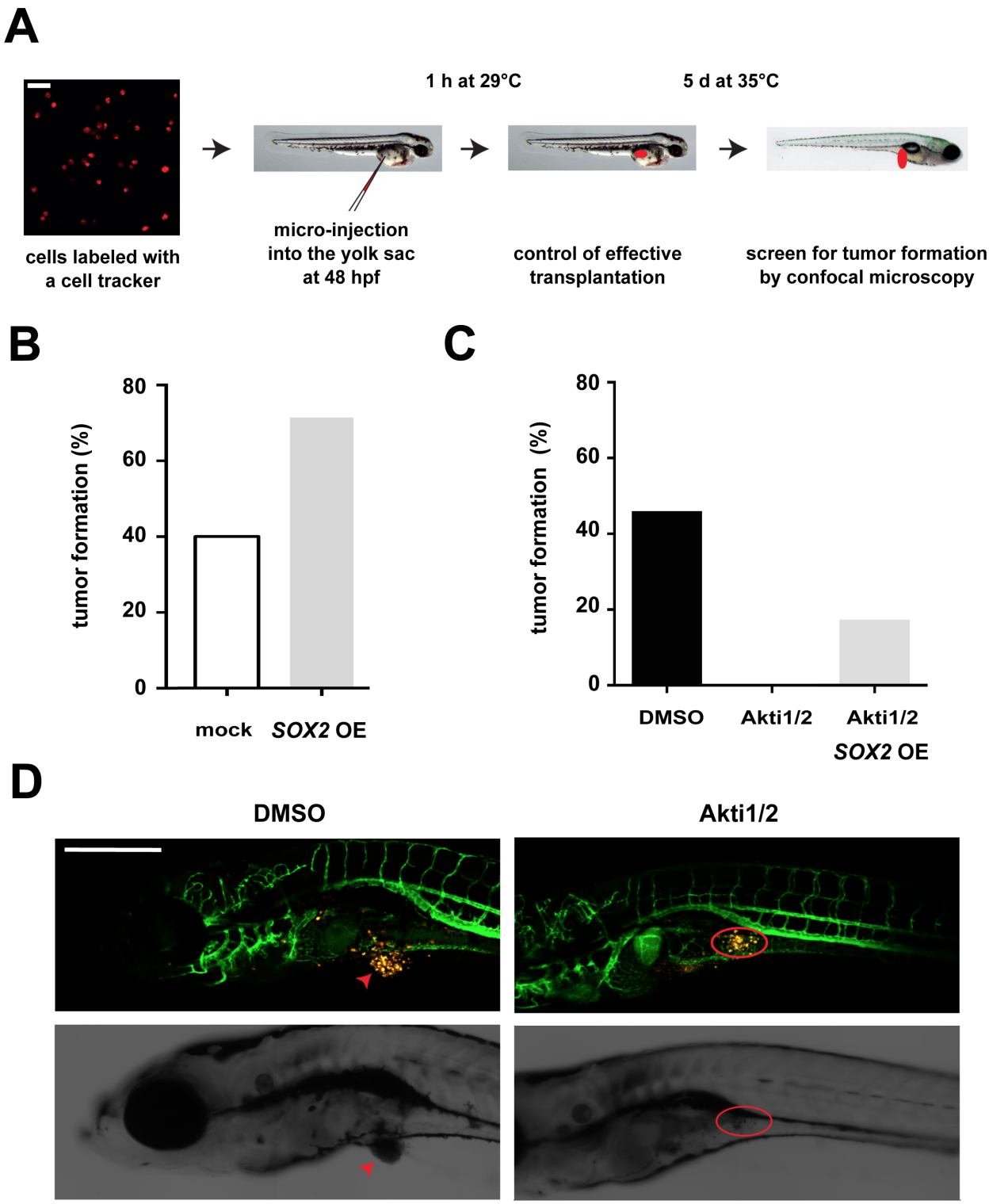

Figure 5: Influence of the AKT/SOX2 axis on *in vivo* tumorigenicity. (A) Schematic illustration of the zebrafish xenotransplantation procedure and assay. Scale bar: 50 µm. **(B)** *SOX2* overexpression facilitates *in vivo* tumor induction. Shown are percentages of fish with tumors upon transplantation with SOX2-overexpressing versus control T47D cells (75 cells per fish and 10 or more fish for each condition). **(C)** AKT kinase inhibition by Akti1/2 (5 µM) prevents tumor formation in T47D xenotransplanted fish. However, tumor formation in AKT inhibitor-treated embryos is partially restored by concomitant *SOX2* overexpression. At least $n = 10$ embryos were analyzed per group. **(D)** Representative confocal pictures of T47D-induced tumor formation and AKT inhibitor effects. Note that in mock-treated control animals T47D cells (yellow) grow out to form a solid tumor mass (arrow, left), whereas dispersed T47D cells persist in the yolk sac of Akti1/2-treated fish (red circle, right). Transgenic *fli:eGFP* zebrafish are used to allow visualization of interactions with host vessels. Scale bar: 500 µm.

with AKT/pAKT in the cytosol (Figure 6A). Interestingly, treatment with MK-2206 induced a more pronounced relative decline of SOX2 protein in cytosolic as compared to nuclear fractions, suggesting that clearance of SOX2 protein may preferentially occur via the compartment where also pAKT is retained (Figure 6A). This is also supported by confocal laser scanning microscopy, revealing a partial cytoplasmic co-localization of SOX2 and pAKT proteins in particular at the nuclear boundary of BC cells (Figure 6B).

The human SOX2 protein sequence (NM_003106.3) harbors an AKT recognition motif (RPRRX-S/T) and a putative phosphorylation site (Thr116 in human, Thr118 in mouse [31]) near the C-terminal end of its high-mobility-group (HMG) DNA-binding domain (Figure 6C). The AKT recognition motif actually coincides with the nuclear localization signal (NLS) of SOX2 [32], suggesting that AKT may associate with SOX2 to modulate its nuclear entry by phospho-modification. Despite the expected transient nature of such enzyme-substrate relations, we succeeded in confirming a direct physical interaction of SOX2 and AKT proteins by co-immunoprecipitation (Figure 6D). Albeit only a small fraction of total AKT co-enriched with SOX2, the recovery of AKT was shown to be specific over internal controls (GAPDH and RPS6) and increased upon its membrane dissociation with SDS (Figure 6D, right panel). The identity of AKT and SOX2 proteins was further confirmed by peptide fingerprinting (not shown).

To explore the regulation of SOX2 protein by AKT in more detail, the *mCherry-SOX2* protein was lentivirally introduced into BC cell lines and primary cells and its expression induced prior to MK-2206 treatment. As noted for the endogenous protein, AKT inhibition also effectively reduced ectopic SOX2, whose expression was driven from an inducible heterologous promoter (Figure 6E). These data clearly demonstrate that pAKT regulates SOX2 expression by influencing protein turnover. Further supporting the post-translational nature of this effect, cycloheximide treatment efficiently depleted BC cells of proteins with a comparable short half-life (e.g. cyclin D3) but only modestly affected SOX2, indicating that SOX2 protein has a comparably longer half-life in BC (Figure 6F) and a complete inhibition of SOX2 protein could not be achieved as fast through translational repression. We therefore conclude that cells of stalled AKT kinase activity clear SOX2 protein by post-translational mechanisms. Interestingly, whereas this molecular dependence was evident in all BC cell lines and primary samples tested, a comparable tight coupling of SOX2 protein on pAKT activity was not consistently detected in other tumor types (e.g. ovarian and squamous neck carcinoma cell lines), suggesting an involvement of yet unknown tissue-specific factors or even alternative regulatory principles in other cell types (Supplementary Figure 6).

Proteasomal clearance of cytoplasmic SOX2 upon AKT inhibition

Live cell imaging visualizing *mCherry-SOX2* protein revealed a bright nuclear signal upon induction with doxycycline (Figure 7A, left), which persisted over several days. In the presence of the AKT inhibitor MK-2206, however, a rapid redistribution of the fluorescent signal from an exclusively nuclear to a nuclear-cytoplasmic signature was observed (Figure 7A and 7B). Cytoplasmic signal retention commenced at about 30 min after the onset of AKT inhibition and became most apparent within 2 to 4 hours. This timing suggested a shifted nucleo-cytoplasmic equilibrium of pre-existing SOX2 protein as predominant cause of signal retention. Indeed, cytoplasmic signal formation was readily abolished and the SOX2 signature effectively retained in the nucleus, when nuclear export was first blocked with leptomycin B and AKT kinase activity stalled with MK-2206 thereafter (Figure 7A, right).

Long-term exposure to MK-2206 for 48 hours instead caused a significant depletion of endogenous SOX2 protein and ectopically expressed *mCherry-SOX2* alike (see Figure 6E for comparison). Interestingly, co-treatment of cells with leptomycin B and MK-2206 allowed for a partial rescue of SOX2 protein even at extended points in time (Figure 7C), suggesting that nuclear retention may have a protective influence on SOX2 protein.

Vice versa, we hypothesized that a cytoplasmic accumulation of SOX2 in AKT-inhibited cells promotes its degradation and that proteasomal inhibitors may counteract this effect. To test this assumption, BC cells were treated with MK-2206 with or without the addition of the proteasomal inhibitor bortezomib. Indeed, co-treatment with bortezomib dose-dependently inhibited the MK-2206-induced SOX2 degradation (Figure 7D). These observations were re-confirmed by confocal microscopy of endogenous SOX2 protein that once again documented a disappearance of SOX2 signal upon AKT inhibition, and a restoration of SOX2 protein in BC cells co-treated with MK-2206 and bortezomib (Figure 7E). Notably however, the SOX2 protein was only restored in the cytosol of double-treated cells, indicating that in the presence of AKT kinase inhibition nuclear import of SOX2 was perturbed.

Taken together, our results highlight the importance of the AKT/SOX2 axis for BC clonogenicity and *in vivo* tumorigenicity, and indicate AKT inhibitors as molecules targeting *SOX2*-positive BC (stem) cells via SOX2 protein depletion. Mechanistically, AKT kinase activity promotes SOX2 nuclear entry, thereby influencing its protein turnover (see Supplementary Figure 9 for summary and schematic illustration).

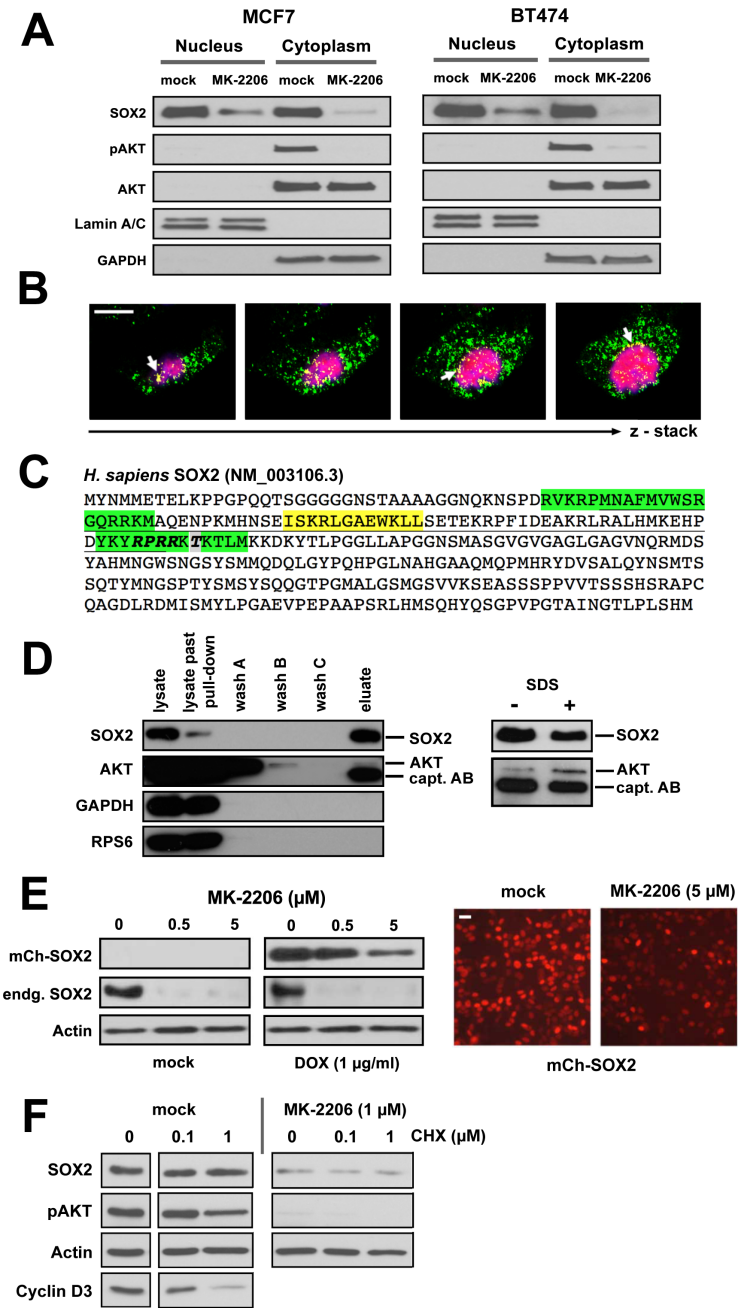

Figure 6: AKT and SOX2 proteins physically interact in BC cells. (A) Expression and subcellular localization of SOX2, pAKT, and AKT proteins in BC cell lines cultured with or without MK-2206 (5 μM) for 48 hours. Lamin A/C and GAPDH were used as nuclear and cytosolic marker proteins, respectively. **(B)** Confocal laser scanning microscope images demonstrating co-localization of pAKT (green) and SOX2 (red) proteins in MCF7 cells. Shown are consecutive sections of a z-stack recording. Co-localization (yellow) is particularly prominent at the nuclear boundary (arrows). Scale bar: 10 μm. **(C)** Sequence analysis of the human SOX2 protein (NCBI Ref. NM_003106.3). The High Mobility Group (HMG) DNA-binding domain is underlined. Bipartite nuclear localization signal (NLS) in green, nuclear export signal (NES) in yellow. Note an AKT recognition motif (RPRR-X_S/T, bold) and a *bona fide* AKT phosphorylation site Thr116 (grey) within the NLS motif of SOX2. **(D)** Immunoblot analysis documenting co-precipitation of SOX2 and AKT proteins from MCF7 cell lysates and specificity of this interaction over internal controls (GAPDH, RPS6). Note that the detection reagent (peroxidase conjugated anti-rabbit IgG) also stains the capture antibody (rabbit anti-human SOX2). **(E)** MK-2206 treatment inhibits the expression of ectopic SOX2 protein (driven by an exogenous *mCherry-SOX2* fusion construct stably integrated into MCF7 cells), as illustrated by immunoblotting (left) and fluorescence life-microscopy (right). Doxycycline (1 μg/ml) was added for 24 hours to induce the ectopic *mCherry-SOX2* protein, then washed out, and MK-2206 (5 μM) or mock-control added for another 48 hours. Scale bar: 25 μm. **(F)** Induction of a translational arrest by cycloheximide (0.1 –1 μM for 48 hours) has only a minor effect on endogenous SOX2 levels. Note that the strong inhibitory effect of MK-2206 on SOX2 protein expression persists in spite cycloheximide-induced translation arrest, indicating direct regulatory effects of pAKT on SOX2 (+/− MK-2206, left vs. right).

DISCUSSION

Breast carcinoma is the most common type of cancer and one of the leading causes of cancer death in women worldwide. In spite recent progresses in therapy, BC patients carry a life-long risk of disease recurrence. BC relapse is thought to originate from clonogenic breast CSCs that metastasize, survive anti-tumor therapies and eventually re-initiate disease. Understanding the molecular mechanisms defining breast CSCs may lead to the discovery of molecules effectively targeting this cell population.

The pluripotency-associated protein SOX2 is a key regulator of self-renewal in pluripotent stem cells and was furthermore shown to determine developmental cell fate decisions by interactions with tissue-specific factors [33]. In the adult, SOX2 marks certain stem and progenitor cells important for tissue homeostasis and repair [2, 34, 35]. Recently, an increasing amount of data indicates SOX2 expression in various cancers [3–13]. Here, the SOX2 expression pattern highly depends upon the tissue of origin. In squamous lung carcinoma, for example, SOX2 expression is mostly linked to amplifications at its chromosomal locus 3q26. Consistently, SOX2 is homogenously detected in all tumor cells where it promotes cell growth as a lineage-survival oncogene [4, 10]. In contrast, in breast and ovarian carcinoma SOX2 expression occurs in the absence of *SOX2* gene amplifications and appears enriched in putative CSCs [7, 14]. In line, SOX2 knockdown reduces sphere formation and *in vivo* tumorigenicity in breast as well as ovarian carcinoma cells [11, 25]. Moreover, even breast carcinoma cell lines with inherently low SOX2 levels as observed in 2D cultures (e.g. HS578T or MDA-MB468) are able to activate the gene dynamically when cultured under conditions that promote CSCs (Supplementary Figure 1). This suggests that SOX2 may have an even broader clinical significance in BC than presently anticipated and may regulate also the biology of tumors where no prominent expression is detected in standard screening procedures.

Next to a small set of classical disease-defining genes such as *BRCA-1/2*, the estrogen receptor or *HER2/neu*, the canonical PI3K/AKT/mTOR signaling pathway forms another mutational hotspot in breast cancer [36]. No less than 30–40% of breast cancers contain constitutively active forms of either PI3K or loss-of-function mutations in its upstream suppressor PTEN [26, 37]. This also concerns the particular cell lines investigated here, which either carry a *PI3K-CA* mutation (MCF7, BT474, and T47D) or *PTEN*$^{-}$ alleles (e.g. BT549 and MDA-MB468, see Supplementary Table 1 for comprehensive overview). Underscoring a particular significance of AKT signaling in BC, nuclear stabilization of AKT was recently shown to enhance stem cell-like features in BC cell lines [38]. In line with these results, we observed that, in contrast to conventional cytostatics, treatment with the allosteric pan-AKT kinase inhibitor MK-2206 not only reduced overall BC cell growth, but also suppressed SOX2-expressing putative CSCs and furthermore impaired BC cell clonogenicity and *in vivo* tumorigenicity. Mechanistically, exposure to different PI3K or AKT inhibitors strongly reduced SOX2 protein levels suggesting that PI3K/AKT signaling may regulate breast CSCs via direct modulation of SOX2. In line with this notion and verifying SOX2 as a functional downstream target of AKT in BC, overexpression of SOX2 was able to rescue sphere formation in AKT-inhibited cells, albeit the reduced size of the rescued spheres suggested that other AKT-dependent effects (e.g. induction of cell proliferation) might not be equally restored (see Supplementary Figure 5). Importantly, these data could be confirmed *in vivo* in xenotransplantation experiments where treatment with AKT inhibitors effectively suppressed tumor induction from control, but not from SOX2-overexpressing BC cells.

To explore how pAKT regulates SOX2 expression in BC, an ectopic *mCherry-SOX2* protein was introduced into BC cell lines and primary tumor cells. In the presence of AKT inhibitors, a rapid cytoplasmic accumulation of SOX2 signal along with a relative intensity decline in the nucleus was observed. These effects commenced within minutes after addition of the inhibitor and became most prominent after 2–4 hours of treatment. A putative contribution of *de novo* protein synthesis to this effect cannot be excluded. However, the rapid onset of events and the documented long half-life of SOX2 protein (Figure 6F) emphasize a subcellular redistribution of pre-existing SOX2 protein as the main cause of cytoplasmic signal retention.

At extended incubation times, a successive disappearance of the SOX2 signal in AKT inhibitor-treated cells was noted. The relative decline in SOX2 protein was more pronounced in cytoplasmic than nuclear fractions, suggesting an involvement of cytosolic proteasomal degradation (Figure 6A). Indeed, addition of the proteasomal inhibitor bortezomib to AKT inhibitor-treated cells was able to rescue SOX2 protein expression in the cytosol even at extended incubation times. We therefore conclude that in BC cells AKT modulates SOX2 steady-state levels by counteracting its proteasomal degradation in the cytosol. Underscoring the regulatory role of protein degradation, Wang and co-workers recently defined the ubiquitin-conjugating enzyme Ube2s as a mediator of Sox2 expression in murine ES cells [39].

Mechanistically, our data show that AKT co-localizes and physically interacts with SOX2 and suggest that the nucleo-cytoplasmic distribution of SOX2 is influenced by AKT kinase activity. Supporting this notion, an AKT recognition motif (RPRR-X_T_{116}) was identified within the nuclear localization signal of SOX2, emphasizing phosphorylation as a probable means to modulate SOX2 nuclear entry. Of note, an evolutionary

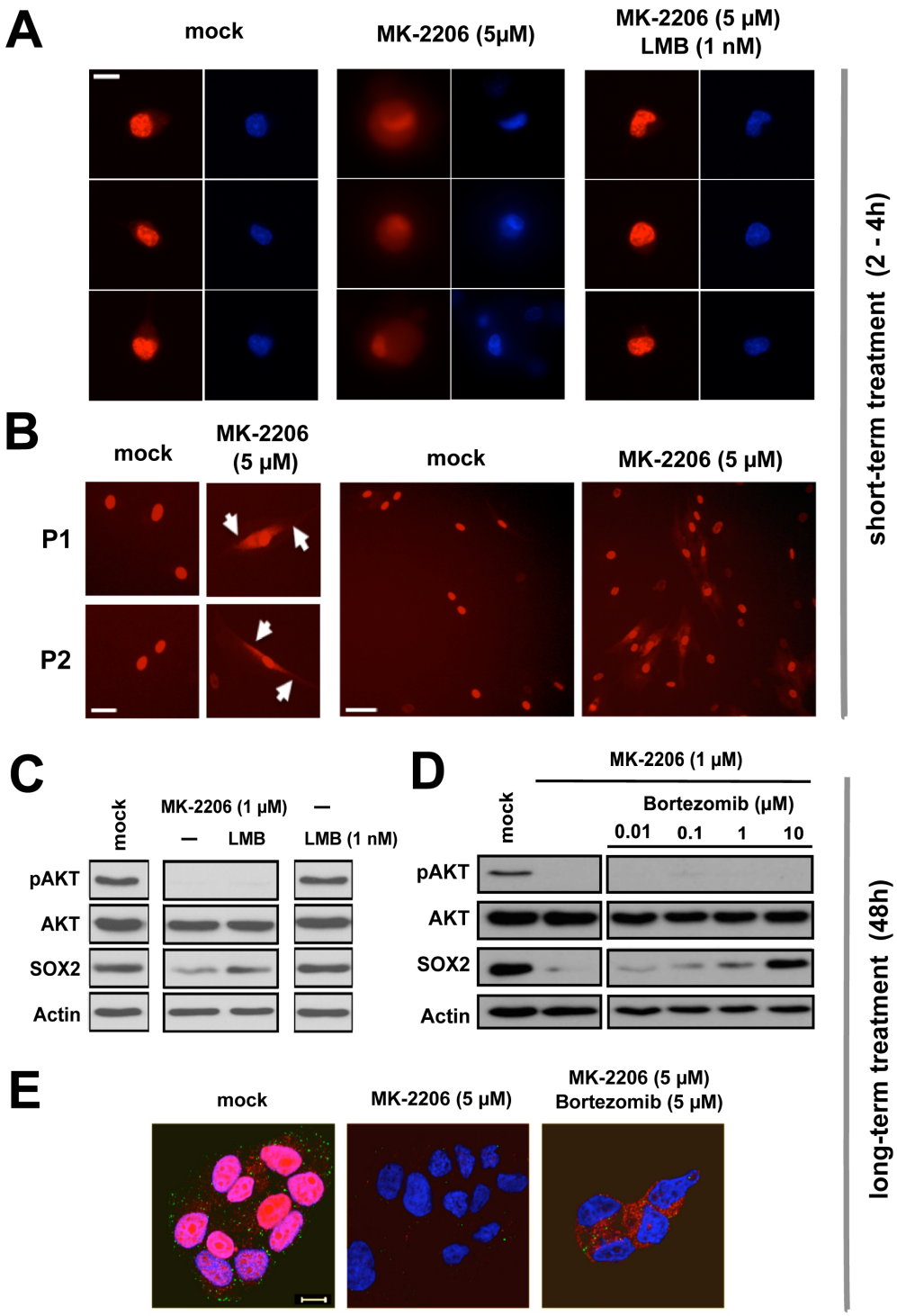

Figure 7: Proteasomal clearance of cytoplasmic SOX2 upon AKT inhibition. **(A)** Rapid cytoplasmic accumulation of *mCherry-SOX2* protein signal in BT474 cells treated with 5 μM MK-2206 for 2–4 hours (left to center), and phenotypic restoration upon inhibition of nuclear export with leptomycin B (1 nM, center to right). DNA was stained with Hoechst33342 to indicate nuclei. Scale bar: 10 μm. **(B)** Verification of cytoplasmic *mCherry-SOX2* signal retention in primary patient-derived cells (P1 and P2) treated with MK-2206. Scale bars: 25 μm (left) and 50 μm (right). **(C)** Immunoblot re-confirming depletion of SOX2 protein by MK-2206 (1 μM) and rescue of SOX2 signal in MK-2206 and leptomycin B double-treated cells at 48 hours. **(D)** Immunoblot documenting a dose-dependent rescue of endogenous SOX2 protein in BC cells co-treated with MK-2206 and the proteasome inhibitor bortezomib for 48 hours. **(E)** Corresponding confocal image sections illustrating a depletion of SOX2 protein signal by MK-2206 (left to center) and the restoration of cytoplasmic SOX2 in MK-2206 and bortezomib double-treated MCF7 cells (center to right). Note that in AKT inhibitor-treated cells, bortezomib treatment can rescue SOX2 protein expression but not relocate it to the nucleus. Depicted are cells 48 hours after treatment with the indicated drugs. Red: SOX2; green: pAKT; blue: DAPI. Scale bar: 10 μm.

conserved phosphorylation site also exists in murine Sox2 and was functionally linked to the reprogramming of murine fibroblasts into induced pluripotent stem (iPS) cells [31] and shown to influence Sox2 protein stability in murine ESCs [40]. Interestingly, a Thr_{116} Ala single-site mutation of this previously reported locus is insufficient to block SOX2 nuclear import in BC cells (Supplementary Figure 7), suggesting an involvement of additional AKT–dependent phosphorylation sites within SOX2, as reinforced by *in vitro* kinase assays (data not shown).

To our knowledge, a correlation between AKT kinase activity and SOX2 nuclear entry has not yet been previously reported. In lack of a decisive phosphorylation site mutant, transport assays involving the nuclear export inhibitor leptomycin B (LMB) were performed to provide experimental evidence of altered SOX2 protein transport in anti-AKT treated cells. Indeed, pre-treatment with LMB prevented MK-2206 induced re-distribution and cytoplasmic retention of *mCherry-SOX2* signal, and at extended incubation times LMB treatment partially restored SOX2 levels, suggesting that the established nuclear retention has a protective effect on SOX2.

In mice, Akt has been suggested to indirectly repress *Sox2* transcription via a regulatory circuit involving FoxO1 [41]. Moreover, AKT was recently reported to modulate *SOX2* transcriptional activity via p27 and a regulatory circuit involving miR-30a in human nasopharyngeal cancers [42]. While these reports jointly underscore a functional correlation of AKT and SOX2, we found no evidence for such molecular interactions in BC cells (Supplementary Figure 8 and data not shown). *Vice versa*, the robust effect of AKT inhibition on SOX2 protein expression that we document here for BC was not consistently observed in other tumor-derived cell types, e.g. in ovarian or squamous head and neck cell carcinoma lines (Supplementary Figure 6). Jointly, these data reinforce the notion that SOX2 regulation occurs in a highly tissue-specific manner and that learning derived from one experimental system may have only limited predictive value for other indications. These observations are in line with the immanent differences in SOX2 expression pattern and function observed in different cancer types (see before), which strongly suggest that also the molecular regulation of SOX2 turnover might likely depend upon the tissue of origin.

The existence of an AKT recognition motif within the human SOX2 amino acid sequence and the experimental confirmation of a direct physical interaction of AKT and SOX2 proteins via co-localization and co-immunoprecipitation strongly suggest an enzyme-substrate relation between the two factors. Moreover, depletion of SOX2 protein and impaired BC clonogenicity required inhibition of AKT kinase itself (as achieved either by MK-2206 or Akti1/2), or of the upstream kinase PI3K by either wortmannin or GCD-0941. Noteworthy, since different inhibitors of AKT or PI3K reduced SOX2 protein in a similar manner, off-target effects are an unlikely explanation for the results presented here. Interestingly, no depletion of SOX2 protein was observed when the mTOR-inhibitor rapamycin was applied. This observation is of particular importance since it indicates relevant differences in drugs designed to target the PI3K/AKT/mTOR-pathway that are currently underway in clinical trials. Moreover, it illustrates that AKT modulates SOX2 protein turnover directly, not indirectly via an mTOR-dependent modulation of protein synthesis, further supporting our previous results.

Finally, we observed that MK-2206 mediated inhibition of pAKT/SOX2 and clonogenicity was sustained throughout serial replating sphere assays, but eventually showed recovery. The transient nature of these inhibitory effects indicates that BC stem/progenitor cells are neither eradicated nor terminally differentiated by the treatment regimen applied here. Whether longer application windows or iterative treatment cycles may indeed induce ultimate cell-fate changes and persistent effects, as recently reported in nasopharyngial carcinoma derived cell lines [42], requires further investigation.

In summary, our investigations uncovered a hitherto unrecognized molecular and functional coupling of AKT and SOX2 proteins that determines tumorigenicity in BC, thus adding a novel perspective onto the promises and limitations of PI3K/AKT/mTOR-inhibitor therapies that are currently under laboratory and clinical investigation in BC.

MATERIALS AND METHODS

Cell culture

Cell lines (DSMZ, Braunschweig, Germany) were cultured according to data sheet. Primary BC samples obtained from patients treated at the Women's University Hospital Tuebingen, Germany, were dissociated to single cells as previously described [11] and cultured in RPMI 1640 medium (R8758, Sigma, St-Louis, MO, USA) supplemented with 15% heat-inactivated FCS (#10500, Gibco, Life Technologies, Grand Island, NY, USA) and 1% v/v Pen/Strep (P4333, Sigma). The study was approved by the Ethics Committee of the University of Tuebingen, Germany. MK-2206, wortmannin, rapamycin, bortezomib (all by Selleckchem, Houston, TX, USA) or Akti1/2, leptomycin B, cycloheximide, and doxycycline (all by Sigma) were resolved or diluted according to data sheet and applied as indicated.

Sphere assay and 3D-culture

Sphere assays were conducted in MEBM medium (CC-3151, Lonza, Basel, Switzerland) supplemented with 4 µg/mL heparin (Ratiopharm, Ulm, Germany), 1x hydrocortisone (CC-4031G, Lonza), 1x insulin (CC-4021G, Lonza), 2% B-27 (#17504, Gibco, Life

Technologies), 20 ng/ml EGF (E9644, Sigma), 20 ng/ml basic FGF (#100-18B, PeproTech, Rocky Hill, NJ, USA), and antibiotics. Unless indicated differently, 1250 cells were seeded into 300 µl medium and propagated in 24-well ultra-low attachment plates (#3473, Corning, NY, USA) at 37°C and 5% CO_2. Sphere numbers were quantified at assay day 5 (i.e. after 120 hours of continuous incubation). Live single cells from trypsinized spheres were used for replating assays. For 3D-cultures, 5×10^5 cells were transferred to 10 ml sphere medium and propagated in 25-cm^2 flasks (#3815, Corning) for 5 days, passaged by trypsinization, and analyzed after another 5 days of sphere cultivation.

Genetic modifications

For genetic manipulation of cells, lentiviral particles encoding *SOX2* shRNAs and GFP [11] or the SRR1-dsRED reporter and a puromycine resistance cassette [24] were produced and used for cell transduction as previously described. In particular, the following sequences were used to generate *SOX2* shRNAs: sh1_fwd: 5′-GATCCCCCAAGGAGAGGCTTCTTGCTGAATTTTTCAAGAGAAAATTCAGCAAGAAGCCTCTCCTTGTTTTTGGAAA-3′; sh1_rev: 5′-AGCTTTTCCAAAAACAAGGAGAGGCTTCTTGCTGAATTTTCTCTTGAAAAATTCAGCAAGAAGCCTCTCCTTGGGG-3′; sh2_fwd:5′-GATCCCCCGAGATAAACATGGCAATCAATTCAAGAGATTGATTGCCATGTTTATCTCGTTTTTGGAAA-3′; sh2_rev: 5′-AGCTTTTCCAAAAACGAGATAAACATGGCAATCAATCTCTTGAATTGATTGCCATGTTTATCTCGGGG-3′. Human *SOX2* cDNA fused N-terminally to *mCherry* was cloned into a Tet_{on} lentiviral gene induction system (Clontech, Mountain View, CA, USA) driven by doxycycline (D9891, Sigma). Phosphorylation-deficient *SOX2* T116A was obtained by site-directed mutagenesis. A myristoylated AKT construct (Addgene, Cambridge, MA, USA) transiently introduced via co-transfection with lipofectamine 2000 (Invitrogen, Life Technologies) was used to overexpress AKT. Efficiently transduced cells were positively selected by antibiotic resistance and FACS.

Real-time PCR

Total RNA was isolated with the RNeasy Mini Kit (Qiagen, Valencia, CA, USA) and cDNA synthesized using a high capacity cDNA reverse transcription kit (Applied Biosystems, Life Technologies). qRT-PCR was performed on an ABI 7500 Light Cycler (Applied Biosystems, Life Technologies) using the FastStart Universal SYBR Green Master mix (Roche, Basel, Switzerland) and the following primer sets for detection of indicated marker genes: *SOX2* (fwd, 5′-AAGACGCTCATGAAGAAGGATAA-3′; rev, 5′-ACTGTCCATGCGCTGGTT-3′), *GAPDH* (fwd, 5′-CTGACTTCAACAGCGACACC-3′; rev, 5′-TAGCCAAATT CGTTGTCATACC-3′), *beta-Actin* (fwd, 5′-AGTCCTGTGGCATCCACGAAAC T-3′; rev, 5′-CACTGTGTTGGCGTACAG GTCTT-3′), and *AKT1* (QuantiTect primer set QT00085379, Qiagen). Expression levels relative to *GAPDH* were calculated using the $\Delta\Delta C_T$ method.

Immunoblotting

Cells were disrupted in 1x Lysis Buffer (#9803, Cell Signaling, Danvers, MA, USA) supplemented with Protease/Phosphatase Inhibitor Cocktail (#78442, Thermo Fisher Scientific, Waltham, MA, USA). Total protein was precipitated and denatured in Laemmli buffer, separated over 12% bis-acrylamide (#161–0148, BioRad, Hercules, CA, USA) gels by Disc-SDS-PAGE, and transferred onto PVDF membrane (#10600021, Amersham, GE Healthcare Life Sciences, Chalfont St. Giles, UK) in a semi-dry blotting apparatus (Trans-Blot Turbo, BioRad). Membranes were blocked with 10% w/v nonfat dry milk (#9999S, Cell Signaling) diluted in TBS 0.1% Tween-20 (p1379, Sigma). Proteins were stained with the following primary antibodies (all by Cell Signaling): anti-SOX2 [either #3579S (rabbit) or #4900S (mouse)], anti-pan AKT (#4691S), anti-pAKT (i.e. pSer473, #4060S), anti-pRPS6 (#4858), anti-Actin (#3700S), anti-lamin A/C (#4777S), anti-GAPDH (#5174P) and detected either by ECL reaction or phospho-imaging. Cell fractionation analyses were performed with a NE-PER Nuclear and Cytoplasmic Extraction kit (Thermo Fisher Scientific) according to the manufacturer's instructions.

Immunoprecipitation

MCF7 cells (100 mg wet pellet weight) were disrupted in Tris/HCl-based Cell Lysis Buffer (#9803, Cell Signaling) supplemented with 1x Protease/Phosphatase Inhibitor Cocktail (#78442, Thermo Fisher Scientific) and incubated with 1 µl of capture antibody (rabbit anti-human SOX2, #3579S, Cell Signaling) for 16 hours at 4°C. Bait-antibody complexes were precipitated with 50 µl (50% slurry bead volume) equilibrated Protein A-Agarose Fast Flow Beads (#92529, Miltenyi Biotech, Bergisch Gladbach, Germany) for 1 hour at 4°C. Bead-protein complexes were sedimented (5 min, 1200 rpm, 4°C) and iteratively (3x) washed with 1 ml cold buffer to resolve non-specifically interactions. Cleared bead-antibody-bait complexes were re-suspended in 100 µl Laemmli buffer, denatured at 95°C for 5 min, and analyzed by immunoblotting.

Microscopy

For life cell microscopy, expression of the *mCherry-SOX2* protein was induced with 1 µg/ml of doxycycline for 24 hours and the medium exchanged preceeding anti-AKT treatment. Images were either recorded at 2–4 hours to document cytoplasmic retention of SOX2 (short-term treatment), or after 48 hours to document

SOX2 protein decay in dependence of AKT (long-term treatment). For immunofluorescence, cells fixed in 4% PFA were permeabilized with 0.1% Triton, stained with antibodies and analyzed. Life cell imaging was performed on IX-50 and IX-81 microscopes (U-RFL-T laser, Olympus, Tokyo, Japan) and confocal images recorded with a LSM 710 microscope (Carl Zeiss, Oberkochen, Germany). Data were processed in ImageJ software (http://imagej.nih.gov/ij) and co-localization analyzed with Zeiss Zen software.

Zebrafish xenografts

Animal experiments and zebrafish husbandry were approved by the "Kantonales Veterinaeramt Basel-Stadt". T47D cells were labeled with the fluorescent CellTracker™ CM-DiI (Life Technologies), a lipophilic fluorescent tracking dye, according to the manufacturer's instructions. Tg (*flk1:eGFP*) zebrafish were maintained, collected, grown and staged in E3 medium at 28.5°C according to standard protocols [43]. For xenotransplantation experiments, zebrafish embryos were anesthetized in 0.4% tricaine (Sigma) at 48 hours post fertilization (hpf) and 75 T47D human BC cells micro-injected into the vessel-free area of the yolk sac. Embryos were incubated for 1 hour at 28.5–29°C for recovery and cell transfer verified by fluorescence microscopy. Fish harboring red cells were incubated at 35°C essentially as described before [30, 44] and the water supplemented with 1 µM Akti1/2 (Sigma) or DMSO at day 0 and day 2.5 post transplantation. On assay day 5, embryos were screened microscopically for tumor cell engraftment using a Zeiss LSM 710 confocal microscope and the number of tumor-bearing fish quantified. For rescue experiments, expression of a *mCherry-SOX2* fusion protein was induced with 1 µg/ml of doxycycline (Sigma) for 24 hours and protein formation verified by fluorescence microscopy prior to transplantation.

Statistics

Unless otherwise indicated, data from ≥ 3 independent biological triplicates was analyzed using the student's *T*-Test $p \leq 0.05$ (*), $p \leq 0.001$ (**), $p \leq 0.0001$ (***). Primary cells were analyzed in technical triplicates. Error bars indicate standard deviations (SD).

ACKNOWLEDGMENTS

We thank Dr. Annette Staebler (Institute for Pathology, University Hospital Tuebingen) for help with tumor sample collection, Dr. Matthias P. Wymann (Department of Biomedicine, University Hospital Basel) for PI3K inhibitors, Dr. Holm Zaehres (Max Planck Institute for Molecular BioMedicine, Muenster, Germany) for provision of a *SOX2* plasmid, Emmanuel Traunecker und Toni Krebs (University Hospital Basel, DBM, FACS sorting unit) for cell sorting and homogenization of strains, and Christine Kruse for experimental support.

FUNDING

This study was performed as contracted research supported by the Baden-Württemberg Stiftung, Germany (Adult Stem Cells Program II, awarded to C.L. and O.R.), and the Deutsche Forschungsgemeinschaft (GRK1302, awarded to K.S.O).

CONFLICTS OF INTEREST

The authors declare no conflict of interest.

REFERENCES

1. Takahashi K, Yamanaka S. Induction of pluripotent stem cells from mouse embryonic and adult fibroblast cultures by defined factors. Cell. 2006; 126:663–676.
2. Sarkar A, Hochedlinger K. The sox family of transcription factors: versatile regulators of stem and progenitor cell fate. Cell stem cell. 2013; 12:15–30.
3. Dong C, Wilhelm D, Koopman P. Sox genes and cancer. Cytogenet Genome Res. 2004; 105:442–447.
4. Bass AJ, Watanabe H, Mermel CH, Yu S, Perner S, Verhaak RG, Kim SY, Wardwell L, Tamayo P, Gat-Viks I, Ramos AH, Woo MS, Weir BA, Getz G, Beroukhim R, O'Kelly M, et al. SOX2 is an amplified lineage-survival oncogene in lung and esophageal squamous cell carcinomas. Nature Genet. 2009; 41:1238–1242.
5. Ben-Porath I, Thomson MW, Carey VJ, Ge R, Bell GW, Regev A, Weinberg RA. An embryonic stem cell-like gene expression signature in poorly differentiated aggressive human tumors. Nature Genet. 2008; 40:499–507.
6. Maier S, Wilbertz T, Braun M, Scheble V, Reischl M, Mikut R, Menon R, Nikolov P, Petersen K, Beschorner C, Moch H, Kakies C, Protzel C, Bauer J, Soltermann A, Fend F, et al. SOX2 amplification is a common event in squamous cell carcinomas of different organ sites. Hum Pathol. 2011; 42:1078–1088.
7. Pham DL, Scheble V, Bareiss P, Fischer A, Beschorner C, Adam A, Bachmann C, Neubauer H, Boesmueller H, Kanz L, Wallwiener D, Fend F, Lengerke C, Perner S, Fehm T, Staebler A. SOX2 expression and prognostic significance in ovarian carcinoma. Int J Gynecol Pathol. 2013; 32:358–367.
8. Schrock A, Bode M, Goke FJ, Bareiss PM, Schairer R, Wang H, Weichert W, Franzen A, Kirsten R, van Bremen T, Queisser A, Kristiansen G, Heasley L, Bootz F, Lengerke C, Perner S. Expression and role of the embryonic protein SOX2 in head and neck squamous cell carcinoma. Carcinogenesis. 2014; 35:1636–1642.

9. Schrock A, Goke F, Wagner P, Bode M, Franzen A, Braun M, Huss S, Agaimy A, Ihrler S, Menon R, Kirsten R, Kristiansen G, Bootz F, Lengerke C, Perner S. Sex determining region Y-box 2 (SOX2) amplification is an independent indicator of disease recurrence in sinonasal cancer. PloS one. 2013; 8:e59201.
10. Wilbertz T, Wagner P, Petersen K, Stiedl AC, Scheble VJ, Maier S, Reischl M, Mikut R, Altorki NK, Moch H, Fend F, Staebler A, Bass AJ, Meyerson M, Rubin MA, Soltermann A, et al. SOX2 gene amplification and protein overexpression are associated with better outcome in squamous cell lung cancer. Mod Pathol. 2011; 24:944–953.
11. Bareiss PM, Paczulla A, Wang H, Schairer R, Wiehr S, Kohlhofer U, Rothfuss OC, Fischer A, Perner S, Staebler A, Wallwiener D, Fend F, Fehm T, Pichler B, Kanz L, Quintanilla-Martinez L, et al. SOX2 expression associates with stem cell state in human ovarian carcinoma. Cancer Res. 2013; 73:5544–5555.
12. Boumahdi S, Driessens G, Lapouge G, Rorive S, Nassar D, Le Mercier M, Delatte B, Caauwe A, Lenglez S, Nkusi E, Brohee S, Salmon I, Dubois C, del Marmol V, Fuks F, Beck B, et al. SOX2 controls tumour initiation and cancer stem-cell functions in squamous-cell carcinoma. Nature. 2014; 511:246–250.
13. Vanner RJ, Remke M, Gallo M, Selvadurai HJ, Coutinho F, Lee L, Kushida M, Head R, Morrissy S, Zhu X, Aviv T, Voisin V, Clarke ID, Li Y, Mungall AJ, Moore RA, et al. Quiescent sox2 (+) cells drive hierarchical growth and relapse in sonic hedgehog subgroup medulloblastoma. Cancer cell. 2014; 26:33–47.
14. Lengerke C, Fehm T, Kurth R, Neubauer H, Scheble V, Muller F, Schneider F, Petersen K, Wallwiener D, Kanz L, Fend F, Perner S, Bareiss PM, Staebler A. Expression of the embryonic stem cell marker SOX2 in early-stage breast carcinoma. BMC cancer. 2011; 11:42.
15. Bollig-Fischer A, Michelhaugh SK, Wijesinghe P, Dyson G, Kruger A, Palanisamy N, Choi L, Alosh B, Ali-Fehmi R, Mittal S. Cytogenomic profiling of breast cancer brain metastases reveals potential for repurposing targeted therapeutics. Oncotarget. 2015; 6:14614–14624.
16. Finicelli M, Benedetti G, Squillaro T, Pistilli B, Marcellusi A, Mariani P, Santinelli A, Latini L, Galderisi U, Giordano A. Expression of stemness genes in primary breast cancer tissues: the role of SOX2 as a prognostic marker for detection of early recurrence. Oncotarget. 2014; 5:9678–9688.
17. Martini M, De Santis MC, Braccini L, Gulluni F, Hirsch E. PI3K/AKT signaling pathway and cancer: an updated review. Ann Med. 2014; 46:372–383.
18. Porta C, Paglino C, Mosca A. Targeting PI3K/Akt/mTOR Signaling in Cancer. Front Oncol. 2014; 4:64.
19. Shaw RJ, Cantley LC. Ras, PI(3)K and mTOR signalling controls tumour cell growth. Nature. 2006; 441:424–430.
20. Korkaya H, Paulson A, Charafe-Jauffret E, Ginestier C, Brown M, Dutcher J, Clouthier SG, Wicha MS. Regulation of mammary stem/progenitor cells by PTEN/Akt/beta-catenin signaling. PLoS Biol. 2009; 7:e1000121.
21. Martelli AM, Evangelisti C, Follo MY, Ramazzotti G, Fini M, Giardino R, Manzoli L, McCubrey JA, Cocco L. Targeting the phosphatidylinositol 3-kinase/Akt/mammalian target of rapamycin signaling network in cancer stem cells. Curr Med Chem. 2011; 18:2715–2726.
22. Gargini R, Cerliani JP, Escoll M, Anton IM, Wandosell F. Cancer stem cell-like phenotype and survival are coordinately regulated by Akt/FoxO/Bim pathway. Stem cells. 2015; 33:646–660.
23. Dontu G, Abdallah WM, Foley JM, Jackson KW, Clarke MF, Kawamura MJ, Wicha MS. *In vitro* propagation and transcriptional profiling of human mammary stem/progenitor cells. Genes Dev. 2003; 17:1253–1270.
24. Wang H, Paczulla A, Lengerke C. Evaluation of stem cell properties in human ovarian carcinoma cells using multi and single cell-based spheres assays. J Vis Exp. 2015; 95:e52259.
25. Leis O, Eguiara A, Lopez-Arribillaga E, Alberdi MJ, Hernandez-Garcia S, Elorriaga K, Pandiella A, Rezola R, Martin AG. Sox2 expression in breast tumours and activation in breast cancer stem cells. Oncogene. 2012; 31:1354–1365.
26. Gonzalez-Angulo AM, Ferrer-Lozano J, Stemke-Hale K, Sahin A, Liu S, Barrera JA, Burgues O, Lluch AM, Chen H, Hortobagyi GN, Mills GB, Meric-Bernstam F. PI3K pathway mutations and PTEN levels in primary and metastatic breast cancer. Mol Cancer Ther. 2011; 10: 1093–1101.
27. Jung K, Gupta N, Wang P, Lewis JT, Gopal K, Wu F, Ye X, Alshareef A, Abdulkarim BS, Douglas DN, Kneteman NM, Lai R. Triple negative breast cancers comprise a highly tumorigenic cell subpopulation detectable by its high responsiveness to a Sox2 regulatory region 2 (SRR2) reporter. Oncotarget. 2015; 6:10366–10373.
28. Eguiara A, Holgado O, Beloqui I, Abalde L, Sanchez Y, Callol C, Martin AG. Xenografts in zebrafish embryos as a rapid functional assay for breast cancer stem-like cell identification. Cell cycle. 2011; 10:3751–3757.
29. Li Y, Drabsch Y, Pujuguet P, Ren J, van Laar T, Zhang L, van Dam H, Clement-Lacroix P, Ten Dijke P. Genetic depletion and pharmacological targeting of alphav integrin in breast cancer cells impairs metastasis in zebrafish and mouse xenograft models. Breast Cancer Res. 2015; 17:28.
30. Konantz M, Balci TB, Hartwig UF, Dellaire G, Andre MC, Berman JN, Lengerke C. Zebrafish xenografts as a tool for *in vivo* studies on human cancer. Ann NY Acad Sci. 2012; 1266:124–137.
31. Jeong CH, Cho YY, Kim MO, Kim SH, Cho EJ, Lee SY, Jeon YJ, Lee KY, Yao K, Keum YS, Bode AM, Dong Z. Phosphorylation of Sox2 cooperates in reprogramming to pluripotent stem cells. Stem cells. 2010; 28:2141–2150.

32. Li J, Pan G, Cui K, Liu Y, Xu S, Pei D. A dominant-negative form of mouse SOX2 induces trophectoderm differentiation and progressive polyploidy in mouse embryonic stem cells. J Biol Chem. 2007; 282:19481–19492.

33. Kondoh H, Kamachi Y. SOX-partner code for cell specification: Regulatory target selection and underlying molecular mechanisms. Int J Biochem Cell Biol. 2010; 42:391–399.

34. Arnold K, Sarkar A, Yram MA, Polo JM, Bronson R, Sengupta S, Seandel M, Geijsen N, Hochedlinger K. Sox2 (+) adult stem and progenitor cells are important for tissue regeneration and survival of mice. Cell stem cell. 2011; 9:317–329.

35. Graham V, Khudyakov J, Ellis P, Pevny L. SOX2 functions to maintain neural progenitor identity. Neuron. 2003; 39:749–765.

36. Di Cosimo S, Scaltriti M, Val D, Rojo F, Guzman M, Jimenez J, Seoane J, Arribas J, Baselga J. The PI3-K/AKT/mTOR pathway as a target for breast cancer therapy. ASCO Annual Meeting Proceedings. 2007; 3511.

37. Sangai T, Akcakanat A, Chen H, Tarco E, Wu Y, Do KA, Miller TW, Arteaga CL, Mills GB, Gonzalez-Angulo AM, Meric-Bernstam F. Biomarkers of response to Akt inhibitor MK-2206 in breast cancer. Clin Cancer Res. 2012; 18:5816–5828.

38. Jain MV, Jangamreddy JR, Grabarek J, Schweizer F, Klonisch T, Cieslar-Pobuda A, Los MJ. Nuclear localized Akt enhances breast cancer stem-like cells through counter-regulation of p21(Waf1/Cip1) and p27(kip1). Cell cycle. 2015; 14:2109–2120.

39. Wang J, Zhang Y, Hou J, Qian X, Zhang H, Zhang Z, Li M, Wang R, Liao K, Wang Y, Li Z, Zhong D, Wan P, Dong L, Liu F, Wang X, et al. Ube2s regulates Sox2 stability and mouse ES cell maintenance. Cell Death Differ. 2015 Aug 21.doi: 10.1038/cdd.2015.106. [Epub ahead of print] PMID:26292759.

40. Fang L, Zhang L, Wei W, Jin X, Wang P, Tong Y, Li J, Du JX, Wong J. A methylation-phosphorylation switch determines Sox2 stability and function in ESC maintenance or differentiation. Mol Cell. 2014; 55:537–551.

41. Ormsbee Golden BD, Wuebben EL, Rizzino A. Sox2 expression is regulated by a negative feedback loop in embryonic stem cells that involves AKT signaling and FoxO1. PloS one. 2013; 8:e76345.

42. Qin J, Ji J, Deng R, Tang J, Yang F, Feng GK, Chen WD, Wu XQ, Qian XJ, Ding K, Zhu XF. DC120, a novel AKT inhibitor, preferentially suppresses nasopharyngeal carcinoma cancer stem-like cells by downregulating Sox2. Oncotarget. 2015; 6:6944–6958.

43. Choi J, Dong L, Ahn J, Dao D, Hammerschmidt M, Chen JN. FoxH1 negatively modulates flk1 gene expression and vascular formation in zebrafish. Dev Biol. 2007; 304:735–744.

44. Haldi M, Ton C, Seng WL, McGrath P. Human melanoma cells transplanted into zebrafish proliferate, migrate, produce melanin, form masses and stimulate angiogenesis in zebrafish. Angiogenesis. 2006; 9:139–151.

Molecular and functional interactions between AKT and SOX2 in breast carcinoma

Supplementary Materials

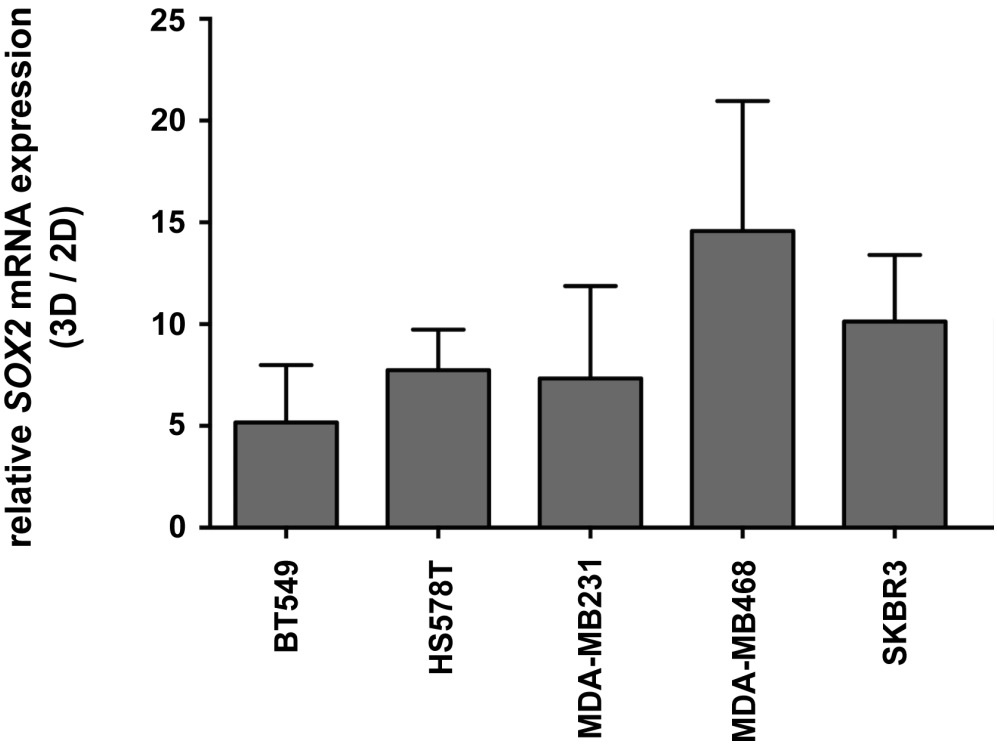

Supplementary Figure S1: Induction of *SOX2* gene expression in *SOX2*-negative/low BC cell lines grown under 3D- versus 2D-culture conditions. Real-time PCR-based quantification of ***SOX2*** mRNA in the indicated BC cell lines grown under CSC-enriching 3D-conditions or standard 2D-conditions. Shown are fold changes in relative *SOX2* expression levels in 3D versus 2D cultures normalized to *GAPDH* expression, as deduced from three independent experiments.

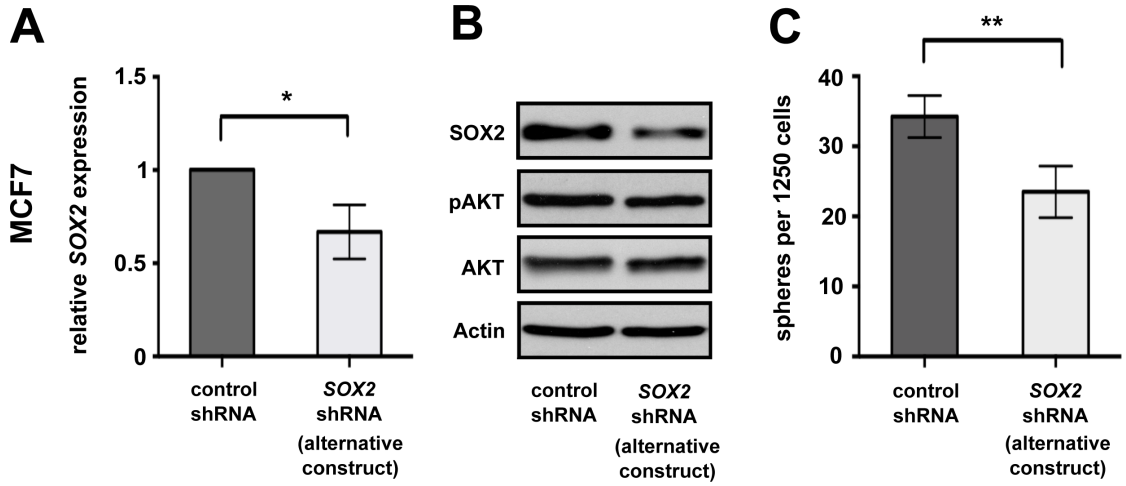

Supplementary Figure S2: Verification of *SOX2* knockdown phenotypes using an alternative shRNA. (**A**) Reduced *SOX2* mRNA and (**B**) protein expression, and (**C**) impaired sphere formation in MCF7 cells transduced with an alternative *SOX2* shRNA vs. control lentiviral particles. Note essentially unaltered (p)AKT levels in cells with impaired *SOX2* expression (B).

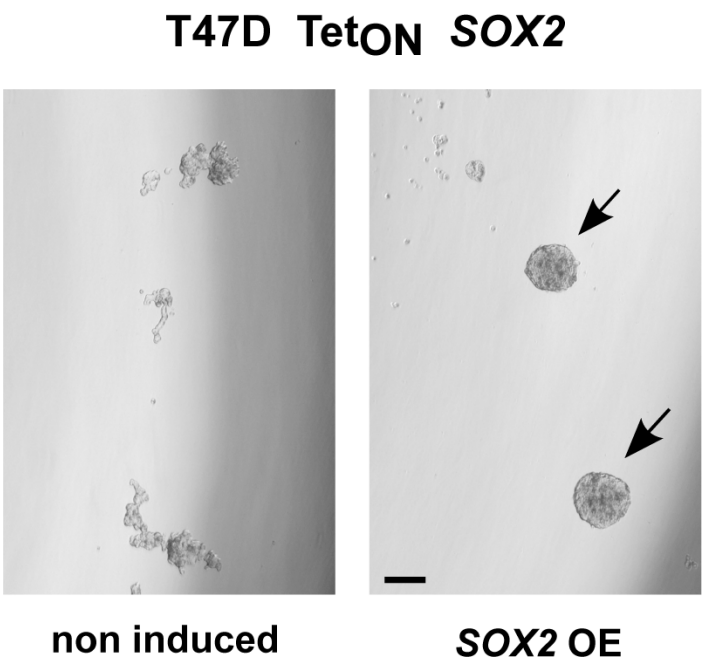

Supplementary Figure S3: *SOX2* expression induces sphere formation from T47D cells. Overview images documenting the supportive role of *SOX2* expression on sphere formation from T47D cells. Shown are representative pictures of mock-treated (non induced, left) and *SOX2*-overexpressing T47D cells (1 µg/ml doxycycline, right) after 5 days of cultivation in sphere assay medium. Scale bar: 100 µm.

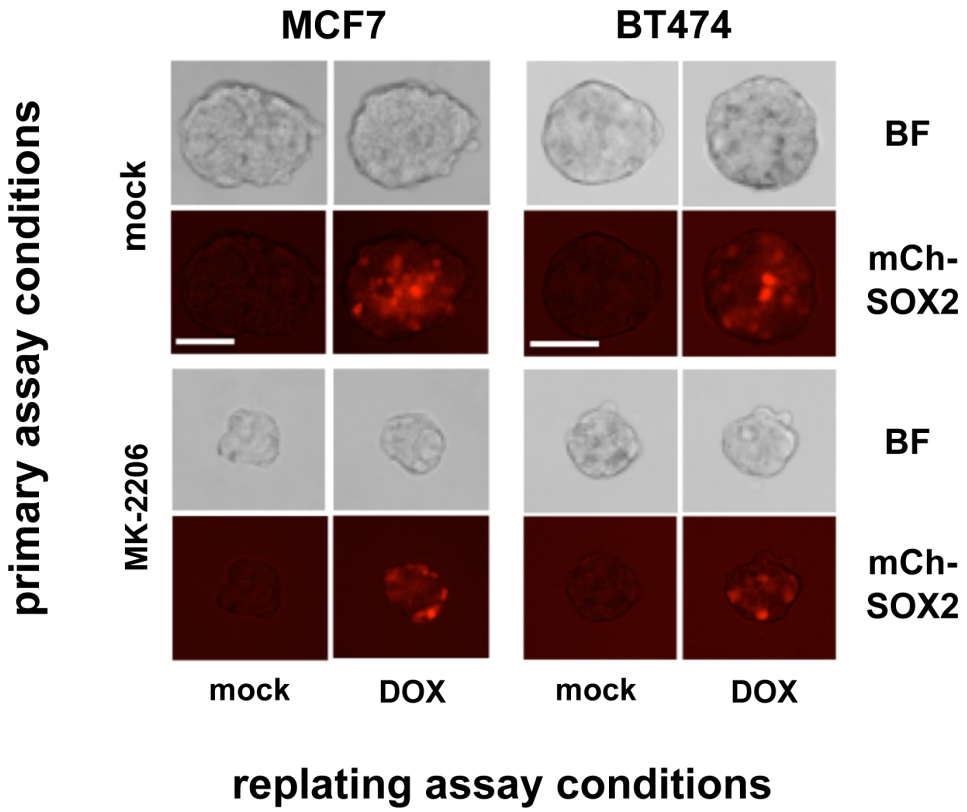

Supplementary Figure S4: Verification of inducible mCherry-SOX2 protein expression in replated spheres. Shown are representative single sphere images of MCF7 and BT474 cells derived from replated spheres (1st replating assay), documenting effective SOX2 protein induction in response to addition of 1 µg/ml doxycycline (DOX) to 3D cultures. Samples were treated with 5 µM MK-2206 or mock control in the first sphere assay, and subsequently re-seeded into mock medium with or without DOX. Note a reduction in sphere size upon MK-2206 treatment (bright field, BF, top panels), and a robust induction of the fusion protein by doxycycline as verified by fluorescent microscopy (mCherry-SOX2, bottom panels). Scale bars: 100 µm.

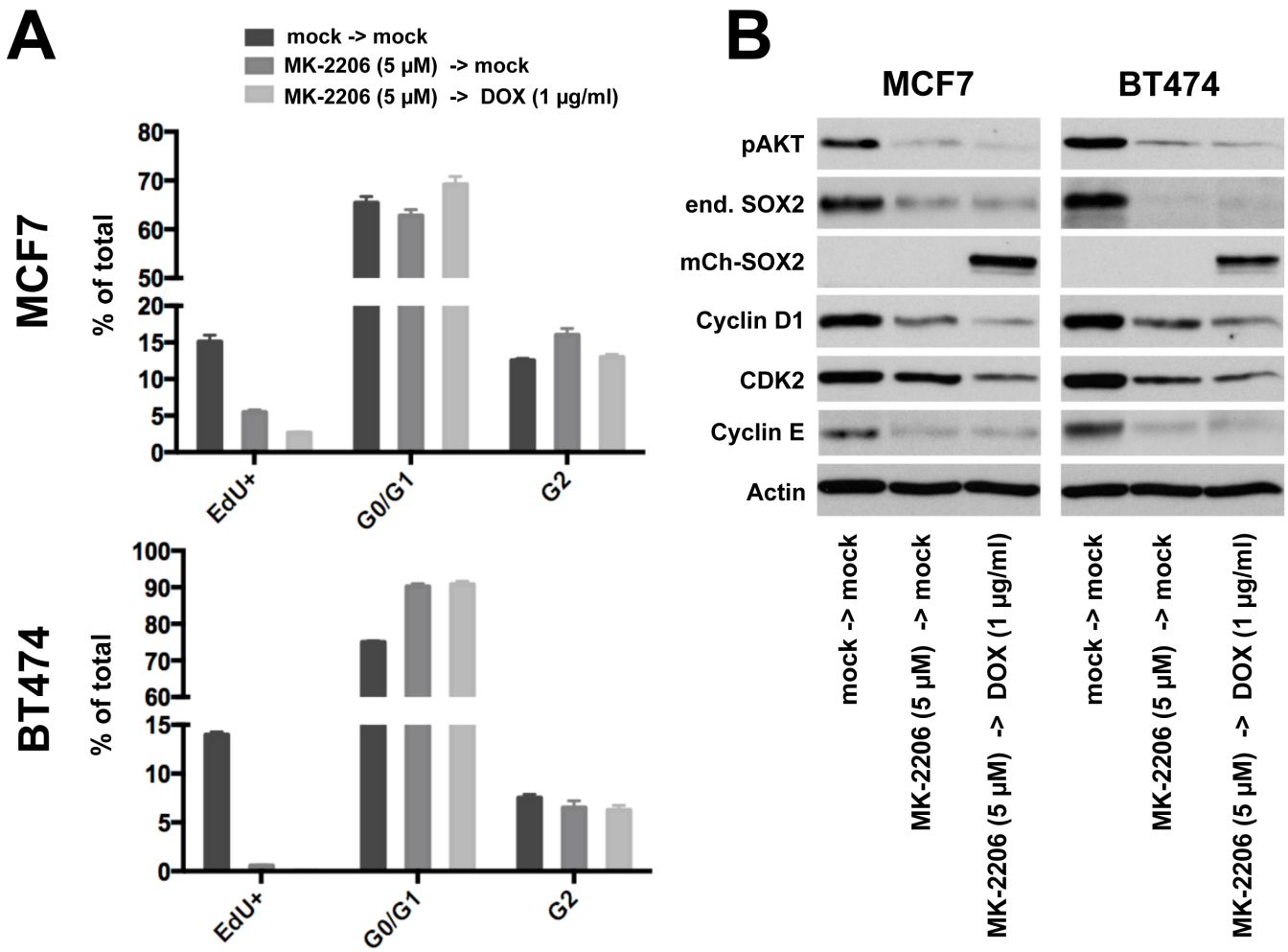

Supplementary Figure S5: Ectopic *SOX2* induction fails to restore proliferation defects in AKT-inhibited cells. (**A**) Cell-cycle analysis of the indicated BC cell lines grown for 2.5 days with or without the AKT inhibitor MK-2206 (5 µM) followed by further 2.5 days of incubation in fresh medium in the absence or presence of doxycycline (1 µg/ml) to induce expression of mCherry-SOX2. Cells were labeled with 5-ethynyl-2′-deoxyuridine (EdU) for 2 hours and stained with DAPI prior to flow cytometry. Note that inhibition of AKT imposes a proliferation defect on cells that is not restored by SOX2. (**B**) Corresponding immunoblot analyses documenting perturbed expression of key cell cycle regulators (i.e. cyclin D1, cyclin E, and CDK2) in AKT-inhibited cells irrespective of SOX2 expression.

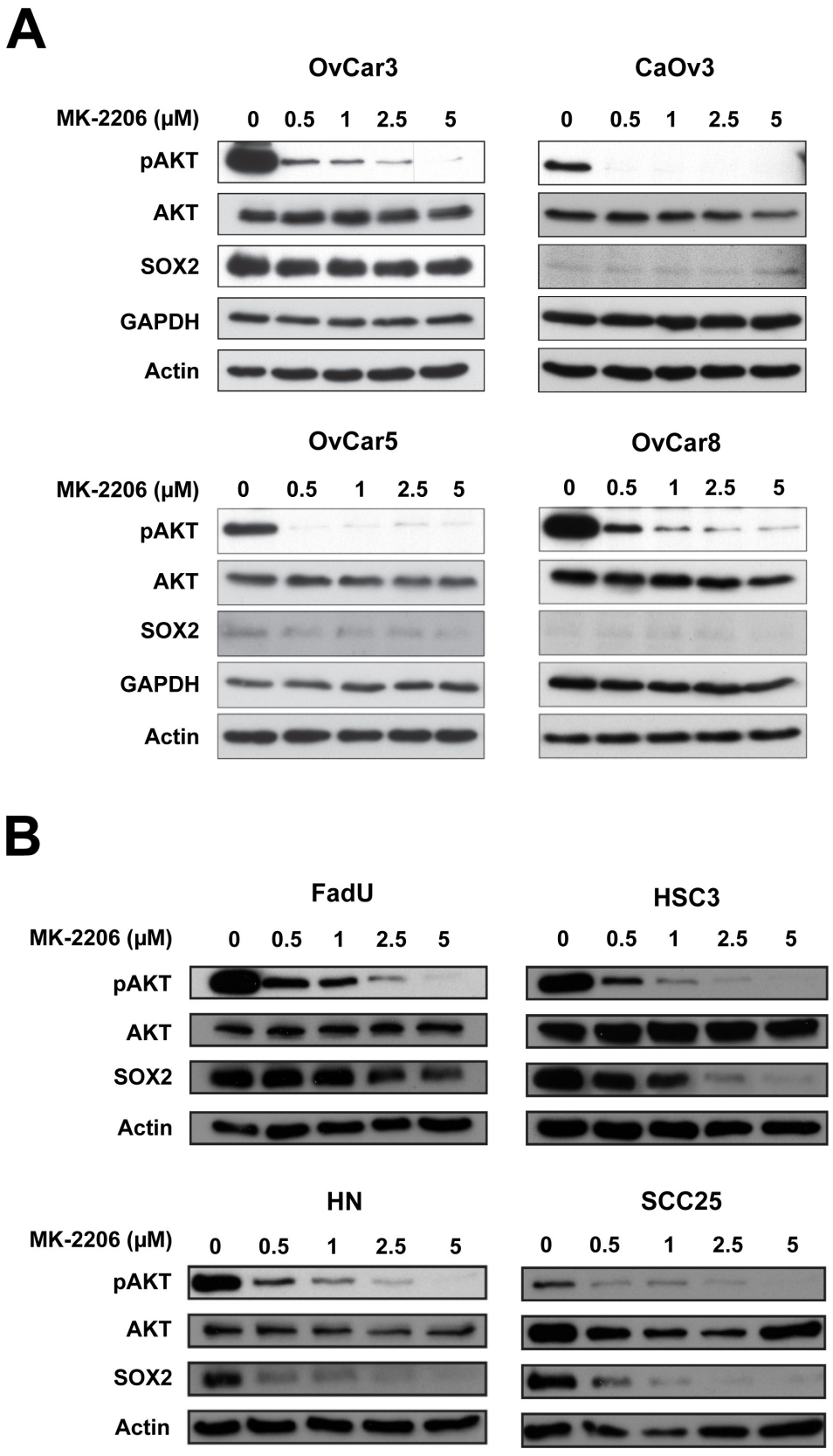

Supplementary Figure S6: Variable effects of AKT inhibition on SOX2 protein levels in other tumor entities. Side-by-side analysis of pAKT, AKT, and SOX2 protein levels upon 48 hours treatment with different doses of MK-2206 in four ovarian (OvCar3, CaOv3, OvCar5, and OvCar8, A) and four squamous head and neck cell carcinoma cell lines (FadU, HSC3, HN, and SCC25, B). Anti-GAPDH and/or anti-actin staining are shown for loading control.

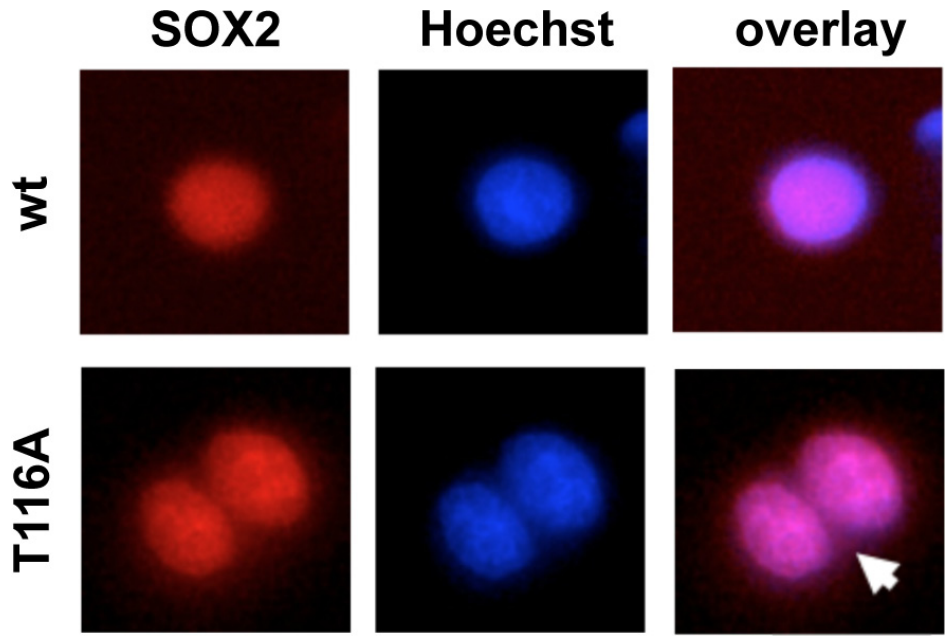

Supplementary Figure S7: Subcellular localization of a mCherry-SOX2 (T116A) phosphorylation site mutant. Live cell microscopic investigation of the steady-state subcellular localization of inducible mCherry-SOX2 constructs (red) in wild-type (wt) or T116A mutant MCF7 cells 24 hours after addition of doxycycline (1 µg/ml). Nuclei were stained with DAPI (blue). Note a bright nuclear staining indicative of persisting nuclear import also of the mutant SOX2 protein arrow. Scale bar: 10 µm.

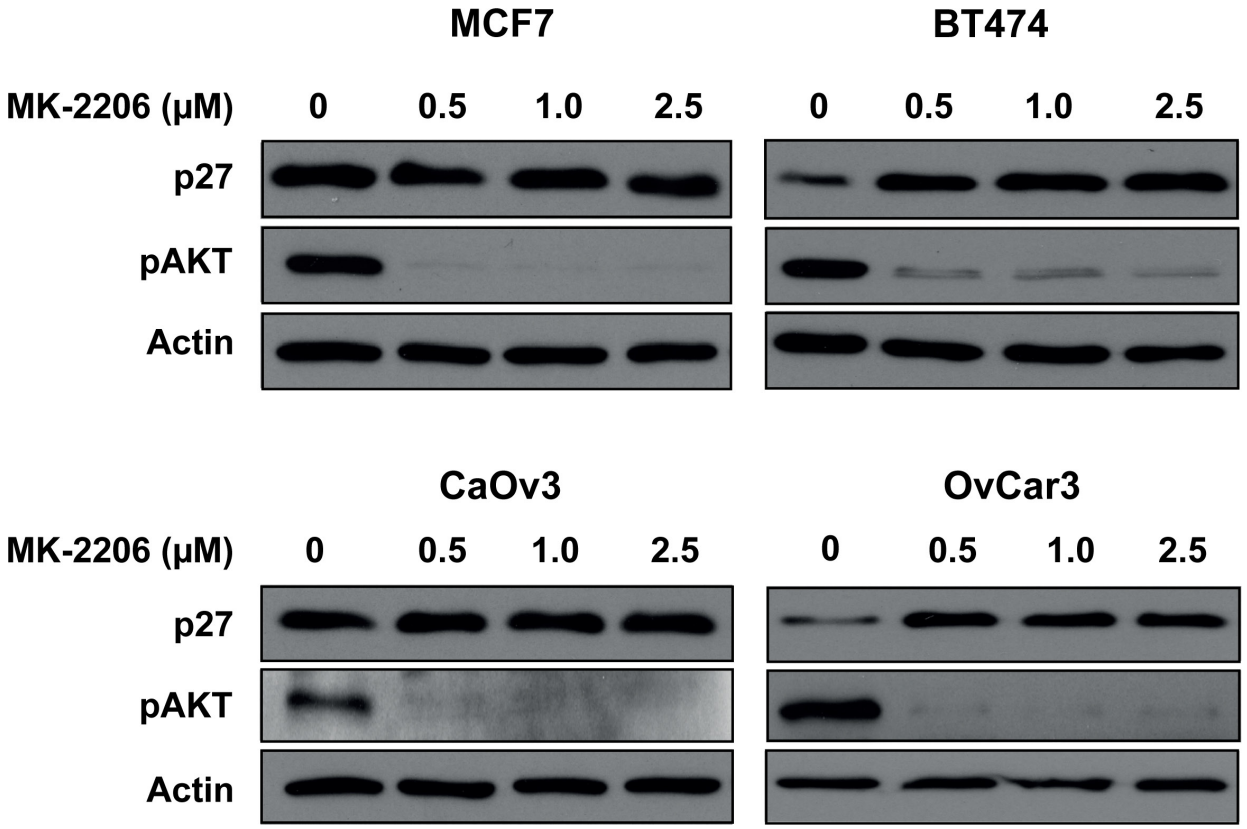

Supplementary Figure S8: No consistent correlation of p27 and pAKT expression in breast and ovarian carcinoma cell lines. Side-by-side analysis of p27 and pAKT protein levels 48 hours upon treatment with the indicated doses of MK-2206 in two breast (MCF7, BT474; top) and two ovarian carcinoma cell lines (CaOv3, OvCar3; bottom). Note that p27 expression is inconsistently affected by AKT kinase inhibition in these tumor cell lines. Anti-actin staining is shown for reference.

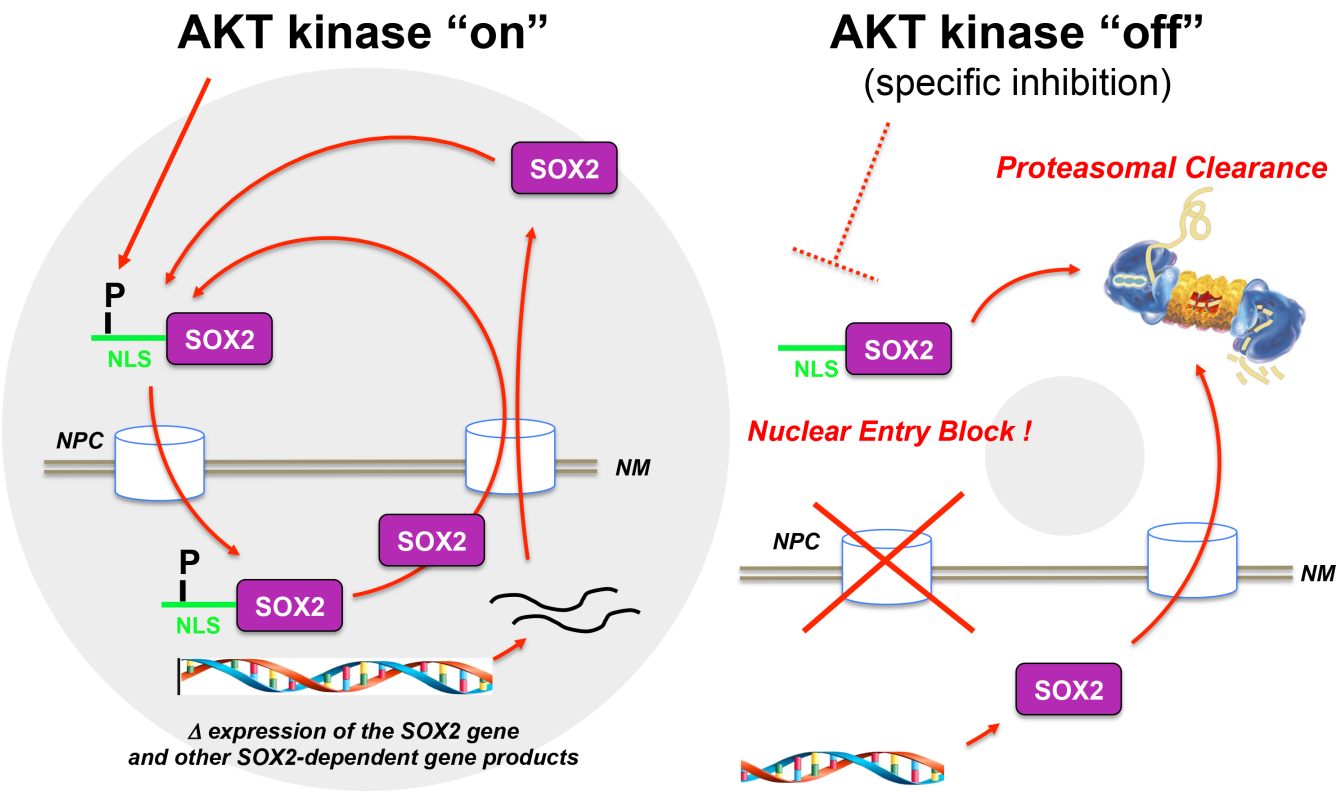

Supplementary Figure S9: AKT kinase determines BC clonogenicity via regulation of SOX2 nuclear entry and protein turnover. AKT kinase activity (left) promotes SOX2 nuclear entry likely involving phosphor-modification of the SOX2 nuclear import signal (NLS). At steady-state, an equilibrium between nuclear entry and export of SOX2 protein is established that involves auto-regulatory mechanisms. AKT kinase inhibition (right) induces a nuclear entry block of SOX2, leading to (i) a rapid cytoplasmic retention of pre-formed SOX2 protein and (ii) to a gradual proteasomal clearance of SOX2 in the cytosol. A functional correlation between SOX2 protein expression and BC cell clonogenicity, as deduced from tumor formation assays *in vitro* and *in vivo*, is illustrated by grey lobes. NPC, nuclear pore complex; NM, nuclear membrane.

Supplementary Table 1: Human breast cancer cell lines used in this investigation. Index list of the human breast cancer cell lines investigated with reference to parental tumor source, classification, and standard gene markers [1–3]

Cell Line	Primary Tumor	Classification	*ER* +/–	*HER2* +/–	*PR* +/–	*PTEN*^{loss}	*PI3KCA*	*Mutant TP53*
BT474	Invasive ductal carcinoma	Luminal B	+	+	+	–	+	+
BT549	Invasive ductal carcinoma	Claudin-low	–	–	–	+		+
HS578T	Carcinosarcoma	Claudin-low	–	–	–			+
MCF-7	Invasive ductal carcinoma	Luminal A	+	–	+	–	+	–
MDA-MB231	Invasive ductal carcinoma	Claudin-low	–	–	–	–	–	+
MDA-MB468	Adenocarcinoma	Basal	–	–	–	+	–	+
SKBR3	Invasive ductal carcinoma	HER2	–	+	–	–	–	+
T47D	Invasive ductal carcinoma	Luminal A	+	–	+	–	+	+

Supplementary Table 2: Histopathological characteristics of the investigated primary breast carcinoma samples P1 and P2

Patient	Histology	subtype	ER status	PR status	HER 2 status	Tumor size	Grading	Nodal Status
P1	Labular	Luminal	+	+	–	pT2	II	neg
P2	Ductulolobular	HER2	+	+	+	pT2	II	neg

REFERENCES

1. Holliday DL, Speirs V. Choosing the right cell line for breast cancer research. Breast Cancer Res. 2011; 13:215.
2. Lacroix M, Leclercq G. Relevance of breast cancer cell lines as models for breast tumours: an update. Breast Cancer Res Treat. 2004; 83:249–289.
3. Sangai T, Akcakanat A, Chen H, Tarco E, Wu Y, Do KA et al. Biomarkers of response to Akt inhibitor MK-2206 in breast cancer. Clin. Cancer Res. 2012; 18:5816–5828.

Paper III

Prominent Oncogenic Roles of EVI1 in Breast Carcinoma.

Wang H, Schaefer T, Konantz M, Braun M, Varga Z, Paczulla AM, Reich S, Jacob F, Perner S, Moch H, Fehm TN, Kanz L, Schulze-Osthoff K, Lengerke C.

Cancer Res. 2017 Apr 15;77(8):2148-2160. Epub 2017 Feb 16.

Published OnlineFirst February 16, 2017; DOI: 10.1158/0008-5472.CAN-16-0593

Tumor and Stem Cell Biology

Cancer Research

Prominent Oncogenic Roles of EVI1 in Breast Carcinoma

Hui Wang[1,2], Thorsten Schaefer[1], Martina Konantz[1], Martin Braun[3], Zsuzsanna Varga[4], Anna M. Paczulla[1], Selina Reich[2], Francis Jacob[1], Sven Perner[5], Holger Moch[4], Tanja N. Fehm[6,7], Lothar Kanz[2], Klaus Schulze-Osthoff[8,9], and Claudia Lengerke[1,2,10]

Abstract

Overexpression of the EVI1 oncogene is associated typically with aggressive myeloid leukemia, but is also detectable in breast carcinoma where its contributions are unexplored. Analyzing a tissue microarray of 608 breast carcinoma patient specimens, we documented EVI1 overexpression in both estrogen receptor–positive (ER^+) and estrogen receptor–negative (ER^-) breast carcinomas. Here, we report prognostic relevance of EVI1 overexpression in triple-negative breast carcinoma but not in the HER2-positive breast carcinoma subset. In human breast cancer cells, EVI1 silencing reduced proliferation, apoptosis resistance, and tumorigenicity, effects rescued by estrogen supplementation in ER^+ breast carcinoma cells. Estrogen addition restored ERK phosphorylation in EVI1-silenced cells, suggesting that EVI1 and estradiol signaling merge in MAPK activation. Conversely, EVI1 silencing had no effect on constitutive ERK activity in $HER2^+$ breast carcinoma cells. Microarray analyses revealed G-protein–coupled receptor (GPR) signaling as a prominent EVI1 effector mechanism in breast carcinoma. Among others, the GPR54-ligand KISS1 was identified as a direct transcriptional target of EVI1, which together with other EVI1-dependent cell motility factors such as RHOJ regulated breast carcinoma cell migration. Overall, our results establish the oncogenic contributions of EVI1 in ER- and HER2-negative subsets of breast cancer. *Cancer Res; 77(8); 2148–60. ©2017 AACR.*

Introduction

Breast carcinoma is the most common malignant tumor and predominant cause of cancer-related death in women worldwide. During the last years, increasing breast carcinoma heterogeneity has been documented concerning mutational background, histopathology, dissemination patterns and efficacy of surgical, antihormonal, chemotherapy, or radiotherapies. Despite high initial remission rates, especially in early-stage disease, breast carcinoma patients carry a significant life-long risk for disease relapse (1). Recent research has focused on so-called breast carcinoma stem cells (CSC) as mediators of tumor relapse after long latency (2) as well as on stemness proteins as CSC biomarkers and potential drug targets (3, 4).

The *EVI1* gene is part of the complex MECOM locus on human chromosome 3q26 and encodes a zinc finger transcription factor that is expressed in long-term repopulating hematopoietic stem cells (HSC; refs. 5, 6). In acute myeloid leukemia (AML), *EVI1* overexpression can occur due to chromosomal rearrangements or as a reflection of the stem cell origin of the disease, but in either case predicts very adverse prognosis (7). *EVI1* expression has also been reported in solid tumors including breast carcinoma (8, 9), where it is still largely understudied with respect to relevance, functional roles, and molecular regulation.

Here, we performed a comprehensive expression and functional analysis of *EVI1* in human breast carcinoma. By analyzing a tissue microarray (TMA) of 608 patient samples, we found high EVI1 protein expression in breast carcinoma regardless of the ER status. A detailed clinicopathologic investigation uncovered a prognostic significance of EVI1 expression in ER- and especially triple-negative breast carcinoma, which was however not observed in $HER2^+$ tumor subsets. Although EVI1 depletion impaired cell-cycle progression, apoptosis resistance, and MAPK signaling in both estrogen receptor–negative (ER^-) and estrogen receptor–positive (ER^+) breast carcinoma cells, addition of estrogen could rescue these effects only in ER^+ cells. Moreover, similar as in patients, HER2 overexpression appeared to overrule EVI1 effects on MAPK signaling, explaining why EVI1 expression is of particular clinical relevance in the ER^- $HER2^-$ tumor subset. Finally, we identified the GPR54-ligand KISS1 as a novel transcriptional target of EVI1, which promotes breast carcinoma cell

[1]Department of Biomedicine, University of Basel and University Hospital Basel, Basel, Switzerland. [2]Department of Hematology, Oncology, Rheumatology, Immunology and Pulmonology, University of Tuebingen, Tuebingen, Germany. [3]Department of Prostate Cancer Research, Institute of Pathology, University Hospital of Bonn, Bonn, Germany. [4]Pathology and Molecular Pathology, University Hospital Zurich, Zurich, Switzerland. [5]Institute of Pathology, Campus Luebeck and Research Center Borstel, Leibniz Center for Medicine and Biosciences, Luebeck and Borstel, Germany. [6]Department of Gynecology and Obstetrics, University Hospital Duesseldorf, Duesseldorf, Germany. [7]Women's Hospital, University Hospital Tuebingen, Tuebingen, Germany. [8]Interfaculty Institute for Biochemistry, University of Tuebingen, Tuebingen, Germany. [9]German Cancer Consortium (DKTK) and German Cancer Research Center (DKFZ), Heidelberg, Germany. [10]Clinic for Hematology, University of Basel and University Hospital Basel, Basel, Switzerland.

Note: Supplementary data for this article are available at Cancer Research Online (http://cancerres.aacrjournals.org/).

Corresponding Author: Claudia Lengerke, University Hospital Basel, Hebelstr. 20, Basel 4031, Switzerland. Phone: 0041-61-5565129; Fax: 0041-61-2654450; E-mail: claudia.lengerke@unibas.ch

doi: 10.1158/0008-5472.CAN-16-0593

©2017 American Association for Cancer Research.

Downloaded from cancerres.aacrjournals.org on December 3, 2017. © 2017 American Association for Cancer Research.

Published OnlineFirst February 16, 2017; DOI: 10.1158/0008-5472.CAN-16-0593

migration. In sum, our report identifies *EVI1* as an oncogene that profoundly regulates breast carcinoma biology and that is of particular importance for estrogen-independent HER2-negative tumors.

Materials and Methods

Human tumor samples and TMA analysis

Handling of patient samples and data analyses were performed in accordance with federal and state laws and approved by the local ethics committee. The TMA included samples from 608 human primary breast carcinoma (primary or recurrent) histologically processed and diagnosed at the Institute for Pathology and Molecular Pathology, University Hospital Zurich (Zurich, Switzerland) as described (10). Immunohistochemistry using rabbit anti-EVI1 antibodies (Cell Signaling Technology) and digital expression analysis were performed as published (11). Briefly, a semi-quantitative image analysis software (Tissue Studio v.2, Definiens AG) was applied to digitalized TMA slides, obtaining a continuous spectrum of average brown staining intensity of tumor cell nuclei in arbitrary units. Subsequently, EVI1 expression was categorized in low, medium, or high according to the 25th and 75th percentiles of all measured expression values. FISH was used to detect *EVI1* copy-number gains and rearrangements using the *EVI1*-flanking BAC clones CTD-2079P9 and RP11-264O10 for probe labeling (12).

Cell lines and culture

Breast carcinoma cell lines (DSMZ) were bought in 2012 and reauthenticated by DSMZ in September 2014 and August 2015, respectively, using a nanoplex PCR for specific DNA profiles in eight different highly polymorphic short tandem repeat loci. In addition, samples were tested for the presence of rodent mitochondrial DNA from mouse, rat, Chinese, and Syrian hamster. Cells were cultivated according to data sheet. Breast carcinoma primary tissue samples were dissociated to single cells and cultured as described (4). Estradiol (Sigma-Aldrich), Kisspeptin-10 (Kp-10; Santa Cruz Biotechnology), and RKI-1447 (Selleckchem) were used as indicated.

Lentiviral production and transduction

EVI1-specific or control shRNAs were designed using the MISSION TRC shRNA software tool and integrated into the pLKO.1-Puro vector system (Sigma) for lentiviral production. *EVI1* overexpression and control vectors (13) were kindly provided by Olga Kustikova and Christopher Baum (Hannover Medical School, Hannover, Germany). For inducible overexpression, *EVI1* or *KISS1* cDNAs (the latter cloned from MDA-MB-231 cells using primers as indicated in Supplementary Table S2) were integrated into a pLVX vector system to drive expression by doxycycline (Sigma) from a Tet_{on} lentiviral system (Clontech). Lentiviral particles were produced and cells transduced as described (14).

siRNA treatment

Primary breast carcinoma cells were cultured for 24 hours with a mixture of 3 independent siRNAs against EVI1 and respectively 2 control siRNAs (Life Technologies) together with lipofectamine (Invitrogen) in penicillin/streptomycin-free culture medium as described (14, 15). Cells were then cultured under standard conditions for another 24 hours and then harvested for mRNA and functional assays.

RNA isolation, cDNA synthesis, and real-time PCR

RNA was extracted with an RNeasy kit (Qiagen) and cDNA synthesized using a Thermo Script RT-PCR System (Invitrogen). Reverse transcripts were amplified by qRT-PCR and quantified upon incorporation of SYBR Green on an ABI 7500 workstation. Relative expression levels were calculated after normalization to the reference gene *GAPDH* using the $\Delta\Delta C_T$ method. *CDKN1A*, *CDKN1B*, *BIK*, and *BBC3* primers were purchased from Qiagen (SYBR Green QuantiTect Primer Assays). Other primer sequences are given in Supplementary Table S2.

Cell growth, cell-cycle, proliferation, and apoptosis assays

To assess cell growth, 50,000 cells were plated and quantified after trypsinization on days 3, 6, and 9 postseeding. Cell proliferation was investigated by incorporation of BrdUrd or EdU as detailed in the manufacturers' protocols (BrdUrd: BD Biosciences; Click-iT, EdU kit: baseclick). Cell-cycle and apoptosis assays were performed as described (15). Cells were analyzed by flow cytometry for their DNA content on a FACS Fortessa machine using FlowJo software (FlowJo enterprise). For apoptosis assays, 5×10^4 cells/mL were incubated overnight and then treated either for 16 hours with staurosporine (2.5 μmol/L; Sigma-Aldrich) or for 24 hours with SuperKiller TRAIL (50 ng/mL; Enzo Life Sciences).

Immunoblotting

Immunoblotting was performed as described (4) using the following primary antibodies (Cell Signaling Technology): anti-pan AKT (#4691S), anti-pAKT (pSer473, #4060S), anti-ERK1/2 (#4695), anti-pERK1/2 (Thr202/Tyr204, #4377), anti-GAPDH (#5174P), anti-EVI1 (#2593), anti-p21 (#2947), anti-p27 (#3688), anti-CDK2 (#2546), and anti-β-actin (#3700S). Fluorescently labeled or HRP-conjugated secondary antibodies were used as described (14, 15).

Microarray gene expression analysis

Microarrays analyses were performed in triplicates from control and *EVI1* knockdown MDA-MB-231 cells (obtained with either one of two independent *EVI1*-specific shRNAs). RNA was extracted with an RNeasy Mini kit (Qiagen). Concentration and purity of RNA samples were determined with a NanoDrop photometer (peqlab), and integrity confirmed on a 2100 Bioanalyzer (Agilent Technologies). Only RNA samples with RIN values $\geq$ 7.5 were considered. Per condition, 100 ng of RNAs were used to prepare cyanine-3–labeled cRNA for hybridizations, which were performed according to standard protocols using Agilent SurePrint G3 Human Gene Expression 8×60K v2 Microarrays. After extensive washing, fluorescence intensities were detected with the Scan Control A.8.4.1 software (Agilent) on an Agilent DNA Microarray Scanner and extracted from images using Feature Extraction 10.7.31 software (Agilent). Quantile normalization was applied to the data set, and correlation analysis was performed. Fold-change calculations identified differentially expressed genes, and Panther analysis most prominently affected pathways in *EVI1* knockdown versus control cells. Array data have been deposited in NCBI's Gene Expression Omnibus and are accessible through GEO Series accession number GSE95272 (https://www.ncbi.nlm.nih.gov/geo/query/acc.cgi?acc=GSE95272).

Chromatin immunoprecipitation

Chromatin immunoprecipitation (ChIP) was performed as described (16). Briefly, 1×10^7 control or *EVI1*-overexpressing

Downloaded from cancerres.aacrjournals.org on December 3, 2017. © 2017 American Association for Cancer Research.

Published OnlineFirst February 16, 2017; DOI: 10.1158/0008-5472.CAN-16-0593

Hs 578T cells were fixed in 1% formaldehyde, sonicated, precleared, and incubated with 10 μg anti-EVI1 or isotype control antibodies overnight at 4°C. Complexes were washed, DNA-extracted, precipitated, and amplified by RT-PCR using primers sets homologous to regions of the human *KISS1* promoter. Nonimmunoprecipitated chromatin was used as input control. Primers flanking the EVI1-binding site in the *BCL2L1* promoter and at a previously described nonbinding site served as positive and negative controls, respectively (17).

Migration assay

The established "wound healing assay" was performed to assess cell migration (18). Briefly, cells were grown to confluence in 24-well plates and incubated with 5 μg/mL aphidicolin (Sigma-Aldrich, A4487) and reduced FCS concentrations (2%) to stall proliferation. Subsequently, the monolayer was injured with a pipette tip and detached cells removed by iterative washing, leaving an approximately 200-μm wide unsettled zone free for lateral repopulation. Migration into these "wound areas" was followed on an Axio Vert.A1 microscope (Zeiss) and quantified by Fiji Imaging software at 0, 12, and 24 hours of incubation with or without addition of doxycycline, Kp-10, or RKI-1447 as indicated.

Zebrafish xenograft experiments

Animal experiments and zebrafish husbandry were approved by the "Kantonales Veterinaeramt Basel-Stadt." Xenotransplantation and assessment of tumor cell engraftment were performed as described (4, 19). In brief, 75 to 100 breast carcinoma cells labeled with the fluorescent CellTracker (Life Technologies) were micro-injected at 48 hours postfertilization into the vessel-free area of the yolk sac of transgenic Tg(flk1:eGFP) zebrafish embryos anesthetized in 0.4% tricaine (20). For rescue experiments, the fish water was supplemented with 100 nmol/L estradiol (Sigma) or carrier (DMSO) at days 0 and 2.5 posttransplantation. Tumor development was assessed microscopically at day 5 postinjection (19, 21). For pERK inhibition, the fish water was supplemented with 200 nmol/L of CI-1040 at days 1 and 2 posttransplantation.

Mouse xenograft experiments

NOD.Cg-Prkdc^{scid} IL2rg^{tmWjl}/Sz(NSG) mice purchased from The Jackson Laboratory were maintained under pathogen-free conditions according to federal and state regulations. Control and EVI1 knockdown MDA-MB-231 cells (1×10^6) mixed with Matrigel (1:1; BD Biosciences) were co-laterally implanted by subcutaneous injection into the flanks of individual mice and occurrence of tumors monitored by palpation as reported (15). Tumor area was assessed *in situ* using the Fiji software, and tumor weight was measured after excision.

Statistical analyses

Unless otherwise indicated, data from ≥3 independent biological experiments performed in technical triplicates were analyzed. Results are shown as mean ± SD. *P* values were calculated by two-tailed, unpaired Student *t* tests or as specified and *P* values indicated with * for <0.05, ** for <0.01, and *** for <0.001. Retrospective survival analyses of breast carcinoma patients were performed by the Kaplan–Meier method using log-rank (Mantel–Cox), Breslow, and Tarone–Ware tests.

Results

EVI1 gene and protein expression in human breast carcinoma

First, we assessed *EVI1* gene and protein expression in 12 primary human breast carcinoma samples (Fig. 1A) and 8 breast carcinoma cell lines (Fig. 1B and C; ER$^-$: MDA-MB-231, BT-549, Hs 578T, MDA-MB-468, SK-BR-3, and ER$^+$: BT-474, T-47D, MCF7). EVI1 expression was detected in several samples irrespective of the ER status. To cover a comprehensive range of endogenous EVI1 expression for subsequent functional investigations, two ER$^-$ (MDA-MB-231 and Hs 578T) and two ER$^+$ breast carcinoma cell lines (T-47D and MCF7) were chosen and investigated alongside with four primary patient-derived cell samples of different ER status (P1–P4).

Furthermore, we employed immunohistochemistry to investigate EVI1 protein expression on a TMA of 608 breast carcinoma samples (10). Reliable and biologically interpretable results were obtained from 527 samples, 512 of which information on ER status was available. Consistent with our previous data, EVI1 protein was detected at variable degrees (Fig. 1D) in both ER$^-$ ($n = 91$) and ER$^+$ ($n = 421$) tumors (Fig. 1D and Supplementary Table S1). However, a significant correlation between EVI1 expression levels and survival was only observed in the ER$^-$ subgroup ($n = 91$ patients; 5-year survival: $P = 0.011$, overall survival: $P = 0.026$) but not in the ER$^+$ subgroup ($n = 421$ patients) or the whole patient cohort analyzed together (Supplementary Fig. S1A). Interestingly, the influence of EVI1 expression on overall survival was most pronounced in triple-negative breast carcinoma ($P = 0.006$), but lost when ER$^-$/HER2$^+$ subsets were separately analyzed (Supplementary Fig. S1A). Together, these data suggest that EVI1 expression is of particular significance in breast carcinoma that is not driven by active ER and HER2 signaling.

ER- and triple-negative breast carcinoma subgroups, in which EVI1 showed prognostic relevance, were subjected to further analysis of clinico-pathologic parameters. High EVI1 expression associated indeed with enhanced distant metastasis rate ($P = 0.046$ and $P = 0.027$, respectively; Supplementary Fig. S1A), indicating a putative functional contribution to tumor cell dissemination/migration. To investigate the mechanisms responsible for EVI1 overexpression, we performed FISH analyses. Unlike in leukemia (22), we could not detect *EVI1* gene rearrangements or copy-number gains except in 2 of 512 breast carcinoma patients (Fig. 1E; Supplementary Fig. S1B).

Based on these data, we conclude that EVI1 expression is frequently observed in human breast carcinoma, where it is mostly driven by yet unknown regulatory events, and might be particularly relevant for estrogen-independent HER2-negative tumors.

EVI1 induces cell proliferation and apoptosis resistance

To examine the functional significance of *EVI1* in breast carcinoma, we performed *EVI1* knockdown experiments in two ER$^-$ (MDA-MB-231 and Hs 578T) and one ER$^+$ (T-47D) breast carcinoma cell line and two patient-derived primary breast carcinoma samples per condition (ER$^+$: P1, P2; ER$^-$: P3, P4). Cells were transduced with lentiviral particles carrying either noncoding or two alternate *EVI1* shRNAs. Transduction with either shRNAs downregulated EVI1 protein and mRNA expression when compared with controls (Fig. 2A; Supplementary Figs. S2A–S2B and S3A). Throughout all analyzed samples, *EVI1* knockdown cells

Downloaded from cancerres.aacrjournals.org on December 3, 2017. © 2017 American Association for Cancer Research.

Published OnlineFirst February 16, 2017; DOI: 10.1158/0008-5472.CAN-16-0593

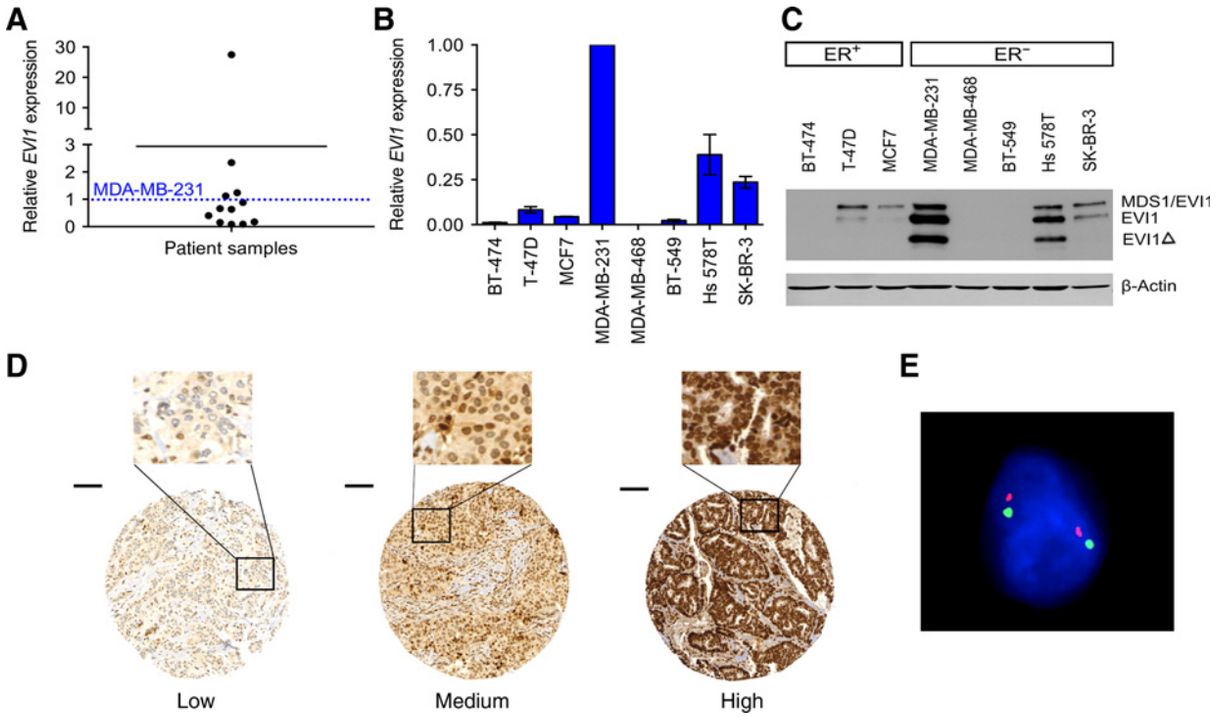

Figure 1.

Differential expression of *EVI1* in human breast carcinoma cells. **A** and **B,** qRT-PCR analysis of *EVI1* expression in 12 primary breast carcinoma samples (**A**) and eight breast carcinoma cell lines (**B**). Indicated are *EVI1* expression levels relative to MDA-MB-231 cells (dotted line); mid-line illustrates average expression (**A**). **C,** Immunoblots documenting variable degrees of EVI1 protein expression in ER^+ and ER^- breast carcinoma cell lines. Predominant isoforms (MDS/EVI1, EVI1, and EVI1Δ) are indicated. β-Actin was used as loading control. **D,** Immunohistological image sections illustrating different degrees (weak, medium, strong) of EVI1 expression in breast carcinoma TMA samples. Overview pictures (bottom, scale bars, 100 μm), inlays at higher magnification (top). **E,** Representative FISH analysis showing normal distribution of EVI1 copy numbers in breast carcinoma. Red and green FISH probes, respectively, flank the *EVI1* gene locus. Nucleus, DAPI, blue.

showed a clear growth defect when compared with corresponding control cells (Fig. 2B; Supplementary Figs. S2C and S3B).

The lower growth rates observed in *EVI1* knockdown cells could be caused by decreased proliferation or enhanced apoptosis rates, both of which are modulated by EVI1 in other cell types (22). Indeed, knockdown of *EVI1* enhanced basal breast carcinoma cell apoptosis (Fig. 3A; Supplementary Figs. S2D and Fig. S3C) as well as apoptosis sensitivity in response to staurosporine or the death ligand TRAIL (Fig. 3B; Supplementary Fig. S3D). In addition, cell-cycle analyses revealed a G_1–S phase transition defect upon *EVI1* knockdown (Fig. 3C; Supplementary Fig. S3E), indicating a proliferation defect. Supporting this notion, BrdUrd incorporation was also diminished (Fig. 3D; Supplementary Fig. S3F). In line, key checkpoint regulators that block G_1–S phase transition, such as the cyclin-dependent kinase inhibitors 1A and 1B ($p21^{Cip1}$ and $p27^{Kip1}$), were upregulated in *EVI1* knockdown MDA-MB-231 cells, while their mutual downstream target CDK2 was decreased (Supplementary Fig. S4).

Stimulation of the ER pathway rescues pERK expression and growth in *EVI1* knockdown breast carcinoma cells

Intriguingly, the profound growth-modulatory effects of EVI1 were observed independent of the ER status, which is in apparent contrast to the prognostic significance of EVI1 expression especially in ER^- breast carcinoma patients. Indeed, the *in vitro* findings in ER^+ breast carcinoma cells could be biased by lack or reduced ER stimulation under standard cultivation conditions. Confirming this hypothesis, addition of estradiol greatly restored growth of *EVI1* knockdown ER^+ T-47D but not ER^- MDA-MB-231 breast carcinoma cells (Fig. 4A). Consistently, estradiol fostered the incorporation of EdU in T-47D but not in MDA-MB-231 *EVI1* knockdown cells (Fig. 4B). We conclude that active estrogen signaling overrules EVI1-mediated growth effects, and, therefore, EVI1-mediated growth induction may be more critical for patients with ER^- tumors that do not equally respond to natural estrogen.

ERK and AKT kinases are key regulators of cell proliferation and survival downstream of estrogen signaling (23–25). We thus wondered whether EVI1 also acts via activation of these kinases in breast carcinoma. No consistent pAKT suppression was observed in *EVI1* knockdown cells (Fig. 4C and F), although *EVI1* overexpression indeed induced pAKT levels (Fig. 4D). However, an overt decrease in phosphorylated (i.e., activated) ERK levels was reproducibly noted upon *EVI1* knockdown throughout the analyzed ER^- and ER^+ breast carcinoma samples (Fig. 4C and Supplementary Fig. S5A), indicating the ERK pathway as a dominant growth axis regulated by EVI1. Indeed, treatment with MEK inhibitors (CI-1040, trametinib, or AZD6244) that act upstream of ERK (26) similarly suppressed cell growth and cycle progression of MDA-MB-231 and T-47D cells (Supplementary Fig. S5B–S5F). Further supporting this notion, addition of estradiol enhanced ERK, but not AKT,

Downloaded from cancerres.aacrjournals.org on December 3, 2017. © 2017 American Association for Cancer Research.

Published OnlineFirst February 16, 2017; DOI: 10.1158/0008-5472.CAN-16-0593

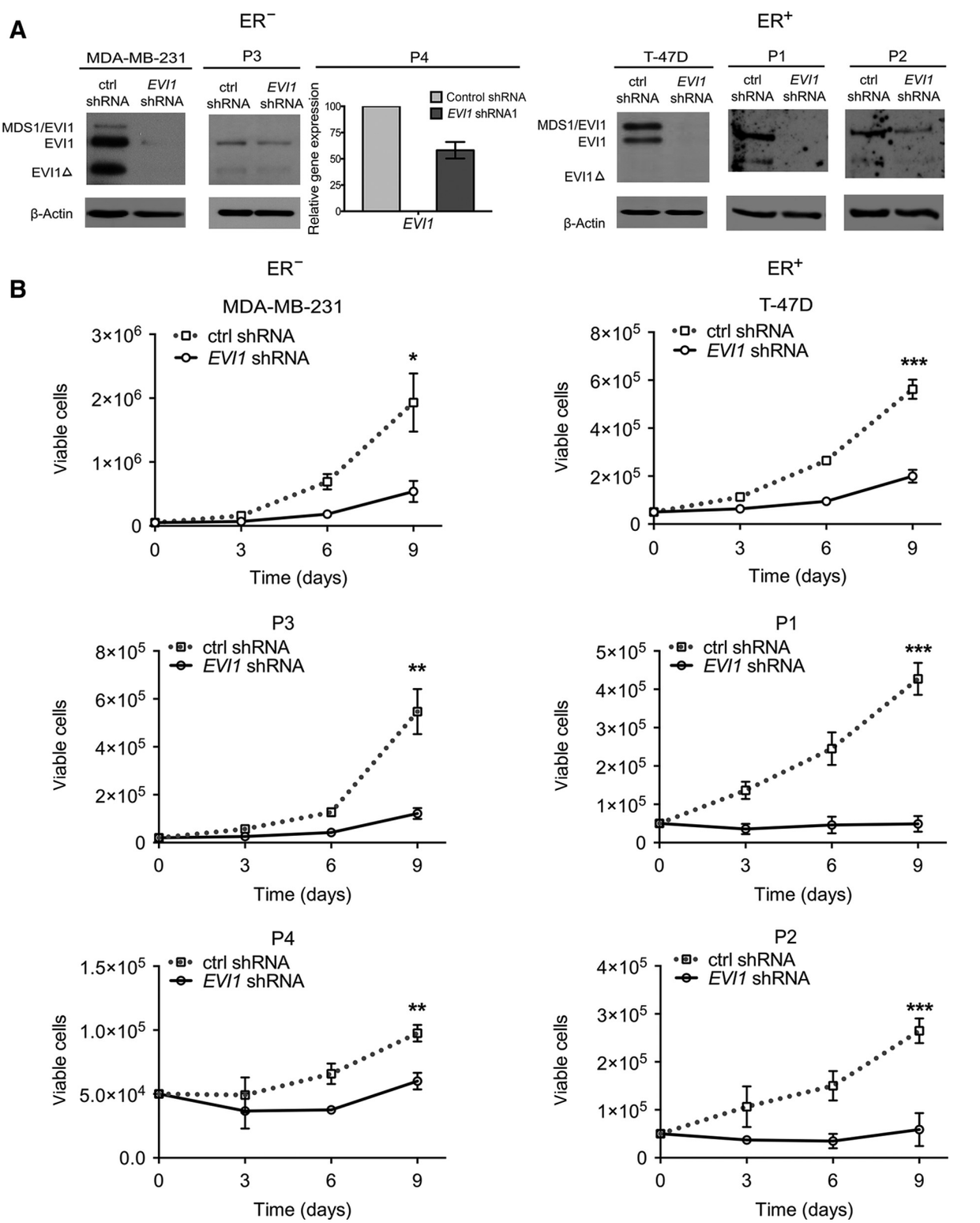

Figure 2.

EVI1 promotes breast carcinoma cell growth *in vitro*. **A,** Immunoblot and qRT-PCR analyses documenting efficient depletion of EVI1 expression in *EVI1* knockdown versus control breast carcinoma cell lines and primary patient-derived cell samples. ER^- (MDA-MB-231, P3 and P4, left) and ER^+ (T-47D, P1 and P2, right). Due to low protein levels in patient sample P4, depletion of EVI1 expression was confirmed by RT-PCR. **B,** Growth curves illustrating a proliferation defect in *EVI1* knockdown vs. control cells. ER^- cells (left); ER^+ cells (right). Plotted are mean values ± SD *, $P < 0.05$; **, $P < 0.01$; ***, $P < 0.001$.

Downloaded from cancerres.aacrjournals.org on December 3, 2017. © 2017 American Association for Cancer Research.

Published OnlineFirst February 16, 2017; DOI: 10.1158/0008-5472.CAN-16-0593

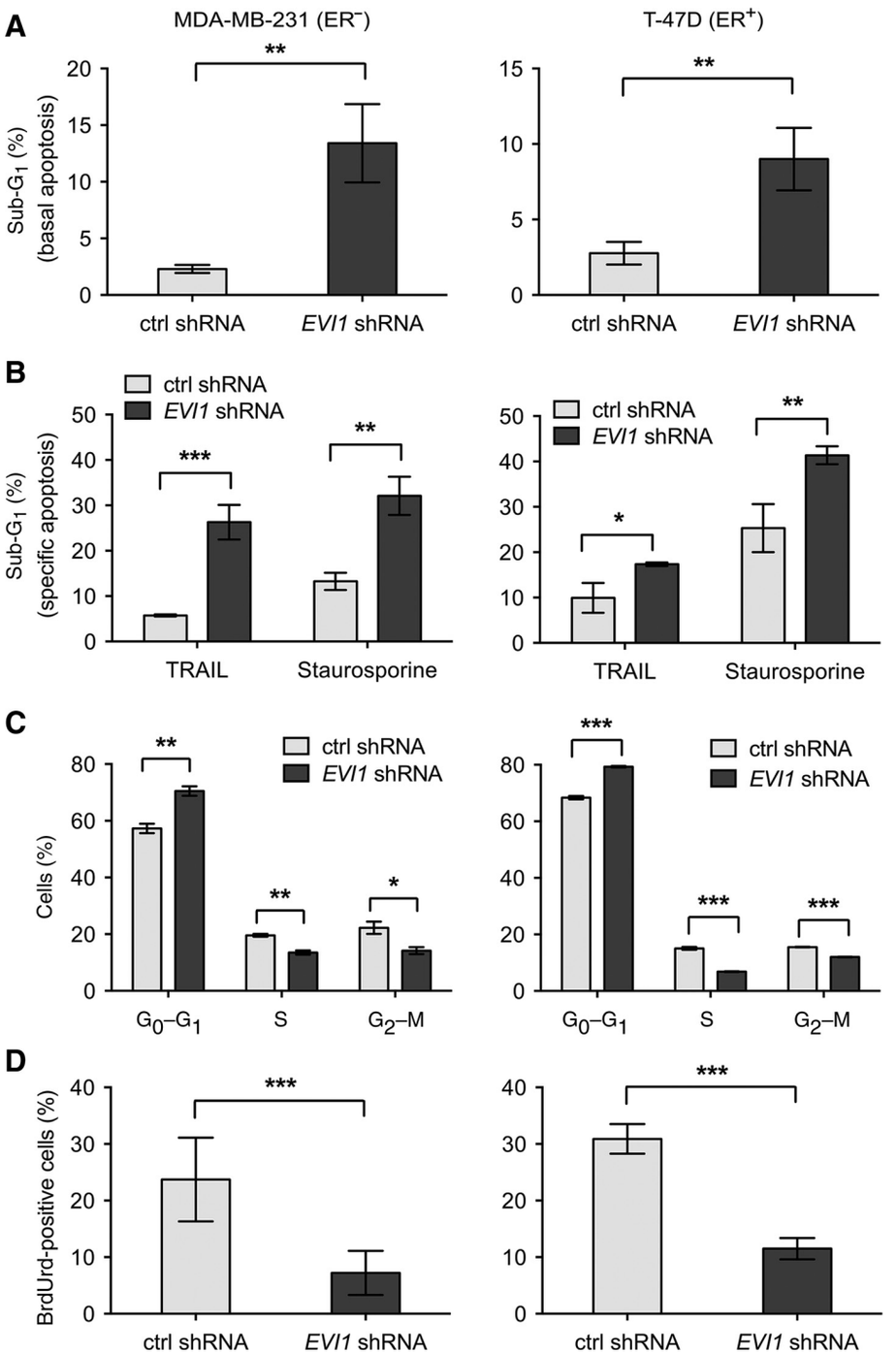

Figure 3.

EVI1 affects apoptosis regulation and cell-cycle progression in breast carcinoma. *EVI1* knockdown MDA-MB-231 (left plots) and T-47D cells (right plots) reveal elevated basal apoptosis (**A**), increased apoptosis sensitivity in response to TRAIL and staurosporine (**B**), increased cell-cycle arrest (**C**), and reduced BrdUrd incorporation (**D**) compared with control shRNA–treated cells. Shown are mean values ± SD. *, $P < 0.05$; **, $P < 0.01$; ***, $P < 0.001$.

phosphorylation in *EVI1* knockdown ER$^+$ T-47D but not ER$^-$ MDA-MB-231 breast carcinoma cells (Fig. 4C). *EVI1* overexpression consistently upregulated pERK in MCF7, T-47D, and MDA-MB-468 cells, and displayed synergistic effects with estradiol in ER$^+$ T-47D cells (Fig. 4D–E). Interestingly, the rescue of cell growth induced by β-estradiol in *EVI1* knockdown cells was abrogated by cotreatment with either the ER-blocking reagent tamoxifen or the MEK inhibitor CI-1040 (Supplementary Fig. S5G).

As also HER2 mediates growth-stimulatory effects via the MAPK/ERK signaling axis in breast carcinoma, we further examined the significance of *EVI1* knockdown on HER-dependent ERK phosphorylation and found that, although loss of EVI1 signaling effectively depleted pERK in HER2$^-$ breast carcinoma cells, ERK phosphorylation remained essentially unaltered in the investigated HER2$^+$ samples (Fig. 4F, left vs. right plots). Together, these data suggest that EVI1, ER, and HER2 signaling functionally impinge on phosphor-modulation of ERK as a common downstream pathway.

Downloaded from cancerres.aacrjournals.org on December 3, 2017. © 2017 American Association for Cancer Research.

Published OnlineFirst February 16, 2017; DOI: 10.1158/0008-5472.CAN-16-0593

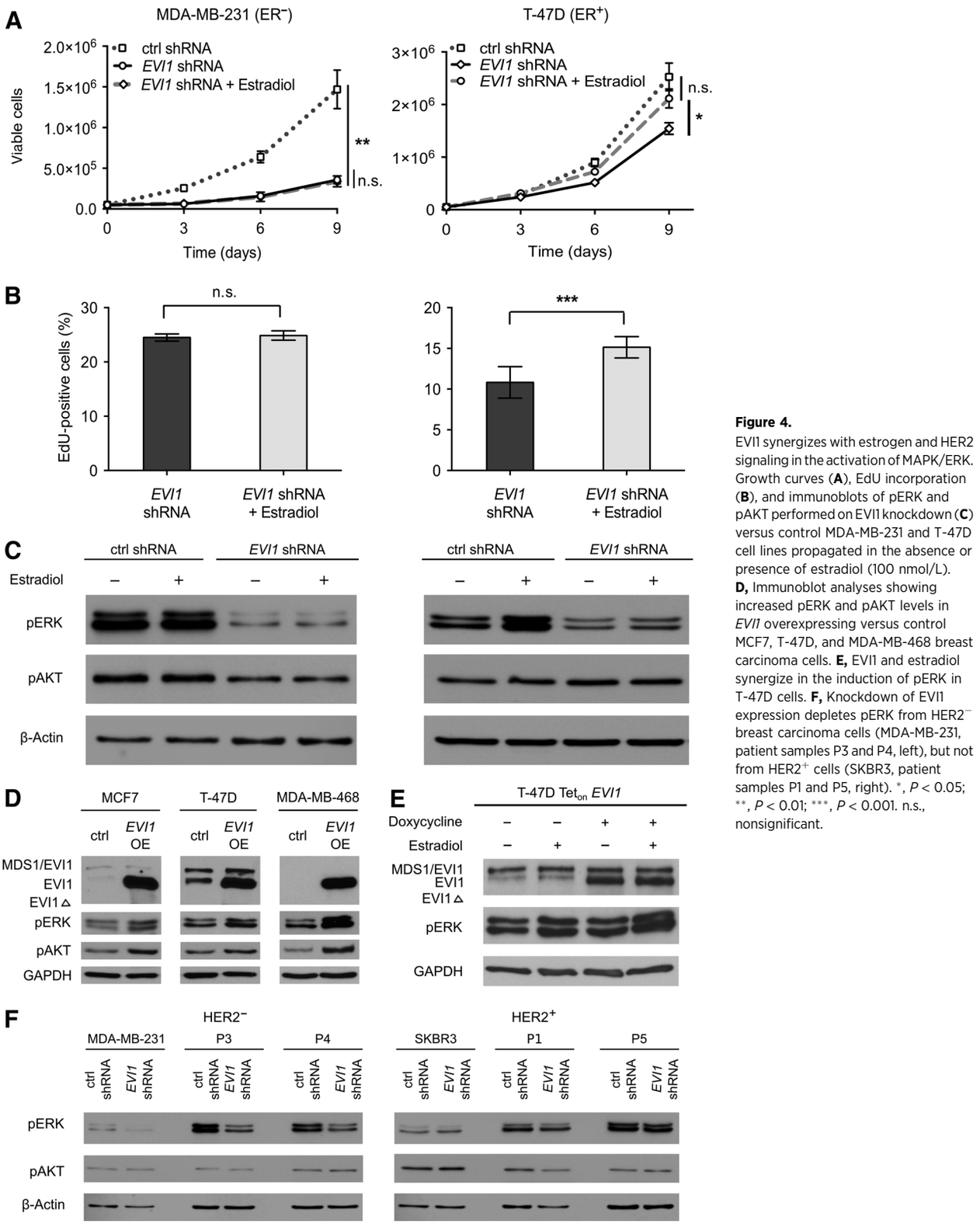

Figure 4.

EVI1 synergizes with estrogen and HER2 signaling in the activation of MAPK/ERK. Growth curves (**A**), EdU incorporation (**B**), and immunoblots of pERK and pAKT performed on EVI1 knockdown (**C**) versus control MDA-MB-231 and T-47D cell lines propagated in the absence or presence of estradiol (100 nmol/L). **D,** Immunoblot analyses showing increased pERK and pAKT levels in *EVI1* overexpressing versus control MCF7, T-47D, and MDA-MB-468 breast carcinoma cells. **E,** EVI1 and estradiol synergize in the induction of pERK in T-47D cells. **F,** Knockdown of EVI1 expression depletes pERK from $HER2^-$ breast carcinoma cells (MDA-MB-231, patient samples P3 and P4, left), but not from $HER2^+$ cells (SKBR3, patient samples P1 and P5, right). *, $P < 0.05$; **, $P < 0.01$; ***, $P < 0.001$. n.s., nonsignificant.

EVI1 knockdown suppresses tumor formation *in vivo*

Next, we used xenotransplantation assays to examine the relevance of *EVI1* for *in vivo* tumorigenesis from human breast carcinoma cells. Equal numbers of *EVI1* knockdown and control MDA-MB-231 cells (ER^-HER2^-) were injected subcutaneously into contralateral flanks of immuno-permissive NSG mice, and

Downloaded from cancerres.aacrjournals.org on December 3, 2017. © 2017 American Association for Cancer Research.

Published OnlineFirst February 16, 2017; DOI: 10.1158/0008-5472.CAN-16-0593

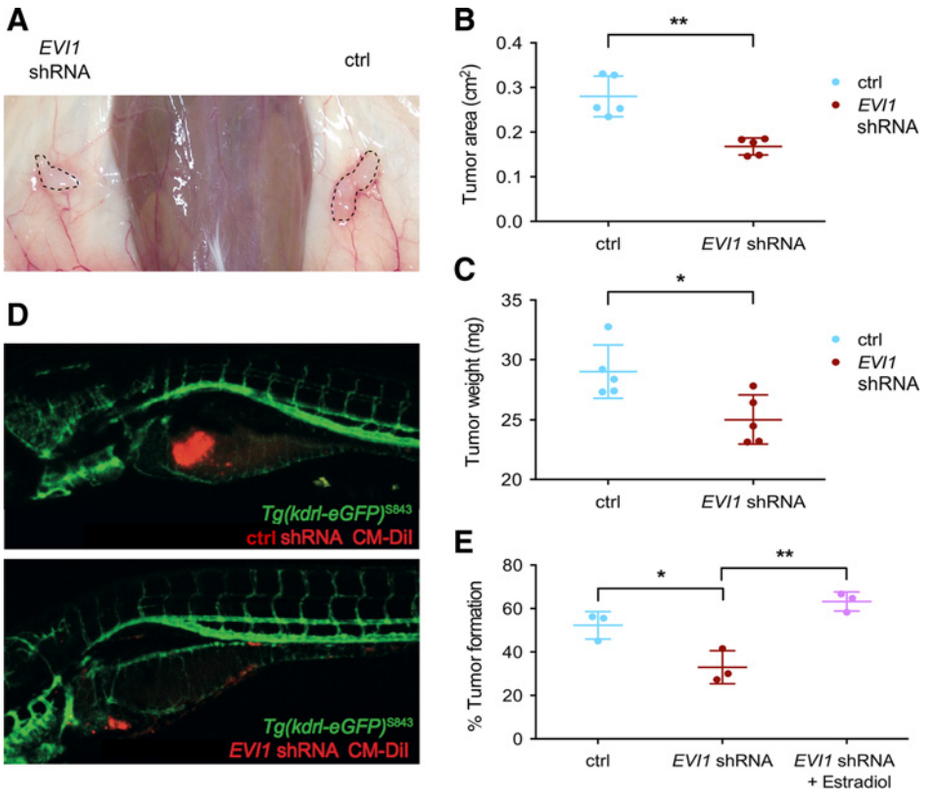

Figure 5.

EVI1 knockdown impairs tumor growth *in vivo*. **A,** ER$^-$ MDA-MB-231 control (right) and *EVI1* knockdown cells (left) were contralaterally injected subcutaneously into NSG mice. Illustrated is a representative example of tumor formation after a follow-up of 12 days. Note that *EVI1* knockdown cells generate smaller tumors (left). **B** and **C,** Corresponding quantitative analysis of tumor area and tumor masses ($n = 5$). *P* values were calculated by a Mann–Whitney test. **D,** Seventy-five to 100 CM-DiI–labeled control or EVI1 knockdown breast carcinoma cells were transplanted into the yolk sac of *Tg(kdrl:eGFP)* fish embryos and analyzed at day 5 posttransplantation by confocal microscopy for tumor formation (red). **E,** Estradiol treatment (100 nmol/L estradiol, 3 days before treatment of cells *in vitro* and afterwards added to the fish water) restores reduction of tumor formation upon *EVI1* knockdown in ER$^+$ T-47D cells. *, $P < 0.05$; **, $P < 0.01$.

tumor formation was assayed over time. At 12 days posttransplantation, smaller tumors were documented from *EVI1* knockdown cells versus control cells (Fig. 5A–C), indicating that *EVI1* influences *in vivo* tumorigenicity. Immunoblot analysis confirmed persistent knockdown of *EVI1* and impaired phosphorylation of ERK in excised tumors (Supplementary Fig. S6A). These data were confirmed in a previously established zebrafish xenotransplant model (4, 19). Consistent with the results obtained in mouse, both *EVI1* knockdown ER$^+$ T-47D and ER$^-$ MDA-MB-231 cells induced fewer tumors than corresponding control cells, whereas estrogen supplementation rescued *in vivo* tumor formation selectively from ER$^+$ cells (Fig. 5D–E; Supplementary Fig. S6B). Moreover, the MEK inhibitor CI-1040 was able to block the rescue effect of β-estradiol *in vivo* (Supplementary Fig. S6C). In line with their reduced *in vivo* tumorigenicity, *EVI1* knockdown cells also displayed impaired mammosphere formation *in vitro* (Supplementary Fig. S6D). These data indicate that, although *EVI1* may not be a specific CSC marker in breast carcinoma, it coregulates the stem cell compartment.

Identification of GPCR signaling–associated molecules as *EVI1* downstream targets

To further explore the molecular mechanisms underlying *EVI1*-driven effects in breast carcinoma, we analyzed the transcriptome of control and *EVI1* knockdown MDA-MB-231 cells using gene expression microarrays. A total of 816 differentially expressed genes were identified in *EVI1* knockdown versus control cells, of which 324 were up- and 492 downregulated. Panther analysis identified cell(-cell) adhesion, cell communication, signal transduction, developmental and immune system process regulation as the predominantly influenced biological processes, and receptors, cell-adhesion, and respectively extracellular matrix proteins as the most significantly affected protein classes (Fig. 6A). Furthermore, GeneSpring analyses revealed "G protein–coupled receptor (GPCR) signaling" molecules, such as *KISS1*, *EDN1*, *PTGFR*, and *PIK3CG* (Fig. 6B and C), as the most influenced pathway, next to cell-cycle control and progression (with perturbed expression levels of several key regulators such as *CDKN1A*, *CDKN1C*, *CCNA1*, and *CDK1*), apoptosis resistance (with upregulation of proapoptotic genes such as *BIK*, *BMF*, and *BBC3*), and ERBB signaling–related molecules (e.g., *EREG*, *DUSP5*, and *NRG2*). Heat maps of these individual categories are depicted in Fig. 6C and Supplementary Fig. S7A and S7B with a cut-off of 2-fold and 1.5-fold expression changes, respectively. *EVI1*-dependent expression changes of 15 exemplary candidate genes were further validated by qRT-PCR (Supplementary Fig. S7C).

To identify potential direct target genes of *EVI1* in breast carcinoma, we next investigated the expression of candidate genes in response to *EVI1* overexpression (Supplementary Fig. S7D). Among these, the GPR54-ligand *KISS1* stood out as one of the most strongly influenced genes. In addition, the induction of *KISS1* mRNA displayed a clear dose-dependency on *EVI1* transcript levels (Fig. 7A). Furthermore, codepletion of *EVI1* and *KISS1* mRNA was observed in primary breast carcinoma cells treated with siRNAs against *EVI1* versus corresponding control siRNA–treated cells (Supplementary Fig. S7E). Moreover, promoter analysis of *KISS1* revealed several potential EVI1-binding sites within *KISS1* regulatory elements (Supplementary Fig. S8A), reinforcing *KISS1* as a putative direct transcriptional target of EVI1. Based on this analysis, four promoter regions of *KISS1* were selected (Supplementary Fig. S8A) and assessed for EVI1 binding in ChIP assays. Higher enrichment rates were indeed observed in

Downloaded from cancerres.aacrjournals.org on December 3, 2017. © 2017 American Association for Cancer Research.

Published OnlineFirst February 16, 2017; DOI: 10.1158/0008-5472.CAN-16-0593

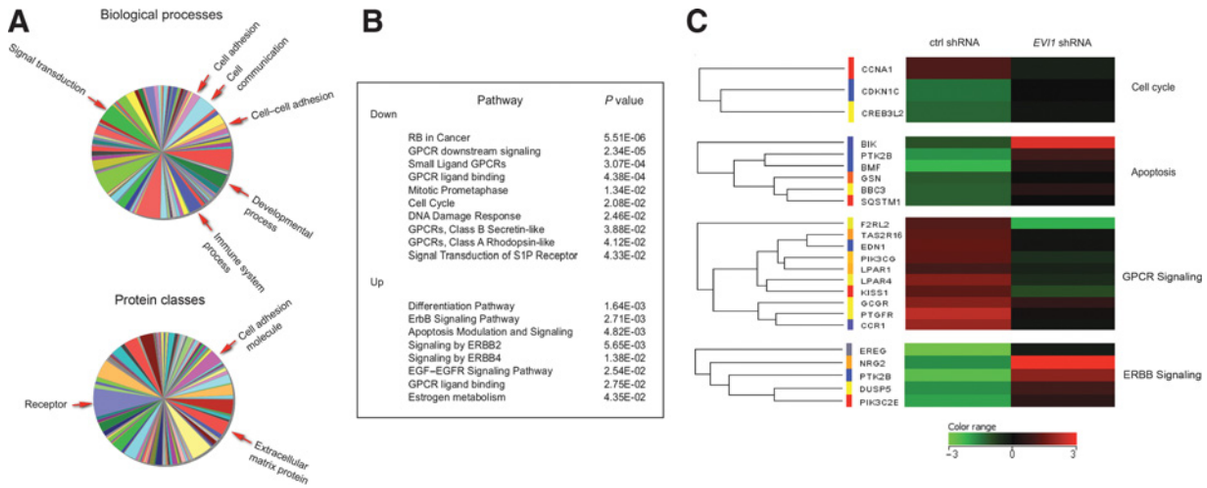

Figure 6.

Gene expression patterns associated with *EVI1* knockdown. **A,** Panther classification linking gene signatures from *EVI1* knockdown transcriptome analysis to Biological Process and Protein Classes. Significantly modulated gene/protein classes are indicated. **B,** Index list of pathways significantly modulated by *EVI1* knockdown (i.e., $P < 0.05$). **C,** Heat maps depicting 24 individual gene entries whose expression significantly differs in a microarray analysis of control vs. *EVI1* knockdown MDA-MB-231 cells. Genes most strongly affected by *EVI1* knockdown functionally cluster in the categories cell-cycle regulation, apoptosis, GPCR, and ERBB signaling.

EVI1-overexpressing versus control cells especially at the most distal promoter site (–4880 to –4761 bp, Fig. 7B). Thus, these data identify the *KISS1* promoter as a yet-unrecognized target region for EVI1 in breast carcinoma (see also Supplementary Fig. S8 for control and schematic illustration of binding sites). We therefore conclude that, next to modulating expression of cell-cycle– and apoptosis-relevant genes (Fig. 6B and C and Supplementary Fig. S7B–S7C), EVI1 directly influences GPCR signaling via transcriptional modulation of the GPR54 ligand KISS1.

Differential role of KISS1 in EVI1-mediated cell migration, cell growth, and ERK activation

KISS1 was originally identified as a metastasis suppressor (27, 28), and more recently described to enhance motility and invasiveness of ER^- breast carcinoma cells (29, 30). We thus hypothesized that EVI1 contributes to these processes at least in part via transcriptional regulation of KISS1. Indeed, migration assays revealed that knockdown of EVI1 strongly impaired the motility of ER^- MDA-MB-231 (Fig. 7C–F) and Hs 578T cells (Supplementary Fig. S9A–S9B), whereas overexpression of EVI1 overtly increased cell mobility (Fig. 7G and H; Supplementary Fig. S9C–S9D). Supporting the role of KISS1 as a downstream target in EVI1-dependent migration, exposure of cells to the GPR54-ligand Kisspeptin-10 (Kp-10), a gene product of KISS1 shown to enhance ER^- breast carcinoma cell motility (Supplementary Fig. S10A), indeed rescued the migration defects observed in *EVI1* knockdown MDA-MB-231 cells (Fig. 7C and D). Supporting these data, overexpression of KISS1 itself also rescued migration in EVI1 knockdown MDA-MB-231 (Fig. 7E and F and Supplementary Fig. S10A–S1B) and Hs 578T cells (Supplementary Fig. S9A–S9B).

Noteworthy, several further modulators of cell motility and adhesion were found to be regulated by EVI1 in our microarray analysis, including RhoJ and TIE1, two molecules that had not been linked to EVI1 or breast carcinoma cell migration before. Exemplifying the functional relevance of also these findings, inhibition of RHO/ROCK signaling with RKI-1447 impaired EVI1-induced breast carcinoma cell mobility in migration assays (Fig. 7G and H and Supplementary Fig. S9C–S9D).

Interestingly, supplementation with Kisspeptin (Kp-10), which effectively rescued migration (Fig. 7C and D), could not restore cell growth in *EVI1* knockdown cells (Supplementary Fig. S10C). Consistently, neither treatment with Kisspeptin (Kp-10) nor KISS1 overexpression influenced pERK activity (Supplementary Fig. S10D). Vice versa, treatment of breast carcinoma cells with the MAPK inhibitor CI-1040 effectively suppressed pERK and cell growth (Supplementary Fig. S5B, S5C, and S5F) but did not influence breast carcinoma cell migration (Supplementary Fig. S10F–G). In particular, treatment with CI-1040 did not abrogate EVI1-induced KISS1 overexpression (Supplementary Fig. S10E) and related breast carcinoma cell migration, reinforcing the idea that these effects are independent of the MAPK pathway (Fig. 7I).

Taken together, we demonstrate a functional relevance of *EVI1* gene expression for breast carcinoma cell growth that involves modulation of pERK signaling (see Fig. 7I for schematic illustration). In part complementary to ER signaling and eventually overruled by constitutive ERK activity in $HER2^+$ breast carcinoma, EVI1-mediated effects achieve pivotal significance in ER^- $HER2^-$ breast carcinoma, where EVI1 expression is of prognostic significance. Moreover, we present evidence for a hitherto unrecognized EVI1-KISS1-GPR54 axis that—independently of ERK signaling—modulates breast carcinoma cell motility, suggesting that also the capacity to induce metastasis may be intimately linked to EVI1. Thus, our work identifies EVI1 as a novel critical determinant of breast carcinoma cell biology that is of particular importance for estrogen-independent $HER2^-$ breast carcinoma.

Discussion

Initially identified as a retroviral insertion region in hematopoietic cells (31), EVI1 has been intensely studied in HSCs and

Downloaded from cancerres.aacrjournals.org on December 3, 2017. © 2017 American Association for Cancer Research.

Published OnlineFirst February 16, 2017; DOI: 10.1158/0008-5472.CAN-16-0593

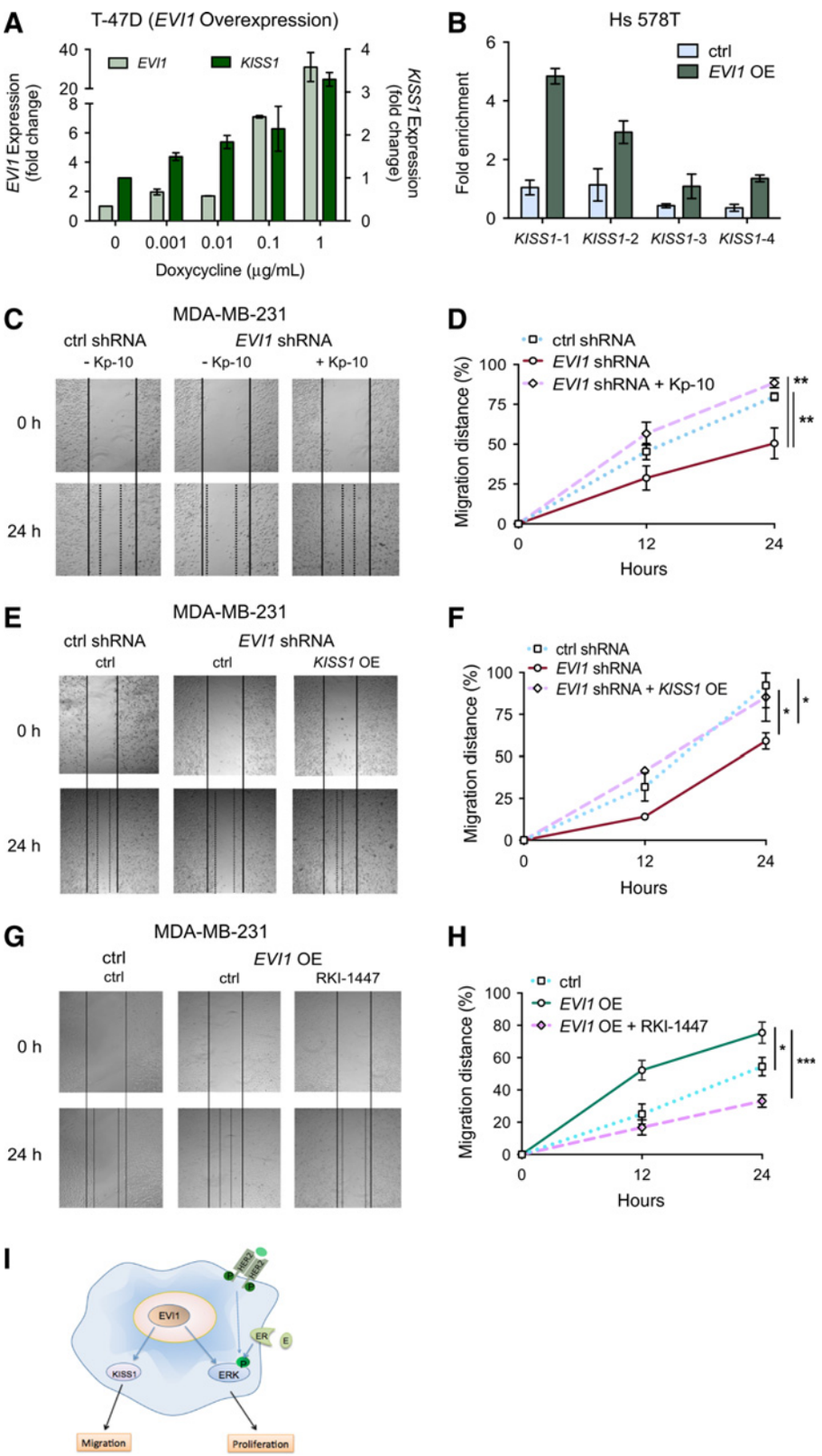

Figure 7.

EVI1 regulates breast carcinoma cell migration via modulation of GPR54/KISS1 and RHO/ROCK signaling. **A,** qRT-PCR analyses documenting dose-dependent coinduction of *EVI1* and *KISS1* in inducible *EVI1*-overexpressing T-47D cells. **B,** ChIP analysis illustrating direct recruitment of EVI1 to regulatory *KISS1* promoter elements in Hs 578T control and more strongly in *EVI1*-overexpressing cells. **C–F,** Supplementation with the soluble *KISS1* gene product Kp-10 (1 μmol/L; **C** and **D**), or overexpression of KISS1 itself (**E** and **F**) ameliorates migration defects imposed by EVI1 knockdown in MDA-MB-231 breast carcinoma cells. Overview images (left); corresponding assay quantifications (right). **G** and **H,** Migration assays documenting increased mobility of MDA-MB-231 cells in response to EVI1 overexpression, whereas treatment with the RHO/ROCK pathway inhibitor RKI-1447 impairs the mobility of EVI1-overexpressing MDA-MB-231 cells. Image sections (**G**, left) and corresponding assay quantification (**H**, right). **I,** Integrated scheme of *EVI1*-dependent signaling pathways influencing breast carcinoma cell migration and growth *, $P < 0.05$; **, $P < 0.01$; ***, $P < 0.001$.

Downloaded from cancerres.aacrjournals.org on December 3, 2017. © 2017 American Association for Cancer Research.

Published OnlineFirst February 16, 2017; DOI: 10.1158/0008-5472.CAN-16-0593

AML where it represents a marker of adverse prognosis. EVI1 is also expressed in other tissues such as brain, lung, and kidney (32–34). Pointing toward its significance in early organogenesis, *Evi1* knockout mice are embryonically lethal and show broad hypocellularity and patterning defects (35, 36). The molecular regulation and functional relevance of EVI1 expression in breast carcinoma however are largely unexplored.

Analysis of a large cohort of primary samples did not detect significant gene rearrangements or copy-number gains, indicating that activation of the *EVI1* locus in breast carcinoma follows different principles than in myeloid leukemia, such as regulation via miRNAs (8). Consistently, a common *EVI1* polymorphism (rs6774494 A>G) targeted by miR-206/133b was suggested to predict adverse outcome in postmenopausal breast carcinoma patients (37). Interestingly, immunohistochemical analyses of our patient cohort identified EVI1 protein as a prognostic marker in ER^- but not ER^+ breast carcinoma, supporting previous mRNA-based studies (8, 38). Importantly, when the ER^- cohort was further subdivided in ER^-HER2^+ and triple-negative breast carcinoma, EVI1 expression influenced survival specifically in the latter. In this subgroup, high EVI1 expression further associated with enhanced distant metastases.

Functional studies documented a profound growth defect in *EVI1* knockdown versus control cells, resulting from impaired proliferation, cell-cycle progression, and apoptosis resistance. Interestingly, addition of estrogen to ER^+ but not ER^- cells restored the impaired ERK activation and proliferation. Furthermore, both effects of β-estradiol were abrogated by cotreatment with either the ER-blocking reagent tamoxifen or the MAPK inhibitor CI-1040, which highlights the specificity of the observed effects and indicates that EVI1 and β-estradiol merge in pERK activation to regulate breast carcinoma cell growth. However, an inverse correlation was documented between EVI1 expression and tumor size in triple-negative breast carcinoma and by trend also in the ER^- subgroup. We hypothesize that the subgroup of breast carcinoma presenting with large primary tumor size and negative to low EVI1 expression is driven by aggressive, yet EVI1-unrelated molecular mechanisms.

Our analyses reliably identified the significance of EVI1 expression in the absence of endogenous estrogen signaling. In contrast, in the ER^+ breast carcinoma cohort, such analyses might be complicated by the fact that these patients receive antiestrogen treatments. The importance of EVI1 expression might differ depending on the patient response and efficacy of such treatments. Our functional data show that EVI1 also severely regulates the growth of ER^+ breast carcinoma cells, if estrogen is not provided. Unfortunately, we have no detailed and complete information on the mode and efficacy of antiestrogen treatments of the ER^+ breast carcinoma patients. Thus, although our analyses support the notion that EVI1 could affect breast carcinoma independently of ER signaling, assessment of the relevance of EVI1 in ER^+ breast carcinoma requires further patient stratification according to the response to antiestrogen treatment.

Suppression of EVI1 expression consistently inhibited MAPK activation in $HER2^-$ but not $HER2^+$ breast carcinoma. Thus, potential inhibitory effects of *EVI1* knockdown on MAPK signaling might be overruled by constitutive HER2 activity. This assumption is consistent with the results in patients where EVI1 expression levels were prognostically relevant in triple-negative breast carcinoma, but not in $ER^- HER2^+$ subsets. Thus, EVI1, estrogen, and HER2 signaling might converge on MAPK signaling as a common downstream effector controlling breast carcinoma cell growth. Growth-stimulatory properties of estrogen in breast carcinoma also involve transcriptional induction of cyclin D1 (39) and suppression of CDK inhibitors, such as $p21^{Cip1}$ or $p27^{Kip1}$ (40). Indeed, our investigations uncovered that also these growth-regulatory events are influenced by EVI1 and, moreover, that EVI1 modulates the expression of several further key cell-cycle regulators (e.g., CDKN1A, CDKN1B, CDKN1C, CCNA1, and CDK1).

In addition, our data suggest that EVI1 enhances apoptosis resistance in breast carcinoma by inducing a concerted suppression of pro- and induction of antiapoptotic genes. In line with previous data (14, 17), we found a physical association of EVI1 with the *BCL-XL* promoter. Previous links between EVI1 and apoptosis include direct blocking interactions with JNK in hematopoietic cells, and the inhibition of apoptosis through a PI3K-dependent mechanism in colon cancer cells (41, 42). EVI1 is further discussed as a stem cell factor in hematopoiesis and leukemia (22), but in breast carcinoma, it rather homogenously marked tumor cells, at least in cases of high EVI1 expression. Nevertheless, *EVI1* knockdown affected the frequency of *in vivo* tumor– as well as *in vitro* mammosphere–initiating breast carcinoma cells. These data suggest that, even though not confined to breast CSCs, EVI1 expression might also regulate this compartment.

Intriguingly, we identified migration as a novel cellular function promoted by EVI1 in breast carcinoma. In particular, *EVI1* knockdown impaired the breast carcinoma cell mobility, whereas its overexpression enhanced migration. Gene microarray and qRT-PCR experiments surprisingly uncovered, next to regulators of cell cycle and apoptosis, several factors implicated in cell communication and GPCR signaling as downstream effectors of EVI1. Of these, we analyzed in more detailed the GPR54-ligand KISS1, which ChIP assays identified as a novel transcriptional target of EVI1. The EVI1-KISS1 ligand axis promoted motility of ER^- breast carcinoma cells, in line with previously reported roles of KISS1 on mobility and adhesion in this disease entity (29, 30). Interestingly, although KISS1 has been reported as an upstream regulator of ERK (43), stimulation with the GPR54-ligand Kp-10 was not able to restore pERK and proliferation of EVI1 knockdown breast carcinoma cells, although it did influence breast carcinoma cell migration. Vice versa, MAPK inhibition effectively suppressed cell growth but did not alter migration, again reinforcing the idea that the EVI1-KISS1 migratory axis acts independently of pERK. Besides KISS1, we identified additional established (e.g., CXCR4, CCR1, AKAP12; refs. 44–46) as well as novel factors in breast carcinoma cell migration as targets of EVI1. For instance, TIE1, a modulator of angiogenesis and cell adhesion (47), and RhoJ, a modulator of the RHO/ROCK-dependent cell motility (48), were found to be modulated by EVI1, suggesting that this transcription factor serves as a master regulator of breast carcinoma cell motility.

Taken together, our data identify EVI1 as a potent oncoprotein regulating breast carcinoma cell proliferation, apoptosis resistance, and migration. Interestingly, estrogen and HER2 signaling as well as EVI1-mediated transcriptional modulation seemingly merge to stimulate MAPK signaling. This functional convergence identifies EVI1 as a major driver of cell growth acting independently of estrogen signaling. EVI1 and downstream MAPK activation might represent therapeutic targets in patients suffering from $HER2^- ER^-$

Downloaded from cancerres.aacrjournals.org on December 3, 2017. © 2017 American Association for Cancer Research.

Published OnlineFirst February 16, 2017; DOI: 10.1158/0008-5472.CAN-16-0593

or ER^+ breast carcinoma resistant to antiestrogen therapies. Finally, targeting the newly identified EVI1-GPR54-KISS1 axis, for example by GPR54 inhibitors, may be considered for the treatment of metastasizing ER^- breast carcinoma. Effective targeting of EVI1-induced breast carcinoma cell migration might however require either inhibition of EVI1 itself or joint suppression of additional migratory pathways (e.g., RHO/ROCK signaling).

Disclosure of Potential Conflicts of Interest

C. Lengerke reports receiving a commercial research grant from Roche Postdoctoral Fellowship Grant and has provided expert testimony for Celgene, Amgen, and Gilead (contributions to travel expenses to scientific conferences). No potential conflicts of interest were disclosed by the other authors.

Authors' Contributions

Conception and design: H. Wang, T. Schaefer, C. Lengerke
Development of methodology: H. Wang, T. Schaefer, M. Konantz, C. Lengerke
Acquisition of data (provided animals, acquired and managed patients, provided facilities, etc.): H. Wang, T. Schaefer, M. Konantz, M. Braun, Z. Varga, A.M. Paczulla, S. Reich, S. Perner, H. Moch, T.N. Fehm, L. Kanz, C. Lengerke
Analysis and interpretation of data (e.g., statistical analysis, biostatistics, computational analysis): H. Wang, T. Schaefer, M. Konantz, M. Braun, Z. Varga, A.M. Paczulla, F. Jacob, S. Perner, T.N. Fehm, K. Schulze-Osthoff, C. Lengerke
Writing, review, and/or revision of the manuscript: H. Wang, T. Schaefer, M. Braun, F. Jacob, S. Perner, H. Moch, T.N. Fehm, K. Schulze-Osthoff, Claudia Lengerke
Administrative, technical, or material support (i.e., reporting or organizing data, constructing databases): M. Braun, H. Moch, L. Kanz, C. Lengerke
Study supervision: H. Moch, C. Lengerke

Acknowledgments

We thank Olga Kustikova and Christopher Baum for provision of *EVI1* plasmids, and Joelle Müller for technical support in zebrafish experiments.

Grant Support

This study was performed as contracted research supported by the Baden-Württemberg Stiftung (Adult Stem Cells Program II) and by grants from the Deutsche Forschungsgemeinschaft to S. Perner (PE 1179/4-1) and the Schweizer Nationalfonds to C. Lengerke (310030_149735).

The costs of publication of this article were defrayed in part by the payment of page charges. This article must therefore be hereby marked *advertisement* in accordance with 18 U.S.C. Section 1734 solely to indicate this fact.

Received March 1, 2016; revised November 29, 2016; accepted January 8, 2017; published OnlineFirst February 16, 2017.

References

1. Sestak I, Cuzick J, Dowsett M, Lopez-Knowles E, Filipits M, Dubsky P, et al. Prediction of late distant recurrence after 5 years of endocrine treatment: A combined analysis of patients from the Austrian breast and colorectal cancer study group 8 and arimidex, tamoxifen alone or in combination randomized trials using the PAM50 risk of recurrence score. J Clin Oncol 2015;33:916–22.
2. Pandya K, Meeke K, Clementz AG, Rogowski A, Roberts J, Miele L, et al. Targeting both Notch and ErbB-2 signalling pathways is required for prevention of ErbB-2-positive breast tumour recurrence. Br J Cancer 2011;105:796–806.
3. Lengerke C, Fehm T, Kurth R, Neubauer H, Scheble V, Muller F, et al. Expression of the embryonic stem cell marker SOX2 in early-stage breast carcinoma. BMC Cancer 2011;11:42.
4. Schaefer T, Wang H, Mir P, Konantz M, Pereboom TC, Paczulla AM, et al. Molecular and functional interactions between AKT and SOX2 in breast carcinoma. Oncotarget 2015;6:53540–56.
5. Fears S, Mathieu C, Zeleznik-Le N, Huang S, Rowley JD, Nucifora G. Intergenic splicing of MDS1 and EVI1 occurs in normal tissues as well as in myeloid leukemia and produces a new member of the PR domain family. Proc Natl Acad Sci U S A 1996;93:1642–7.
6. Saito Y, Kaneda K, Suekane A, Ichihara E, Nakahata S, Yamakawa N, et al. Maintenance of the hematopoietic stem cell pool in bone marrow niches by EVI1-regulated GPR56. Leukemia 2013;27:1637–49.
7. Eppert K, Takenaka K, Lechman ER, Waldron L, Nilsson B, van Galen P, et al. Stem cell gene expression programs influence clinical outcome in human leukemia. Nat Med 2011;17:1086–93.
8. Patel JB, Appaiah HN, Burnett RM, Bhat-Nakshatri P, Wang G, Mehta R, et al. Control of EVI-1 oncogene expression in metastatic breast cancer cells through microRNA miR-22. Oncogene 2011;30:1290–301.
9. Nanjundan M, Nakayama Y, Cheng KW, Lahad J, Liu J, Lu K, et al. Amplification of MDS1/EVI1 and EVI1, located in the 3q26.2 amplicon, is associated with favorable patient prognosis in ovarian cancer. Cancer Res 2007;67:3074–84.
10. Theurillat JP, Zurrer-Hardi U, Varga Z, Storz M, Probst-Hensch NM, Seifert B, et al. NY-BR-1 protein expression in breast carcinoma: A mammary gland differentiation antigen as target for cancer immunotherapy. Cancer Immunol Immunother 2007;56:1723–31.
11. Braun M, Kirsten R, Rupp NJ, Moch H, Fend F, Wernert N, et al. Quantification of protein expression in cells and cellular subcompartments on immunohistochemical sections using a computer supported image analysis system. Histol Histopathol 2013;28:605–10.
12. Scheble VJ, Braun M, Beroukhim R, Mermel CH, Ruiz C, Wilbertz T, et al. ERG rearrangement is specific to prostate cancer and does not occur in any other common tumor. Mod Pathol 2010;23:1061–7.
13. Maetzig T, Brugman MH, Bartels S, Heinz N, Kustikova OS, Modlich U, et al. Polyclonal fluctuation of lentiviral vector-transduced and expanded murine hematopoietic stem cells. Blood 2011;117:3053–64.
14. Konantz M, Andre MC, Ebinger M, Grauer M, Wang H, Grzywna S, et al. EVI-1 modulates leukemogenic potential and apoptosis sensitivity in human acute lymphoblastic leukemia. Leukemia 2013;27:56–65.
15. Bareiss PM, Paczulla A, Wang H, Schairer R, Wiehr S, Kohlhofer U, et al. SOX2 expression associates with stem cell state in human ovarian carcinoma. Cancer Res 2013;73:5544–55.
16. Bonadies N, Foster SD, Chan WI, Kvinlaug BT, Spensberger D, Dawson MA, et al. Genome-wide analysis of transcriptional reprogramming in mouse models of acute myeloid leukaemia. PLoS One 2011;6:e16330.
17. Pradhan AK, Mohapatra AD, Nayak KB, Chakraborty S. Acetylation of the proto-oncogene EVI1 abrogates Bcl-xL promoter binding and induces apoptosis. PLoS One 2011;6:e25370.
18. Rodriguez LG, Wu X, Guan JL. Wound-healing assay. Methods Mol Biol 2005;294:23–9.
19. Konantz M, Balci TB, Hartwig UF, Dellaire G, Andre MC, Berman JN, et al. Zebrafish xenografts as a tool for in vivo studies on human cancer. Ann N Y Acad Sci 2012;1266:124–37.
20. Choi J, Dong L, Ahn J, Dao D, Hammerschmidt M, Chen JN. FoxH1 negatively modulates flk1 gene expression and vascular formation in zebrafish. Dev Biol 2007;304:735–44.
21. Haldi M, Ton C, Seng WL, McGrath P. Human melanoma cells transplanted into zebrafish proliferate, migrate, produce melanin, form masses and stimulate angiogenesis in zebrafish. Angiogenesis 2006;9:139–51.
22. Wieser R.The oncogene and developmental regulator EVI1: expression, biochemical properties, and biological functions. Gene 2007;396:346–57.
23. Saha Roy S, Vadlamudi RK. Role of estrogen receptor signaling in breast cancer metastasis. Int J Breast Cancer 2012;2012:654698.
24. Moriarty K, Kim KH, Bender JR. Minireview: Estrogen receptor-mediated rapid signaling. Endocrinology 2006;147:5557–63.
25. Improta-Brears T, Whorton AR, Codazzi F, York JD, Meyer T, McDonnell DP. Estrogen-induced activation of mitogen-activated protein kinase requires mobilization of intracellular calcium. Proc Natl Acad Sci U S A 1999;96:4686–91.
26. Rinehart J, Adjei AA, Lorusso PM, Waterhouse D, Hecht JR, Natale RB, et al. Multicenter phase II study of the oral MEK inhibitor, CI-1040, in patients

Downloaded from cancerres.aacrjournals.org on December 3, 2017. © 2017 American Association for Cancer Research.

Published OnlineFirst February 16, 2017; DOI: 10.1158/0008-5472.CAN-16-0593

with advanced non-small-cell lung, breast, colon, and pancreatic cancer. J Clin Oncol 2004;22:4456–62.
27. Lee JH, Miele ME, Hicks DJ, Phillips KK, Trent JM, Weissman BE, et al. KiSS-1, a novel human malignant melanoma metastasis-suppressor gene. J Natl Cancer Inst 1996;88:1731–7.
28. Welch DR, Hunter KW. A new member of the growing family of metastasis suppressors identified in prostate cancer. J Natl Cancer Inst 2003;95:839–41.
29. Cvetkovic D, Dragan M, Leith SJ, Mir ZM, Leong HS, Pampillo M, et al. KISS1R induces invasiveness of estrogen receptor-negative human mammary epithelial and breast cancer cells. Endocrinology 2013;154:1999–2014.
30. Zajac M, Law J, Cvetkovic DD, Pampillo M, McColl L, Pape C, et al. GPR54 (KISS1R) transactivates EGFR to promote breast cancer cell invasiveness. PLoS One 2011;6:e21599.
31. Mucenski ML, Taylor BA, Ihle JN, Hartley JW, Morse HC 3rd, Jenkins NA, et al. Identification of a common ecotropic viral integration site, Evi-1, in the DNA of AKXD murine myeloid tumors. Mol Cell Biol 1988;8:301–8.
32. Perkins AS, Mercer JA, Jenkins NA, Copeland NG. Patterns of Evi-1 expression in embryonic and adult tissues suggest that Evi-1 plays an important regulatory role in mouse development. Development 1991;111:479–87.
33. Dutta P, Bui T, Bauckman KA, Keyomarsi K, Mills GB, Nanjundan M. EVI1 splice variants modulate functional responses in ovarian cancer cells. Mol Oncol 2013;7:647–68.
34. Deng X, Cao Y, Liu Y, Li F, Sambandam K, Rajaraman S, et al. Overexpression of Evi-1 oncoprotein represses TGF-beta signaling in colorectal cancer. Mol Carcinog 2013;52:255–64.
35. Hoyt PR, Bartholomew C, Davis AJ, Yutzey K, Gamer LW, Potter SS, et al. The Evi1 proto-oncogene is required at midgestation for neural, heart, and paraxial mesenchyme development. Mech Dev 1997;65:55–70.
36. Buonamici S, Chakraborty S, Senyuk V, Nucifora G. The role of EVI1 in normal and leukemic cells. Blood Cells Mol Dis 2003;31:206–12.
37. Wang TY, Huang YP, Ma P. Correlations of common polymorphism of EVI-1 gene targeted by miRNA-206/133b with the pathogenesis of breast cancer. Tumour Biol 2014;35:9255–62.
38. Gyorffy B, Lanczky A, Eklund AC, Denkert C, Budczies J, Li Q, et al. An online survival analysis tool to rapidly assess the effect of 22,277 genes on breast cancer prognosis using microarray data of 1,809 patients. Breast Cancer Res Treat 2010;123:725–31.
39. Dos Santos E, Dieudonne MN, Leneveu MC, Serazin V, Rincheval V, Mignotte B, et al. Effects of 17beta-estradiol on preadipocyte proliferation in human adipose tissue: Involvement of IGF1-R signaling. Horm Metab Res 2010;42:514–20.
40. Dupont J, Karas M, LeRoith D. The potentiation of estrogen on insulin-like growth factor I action in MCF-7 human breast cancer cells includes cell cycle components. J Biol Chem 2000;275:35893–901.
41. Kurokawa M, Mitani K, Yamagata T, Takahashi T, Izutsu K, Ogawa S, et al. The evi-1 oncoprotein inhibits c-Jun N-terminal kinase and prevents stress-induced cell death. EMBO J 2000;19:2958–68.
42. Liu Y, Chen L, Ko TC, Fields AP, Thompson EA. Evi1 is a survival factor which conveys resistance to both TGFbeta- and taxol-mediated cell death via PI3K/AKT. Oncogene 2006;25:3565–75.
43. Szereszewski JM, Pampillo M, Ahow MR, Offermanns S, Bhattacharya M, Babwah AV. GPR54 regulates ERK1/2 activity and hypothalamic gene expression in a Galpha(q/11) and beta-arrestin-dependent manner. PLoS One 2010;5:e12964.
44. Xu C, Zhao H, Chen H, Yao Q. CXCR4 in breast cancer: Oncogenic role and therapeutic targeting. Drug Des Devel Ther 2015;9:4953–64.
45. Li Y, Wu J, Zhang P. CCL15/CCR1 axis is involved in hepatocellular carcinoma cells migration and invasion. Tumour Biol 2016;37:4501–7.
46. Finger EC, Castellini L, Rankin EB, Vilalta M, Krieg AJ, Jiang D, et al. Hypoxic induction of AKAP12 variant 2 shifts PKA-mediated protein phosphorylation to enhance migration and metastasis of melanoma cells. Proc Natl Acad Sci U S A 2015;112:4441–6.
47. Chan B, Yuan HT, Ananth Karumanchi S, Sukhatme VP. Receptor tyrosine kinase Tie-1 overexpression in endothelial cells upregulates adhesion molecules. Biochem Biophys Res Commun 2008;371:475–9.
48. Wilson E, Leszczynska K, Poulter NS, Edelmann F, Salisbury VA, Noy PJ, et al. RhoJ interacts with the GIT-PIX complex and regulates focal adhesion disassembly. J Cell Sci 2014;127:3039–51.

Downloaded from cancerres.aacrjournals.org on December 3, 2017. © 2017 American Association for Cancer Research.

Published OnlineFirst February 16, 2017; DOI: 10.1158/0008-5472.CAN-16-0593

Cancer Research
The Journal of Cancer Research (1916–1930) | The American Journal of Cancer (1931–1940)

AACR American Association for Cancer Research

Prominent Oncogenic Roles of EVI1 in Breast Carcinoma

Hui Wang, Thorsten Schaefer, Martina Konantz, et al.

Cancer Res 2017;77:2148-2160. Published OnlineFirst February 16, 2017.

Updated version	Access the most recent version of this article at: doi:10.1158/0008-5472.CAN-16-0593
Supplementary Material	Access the most recent supplemental material at: http://cancerres.aacrjournals.org/content/suppl/2017/02/16/0008-5472.CAN-16-0593.DC1

Cited articles	This article cites 48 articles, 12 of which you can access for free at: http://cancerres.aacrjournals.org/content/77/8/2148.full#ref-list-1

E-mail alerts	Sign up to receive free email-alerts related to this article or journal.
Reprints and Subscriptions	To order reprints of this article or to subscribe to the journal, contact the AACR Publications Department at pubs@aacr.org.
Permissions	To request permission to re-use all or part of this article, use this link http://cancerres.aacrjournals.org/content/77/8/2148. Click on "Request Permissions" which will take you to the Copyright Clearance Center's (CCC) Rightslink site.

Downloaded from cancerres.aacrjournals.org on December 3, 2017. © 2017 American Association for Cancer Research.

Supplementary Figure and Table Legends

Supplementary Figure S1: Analysis of EVI1 expression within a BC patient cohort. **A,** Kaplan-Meier overall survival curves according to EVI1 expression in all BC cases as well as in ER+, ER-, ER-HER2+ and triple-negative BC subgroups (top), and more detailed clinico-pathological information according to EVI1 expression in all BC cases and ER-negative BC subgroups (bottom). **B,** FISH analysis indicating *EVI1* copy gain in 2 out of 515 analyzed BC samples.

Supplementary Figure S2: Validation of effects using an alternative *EVI1* shRNA. **A,** qRT-PCR analysis of *EVI1* and *MDS1/EVI1* expression in control vs. *EVI1* knockdown MDA-MB-231 cells using an alternative shRNA construct (*EVI1* shRNA alternate). Indicated are *EVI1* and *MDS1/EVI1* expression levels relative to *GAPDH* ($\Delta\Delta$Ct method) and normalized to control cells (100%). **B,** Corresponding immunoblots verifying efficient reduction of EVI1 protein expression also for the alternative shRNA construct. Anti-β-actin staining is shown for loading control. **C,** Growth curves illustrating a growth defect in *EVI1* knockdown MDA-MB-231 cells treated with the alternative shRNA vs. respective control lentiviral particles. **D,** Elevated basal apoptosis in MDA-MB-231 cells transduced with the alternative *EVI1* shRNA. Cells were stained with PI and apoptosis deduced from the percentage of sub-G1 cells.

Supplementary Figure S3: Verification of *EVI1*-related phenotypic observations in Hs 578T cells. **A,** Immunoblots of whole cell lysates derived from control vs.

EVI1 knockdown Hs 578T cells. Anti-β-actin staining is shown for loading control. **B,** Growth curves illustrating a growth defect in *EVI1* knockdown Hs 578T cells vs. respective controls. **C,** Elevated basal apoptosis in *EVI1* knockdown Hs 578T cells as compared to controls. Cells were stained with PI and apoptosis deduced from the percentage of sub-G1 cells. **D,** *EVI1* knockdown sensitizes Hs 578T cells to TRAIL-induced apoptosis. **E/F,** EVI1 affects cell cycle progression. Induction of a G0/G1 defect (E) and reduced BrdU incorporation (F) in *EVI1* knockdown Hs 578T cells.

Supplementary Figure S4: EVI1 affects cell cycle regulatory molecules in BC. **A,** Immunoblots of whole cell lysates derived from control vs. *EVI1* knockdown MDA-MB-231 cells. Note an induction of $p21^{Cip1}$ and $p27^{Kip1}$ and a decrease in CDK2 expression in response to *EVI1* knockdown. Anti-ß-actin staining is shown for loading control. **B,** qRT-PCR analysis of *CDKN1A* (p21) and *CDKN1B* (p27) gene expression in *EVI1* knockdown MDA-MB-231 cells. Respective expression levels in control cells were set to 1.

Supplementary Figure S5: MAPK inhibition modulates BC cell cycle progression and abrogates estrogen-mediated growth rescue in *EVI1* knockdown cells. **A,** Immunoblot analysis verifying downregulation of pERK in MDA-MB-231 (left) and T-47D cells (right) treated with two or three different *EVI1* shRNAs [*EVI1* shRNA; *EVI1* shRNA (alternate); *EVI1* shRNA(alternate2)] as compared to lentivirally transduced control shRNAs. **B-E,** Effects of MEK inhibitors and pERK

suppression on growth, cell cycle and apoptosis. **B,** Growth curves of MDA-MB-231 (left) and T-47D (right) cells treated with the MEK inhibitor CI-1040 (5 μM) *vs.* DMSO control. **C,** Cell cycle analyses of MDA-MB-231 (left) and T-47D (right) cells treated with different concentrations of MEK inhibitor CI-1040. Note a dose-dependent induction of a G0/G1-defect in MEK inhibitor-treated cells. **D,** Verification of a G0/G1-defect in MDA-MB-231 cells treated with two alternative MEK inhibitors (1 μM Trametinib or 4 μM AZD6244). **E,** Elevated specific apoptosis in MEK inhibitor-treated MDA-MB-231 cells vs. DMSO-treated control cells. Cells were stained with PI and apoptosis was deduced from the percentage of sub-G1 cells. **F,** Immunoblot analysis of pERK levels in T-47D cells treated with different MEK inhibitors: CI-1040 (5 μM), AZD6244 (4 μM) and Trametinib (1 μM). **G,** Estrogen supplementation does not rescue growth of *EVI1* knockdown cells treated with tamoxifen (10 μM) or CI-1040 (5 μM). Indicated are cell numbers derived from equally plated control (sh-noncoding) and *EVI1*-shRNA-treated T-47D cells cultured over 9 days with vehicle control, β-estradiol (100 nM), or β-estradiol together with tamoxifen (10 μM) or CI-1040 (5 μM).

Supplementary Figure S6: Effect of *EVI1* knockdown on tumorigenicity *in vivo* and clonogenicity *in vitro*. **A,** Immunoblot analysis of whole cell lysates derived from tumors excised from xenotransplanted NSG mice, documenting persistent EVI1 knockdown and pERK inhibition *in vivo*. **B,** Quantification of tumor formation from control and *EVI1* knockdown MDA-MD-231 cells in zebrafish. Note that, in contrast to ER+ BC cells, tumor formation could not be restored from

transplanted *EVI1* knockdown ER- cells exposed to 100 nM estradiol for 72 hours before and after transplantation. P-values were calculated by a Mann-Whitney test. **C,** Quantification of tumor formation from *EVI1* knockdown ER+ T-47D cells treated with β-estradiol (100 nM), CI-1040 (200 nM) or the combination of both drugs in zebrafish. P-values were calculated by the application of a Chi-square test. **D,** *EVI1* knockdown T-47D cells show an impaired formation of mammospheres in an *in vitro* surrogate assay of BC tumorigenicity.

Supplementary Figure S7: Gene expression patterns associated with EVI1 knockdown or overexpression in BC. **A/B,** Gene expression profiles from MDA-MB-231 cells transduced either with control or EVI1 shRNA lentiviral particles. Shown are genes involved in GPCR signaling (A) and cell cycle regulation (B). Heat maps illustrate genes with EVI1-dependent expression differences of >1.5 fold. **C,** qRT-PCR verification of differential expression for 15 candidate genes as identified from the microarray data set. **D,** qRT-PCR analysis of candidate genes in EVI1-overexpressing vs. control Hs 578T cells indicate *KISS1* as the most robustly regulated gene. Indicated are fold changes in gene expression in EVI1-modified versus control cells (C-D). **E,** qRT-PCR documenting co-depletion of *EVI1* and *KISS1* mRNA in two primary ER- BC cell samples (P3 and P4) treated for 48 hours with *EVI1*-specific or control siRNAs. Shown are fold changes in mRNA expression in *EVI1* knockdown vs. control cells for each patient sample.

Supplementary Figure S8: EVI1 ChIP analyses of the *KISS1* promoter. **A,**

Schematic illustration of *KISS1* promoter regions with potential EVI1-binding sites (*KISS1-1* to *KISS1-4*) therein. **B,** To provide a positive control for the ChIP results presented in Figure 7D, and a respective negative control using non-specific primers, ChIP analyses were performed to analyze occupancy of the *BCL2L1* promoter by EVI1 protein using primer sets as described.

Supplementary Figure S9: Verification of the effects of KISS1 overexpression and respectively RKI-1447 treatment on BC cell migration using an alternative cell line (Hs 578T). **A,** Migration ("wound healing") assays of control and *EVI1*-knockdown Hs 578T BC cells with or without concomitant KISS1 overexpression. Stable EVI1 knockdown or control cells were obtained via lentiviral transduction of Hs578T cells engineered to conditionally express KISS1 upon doxycycline treatment. Doxycyline was added at 1 µg/ml 24 hours before and during (12 hours) of the migration assay. Note that KISS1 overexpression indeed induces migration and rescues the impaired motility of EVI1 knockdown cells. **B,** Semi-quantitative analysis of the migration effects depicted in panel A at 12 hours after start of the migration assay. **C,** Migration assays of control and EVI1-overexpressing Hs 578T BC cells with or without concomitant treatment with the RHO/ROCK inhibitor RKI-1447 (2 µM). Note that EVI1 overexpression enhances cell migration, whereas RKI-1447 treatment impairs this effect. **D,** Semi-quantitative analysis of the migration effects depicted in panel C at 12 hours after start of the migration assay.

Supplementary Figure S10. Differential role of KISS1 in *EVI1*-mediated cell migration, cell growth and ERK activation. **A,** Stimulatory effect of Kisspeptin (Kp-10, left) and KISS1 overexpression (*KISS1* OE, right) on the migration of MDA-MB-231 cells. **B,** qRT-PCR confirmation of *KISS1* mRNA induction in MDA-MB-231 and Hs 578T cells transduced with the Tet_{on} lentiviral vector system and cultured for 24 hours in the presence of doxycycline (1 µg/ml). **C,** Growth curves of MDA-MB-231 (ER-) and T-47D (ER+) cells transduced either with control or *EVI1* shRNA lentiviral particles and grown in the absence or presence of Kp-10 (1 µM). Note that Kp-10 supplementation cannot restore the growth defects imposed by knockdown of *EVI1.* **D,** Neither supplementation with Kp-10 (500 nM or 1000 nM) nor KISS1 overexpression induces pERK in MDA-MB-231 cells. **E,** qRT-PCR analysis of *KISS1* mRNA in *EVI1*-overexpressing MDA-MB-231 cells treated with MEK inhibitor CI-1040. **F-G,** Treatment with the MEK inhibitor CI-1040 (5 µM) does not alter EVI1-dependent migration. Migration assays of control, *EVI1*-overexpressing (F) and *KISS1*-overexpressing (G) MDA-MB-231 cells in the presence or absence of CI-1040 (5 µM).

Supplementary Table 1: Stratification of BC-TMA patient samples according to EVI1 expression levels in relation to histological, ER and HER2 status.

Supplementary Table 2: Index list of primer sequences as used for qRT-PCR, ChIP analyses and the cloning of *KISS1* from cDNA DNA.

A

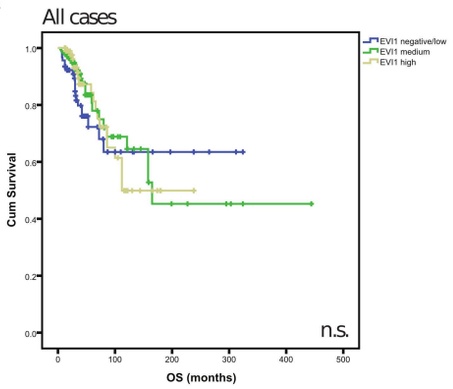

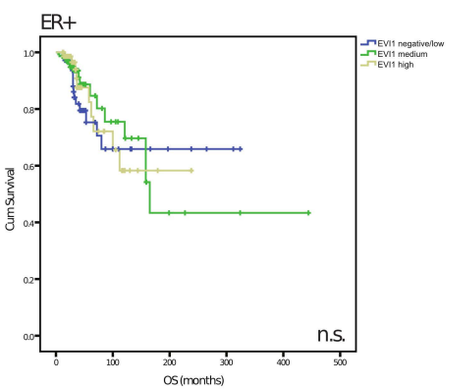

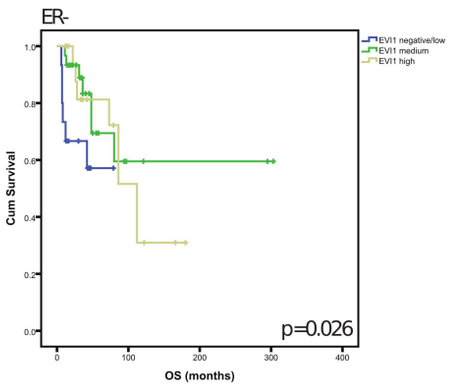

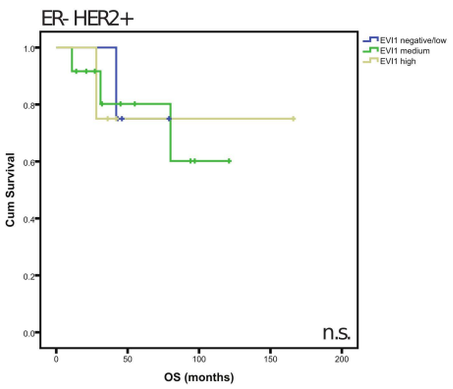

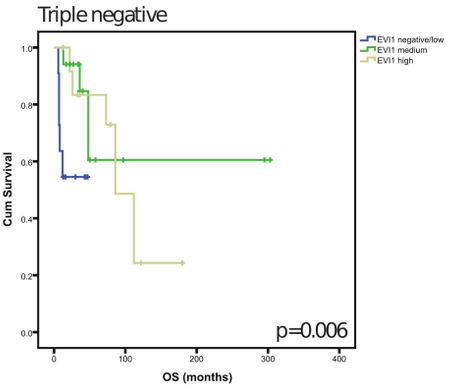

All cases		EVI1 negative/low	EVI1 medium	EVI1 high	Univariate p-value
	pT				
	pT1	41	104	66	0.030 (Chi Square)
	pT2	59	116	61	
	pT3	18	19	7	
	pT4	10	9	9	
	pN				
	pN0	32	92	48	n.s.
	pN1-3	80	135	78	
	Grade				
	G1	15	32	33	0.008 (Chi-Square)
	G2	67	136	55	
	G3	45	78	54	
	pM				n.s.
	OS				n.s.
	5-J survival				n.s.
	other factors				n.s.

ER-					
	pT				
	pT1	9	10	12	n.s.
	pT2	9	23	10	
	pT3	4	4	1	
	pT4	1	2	4	
		23	39	27	
	pN				
	pN0	6	17	9	n.s.
	pN1-3	13	19	14	
		19	36	23	
	Grade				
	G1	1	2	1	n.s.
	G2	5	10	5	
	G3	17	27	21	
		23	39	27	
	pM				
	pM0	20	39	22	0.046 (Chi-Square)
	pM1	3	1	6	
	OS				0.026 (Breslow)
	5 year survival				0.011 (Spearman)
	other factors				n.s.

ER-/Her2+		EVI1 negative/low	EVI1 medium	EVI1 high	Univariate p-value
	pT				
	pT1	7	6	3	n.s.
	pT2-4	3	8	3	
	pN				
	pN0	4	5	2	n.s.
	pN1-3	5	9	4	
	Grade				
	G1	0	1	0	n.s.
	G2	1	4	2	
	G3	9	9	4	
	pM				
	pM0	8	13	5	n.s.
	pM1	2	1	1	
	OS				n.s.
	5-J survival				n.s.
	other factors				n.s.

Triple negative					
	pT				
	pT1	2	2	8	0.01 (Chi-Square)
	pT2	9	18	8	
	pT3	4	6	0	
	pT4	0	4	3	
	pN				
	pN0	2	12	7	n.s.
	pN1-3	8	9	10	
	Grade				
	G1	1	1	1	n.s.
	G2	4	6	3	
	G3	8	17	16	
	pM				
	pM0	12	25	16	0.027 (Chi-Square)
	pM1	1	0	5	
	OS				0.006
	5 year survival				N.A.
	other factors				n.s.

B

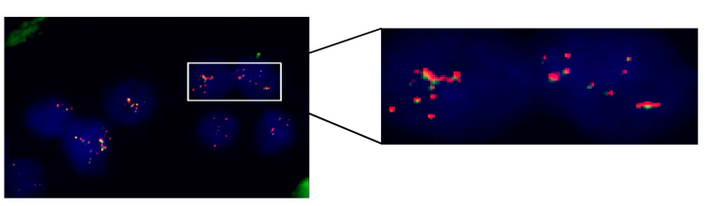

Supplementary Figure 1

Histological subtype	EVI1 positivity		
	Score 1 (low/negative)	**Score 2 (medium)**	**Score 3 (high)**
Ductal (n=404)	94 (23.2%)	195 (48.3%)	115 (28.5%)
Lobular (n=66)	25 (37.9%)	32 (48.5%)	9 (13.6%)
Other (n=50)	9 (18%)	22 (44%)	19 (38%)
			p=0.012 (Person, Chi Square)
ER status			
ER positive (n=421)	104 (24.7%)	206 (48.9%)	111 (26.4%)
ER negative (n=91)	23 (25.3%)	40 (44%)	28 (30.8)
			p value: n.s.
HER2 status			
HER2 positive (n=79)	25 (31.6%)	37 (46.8%)	17 (21.5%)
HER2 negative (n=448)	105 (23.4%)	219 (48.9%)	124 (27.7%)
			p value: n.s.

Supplementary Table 1

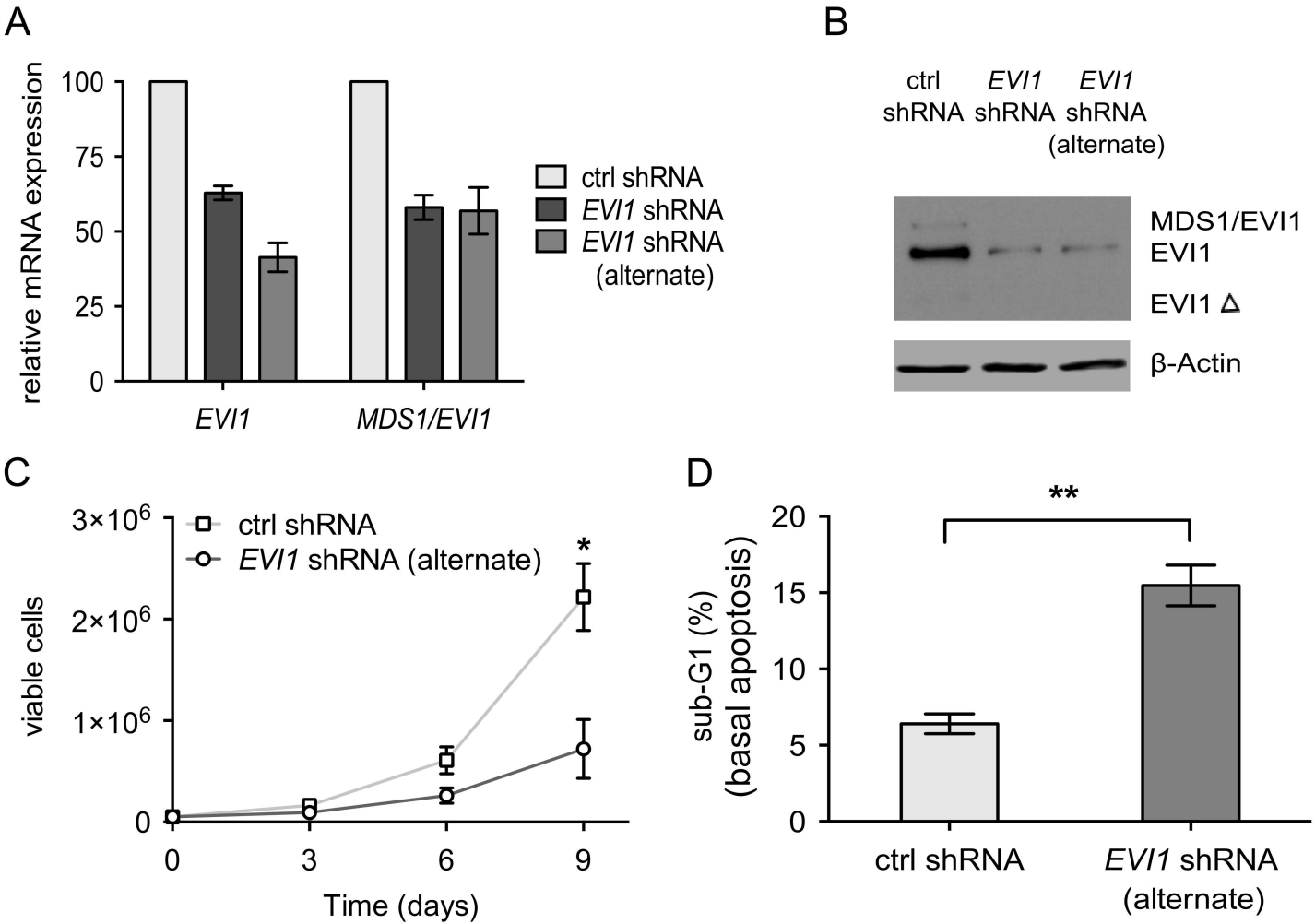

Supplementary Figure 2

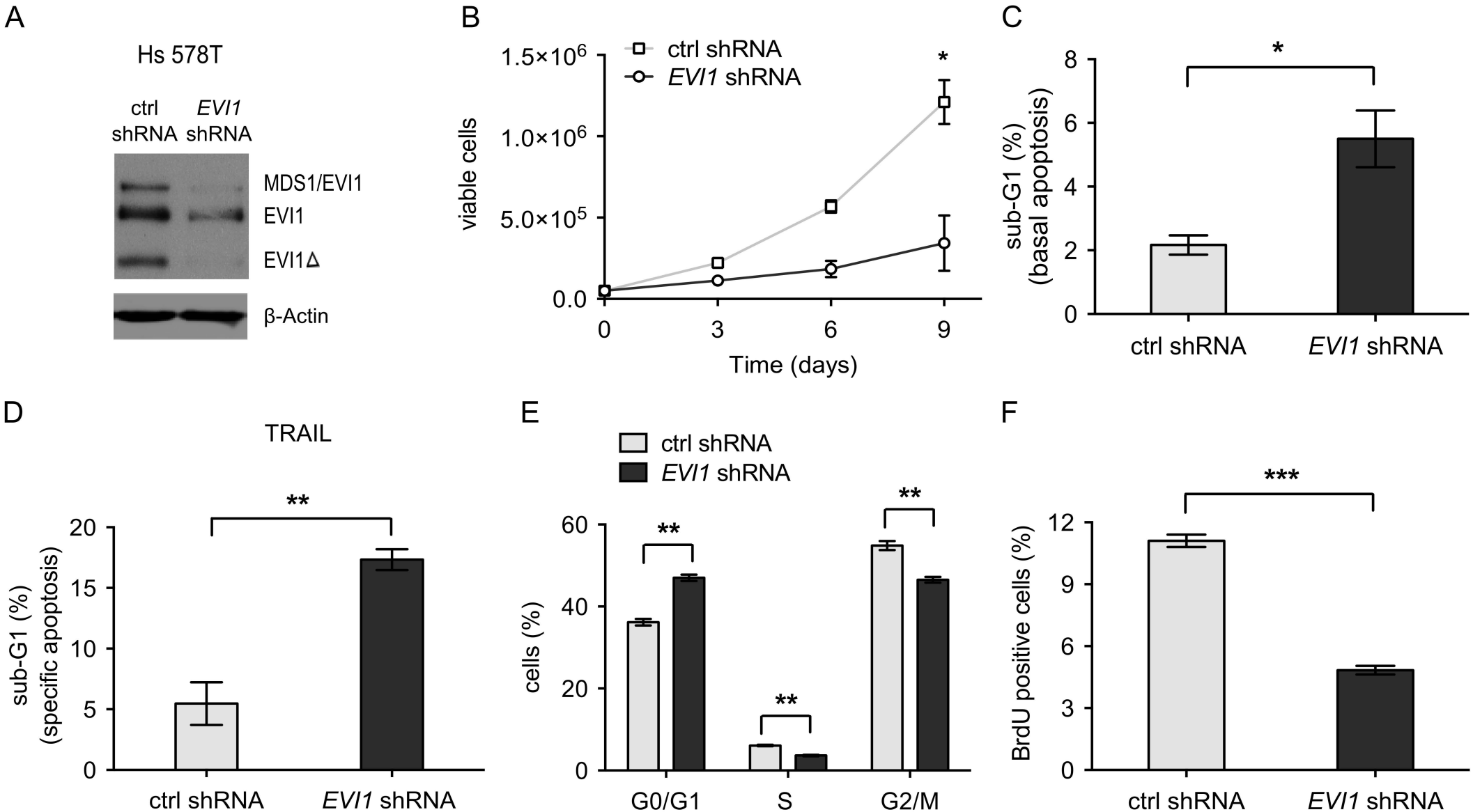

Supplementary Figure 3

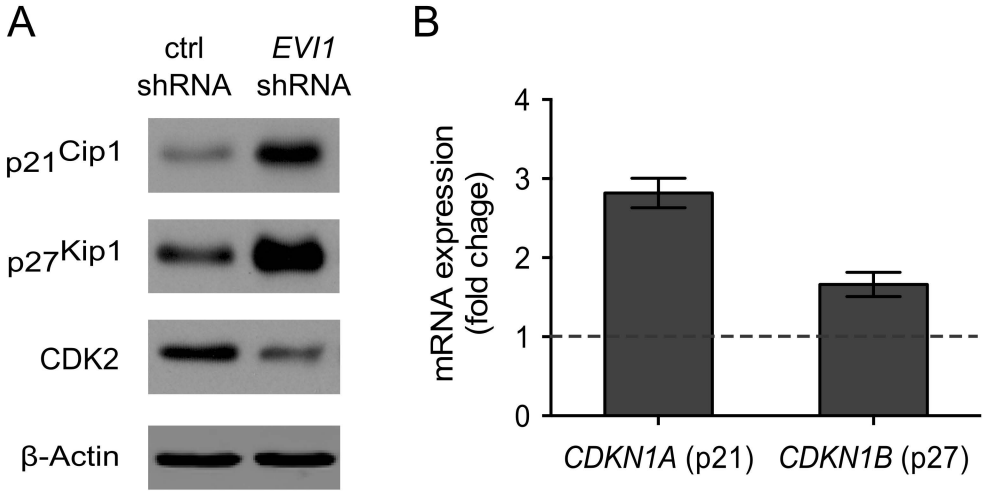

Supplementary Figure 4

A

MDA-MB-231 (ER-)

ctrl shRNA | *EVI1* shRNA (alternate2) | *EVI1* shRNA | *EVI1* shRNA (alternate)

pERK

ERK

β-Actin

T-47D (ER+)

ctrl shRNA | *EVI1* shRNA | *EVI1* shRNA (alternate)

pERK

ERK

β-Actin

B

viable cells

4×10^6
3×10^6
2×10^6
1×10^6
0

ctrl
CI-1040

0 3 6 9

Time (days)

4×10^6
3×10^6
2×10^6
1×10^6
0

ctrl
CI-1040

0 3 6 9

Time (days)

C

cells (%)

80
60
40
20
0

ctrl
CI-1040 1 μM
CI-1040 5 μM
CI-1040 10 μM

G0/G1 S G2/M

100
80
60
40
20
0

ctrl
CI-1040 5 μM
CI-1040 10 μM
CI-1040 20 μM

G0/G1 S G2/M

D

MDA-MB-231

cells (%)

80
60
40
20
0

ctrl
Trametinib
AZD6244

G0/G1 S G2/M

E

MDA-MB-231

sub-G1 (%)

10
8
6
4
2
0

ctrl Trametinib AZD6244

F

MDA-MB-231

ctrl CI-1040 AZD6244 Trametinib

pERK

β-Actin

G

T-47D

viable cells

3×10^5
2×10^5
1×10^5
0

n.s.
*
***
***

ctrl
EVI1 shRNA
EVI1 shRNA + Estradiol
EVI1 shRNA + Estradiol + Tamoxifen
EVI1 shRNA + Estradiol + CI-1040

Supplementary Figure 5

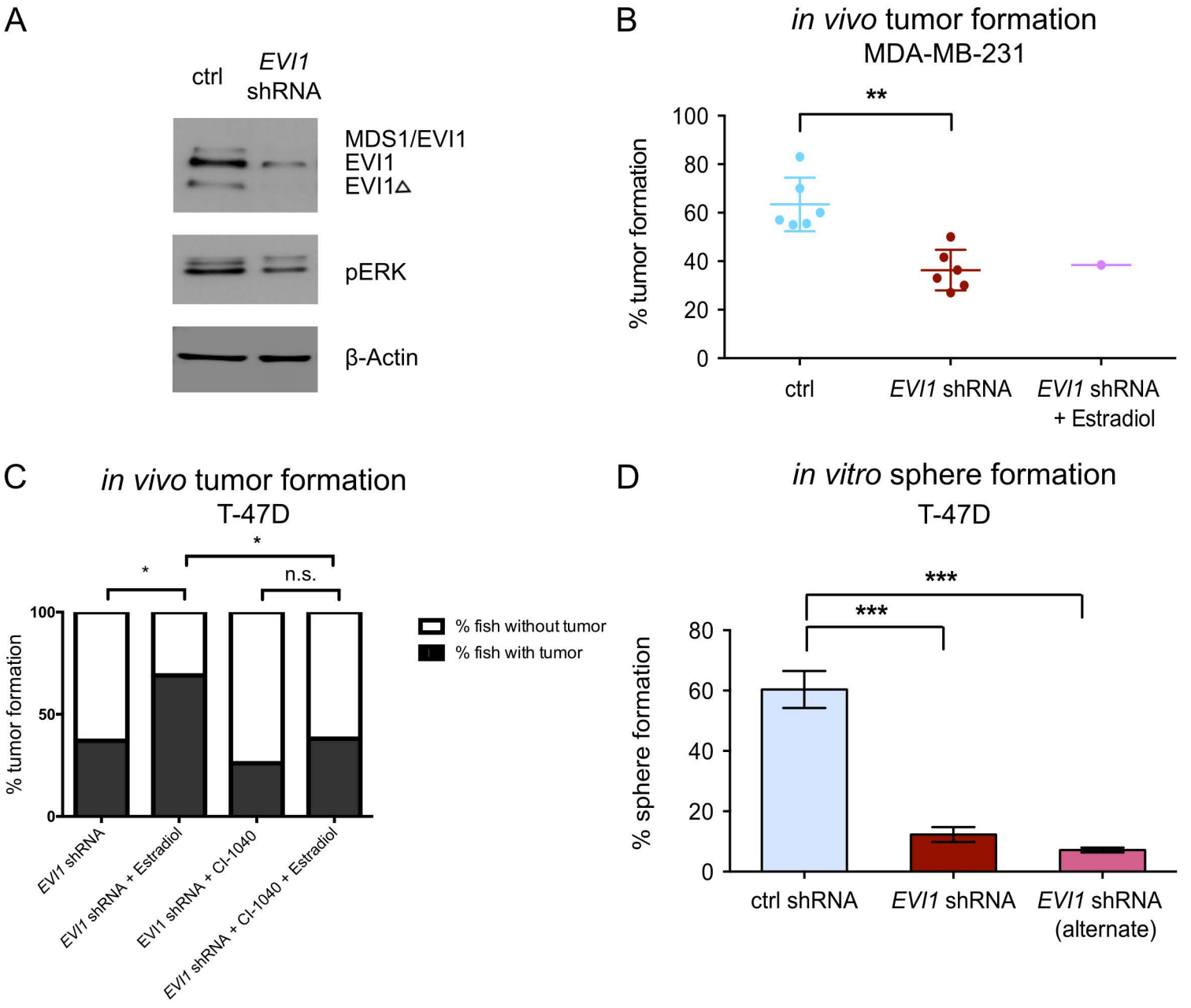

Supplementary Figure 6

A

ctrl shRNA | *EVI1* shRNA | *EVI1* shRNA (alternate)

GPCR signaling related genes

CXCR4
F2RL2
LPAR4
S1PR5
KISS1
PIK3CG
OXTR
PTH1R
PTGFR
MGLL
NPFFR2
S1PR1
GHRH
S1PR3
GRM7
CCR3
ADCY4
EDN1
EDN3
TAS2R
EDN1
NPSR1
HTR1F
LPAR1
ADCY3
GABBR
PTGER
HTR1D
PLCB4
GCGR
PTGFR
CCR1

B

ctrl shRNA | *EVI1* shRNA | *EVI1* shRNA (alternate)

cell cycle related genes

CREB3L3
CDKN1C
CDKN1B
CDKN1B

cell cycle up

CDK1
CCNA2
SKP2
CCNA1
MDM2
CDK1
MCM10
SMC1A
MCM9

cell cycle down

CDK1
CCNA1
POLE
CDK1
MDM2

G1 to S cell cycle control

NEDD1
CDK1
CCNA1
CCNA2
PLK4
CDK1
CEP164

mitotic G2-G2-M phase

Color range
-3 0 3

C

MDA-MB-231 (*EVI1* knockdown)

mRNA expression (fold change)

6
3
0
-3

KISS1
EDN1
PIK3CG
PTGFR
CDK1
CCNA1
CDKN1A (p21)
CDKN1B (p27)
CDKN1C (p57)
BMF1
BMF2
BBC3
BIK
DUSP5
DUSP22

D

Hs 578T (*EVI1* overexpression)

mRNA expression (fold change)

80
60
40
20
0
-20

KISS1
EDN1
CDK1
BBC3
DUSP5
DUSP22
ERBB2

E

relative gene expression

1.00
0.75
0.50
0.25
0.00

control siRNA

P3
P4

EVI1
KISS1

Supplementary Figure 7

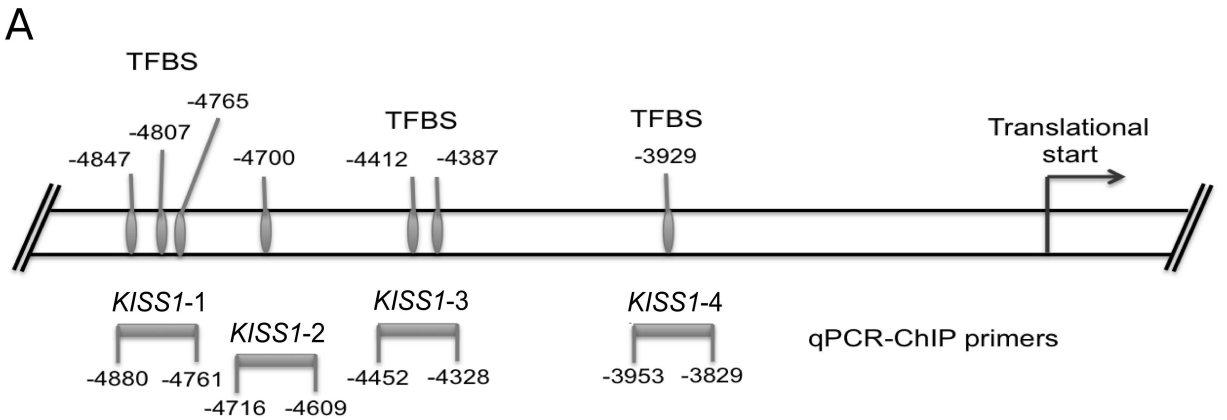

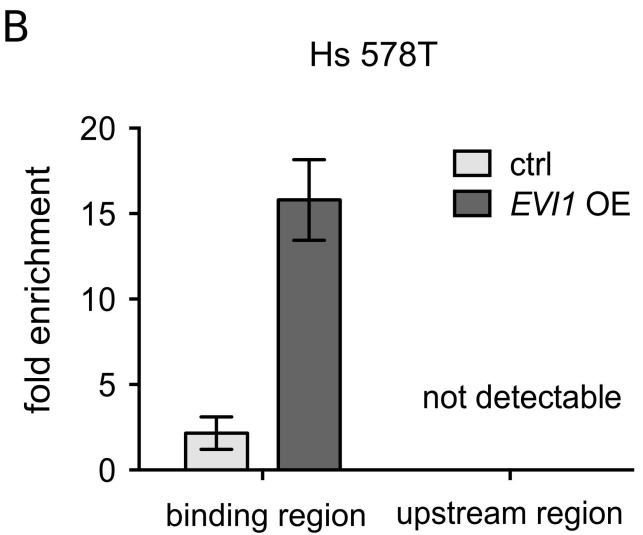

Supplementary Figure 8

Gen name	Forward sequence	Reverse sequence
EVI1	ACCCACTCCTTTCTTTATGGACC	TGATCAGCCAGTTGGAATTGTG
MDS1/EVI1	CCAGCGAATCTAATGTACTTGAGC	CCAGTTATGGATGGGAGATCTTAGAC
mEvi1	ACAACGACATCCCAGGAAAG	CTTGCAGCTCATCTCCAGTG
KISS1	CACTGGTTTCTTGGCAGCTA	GGAGGCCCAGGGATTCTA
EDN1	CCAAGGAGCTCCAGAAACAG	CTCTTTATCCATCAGGGACGA
PIK3CG	CCTCAACCATGAAGGAAACC	GGCAGTTGTCCTCTCTCAGC
PTGFR	GGGATCGGTGGAACTTGAG	GGATTGCAGTCCAGACATCTT
CDK1	TGGATCTGAAGAAATACTTGGATTCTA	CAATCCCCTGTAGGATTTGG
CCNA1	AATGGGCAGTACAGGAGGAC	CCACAGTCAGGGAGTGCTTT
CDKN1C(p57)	GAGCGAGCTAGCCAGCAG	GCGACAAGACGCTCCATC
BMF1	GAGACTCTCTCCTGGAGTCACC	CTGGTTGGAACACATCATCCT
BMF2	AGTTCCACCGGCTTCATGT	TCTTCTCCATTCAAAGCAAGG
SMAD3	GTCTGCAAGATCCCACCAG	GTGCACATTCGGGTCAACT
DUSP5	ACAAATGGATCCCTGTGGAA	CCTCCCTTTTCCCTGACAC
DUP22	GGTGAGAGCTGCCTTGTACACT	GCACAGGATCTCCCAGCA
GAPDH	CTGACTTCAACAGCGACACC	TAGCCAAATTCGTTGTCATACC
ERBB2	GGGAAACCTGGAACTCACCT	CCCTGCACCTCCTGGATA
KISS1-1 (ChIP)	AGGGTCAGTGCTGTCCTCAT	ACCCCTCACTTGTCTGATGC
KISS1-2 (ChIP)	GACCAGGTTGAGCTTGTGCT	TCTCCAGGGCAGAGACTGTT
KISS1-3 (ChIP)	CCCTGTCCTCAAAGTGCTGT	AGAGAGGGGACTTCCAGGTG
KISS1-4 (ChIP)	GCTCTTCGGAGAGGAAACAA	CCATCCTCCACACCCTCTT
BCL-xL (ChIP)	AGGGTAAATGGCATGCATATTAA	TTATAATAGGGATGGGCTCAACCA
Neg. Ctrl. (ChIP)	CTCTCAGGAAGGTCTAGGGGGCG	CGCCCCCGGGAGGGCTCCGGGGC
Kiss1_PLVX	GCCTGGAGAAGGATCCATGAACTCACTGGTTTCT	GCGCGGCCGCGGATCCTCACTGCCCCGCACCTG

Supplementary Table 2

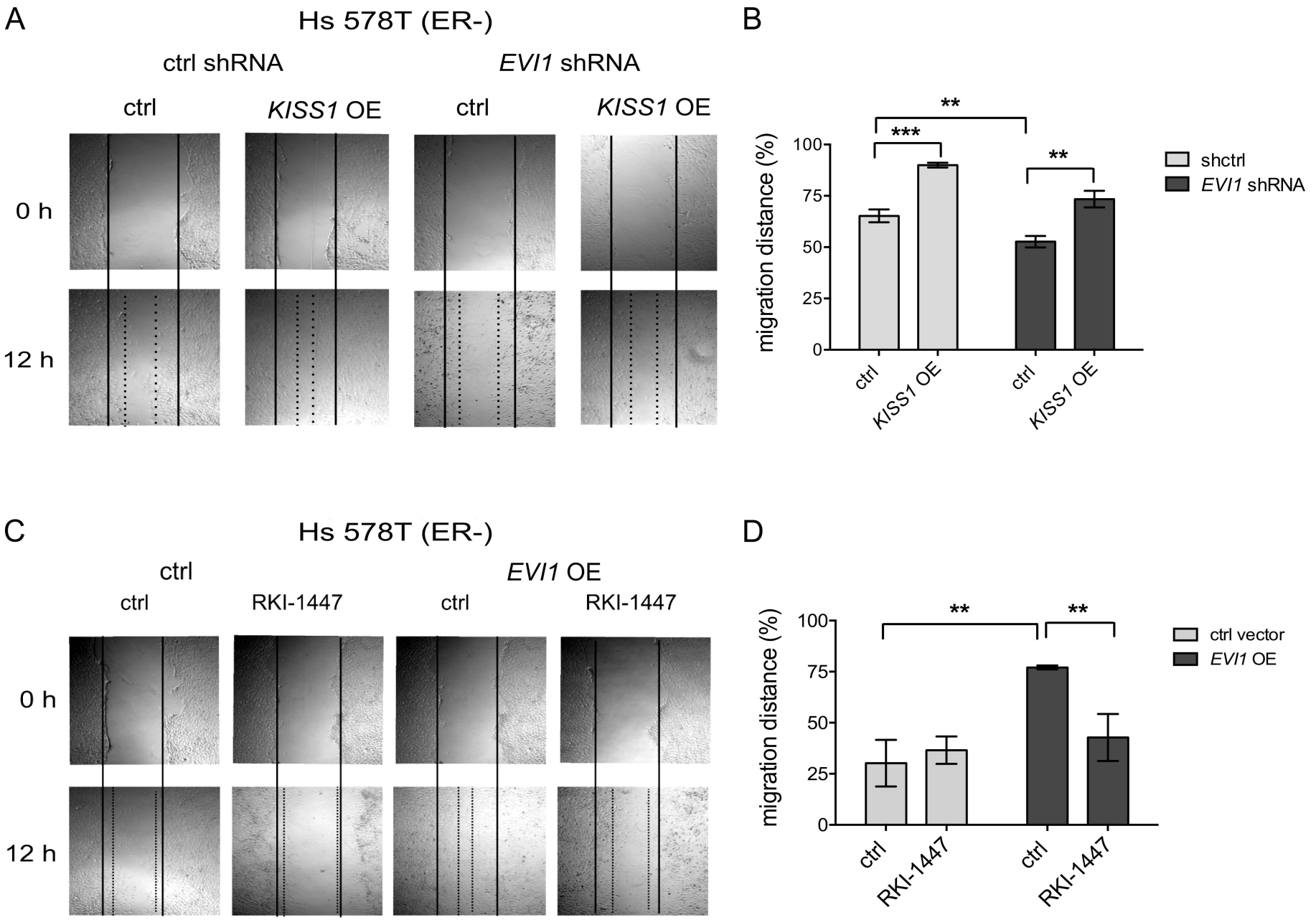

Supplementary Figure 9

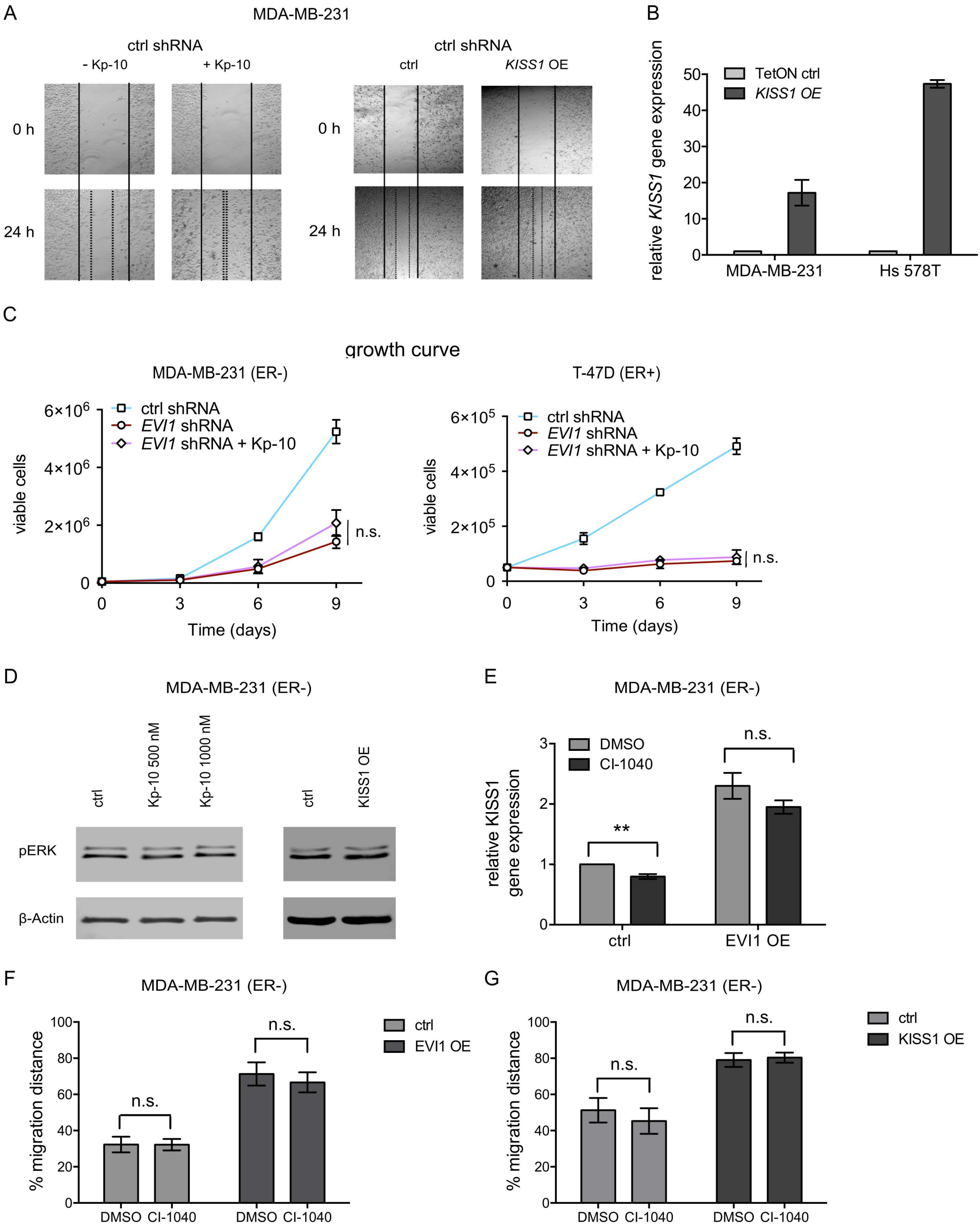

Supplementary Figure 10

Paper IV

Ecotropic viral integration site 1, a novel oncogene in prostate cancer.

Queisser A*, Hagedorn S*, **Wang H***, Schaefer T, Konantz M, Alavi S, Deng M, Vogel W, von Mässenhausen A, Kristiansen G, Duensing S, Kirfel J, Lengerke C, Perner S.

Oncogene. 2017 Mar;36(11):1573-1584. Epub 2016 Sep 12.

Oncogene (2017) **36**, 1573–1584
© 2017 Macmillan Publishers Limited, part of Springer Nature. All rights reserved 0950-9232/17
www.nature.com/onc

ORIGINAL ARTICLE

Ecotropic viral integration site 1, a novel oncogene in prostate cancer

A Queisser[1,2,3,7], S Hagedorn[1,2,3,7], H Wang[4,7], T Schaefer[4], M Konantz[4], S Alavi[1,2,3], M Deng[5], W Vogel[5], A von Mässenhausen[1,2,3], G Kristiansen[2,3], S Duensing[6], J Kirfel[2,3], C Lengerke[4,7] and S Perner[1,2,3,5,7]

Prostate cancer (PCa) is the most commonly diagnosed non-cutaneous cancer in men in the western world. Mutations in tumor suppressor genes and in oncogenes are important for PCa progression, whereas the role of stem cell proteins in prostate carcinogenesis is insufficiently examined. This study investigates the role of the transcriptional regulator *Ecotropic Viral Integration site 1* (*EVI1*), known as an essential modulator of hematopoietic and leukemic stem cell biology, in prostate carcinogenesis. We show that in healthy prostatic tissue, EVI1 expression is confined to the prostate stem cell compartment located at the basal layer, as identified by the stem cell marker CD44. Instead, in a PCa progression cohort comprising 219 samples from patients with primary PCa, lymph node and distant metastases, EVI1 protein was heterogeneously distributed within samples and high expression is associated with tumor progression ($P < 0.001$), suggesting EVI1 induction as a driver event. Functionally, short hairpin RNA-mediated knockdown of EVI1 inhibited proliferation, cell cycle progression, migratory capacity and anchorage-independent growth of human PCa cells, while enhancing their apoptosis sensitivity. Interestingly, modulation of *EVI1* expression also strongly regulated stem cell properties (including expression of the stem cell marker SOX2) and *in vivo* tumor initiation capacity. Further emphasizing a functional correlation between EVI1 induction and tumor progression, upregulation of EVI1 expression was noted in experimentally derived docetaxel-resistant PCa cells. Importantly, knockdown of *EVI1* in these cells restored sensitivity to docetaxel, in part by downregulating anti-apoptotic BCL2. Together, these data indicate EVI1 as a novel molecular regulator of PCa progression and therapy resistance that may control prostate carcinogenesis at the stem cell level.

Oncogene (2017) **36,** 1573–1584; doi:10.1038/onc.2016.325; published online 12 September 2016

INTRODUCTION

Prostate cancer (PCa) is the most commonly diagnosed non-cutaneous cancer and the second most common cancer-related cause of death in men in the western world.[1] Initially, metastasized PCas respond to androgen deprivation therapy; however, the transition of hormone-sensitive tumors to the castration-resistant PCa (CRPC) is inevitable. Owing to its limited response to available treatments, CRPC remains a clinical challenge.

It is assumed that an accumulation of molecular changes contributes to prostate carcinogenesis.[2] Known genetic modifications involved in PCa progression include the androgen receptor signaling pathway, next to tumor suppressor genes such as *PTEN* and *TP53*, and oncogenes such as *MYC*, *EGFR*[3–6] and *TMPRSS2-ETS* gene fusions.[7–10] The zink finger transcriptional regulator *Ecotropic viral integration site 1 (EVI1)* is located on human chromosome 3q26.2,[11] a region showing DNA copy number gains in primary PCa.[12]

Originally described as a retroviral insertion site in murine myeloid tumors, *EVI1* has been mostly studied in hematopoietic stem cells and in myeloid malignancies where its overexpression indicates particularly aggressive disease.[13–16] However, *EVI1* is also expressed in some non-hematopoietic tissues[17] and tumors thereof.[18–21] More recently, a chromatin immunoprecipitation sequencing and microarray analyses performed on ovarian carcinoma suggested that several genes involved in oncogenesis seem to be direct targets of EVI1,[22] highlighting its relevance for cancer biology.

In PCa, *EVI1* expression has been previously documented in a limited number of cell lines,[23,24] but has not been investigated in patient-derived PCa samples or evaluated with respect to functional significance and molecular targets. Here we demonstrate that EVI1 expression influences proliferation, apoptosis resistance, migration and stem cell properties in CRPC cells. In line with these results, EVI1 expression is strongly induced in experimentally generated docetaxel-resistant PCa cells.

The changes leading to CRPC are not fully understood. Emerging evidence points towards the existence of a distinct subpopulation called cancer stem cells (CSCs), which may be involved in tumor initiation, progression and therapy resistance.[25] In healthy tissues, EVI1 expression is confined to the basal cell layer, the prostatic stem cell compartment. It can be speculated that an aberrant activation of stem cell factors such as EVI1 might contribute to PCa CSC formation and thus to PCa initiation.

[1]Section for Prostate Cancer Research, University Hospital of Bonn, Bonn, Germany; [2]Institute of Pathology, University Hospital of Bonn, Bonn, Germany; [3]Center for Integrated Oncology Cologne/Bonn, University Hospital of Bonn, Bonn, Germany; [4]Department of Biomedicine, University Hospital of Basel, Basel, Switzerland; [5]Pathology of the University Medical Center Schleswig-Holstein, Campus Luebeck and the Research Center Borstel, Leibniz Center for Medicine and Biosciences, 23538 Luebeck and 23845 Borstel, Borstel, Germany and [6]Section of Molecular Urooncology, Department of Urology, University of Heidelberg School of Medicine, Heidelberg, Germany. Correspondence: Professor C Lengerke, Department of Biomedicine, University Hospital Basel, Hebelstrasse 20, Basel CH-4031, Switzerland or Professor S Perner, Pathology of the University Hospital of Luebeck and Leibniz Research Center Borstel, Institute of Pathology, Ratzeburger Allee 160, Building 50, Luebeck 23538, Germany.
E-mail: Claudia.Lengerke@unibas.ch or Sven.Perner@uksh.de
[7]These authors contributed equally to this work.
Received 18 February 2016; revised 8 July 2016; accepted 26 July 2016; published online 12 September 2016

At advanced disease stages, the enhanced expression of EVI1 might reflect the stem cell origin of drug resistance and metastatic disease.

Jointly, these data indicate EVI1 overexpression as an important novel factor in PCa biology that could serve as a target for controlling CRPC.

RESULTS

EVI1 expression in benign and malignant prostatic glands and PCa lymph node and distant metastases

We investigated the expression of EVI1 in benign prostatic glands and a progression cohort containing 148 primary PCa samples, 39 lymph node metastases and 32 CRPCs by immunohistochemistry. In benign prostatic glands, EVI1 showed exclusive expression in the basal cell layer co-localizing with CD44, which is expressed by putative stem cells (Figures 1a and b).[26,27] In primary PCa, heterogeneous EVI1 expression was observed with most cells showing either no or modest expression of EVI1 (Figure 1a). However, enhanced and homogeneous expression was observed in lymph node and distant metastases (Figures 1a and c). Next, we performed fluorescence *in situ* hybridization analyses to investigate whether the enhanced EVI1 expression is due to rearrangements or amplification of the *EVI1* gene locus as reported in some leukemia.[17,28] However, we found no evidence of *EVI1* translocation/amplification in our PCa cohort (Supplementary Figure 1a). To further investigate this aspect, nine data sets provided by the c-BioPortal (http://www.cbioportal.org) were additionally examined for copy number variations.[29,30] Within these, the copy number variation of the *MECOM* joint gene gene (including the *EVI1* gene) varied between 0 and 8.2% (Supplementary Figure 1b).[31–39] Moreover, co-occurrence between expression levels of *EVI1* and the established stem cell genes *SOX2* and *PROM1* (Supplementary Figures 1c and d) was observed in the The Cancer Genome Atlas data set ($n = 333$; The Cancer Genome Atlas, Cell 2015).[33] The correlation between

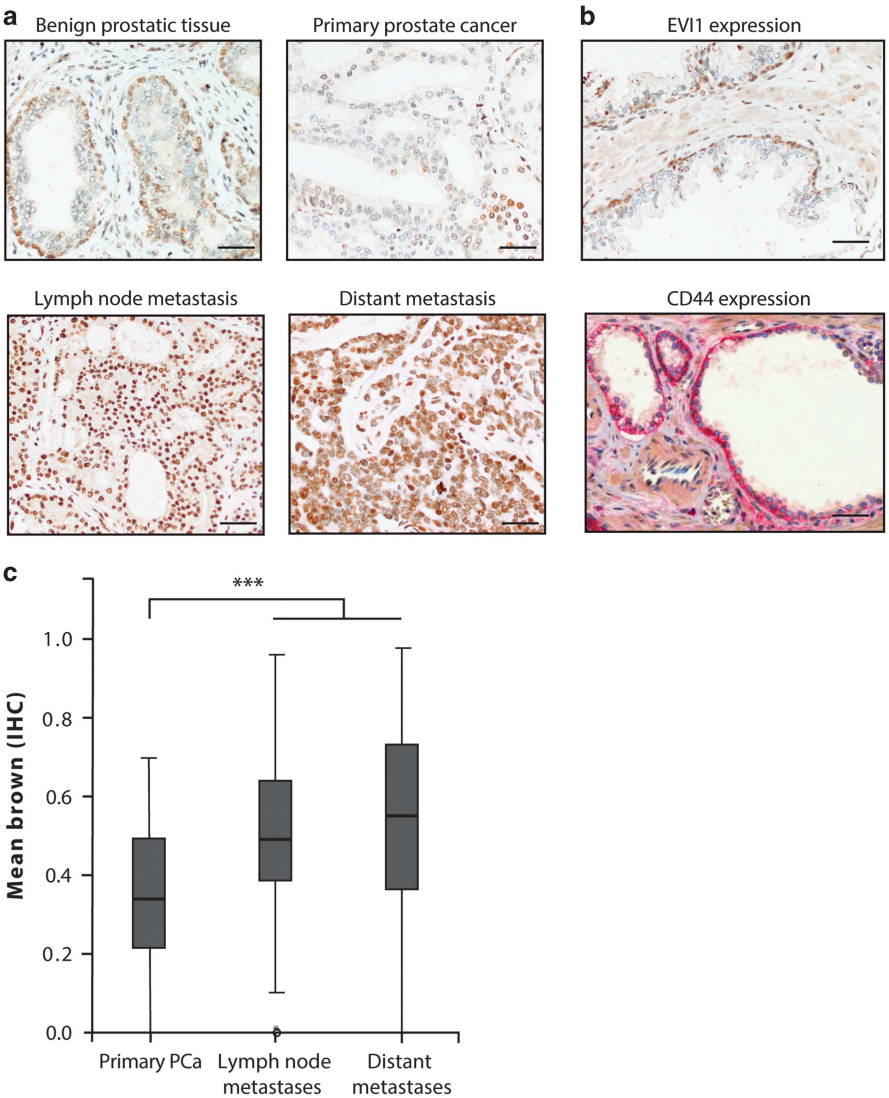

Figure 1. EVI1 is expressed in the basal layer of normal prostatic glands and is significantly higher expressed in lymph node metastases and CRPC. Immunohistochemistry (IHC) staining of EVI1 was performed on primary PCas, lymph node and distant metastases, as well as benign prostatic tissue. (**a**) Representative samples of EVI1 protein expression (brown) in prostatic normal tissue and in neoplastic prostatic tissue are shown. (**b**) IHC staining of EVI1 and the stem cell marker CD44 (magenta) in benign prostatic tissue. (**c**) Boxplot displaying the mean nuclear staining intensity of EVI1 evaluated using the semi-automated image analysis system Definiens (Student's *t*-test one-sided, Bonferroni correction, $^{***}P < 0.001$).

© 2017 Macmillan Publishers Limited, part of Springer Nature.

EVI1 and *SOX2* expression was furthermore confirmed experimentally, as downregulation of *EVI1* reduced *SOX2* and *PROM1* mRNA expression in PCa cells (Supplementary Figure 1e).

Generation of *EVI1* knockdown PCa cells

To investigate the functional significance of EVI1 in PCa cells, we used lentiviral short hairpin RNA (shRNA) technology to downregulate EVI1 expression in PC3 cells (derived from a hormone-refractory PCa bone metastasis),[40] which were identified to robustly express EVI1 (Supplementary Figures 2a and b). PC3 cells were stably transduced with two lentiviral plasmids containing different shRNAs against EVI1. Cultures derived from transduction with either of the two *EVI1* shRNAs (shEVI1#1 and shEVI1#2) showed efficient downregulation of *EVI1* mRNA and protein expression (Figures 2a and b, respectively), when compared with cells transduced with non-coding control shRNA. In addition, three single-cell derived clones showing particularly efficient EVI1 knockdown (PC3 shEVI1 single cell clones A, B and C) were investigated alongside with the aforementioned PC3 shEVI1 bulk cultures (shEVI1#1 and shEVI1#2).

EVI1 knockdown impairs proliferation in PCa cells

Knockdown of EVI1 significantly and dose-dependently reduced cell growth in standard growth assay ($P < 0.001$), with more pronounced effects in single cell-derived EVI1 knockdown clones (Figure 2c). These findings were confirmed using the xCELLigence system, which monitors cell growth in real time (Figure 2d). 5-ethynyl-2'-deoxyuridine analyses confirmed alterations in cell proliferation as indicated by significantly reduced 5-ethynyl-2'-deoxyuridine-positive cell fractions in EVI1 knockdown versus control cells (Figure 3a). To further investigate these findings we analysed the proliferation marker Ki67. Although nearly 100% of control cells stained positive for Ki67, bulk EVI1 knockdown and, even more, the EVI1 knockdown single-cell clones showed a significant reduction in proliferation (Figure 3b, upper panel). In addition, a β-galactosidase senescence assay revealed that EVI1 knockdown cultures contained several β-galactosidase-positive cells, whereas almost no senescent cells could be detected in control cultures (Figure 3b, lower panel). Consistent with the notion that EVI1 expression has impacts on proliferation, knockdown of EVI1 increased the percentage of cells in G0/G1, at the expense of decreased S-phase (Supplementary Figure 3a). The steady-state expression of key cell-cycle mediators was also

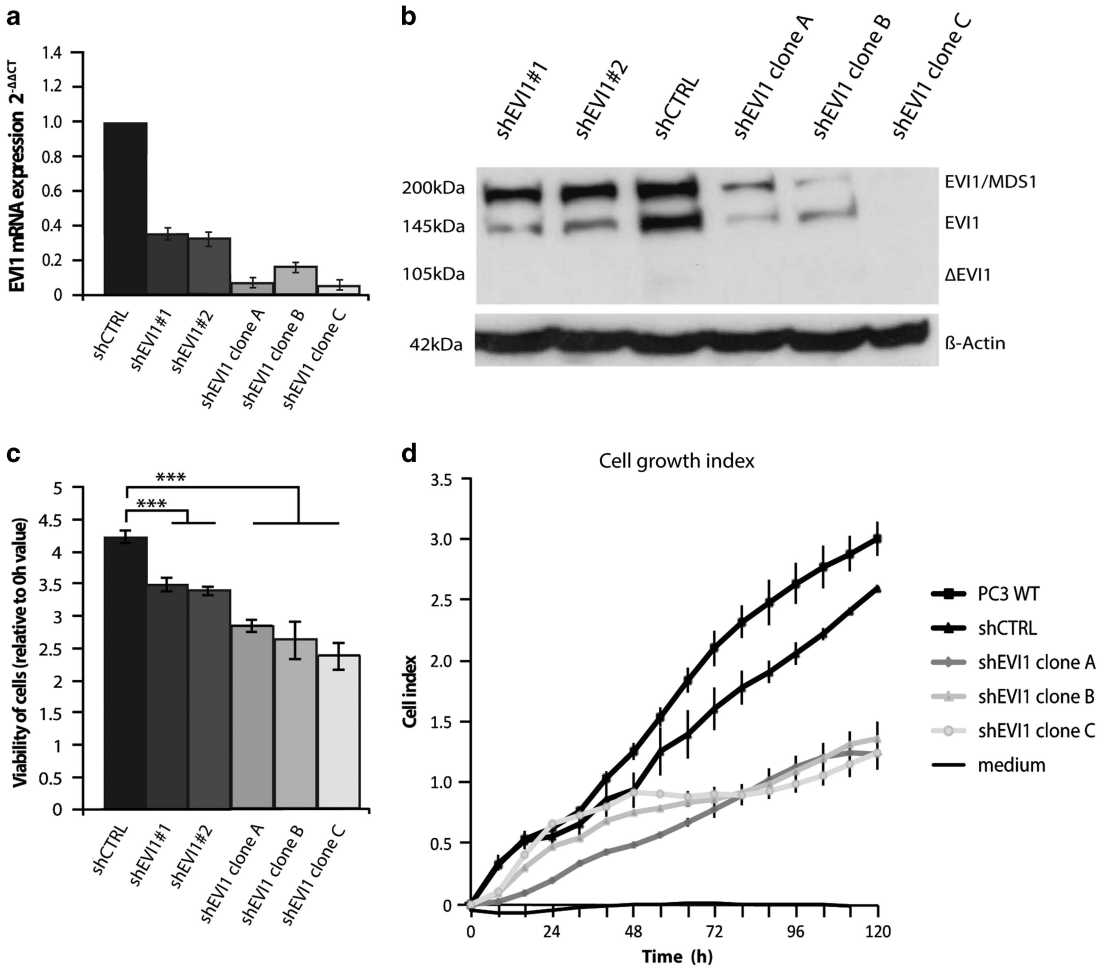

Figure 2. Knockdown of EVI1 expression in PC3 cells reduces cell growth. (**a**) Quantitative real-time PCR analysis of *EVI1* in shEVI1-treated PC3 cells (shEVI1#1, shEVI1#2 and shEVI1 clone A/B/C) and control cells. *EVI1* mRNA expression is displayed relative to the control cells containing non-coding shRNA (shCTRL) after normalization to the housekeeping gene β-actin. (**b**) Immunoblot analyses of protein extracts derived from EVI1 shRNA or control shRNA-treated PC3 cells. (**c**) Cell viability was determined after 72 h using a MTT assay. Bars show the absorbance at 595 nm relative to the 0 h value (independent Student's *t*-test one-sided, Bonferroni correction; ***$P < 0.001$). (**d**) Proliferation of PC3 EVI1 knockdown and control cells as determined by the xCELLigence system throughout a time window of 120 h. Graphs represent the mean cell index of two wells ± s.d. A representative graph of the experiment, which was repeated three times independently, is shown.

© 2017 Macmillan Publishers Limited, part of Springer Nature.

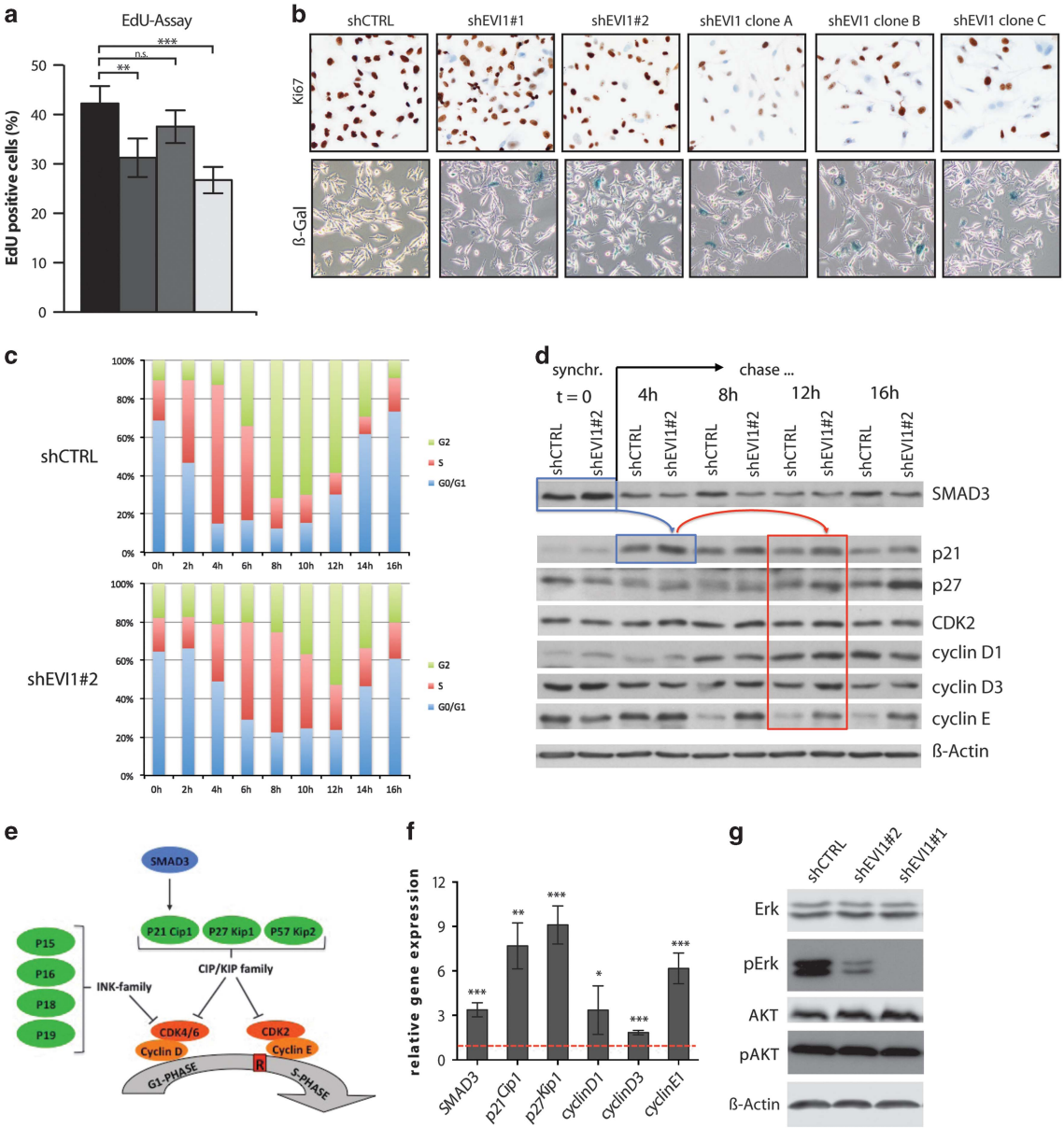

Figure 3. EVI1 knockdown interferes with cell cycle progression and downstream signaling pathways in PC3 cells. ShEVI1 knockdown and control shRNA-treated PC3 cells were analyzed for (**a**) incorporation of 5-ethynyl-2'-deoxyuridine (**b**) Ki67 positivity by immunocytochemistry (ICC; top panels) and β-galactosidase activity to detect senescence (lower panels). (**c**) Cell cycle phase distribution analysis in aphidicolin-synchronized EVI1 knockdown and control PC3 cells, and (**d**) corresponding immunoblot analyses, indicating perturbed expression of key cell cycle regulators in EVI1 knockdown versus control cells. SMAD3/p21 axis (blue box), relevant downstream effectors (red box). (**e**) Scheme to illustrate the relevance of SMAD3 for G1-S phase progression. (**f**) Real-time PCR analysis verifying co-induction of *SMAD3*, *p21* and selected downstream target genes in *EVI1* knockdown versus control PC3 cells. Indicated are ΔΔCt values relative to *GAPDH* and normalized to corresponding expression levels in control PC3 cells (red line). (**g**) Immunoblot analyses to illustrate differential regulation of proliferation-associated mitogen-activated protein kinase signaling, but not AKT signaling in EVI1 knockdown versus control PC3 cells (Student's *t*-test; $*P < 0.05$, $**P < 0.01$ and $***P < 0.001$).

significantly perturbed on EVI1 knockdown (Supplementary Figure 3b). Interestingly, cyclin D1 expression, usually reduced on cell cycle arrest in G0/G1, was enhanced in EVI1 knockdown cells (Supplementary Figure 3b). We therefore hypothesized that the impaired growth observed in EVI1 knockdown versus control cells does not reflect an actual cell cycle arrest, but instead results from a cell cycle delay with extended periods of cyclin D1 expression. To explore this notion, the cell cycle status of control and EVI1 knockdown PC3 cells was synchronized using aphidicolin,[41] which stalls the cell cycle in G0/G1. Aphidicolin was then removed and cells followed progressively for one entire cell cycle, regarding phase distribution and expression of key cell cycle proteins. Indeed, a clear cell cycle delay (and not an arrest) was observed in EVI1 knockdown versus control PC3 cells (Figure 3c). In line, corresponding protein analyses showed shifted expression peaks of key cell cycle mediators (Figure 3d).

Mechanistically, these changes may be mediated by de-repression of SMAD3, a reported direct target of EVI1 transcriptional regulation,[42] which then broadly modulates cell cycle proteins via its downstream target p21Cip1 (Pardali *et al.*;[43] see also scheme in Figure 3e). Supporting these results, modulation of the SMAD3-p21 axis and downstream cell cycle targets were

© 2017 Macmillan Publishers Limited, part of Springer Nature.

confirmed by real-time PCR in EVI1 knockdown versus control PC3 cells (Figure 3f).

The PI3K-pAKT pathway is another major regulator of cell growth that was shown to be influenced by EVI1 expression in colon carcinoma.[44] In PCa, EVI1 knockdown cells did not display overt changes in pAKT or AKT levels as compared with control cells (Figure 3g). A marked reduction in mitogen-activated protein kinase activity, as deduced from reduced pERK but not ERK, was observed upon EVI1 knockdown (Figure 3g).

EVI1 knockdown impairs migration and anchorage-independent growth of PCa cells

As lymph node metastases and CRPC showed higher EVI1 positivity than primary PCa samples, we investigated influences of EVI1 expression on migratory properties by performing an *in vitro* scratch assay. Indeed, EVI1 knockdown reduced migration of bulk and single clone-derived PC3 cells versus controls (Figure 4a).

To investigate mechanisms by which EVI1 expression has impacts on cell migration, we explored by real-time PCR the effect of EVI1 knockdown on the expression of a panel of genes involved in cell migration and metastasis. A direct comparison of bulk transduced shEVI1 cells versus corresponding non-coding shRNA control cells uncovered 31 genes involved in cell mobility (20 up and 11 down) and 33 genes involved in metastases (22 up and 11 down) to be significantly modulated by EVI1 knockdown (Figure 4b and Supplementary Figure 4). For further validation, results were compared with the analysis of two single cell-derived EVI1 shRNA clones (obtained by treatment with an alternative shRNA). Candidate genes modulated greater than fivefold and showing conservation in all three analyses (highlighted in color, Figure 4b) included for example integrin β2 and 3, both involved in RHO-ROCK-mediated cell adhesion.

Finally, in comparison with control PC3 cells, EVI1 knockdown bulk and single cell-derived clones showed reduced anchorage-independent growth capacity as indicated by lower number and smaller size of colonies formed in soft-agar assays (Figures 4c and d).

Downregulation of EVI1 inhibits tumor sphere formation in PC3 cells

The tumor sphere assay is considered as an *in vitro* surrogate assay for CSC activity in carcinomas.[45–47] Our expression results suggest that EVI1 expression might mark healthy and cancerous prostatic stem cells. In line, *EVI1* expression associated with expression of the stem cell genes *SOX2* and *PROM1* (Supplementary Figures 1d and e). Therefore, we used this assay to test the influence of EVI1 expression levels on PCa cell clonogenicity and CSC features. Downregulation of EVI1 led to a dose-dependent impairment in tumor sphere formation in primary and serial replating assays (Figures 5a and b).

In vivo tumorigenicity of PC3 cells is reduced on EVI1 knockdown

To test the importance of EVI1 expression for *in vivo* tumor initiation capacity, tumor formation from PC3 cells was assayed in a previously described zebrafish xenotransplantation model.[48,49] Frequency of tumor formation from fluorescence labeled injected cells was assayed by microscopy (Figure 5c). In line with the *in vitro* results suggesting that EVI1 controls the PCa-initiating cell compartment, PC3 control cells robustly engrafted zebrafish embryos and formed tumors at high frequency, whereas knockdown of EVI1 markedly reduced tumor formation from xenotransplanted PC3 cells (Figures 5d–f).

EVI1 expression associates with docetaxel resistance

Long-term treatment of PC3 cells with docetaxel—a drug that is commonly used for treatment of patients with CRPC—induced a marked upregulation of EVI1 expression (Figure 6a). In leukemia, high EVI1 expression has been associated with apoptosis resistance via upregulation of the anti-apoptotic protein BCL-xL.[15] Therefore, we hypothesized that the elevated levels of EVI1 expression observed in docetaxel-resistant PC3 cells (Figure 6a) induce chemoresistance by modulation of apoptosis. Consistently, knockdown of EVI1 in docetaxel-resistant PC3 cells enhanced their apoptotic response restoring drug sensitivity (Figures 6b and c). To investigate the molecular pathways by which EVI1 modulates apoptosis, we performed a real-time PCR analysis of pro- and anti-apoptotic candidate molecules and identified anti-apoptotic BCL2 (and not BCL-xL) as significantly downregulated in EVI1 knockdown versus control docetaxel-resistant cells (Figure 6d). A marked co-induction of EVI1 and BCL2 expression in drug-resistant PC3 cells was confirmed also on protein level (Figure 6e and Supplementary Figure 5d). To functionally explore the importance of BCL2 as a downstream target of EVI1 mediating docetaxel resistance, we next co-treated docetaxel-resistant PC3 cells with different concentrations of docetaxel and/or the BCL2 inhibitor ABT-199.[50] As previously shown with EVI1 knockdown, treatment with BCL2 inhibitor was able to enhance apoptotic response to docetaxel in formerly resistant PC3 cells (Figures 6f and g and Supplementary Figure 5f). Together, these data indicate that EVI1 expression contributes to docetaxel resistance by enhancing apoptosis resistance via upregulation of anti-apoptotic BCL2.

Consistently with the results reported above in docetaxel-resistant PC3 cells, knockdown of EVI1 also suppressed BCL2 expression and enhanced apoptosis sensitivity in non-resistant PC3 cells (Supplementary Figures 5a–c). Of note, in contrast to docetaxel-resistant cells, control cells showed enhanced sensitivity to treatment with ABT-199 alone (Supplementary Figures 5e vs f), consistent with the notion that resistant cells have enhanced endogenous BCL2 activity and thus require higher dosages of the inhibitor.

DISCUSSION

CRPC is considered incurable and therefore the identification of targets for novel treatment options represents an unmet medical need. It is known that changes in tumor suppressor genes and oncogenes contribute to PCa progression.[3–6] Fifty percent of PCa display gene amplifications spanning the region 3q25–3q27, where also EVI1 is encoded.[12] In myeloid leukemia, increased expression of *EVI1* often involves genetic rearrangements of the *EVI1* locus at chromosomal region 3q26,[17] whereas in ovarian cancer elevated EVI1 expression was associated with high copy number gains.[51] However, *EVI1* copy number gains could not be found in other investigated tumors (for example, pancreatic cancer).[52] Throughout all PCa stages investigated by fluorescence *in situ* hybridization in our cohort, we could neither detect rearrangements nor an amplification of the *EVI1* gene, indicating that the overexpression of EVI1 in PCa may not result from genetic aberrations but result from an alternative mechanism, as also seen in 10–50% of myeloid malignancies.[17] However, analysis of nine further PCa cohorts using the cBioPortal revealed an *EVI1* copy number variation rate varying between 0 and 8.2%. This difference could be explained by the usage of different methods for detecting copy number variations such as Affymetrix SNP 6 Arrays and sequencing. However, the gold standard to detect amplifications/deletions on single-cell level remains the fluorescence *in situ* hybridization analysis. Moreover, mRNA expression data indicated that an EVI1 amplification does not necessarily lead to an enhanced mRNA expression.

© 2017 Macmillan Publishers Limited, part of Springer Nature.

Here we analyzed EVI1 expression on protein level in a PCa progression cohort containing primary PCa and metastatic samples. As control, healthy prostatic tissue was used. In normal prostatic glands, EVI1 expression was detected exclusively in the basal cell layer harboring prostatic stem cells. Higher expression was found in lymph node metastases and CRPC compared with

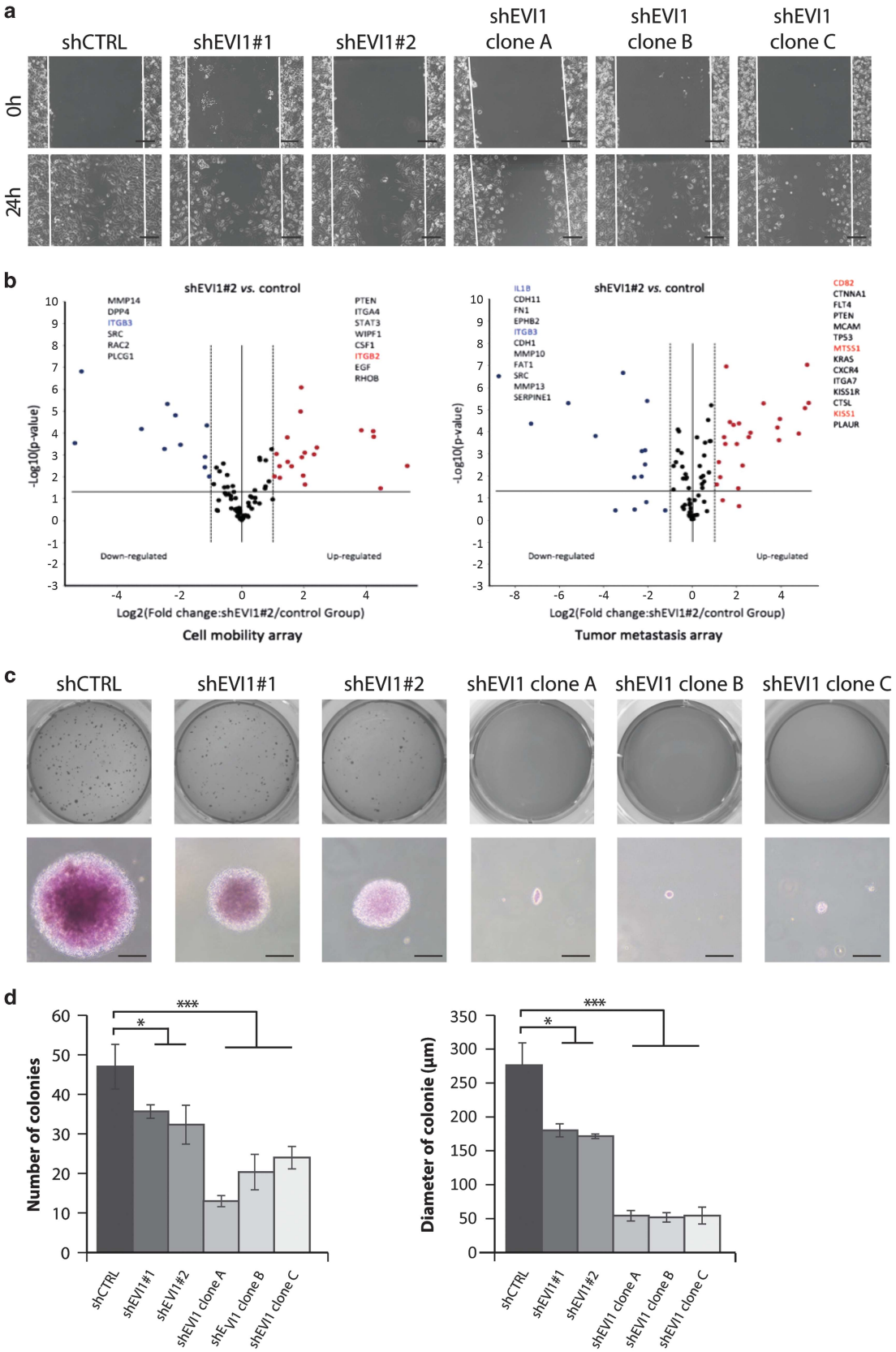

© 2017 Macmillan Publishers Limited, part of Springer Nature.

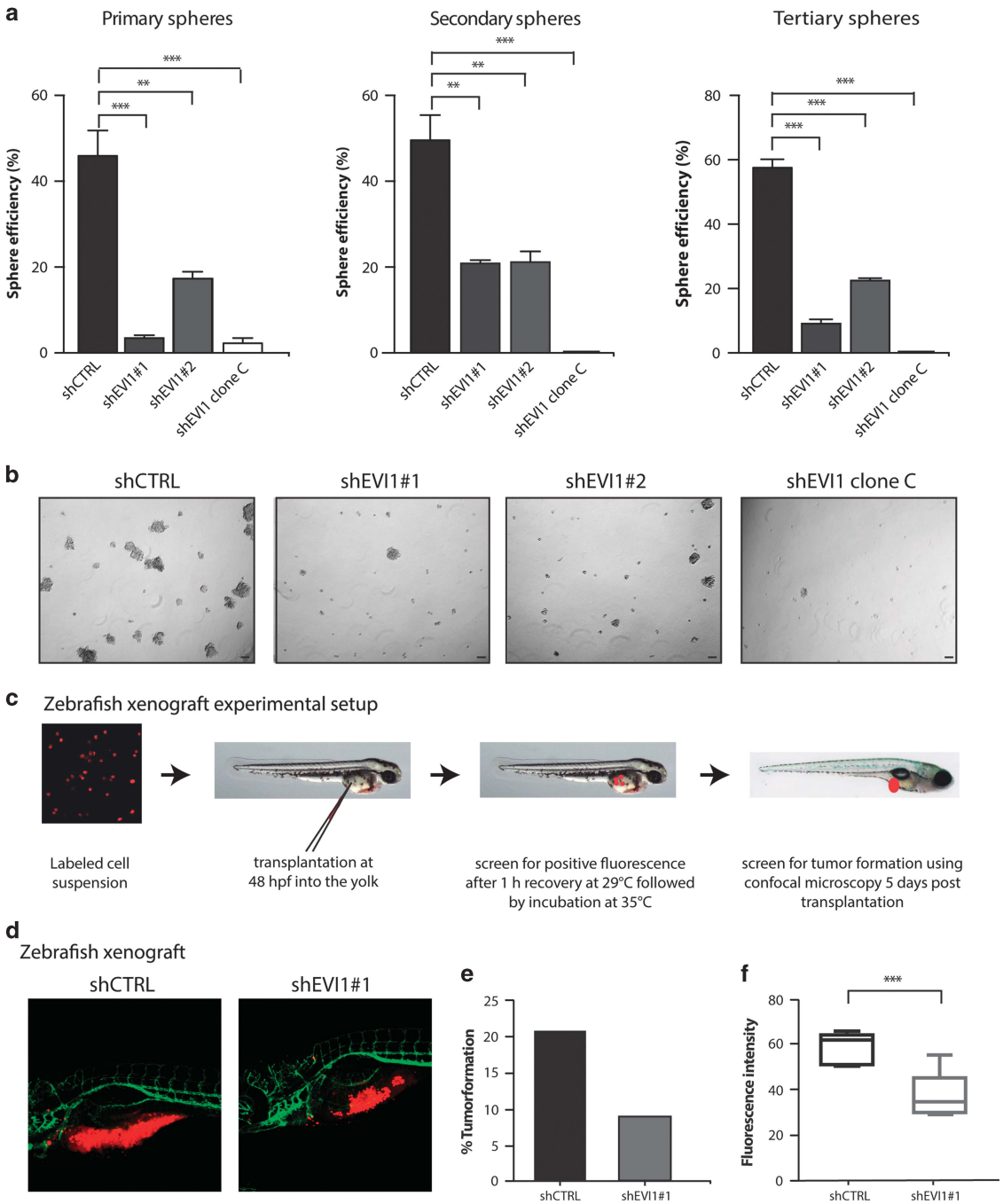

Figure 5. EVI1 regulates tumor sphere formation and *in vivo* tumorigenicity of PC3 cells. (**a**) Quantification of tumor sphere formation from sh*EVI1* and non-coding shRNA control cells throughout primary, secondary and tertiary assay cycles. (**b**) Representative overview pictures of spheres formed from either shEVI1 knockdown or control cells. (**c**) Schematic illustration of the zebrafish xenotransplantation experimental setup. (**d**) Representative pictures of red-labeled *EVI1* shRNA-treated PC3 cells and control cells xenotransplanted into zebrafish embryos. (**e**) Quantification of total number of animals with red label past 5 days and (**f**) the fluorescence intensity of red-labeled xenotransplanted cells as calculated using Fiji software. For each experiment 75–100 cells per fish were transplanted and at least 5 fish for each condition were analyzed (Student's *t*-test; $^{**}P < 0.01$ and $^{***}P < 0.001$).

Figure 4. EVI1 knockdown in PC3 cells reduces migratory potential and anchorage-independent growth. (**a**) Confluent layers of EVI1 knockdown cells (shEVI1#1 and #2), and single cell clones (shEVI1 clones A/B/C), as well as control cells were injured by scratching. Images of scratches were captured at 0 and 24 h. Representative scratch healing images are shown. Scale bar = 200 μm. (**b**) Identification of target genes implicated in cell migration (left panel) and metastasis (right panel) by microarray technology in EVI1 knockdown versus control PC3 cells. Genes with an EVI1-dependent expression fold difference > 5 are indicated by names (left, downregulated and right, upregulated in response to EVI1 knockdown). Conserved hits, identified on EVI1 knockdown in parental mixed cultures and single cell clones, are shown in bold. (**c**) Anchorage-independent growth of shEVI1-treated PC3 cells and control cells were evaluated using soft agar assays. Overview pictures (top) and representative single colonies (bottom) are shown. Scale bar = 100 μm. (**d**) Left: soft agar assay showing the numbers of formed colonies in shEVI1-treated PC3 cells and control cells. Right: soft agar assay showing the size of colonies in sh*EVI1*-treated PC3 cells and control cells (Stundent's *t*-test one-sided, Bonferroni correction; $^{*}P < 0.05$, $^{**}P < 0.01$ and $^{***}P < 0.001$).

© 2017 Macmillan Publishers Limited, part of Springer Nature.

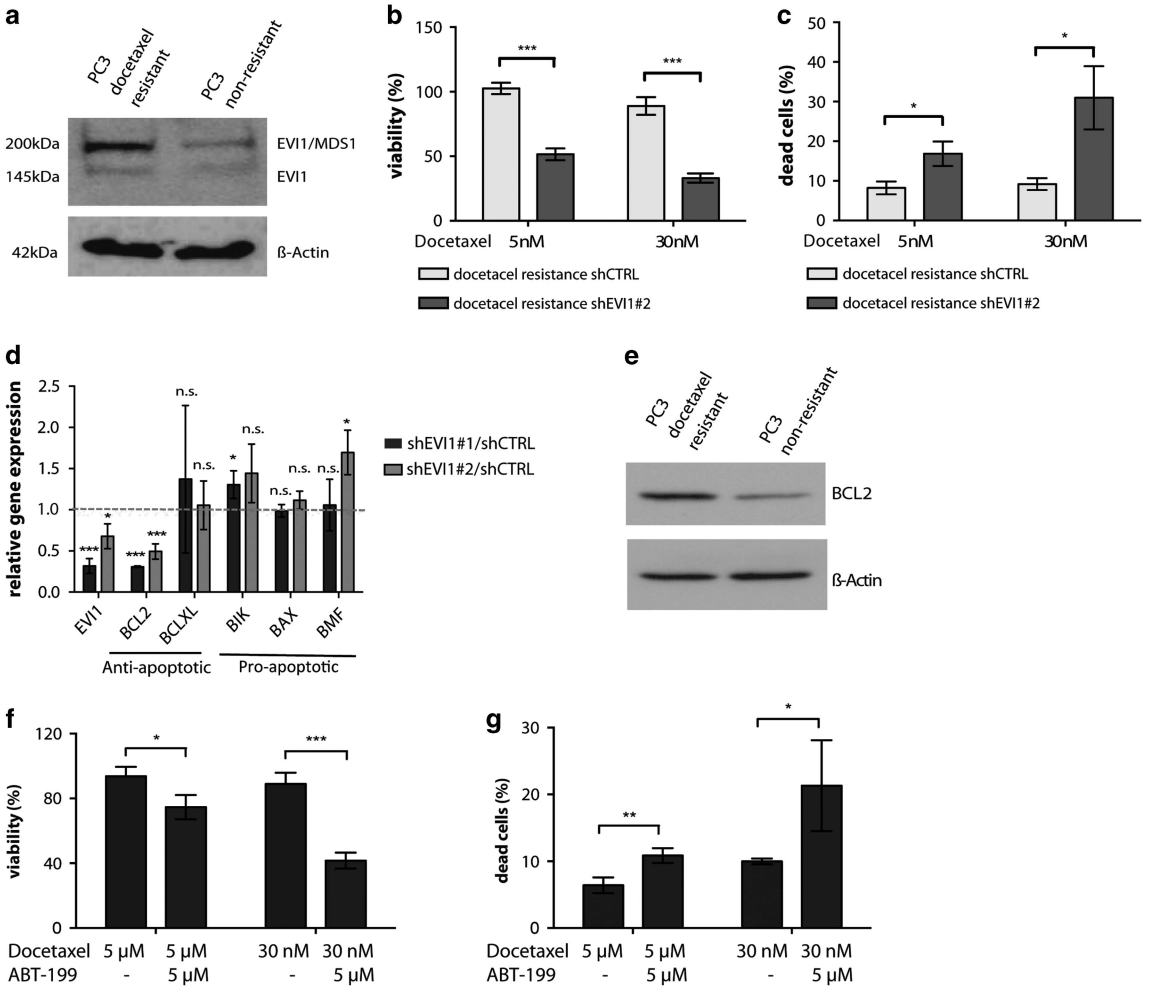

Figure 6. EVI1 expression mediates docetaxel resistance. (**a**) Immunoblot documenting elevated expression of EVI1 protein in docetaxel-resistant PC3 versus wildtype control cells. Anti β-actin staining is shown for reference. Knockdown of EVI1 expression re-sensitized drug-resistant PC3 cells to docetaxel, as deduced from (**b**) impaired cell viability and (**c**) aggravated apoptosis rates in response to docetaxel. (**d**) qPCR investigation documenting co-depletion of *EVI1* and *BCL2* mRNAs in EVI1 knockdown versus control PC3 cells. It is noteworthy that *BCL2* is selectively regulated, whereas other apoptotic mediators (for example, *BCL-XL*, *BIK*, *BAX* and *BMF*) remain largely unaffected by EVI1 knockdown. (**e**) Enhanced expression of BCL2 protein in docetaxel-resistant PC3 cells, as illustrated by immunoblot. (**f** and **g**) Indicating functional synergism, depletion of BCL2 activity with the small compound inhibitor ABT-199 re-sensitized formerly drug-resistant PC3 cells to docetaxel-induced cell death (Student's *t*-test; $*P < 0.05$, $**P < 0.01$ and $***P < 0.001$).

primary PCa, where EVI1 was heterogeneously expressed, indicating a role in PCa progression. On the functional level, EVI1 strongly modulated PCa cell growth. Specifically, EVI1 knockdown led to a profound delay in cell cycle progression accompanied by deregulated expression of several cell cycle proteins. Mechanistically, these changes might be at least in part mediated by de-repression of SMAD3, a known transcriptional target of EVI1,[42] followed by consecutive induction of p21CIP1 expression. Moreover, the suppressed pERK levels observed in EVI1 knockdown versus control cells might further contribute to their impaired growth. Besides proliferation, we furthermore detected pronounced influences of EVI1 on BCL2 expression and apoptosis. Molecularly, EVI1 knockdown PCa cells showed reduced BCL2 levels and functionally enhanced basal apoptosis and docetaxel-induced cell death, consistent with previous observations in acute lymphoblastic leukemia.[15] Interestingly, no alterations in pAKT and AKT levels were observed on EVI1 knockdown, even though EVI1 has been linked to PI3-kinase/p-AKT pathway or c-Jun kinase in other tissues.[17] Overall, these data reflect important tissue-specific differences but support the notion that EVI1 expression in general promotes cell growth, apoptosis resistance and/or G1 progression.[19,52–55]

The influence of EVI1 on cell migration and metastasis has been less investigated. However, in pancreatic cancer cell lines, down-regulation of EVI1 led to a reduced migration,[52] whereas overexpression in ovarian cancer cell conferred migratory potential.[51] In our PCa cohort, higher EVI1 expression was associated with metastatic samples and a functional role of EVI1 in PCa cell migration was confirmed by scratch assays. By analyzing two arrays of genes involved in cell motility and metastasis in EVI1 knockdown and control PCa cells, we identified several candidate genes that potentially mediate these effects, including components of the RHO-ROCK adhesion pathway, CD82, IL1b and matrix metalloproteinases.

Very recently, EVI1 expression was reported in prostatic epithelium and stroma, where it supports cell survival and immaturity in the absence of functional androgen stimulation—a state that might contribute to the development of CRPC.[56] The intratumoral heterogeneity of PCa is reflected in its different histostructural and cellular composition;[26] there are two different theories: the clonal evolution and/or the stem cell model.[26,57]

© 2017 Macmillan Publishers Limited, part of Springer Nature.

Some data suggest that the development of CRPC follows a hierarchical model[26,58] and consists of prostate CSCs originating from androgene receptor-negative cells of the basal layer of the healthy prostatic gland.[25,57,59] Supporting this notion, Schroeder *et al.*[60] demonstrated that the androgen deprivation therapy promoted the development of a CSC phenotype by upregulation of stem cell markers such as SOX2 and CD44.

Together, our study indicates possible roles of EVI1 as a CSC protein, as (1) EVI1 is only expressed in cells of the androgen-negative stem-cell-associated basal layer of normal prostatic glands, where SOX2 and CD44 expression is detected as well,[61] that (2) only a small subset of primary PCa cells heterogeneously express EVI1, and that (3) long-term treatment of PC3 cells with docetaxel—a chemotherapeutic drug normally used as a therapy for CRPC patients—leads to drug resistance and a marked upregulation of EVI1.

Common models used for the evaluation of stem cell features are to test for self-renewal capacity *in vitro* by tumor sphere assay as well as *in vivo* xenotransplantation assays.[62] The zebrafish embryo model has emerged as model to study cancer stem-like cells *in vivo*.[63] Using both the sphere and the zebrafish assays, we could show that the self-renewal capacity was diminished after EVI1 knockdown. Furthermore, the soft agar assay also showed reduced *in vitro* colony formation. Consistently, on the molecular level downregulation of the stem cell factors *SOX2* and *PROM1* was observed on *EVI1* knockdown. These results further support the hypothesis that EVI1 regulates CSC properties in PCa cells.

Importantly, arsenic trioxide was reported to degrade the oncogenic EVI1 protein in leukemic cells inducing differentiation and sensitizing cells to chemotherapy-induced apoptosis.[64,65] If these mechanisms are conserved in PCa cells, treatment with arsenic trioxide might be an effective option for targeting EVI1-positive PCa cancer (stem) cells, which will be the subject of further studies.

Taken together, our immunhistochemical data as well as *in vitro* and *in vivo* studies demonstrate that EVI1 contributes to PCa progression by regulating different oncogenic functions. The data indicate that EVI1 regulates the PCa stem cell compartment responsible for disease initiation and also development of CRPC. However, further studies are necessary to verify EVI1 as a CSC protein, and to identify its molecular partners during this process as well as strategies of targeting it for therapeutic purposes.

MATERIALS AND METHODS

Cohort and tissue microarray construction

Approved by the institutional review board of the University of Tübingen, we studied a PCa progression cohort containing 14 benign prostatic samples, 148 primary PCa samples, 39 lymph node metastases and 32 CRPC samples, primarily of osseous sites. The cohort contains primary tumor material from Middle Europeans, who consecutively underwent radical prostatectomy with curative intent. Regional lymph node metastases were extracted in the context of the radical prostatectomy. Distant metastases were treated with hormone ablation therapy. Tissue microarrays were constructed as described previously.[66]

Immunohistochemistry and immunocytochemistry

Immunohistochemical and immunocytochemistry stains were conducted using the Ventana Benchmark automated staining system (Ventana Medical System, Tuscon, AZ, USA) as described previously.[67] The following antibodies were used: for immunohistochemistry, anti-EVI1 rabbit polyclonal (1:200, C50E12, Cell Signaling Technologies, Danvers, MA, USA) and anti-CD44 mouse monoclonal (1:400, F10-44-2, Abcam, Cambridge, UK), and for immunocytochemistry, anti-Ki-67 rabbit monoclonal (1:100, 30-9, Ventana). Signal detection was performed using the UltraView–DAB detection kit (Ventana Medical System). The EVI1 mean chromogene intensity of the nucleus was determined using the semi-automatic image analysis system (Definiens AG, Munich, Germany). Samples lacking tissues or carcinomas were excluded from analysis.

For Ki67 immunocytochemistry, the percentage of tumor cells with positive nuclear staining was evaluated within 10 randomly selected fields of the whole slide staining (original magnification ×100).

Fluorescence *in situ* hybridization

Please see Supplementary Material.

Data analysis using the c-BioPortal

Please see Supplementary Material.

Cell lines and culture conditions

BPH1, LNCaP, PC3 and DU145 cells were purchased from ATCC (Wesel, Germany) and authenticated by Multiplexon (Heidelberg, Germany). Cells were grown in a humidified atmosphere with 5% CO_2 and 37 °C. PC3 and BPH1 cells were cultured in RPMI-1640 (Biochem GmbH, Karlsruhe, Germany) supplemented with 10% fetal bovine serum (Biochem GmbH) and 1% penicillin/streptomycin (Life Technologies, Darmstadt, Germany). The medium for LNCaP and DU145 was additionally supplemented with 1% NEAA (Life Technologies) and 25 mM HEPES (PAA, Pasching, Austria; cell culture company). HEK293T cells for viral production were purchased form Thermo Scientific (Schwerte, Germany) and were cultured in high glucose HyClone Dulbecco's modified Eagle's medium (Thermo Scientific) supplemented with 10% fetal bovine serum, 1% penicillin/streptomycin and 1% L-glutamin (Life Technologies). To generate docetaxel-resistant PC3 cells, cells were treated with an ascending concentration of docetaxel (Selleckchem, Houston, TX, USA) starting from 2.5 nM up to 30 nM over a time span of 6 months.

Lentiviral transduction

The vector pLKO.1-puro carrying *EVI1* MISSION shRNAs: sh*EVI1*#1: TRCN0000002529 (5′-CCGGGCACTACGTCTTCCTTAAATACTCGAGTATTTAAGGAAGACGTAGTGCTTTTT-3′) and sh*EVI1*#2: TRCN0000002531 (5′-CCGGCCTTTCTTTATGGACCCTATTCTCGAGAATAGGGTCCATAAAGAAAGGTTTTT-3′) or non-coding shRNA were used in this study. Lentiviral particles were generated in HEK293T cells and supernatant containing lentiviral particles was used to infect PC3 cells. Transduced cells were selected with 2 µg/ml puromycin (Sigma-Aldrich, Hamburg, Germany). Individual clones from the PC3 *EVI1* knockdown cells were derived by limited dilution. Investigated were three single cell-derived clones containing EVI1 shRNA (sh*EVI1*#1_clone A/B/C) and two parental/bulk cultures transduced with either one shRNA (sh*EVI1*#1_bulk and sh*EVI1*#2_bulk). As a control, cells containing a non-coding shRNA were used.

Immunoblot analyses

Cells were disrupted in 1 × Lysis Buffer (Cell Signaling) supplemented with Protease/Phosphatase Inhibitor Cocktail (Thermo Fisher Scientific, Darmstadt, Germany). Total protein was precipitated and denatured in Laemmli buffer. Five to 15 µg of which were separated over 8–12% bis-acrylamide (BioRad, Hercules, CA, USA) gels by Disc-SDS–polyacrylamide gel electrophoresis and transferred onto polyvinylidene difluoride membrane (Amersham, GE Healthcare Life Sciences, Chalfont St. Giles, UK). Membranes were blocked with 10% w/v non-fat dry milk (Cell Signaling) diluted in TBS 0.1% Tween-20 (p1379, Sigma).

Antibodies and dilutions are listed in Supplementary Materials.

Quantitative real-time PCR

Total RNA was extracted using the RNeasy kit (Qiagen, Valencia, CA, USA). First-strand cDNA synthesis was performed using the iScript cDNA synthesis kit (BioRad). *EVI1* transcripts were detected by semi-quantitative real-time PCR using the *Power* SYBR Green PCR Master Mix (Life Technologies) with a LightCycler 480 II instrument (Roche, Mannheim, Germany). Primer sequences are listed in Supplementary Table 1 in Supplementary Materials. For each data point, triplicate samples were analyzed in parallel. Expression of *EVI1* mRNA was calculated using the $\Delta\Delta C_t$-method relative to the housekeeping genes *β-actin* or *GAPDH* ($n = 3$). Each experiment was repeated three times individually. For metastasis analysis, Qiagen RT^2 Profiler PCR Arrays (PAHS-028 and PAHS-128) and ViiA 7 real-time PCR System (Applied Biosystems, Waltham, MA, USA) were used according to the manufacturer's instructions.

© 2017 Macmillan Publishers Limited, part of Springer Nature.

Viability and proliferation assays

Viability was assessed using the MTT (3-(4,5-dimethylthiazol-2-yl)-2,5-diphenyltetrazolium bromide) cell proliferation kit (Roche) according to the manufacturer's instructions. After 72 h, cell proliferation was measured by detection of absorbance at 595 nm using the Epoch microplate spectrophotometer (BioTek, Bad Friedrichshall, Germany). Cell growth was displayed relatively to the 0 h value ($n = 3$). Cell proliferation was additionally monitored using the xCELLigence Real Time Cell Analyzer (Roche). Cells were plated in E-Plates 16 (ACEA Biosciences, San Diego, CA, USA). Cell density measurements were performed in duplicates with programmed signal detection every 15 min (up to a total of 120 h; $n = 3$). Data analysis was performed using the RTCA software version 1.2 (Roche). In addition, proliferation and viability were determined using WST-1 assays (Roche). Cells were plated in a 96-well tissue culture plate and treated up to 30 nM docetaxel for 3 days before the incubation with the WST-1 reagent for 1 h. A scanning multi-well spectrophotometer (enzyme-linked immunosorbent assay reader) was used for analysis at a wavelength of 450 nm.

Anchorage-independent cell growth

Cells (5×10^3) were suspended in 0.6% agarose (Thermo Fisher Scientific). Cells were plated in a six-well over a basal layer of 1% agarose and were overlaid with 2 ml of growth medium. After 4 weeks of incubation at 37 °C and 5% CO_2, colonies were visualized by crystal violet staining. Three random fields were captured in each quadrant. The number and size of colonies was measured using ImageJ.

Scratch assay

Cells were grown to confluent monolayers in six-well plates. To inhibit proliferation, cells were incubated with 10 µg/ml mitomycin C (Sigma-Aldrich) for 2 h. The cell monolayer was injured using a 200 µl pipette tip. Cells were washed with PBS to remove cell debris. Images were captured after 0 and 24 h.

Cell cycle analysis

Cell cycle analyses were performed using propidium iodide (Sigma-Aldrich) staining of cells fixed in 70% cold ethanol. Cell proliferation was investigated by incorporation of 5-ethynyl-2'-deoxyuridine as detailed in the manufacturer's protocol (Baseclick, Munich, Germany). Treated cells were positivity assayed by flow cytometry using a Fortessa analyser and Flowjo software (BD Biosciences, Heidelberg, Germany).

Annexin V/7AAD-apoptosis assay

Cells were stained with Annexin V/7AAD using the Annexin V Apoptosis Detection Kit (BD Pharmingen, San Diego, CA, USA) according to the manufacturer's instructions. Apoptotic cells were determined using the BD LSRFortessa analyzer. Analysis was performed using the FlowJo data analysis software (FlowJo, Ashland, OR, USA). Analysis of apoptotic cells includes both, early apoptotic (Annexin V-positive and 7AAD-negative) and dead cells (late apoptotic (Annexin V-positive and 7AAD-positive) plus necrotic cells (Annexin V-negative and 7AAD-positive). Cells were treated with different concentrations of docetaxel and/or ABT199 for 3 days prior Annexin V/7AAD staining.

Senescence assay

The Senescence β-Galactosidase Staining Kit (Cell Signaling) was used according to the manufacturer's instructions. Pictures were recorded at a total magnification of ×200.

Tumor sphere assay

Tumor sphere assays were carried out similar to previously described.[47] Cells (1250) were seeded in 24-well ultra-low attachment plates (Corning, Tewksbury, MA, USA) and the formation of tumor spheres quantified after 5 days of incubation by microscopic inspection for 5 days. Serial replating was performed as previously described.[47]

Zebrafish embryo xenografts

Animal experiments and zebrafish husbandry were approved by the 'Kantonales Veterinaeramt Basel-Stadt'. *EVI1* knockdown and corresponding control cells were labeled with the fluorescent CellTracker CM-DiI (Life Technologies) as previously described,[48,49] Tg(*flk1:eGFP*) zebrafish were maintained, collected, grown and staged in E3 medium at 28.5 °C according to standard protocols.[68] For xenotransplantation experiments, zebrafish embryos were anesthetized in 0.4% tricaine (Sigma-Aldrich) at 48 h post fertilization and 75-100 control or knockdown cells were microinjected into the vessel free area of the yolk. Embryos were incubated for 1 h at 28.5–29 °C for recovery and then screened for the presence of fluorescent human cancer cells in the yolk. Fish harboring red cells were incubated at 35 °C as described before.[69] Five days after transplantation, embryos were screened microscopically for tumor formation using a Zeiss LSM 710 confocal microscope and fluorescence intensity was calculated using Fiji software (http://fiji.sc/Fiji). For each experiment 75–100 cells per fish were transplanted and at least 5 fish for each condition were analyzed.

Statistical data analyses

Data from three or more independent biological replicates are shown with exception of real-time PCR and Array Data, where technical triplicates were analyzed. Mean values are presented and error bars used to indicate s.d. Significance was determined using Student's *t*-test and is indicated as follows: NS > 0.05, * < 0.05, ** < 0.01 and *** < 0.001.

Materials and methods used are available in detail in the Supplementary Section.

CONFLICT OF INTEREST

The authors declare no conflict of interest.

ACKNOWLEDGEMENTS

The study was supported by a grant from the German Research Foundation (Deutsche Forschungsgemeinschaft (PE 1179/11-1)) to SP, the Schweizer Nationalfonds to CL (310030_149735), the Rudolf-Becker-Foundation and the Wilhelm-Sander-Foundation (2011.077.2) to SP and the German Cancer Aid (Mildred-Scheel Doctoral Student Fellowship) to SH. We also acknowledge the TCGA Research Network for providing their cancer data sets.

AUTHOR CONTRIBUTIONS

AQ, SH, HW, CL and SP designed the study. AQ, SH, HW and TS performed the *in vitro* experiments. WV performed the immunohistochemistry stains. MK performed the *in vivo* zebrafish experiments. SA generated the docetaxel-resistant cell lines. SH performed the statistics. MD performed the cBioPortal analysis. AQ, SH, HW, MK, AvM, GK, SD, TS, JK, CL and SP analyzed and interpreted the data. AQ, SH, HW, CL and SP wrote the manuscript.

REFERENCES

1 Siegel RL, Miller KD, Jemal A. Cancer statistics, 2015. *Cancer J Clin* 2015; **65**: 5–29.
2 Fraser M, Berlin A, Bristow RG, van der Kwast T. Genomic, pathological, and clinical heterogeneity as drivers of personalized medicine in prostate cancer. *Urol Oncol* 2015; **33**: 85–94.
3 Beltran H, Rickman DS, Park K, Chae SS, Sboner A, MacDonald TY *et al.* Molecular characterization of neuroendocrine prostate cancer and identification of new drug targets. *Cancer Discov* 2011; **1**: 487–495.
4 De Marzo AM, Platz EA, Sutcliffe S, Xu J, Gronberg H, Drake CG *et al.* Inflammation in prostate carcinogenesis. *Nat Rev Cancer* 2007; **7**: 256–269.
5 Mosquera JM, Beltran H, Park K, MacDonald TY, Robinson BD, Tagawa ST *et al.* Concurrent AURKA and MYCN gene amplifications are harbingers of lethal treatment-related neuroendocrine prostate cancer. *Neoplasia* 2013; **15**: 1–10.
6 Sethi S, Kong D, Land S, Dyson G, Sakr WA, Sarkar FH. Comprehensive molecular oncogenomic profiling and miRNA analysis of prostate cancer. *Am J Transl Res* 2013; **5**: 200–211.
7 Perner S, Demichelis F, Beroukhim R, Schmidt FH, Mosquera JM, Setlur S *et al.* TMPRSS2:ERG fusion-associated deletions provide insight into the heterogeneity of prostate cancer. *Cancer Res* 2006; **66**: 8337–8341.
8 Mosquera JM, Perner S, Demichelis F, Kim R, Hofer MD, Mertz KD *et al.* Morphological features of TMPRSS2-ERG gene fusion prostate cancer. *J Pathol* 2007; **212**: 91–101.
9 Pflueger D, Rickman DS, Sboner A, Perner S, LaFargue CJ, Svensson MA *et al.* N-myc downstream regulated gene 1 (NDRG1) is fused to ERG in prostate cancer. *Neoplasia* 2009; **11**: 804–811.

© 2017 Macmillan Publishers Limited, part of Springer Nature.

10 Tomlins SA, Rhodes DR, Perner S, Dhanasekaran SM, Mehra R, Sun XW *et al.* Recurrent fusion of TMPRSS2 and ETS transcription factor genes in prostate cancer. *Science* 2005; **310**: 644–648.
11 Barjesteh van Waalwijk, van Doorn-Khosrovani S, Erpelinck C, van Putten WL, Valk PJ, van der Poel-van de Luytgaarde S, Hack R *et al.* High EVI1 expression predicts poor survival in acute myeloid leukemia: a study of 319 de novo AML patients. *Blood* 2003; **101**: 837–845.
12 Sattler HP, Lensch R, Rohde V, Zimmer E, Meese E, Bonkhoff H *et al.* Novel amplification unit at chromosome 3q25-q27 in human prostate cancer. *Prostate* 2000; **45**: 207–215.
13 Goyama S, Kurokawa M. Evi-1 as a critical regulator of leukemic cells. *Int J Hematol* 2010; **91**: 753–757.
14 Kataoka K, Kurokawa M. Ecotropic viral integration site 1, stem cell self-renewal and leukemogenesis. *Cancer Sci* 2012; **103**: 1371–1377.
15 Konantz M, Andre MC, Ebinger M, Grauer M, Wang H, Grzywna S *et al.* EVI-1 modulates leukemogenic potential and apoptosis sensitivity in human acute lymphoblastic leukemia. *Leukemia* 2013; **27**: 56–65.
16 Mucenski ML, Taylor BA, Ihle JN, Hartley JW, Morse HC 3rd, Jenkins NA *et al.* Identification of a common ecotropic viral integration site, Evi-1, in the DNA of AKXD murine myeloid tumors. *Mol Cell Biol* 1988; **8**: 301–308.
17 Wieser R. The oncogene and developmental regulator EVI1: expression, biochemical properties, and biological functions. *Gene* 2007; **396**: 346–357.
18 Deng X, Cao Y, Liu Y, Li F, Sambandam K, Rajaraman S *et al.* Overexpression of Evi-1 oncoprotein represses TGF-beta signaling in colorectal cancer. *Mol Carcinogenesis* 2013; **52**: 255–264.
19 Dutta P, Bui T, Bauckman KA, Keyomarsi K, Mills GB, Nanjundan M. EVI1 splice variants modulate functional responses in ovarian cancer cells. *Mol Oncol* 2013; **7**: 647–668.
20 Nayak KB, Kuila N, Das Mohapatra A, Panda AK, Chakraborty S. EVI1 targets DeltaNp63 and upregulates the cyclin dependent kinase inhibitor p21 independent of p53 to delay cell cycle progression and cell proliferation in colon cancer cells. *Int J Biochem Cell Biol* 2013; **45**: 1568–1576.
21 Patel JB, Appaiah HN, Burnett RM, Bhat-Nakshatri P, Wang G, Mehta R *et al.* Control of EVI-1 oncogene expression in metastatic breast cancer cells through microRNA miR-22. *Oncogene* 2011; **30**: 1290–1301.
22 Bard-Chapeau EA, Jeyakani J, Kok CH, Muller J, Chua BQ, Gunaratne J *et al.* Ecotopic viral integration site 1 (EVI1) regulates multiple cellular processes important for cancer and is a synergistic partner for FOS protein in invasive tumors. *Proc Natl Acad Sci USA* 2012; **109**: 2168–2173.
23 Aytekin M, Vinatzer U, Musteanu M, Raynaud S, Wieser R. Regulation of the expression of the oncogene EVI1 through the use of alternative mRNA 5′-ends. *Gene* 2005; **356**: 160–168.
24 Brooks DJ, Woodward S, Thompson FH, Dos Santos B, Russell M, Yang JM *et al.* Expression of the zinc finger gene EVI-1 in ovarian and other cancers. *Br J Cancer* 1996; **74**: 1518–1525.
25 Yu Z, Pestell TG, Lisanti MP, Pestell RG. Cancer stem cells. *Int J Biochem Cell Biol* 2012; **44**: 2144–2151.
26 Chen X, Rycaj K, Liu X, Tang DG. New insights into prostate cancer stem cells. *Cell Cycle* 2013; **12**: 579–586.
27 van Leenders GJ, Schalken JA. Stem cell differentiation within the human prostate epithelium: implications for prostate carcinogenesis. *BJU Int* 2001; **88**: 35–42 discussion 49–50.
28 Volkert S, Schnittger S, Zenger M, Kern W, Haferlach T, Haferlach C. Amplification of EVI1 on cytogenetically cryptic double minutes as new mechanism for increased expression of EVI1. *Cancer Genet* 2014; **207**: 103–108.
29 Cerami E, Gao J, Dogrusoz U, Gross BE, Sumer SO, Aksoy BA *et al.* The cBio cancer genomics portal: an open platform for exploring multidimensional cancer genomics data. *Cancer Discov* 2012; **2**: 401–404.
30 Gao J, Aksoy BA, Dogrusoz U, Dresdner G, Gross B, Sumer SO *et al.* Integrative analysis of complex cancer genomics and clinical profiles using the cBioPortal. *Sci Signal* 2013; **6**: pl1.
31 Baca SC, Prandi D, Lawrence MS, Mosquera JM, Romanel A, Drier Y *et al.* Punctuated evolution of prostate cancer genomes. *Cell* 2013; **153**: 666–677.
32 Barbieri CE, Baca SC, Lawrence MS, Demichelis F, Blattner M, Theurillat JP *et al.* Exome sequencing identifies recurrent SPOP, FOXA1 and MED12 mutations in prostate cancer. *Nat Genet* 2012; **44**: 685–689.
33 Cancer Genome Atlas Research N, The molecular taxonomy of primary prostate cancer. *Cell* 2015; **163**: 1011–1025.
34 Gao D, Vela I, Sboner A, Iaquinta PJ, Karthaus WR, Gopalan A *et al.* Organoid cultures derived from patients with advanced prostate cancer. *Cell* 2014; **159**: 176–187.
35 Grasso CS, Wu YM, Robinson DR, Cao X, Dhanasekaran SM, Khan AP *et al.* The mutational landscape of lethal castration-resistant prostate cancer. *Nature* 2012; **487**: 239–243.
36 Hieronymus H, Schultz N, Gopalan A, Carver BS, Chang MT, Xiao Y *et al.* Copy number alteration burden predicts prostate cancer relapse. *Proc Natl Acad Sci USA* 2014; **111**: 11139–11144.
37 Kumar A, Coleman I, Morrissey C, Zhang X, True LD, Gulati R *et al.* Substantial interindividual and limited intraindividual genomic diversity among tumors from men with metastatic prostate cancer. *Nat Med* 2016; **22**: 369–378.
38 Robinson D, Van Allen EM, Wu YM, Schultz N, Lonigro RJ, Mosquera JM *et al.* Integrative clinical genomics of advanced prostate cancer. *Cell* 2015; **161**: 1215–1228.
39 Taylor BS, Schultz N, Hieronymus H, Gopalan A, Xiao Y, Carver BS *et al.* Integrative genomic profiling of human prostate cancer. *Cancer Cell* 2010; **18**: 11–22.
40 Kaighn ME, Narayan KS, Ohnuki Y, Lechner JF, Jones LW. Establishment and characterization of a human prostatic carcinoma cell line (PC-3). *Invest Urol* 1979; **17**: 16–23.
41 Pedrali-Noy G, Spadari S, Miller-Faures A, Miller AO, Kruppa J, Koch G. Synchronization of HeLa cell cultures by inhibition of DNA polymerase alpha with aphidicolin. *Nucleic Acids Res* 1980; **8**: 377–387.
42 Kurokawa M, Mitani K, Irie K, Matsuyama T, Takahashi T, Chiba S *et al.* The oncoprotein Evi-1 represses TGF-beta signalling by inhibiting Smad3. *Nature* 1998; **394**: 92–96.
43 Pardali K, Kowanetz M, Heldin CH, Moustakas A. Smad pathway-specific transcriptional regulation of the cell cycle inhibitor p21(WAF1/Cip1). *J Cell Physiol* 2005; **204**: 260–272.
44 Liu Y, Chen L, Ko TC, Fields AP, Thompson EA. Evi1 is a survival factor which conveys resistance to both TGFbeta- and taxol-mediated cell death via PI3K/AKT. *Oncogene* 2006; **25**: 3565–3575.
45 Bareiss PM, Paczulla A, Wang H, Schairer R, Wiehr S, Kohlhofer U *et al.* SOX2 expression associates with stem cell state in human ovarian carcinoma. *Cancer Res* 2013; **73**: 5544–5555.
46 Fan X, Liu S, Su F, Pan Q, Lin T. Effective enrichment of prostate cancer stem cells from spheres in a suspension culture system. *Urol Oncol* 2012; **30**: 314–318.
47 Wang H, Paczulla A, Lengerke C. Evaluation of stem cell properties in human ovarian carcinoma cells using multi and single cell-based spheres assays. *J Vis Exp* 2015; **95**: e52259.
48 Konantz M, Balci TB, Hartwig UF, Dellaire G, Andre MC, Berman JN *et al.* Zebrafish xenografts as a tool for in vivo studies on human cancer. *Ann N Y Acad Sci* 2012; **1266**: 124–137.
49 Schaefer T, Wang H, Mir P, Konantz M, Pereboom TC, Paczulla AM *et al.* Molecular and functional interactions between AKT and SOX2 in breast carcinoma. *Oncotarget* 2015; **6**: 43540–43556.
50 Souers AJ, Leverson JD, Boghaert ER, Ackler SL, Catron ND, Chen J *et al.* ABT-199, a potent and selective BCL-2 inhibitor, achieves antitumor activity while sparing platelets. *Nat Med* 2013; **19**: 202–208.
51 Nanjundan M, Nakayama Y, Cheng KW, Lahad J, Liu J, Lu K *et al.* Amplification of MDS1/EVI1 and EVI1, located in the 3q26.2 amplicon, is associated with favorable patient prognosis in ovarian cancer. *Cancer Res* 2007; **67**: 3074–3084.
52 Tanaka M, Suzuki HI, Shibahara J, Kunita A, Isagawa T, Yoshimi A *et al.* EVI1 oncogene promotes KRAS pathway through suppression of microRNA-96 in pancreatic carcinogenesis. *Oncogene* 2014; **33**: 2454–2463.
53 Nwachukwu JC, Mita P, Ruoff R, Ha S, Wang Q, Huang SJ *et al.* Genome-wide impact of androgen receptor trapped clone-27 loss on androgen-regulated transcription in prostate cancer cells. *Cancer Res* 2009; **69**: 3140–3147.
54 Taneja SS, Ha S, Swenson NK, Torra IP, Rome S, Walden PD *et al.* ART-27, an androgen receptor coactivator regulated in prostate development and cancer. *J Biol Chem* 2004; **279**: 13944–13952.
55 McGilvray R, Walker M, Bartholomew C. UXT interacts with the transcriptional repressor protein EVI1 and suppresses cell transformation. *FEBS J* 2007; **274**: 3960–3971.
56 Rosa-Ribeiro R, Nishan U, Vidal RO, Barbosa GO, Reis LO, Cesar CL *et al.* Transcription factors involved in prostate gland adaptation to androgen deprivation. *PLoS ONE* 2014; **9**: e97080.
57 Kerr CL, Hussain A. Regulators of prostate cancer stem cells. *Cuee Opin Oncol* 2014; **26**: 328–333.
58 Li P, Yang R, Gao WQ. Contributions of epithelial-mesenchymal transition and cancer stem cells to the development of castration resistance of prostate cancer. *Mol Cancer* 2014; **13**: 55.
59 Tu SM, Lin SH. Prostate cancer stem cells. *Clin Genitourinary Cancer* 2012; **10**: 69–76.
60 Schroeder A, Herrmann A, Cherryholmes G, Kowolik C, Buettner R, Pal S *et al.* Loss of androgen receptor expression promotes a stem-like cell phenotype in prostate cancer through STAT3 signaling. *Cancer Res* 2014; **74**: 1227–1237.
61 Kregel S, Kiriluk KJ, Rosen AM, Cai Y, Reyes EE, Otto KB *et al.* Sox2 is an androgen receptor-repressed gene that promotes castration-resistant prostate cancer. *PLoS ONE* 2013; **8**: e53701.

© 2017 Macmillan Publishers Limited, part of Springer Nature.

62 Han L, Shi S, Gong T, Zhang Z, Sun X. Cancer stem cells: therapeutic implications and perspectives in cancer therapy. *Acta Pharma Sin B* 2013; **3**: 65–75.
63 Zhang B, Shimada Y, Kuroyanagi J, Nishimura Y, Umemoto N, Nomoto T *et al.* Zebrafish xenotransplantation model for cancer stem-like cell study and high-throughput screening of inhibitors. *Tumour Biol* 2014; **35**: 11861–11869.
64 Kustikova OS, Schwarzer A, Stahlhut M, Brugman MH, Neumann T, Yang M *et al.* Activation of Evi1 inhibits cell cycle progression and differentiation of hematopoietic progenitor cells. *Leukemia* 2013; **27**: 1127–1138.
65 Shackelford D, Kenific C, Blusztajn A, Waxman S, Ren R. Targeted degradation of the AML1/MDS1/EVI1 oncoprotein by arsenic trioxide. *Cancer Res* 2006; **66**: 11360–11369.
66 Scheble VJ, Braun M, Beroukhim R, Mermel CH, Ruiz C, Wilbertz T *et al.* ERG rearrangement is specific to prostate cancer and does not occur in any other common tumor. *Mod Pathol* 2010; **23**: 1061–1067.
67 Braun M, Goltz D, Shaikhibrahim Z, Vogel W, Bohm D, Scheble V *et al.* ERG protein expression and genomic rearrangement status in primary and metastatic prostate cancer--a comparative study of two monoclonal antibodies. *Prostate Cancer Prostatic Dis* 2012; **15**: 165–169.
68 Choi J, Dong L, Ahn J, Dao D, Hammerschmidt M, Chen JN. FoxH1 negatively modulates flk1 gene expression and vascular formation in zebrafish. *Dev Biol* 2007; **304**: 735–744.
69 Haldi M, Ton C, Seng WL, McGrath P. Human melanoma cells transplanted into zebrafish proliferate, migrate, produce melanin, form masses and stimulate angiogenesis in zebrafish. *Angiogenesis* 2006; **9**: 139–151.

Supplementary Information accompanies this paper on the Oncogene website (http://www.nature.com/onc)

© 2017 Macmillan Publishers Limited, part of Springer Nature.

Supplementary Materials and Methods and Figure Legends

Supplementary Material and Methods

Fluorescence *in situ* hybridization (FISH)

FISH experiments were performed as described before.[1] Briefly, differential digoxigenin- or biotin-labeled BAC clones flanking the gene were utilized as probes to detect translocations or amplification of *EVI1*. All samples were independently analyzed by three evaluators (AQ, SH, SP) under a 63x oil immersion objective with a fluorescence microscope (Zeiss, Jena, Germany). A sample was considered translocated or amplified if at least 20% of nuclei displayed a translocation or amplification.

Data analysis using the c-BioPortal

The c-BioPortal, which was developed at Memorial Sloan-Kettering Cancer Center (http://cbioportal.org) provides the possibility of analyzing cancer genomic data online.[2,3] Commonly accessible PCa patient data sets of the cBioportal database were used to analyze the percentage of EVI1 CNVs in PCa. Furthermore, we investigated the co-occurrence between EVI1 and selected stem cell marker genes (*SOX2, CD44, PROM1*) as well as key regulators described in PCa carcinogenesis (*AR, PTEN, ERG, TP53, SPOP*).

Antibodies and Dilutions

Primary antibodies (all by Cell Signaling Technologies) and 1:1000 dilution was used: EVI1 (#2593 (C50E12), 1:1000), BCL2 (#2870), p15 (#4822), p18 (#2896,), p21 (#2947), p27 (#3688), CDK2 (#2546), CDK4 (#2906), CDK6 (#3136), Cyclin D1 (#2926), Cyclin D3 (#2936), Cyclin E (#4129), ERK (#4695), p-ERK (#4377 (197G2)), AKT (#9272), p-AKT (#4058), SMAD3 (#9523) or β-actin (1:5000, mouse

monoclonal, A1978, Sigma-Aldrich). HRP-linked secondary antibodies goat anti-rabbit (1:5000, Cell Signaling Technologies) or goat anti-mouse (1:5000, Santa Cruz Biotechnology, Santa Cruz, CA) were used.

Primer for real-time PCR

Table 1

Gen name	Forward sequence	Reverse sequence
EVI1	ACCCACTCCTTTCTTTATGGACC	TGATCAGCCAGTTGGAATTGTG
SMAD3	GTCTGCAAGATCCCACCAG	GTGCACATTCGGGTCAACT
P21	TGGACCTGTCACTGTCTTGT	TCCTGTGGGCGGATTAG
P27	CCGGCTAACTCTGAGGACAC	AGAAGAATCGTCGGTTGCAG
cyclinD1	CCTCGGTGTCCTACTTCAAATG	GCGGTCCAGGTAGTTCATG
cyclinD3	CATCCATGATCGCCACGG	CTTCGATCTGCTCCTGACAG
cyclinE	ACAGTTGGATTTGCTGGAC	TCTGCTTCTTACCGCTCTGTG
BCL2	ACAGAGGATCATGCTGTACTTAAAAA	TTATTTCATGAGGCACGTTATTATTAG
BCLxL	QIAGEN QUANTITECT PRIMER ASSAY QT00236712	
BIK	QIAGEN QUANTITECT PRIMER ASSAY QT00070777	
BAX	QIAGEN QUANTITECT PRIMER ASSAY QT00031192	
BMF	GAGACTCTCTCCTGGAGTCACC	CTGGTTGGAACACATCATCCT
SOX2	AAGACGCTCATGAAGAAGGATAA	ACTGTCCATGCGCTGGTT
PROM1	ACAGGGAATGGATTGTTGGA	CTCCCATACTTCTTAGTTTCCTCAA
GAPDH	CTGACTTCAACAGCGACACC	TAGCCAAATTCGTTGTCATACC

Supplementary Figure legends

Supplementary Figure 1: Determination of the EVI1 amplification status as well as co-occurrence with stem cell markers and genes involved in PCa oncogenesis. (**a**) The EVI1 gene locus is neither re-arranged nor amplified in PCa patient samples, as analyzed by FISH using digitoxin- and biotin-labled BAC clones flanking the gene. Shown is a representative single cell derived from the analysis of one CRPC patient sample. (**b**) Cross-cancer alteration summary for MECOM (EVI1) within the indicated PCa patient cohorts using the cBioPortal analysis tool. Shown are the percentages of CNV in the different PCa cohorts provided at the cBioPortal. Red: copy number gain, blue: copy number loss. (**c**) Oncoprint data represents PCa samples from one published set (TCGA, Cell, 2015; n=333 patient samples). Shown are only these 7% of patients that demonstrate a genetic alteration of MECOM including not only CNV (amplification or deletion) but also mutations or mRNA up-regulation of the EVI1 gene. (**d**) Table indicating co-occurrent alterations of *EVI1* with stem cell specific genes (*SOX2, CD44, PROM1*) or genes implicated in PCa progression (ERG, STOP,TP53) using cBioPortal (TCGA, Cell, 2015). (**e**) Expression changes of *EVI1* (left) and stem cell factors *SOX2* and *PROM1* in docetaxel-resistant PC3 cells treated with two independent EVI1 shRNAs relative to control treated cells.

Supplementary Figure 2: Verification of stable endogenous EVI1 expression in PC3 cells. (**a**) Quantitative real-time PCR and (**b**) corresponding immunoblot analysis documenting superior endogenous EVI1 mRNA and protein expression, respectively, in PC3 cells over three other PCa cell lines investigated.

Supplementary Figure 3: Perturbed cell cycle regulation in EVI1 knockdown PC3 cells. ShEVI1 and control shRNA treated PC3 cells were analyzed for (**a**) cell cycle phase distribution as deduced from PI staining and (**b**) steady-state protein expression of key cell cycle mediators as investigated by immunoblot.

Supplementary Figure 4: Knockdown of EVI1 expression affects various factors implicated in cell mobility and/or tumor metastasis. (**a/b**) Hit list of potential EVI1 downstream targets whose expression was significantly ($p<0.05$) altered with an expression factor change of >2-fold in shEVI1#2 mix vs. sh control PC3 cells, as uncover by RT profiler PCR array analysis (Qiagen). Listed are EVI1 target genes implicated in (**a**) cell mobility and (**b**) tumor metastasis. Up-regulated genes (top panels), down-regulated factors (bottom panels). (**c**) Intersection charts illustrating individual target gene numbers as identified in either shEVI1#2 mix (blue), shEVI1#1 clone B (orange), or shEVI1#1 clone C (green) PC3 cells. Up-regulated candidate genes (left) vs. down-regulated genes (right). Conserved candidates significantly identified in all three data sets (5 up- and 3 down-regulated in response to EVI1 knockdown, see intersection) are indicated by name.

Supplementary Figure 5: EVI1 influences cell viability and apoptosis induction also in non-resistant PC3 cells. **(a**) AnnexinV staining of shEVI1 and shCTRL treated PC3 cells reveals aggravated spontaneous apoptosis levels upon EVI1 knockdown. (**b**) Knockdown of EVI1 expression likewise enhances induced apoptosis rates as triggered with either 5 or 30 nM of docetaxel. (**c**) Knockdown of EVI expression in PC3 cells with either one of two shRNAs co-depletes the anti-apoptosis factor BCL2 as investigated by qRT-PCR. (**d**) Immunoblot of BCL2 expression in non-resistant PC3 cells and docetaxel-resistant PC3 cells after docetaxel treatment (**e**) Co-treatment with docetaxel and BCL2-inhibitor ABT-199 dose-dependently impairs cell viability in PC3 wild-type cells (non-resistant, left). (**f**) Inhibition of BCL2 activity dose-dependently re-sensitized formerly drug-resistant PC3 cells to treatment with docetaxel**.**

References

1. Braun M, Scheble VJ, Menon R, Scharf G, Wilbertz T, Petersen K*, et al.* Relevance of cohort design for studying the frequency of the ERG rearrangement in prostate cancer. *Histopathology* 2011; **58**:1028-1036.

2. Cerami E, Gao J, Dogrusoz U, Gross BE, Sumer SO, Aksoy BA*, et al.* The cBio cancer genomics portal: an open platform for exploring multidimensional cancer genomics data. *Cancer discovery* 2012; **2**:401-404.

3. Gao J, Aksoy BA, Dogrusoz U, Dresdner G, Gross B, Sumer SO*, et al.* Integrative analysis of complex cancer genomics and clinical profiles using the cBioPortal. *Science signaling* 2013; **6**:pl1.

Supplementary Figure 1

a

EVI1 FISH analysis in metastasis

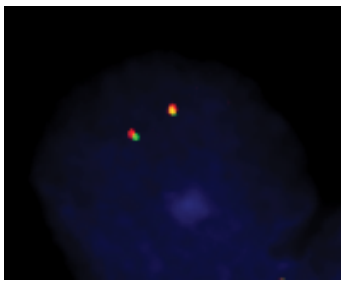

b

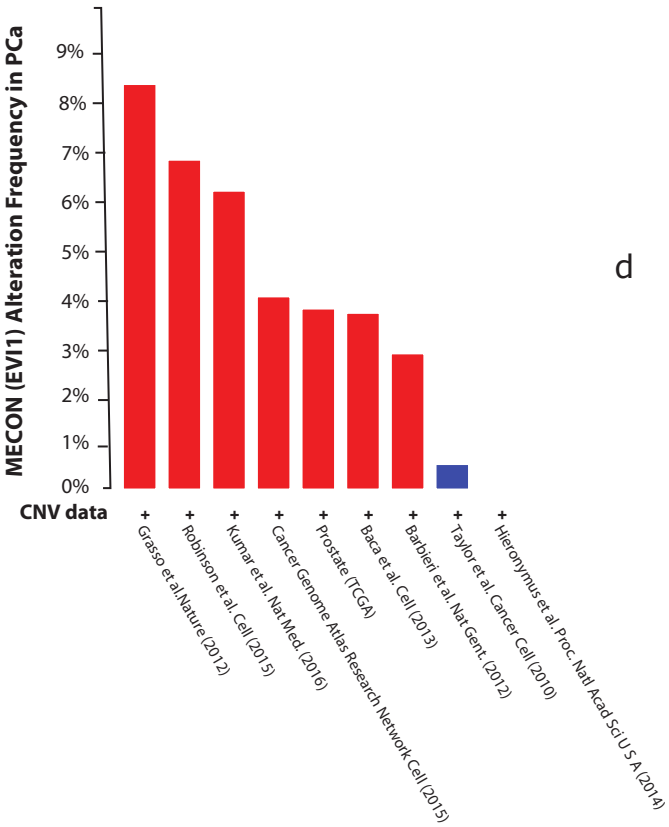

c

Prostate Adenocarcinoma (TCGA, Cell 2015)

All Tumors (333 samples/9 Genes)

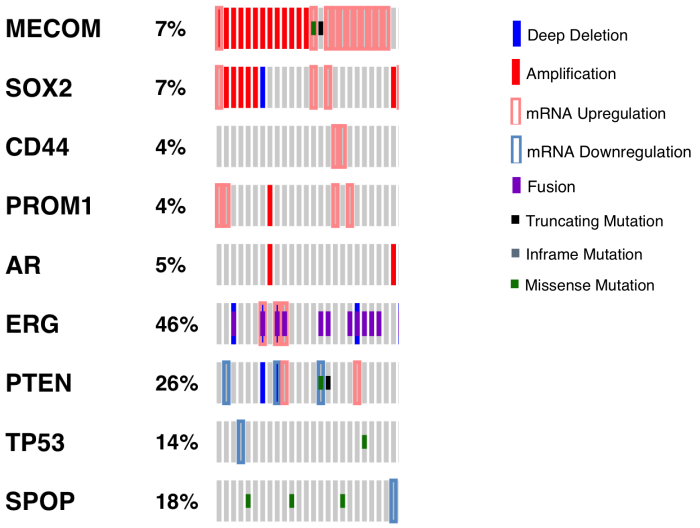

d

Prostate Adenocarcinoma (333 samples) TCGA, Cell 2015				
Gene A	**Gene B**	**p-Value**	**Log Odds Ratio**	**Association**
MECOM	SOX2	<0.001	2.465	Significant co-occurrence
MECOM	PROM1	0.001	2.293	Significant co-occurence
MECOM	CD44	0.239	0.901	Tendency towards co-occurrence
MECOM	TP53	0.312	-0.629	Tendency towards mutual exclusivity
MECOM	SPOP	0.355	-0.438	Tendency towards mutual exclusivity
MECOM	PTEN	0.415	0.198	Tendency towards co-occurrence
MECOM	ERG	0.569	-0.018	Tendency towards mutual exclusivity
MECOM	AR	0.622	-0.292	Tendency towards mutual exclusivity

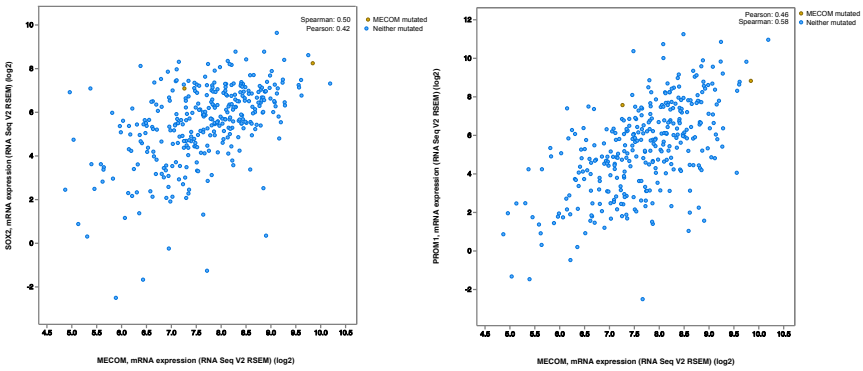

e

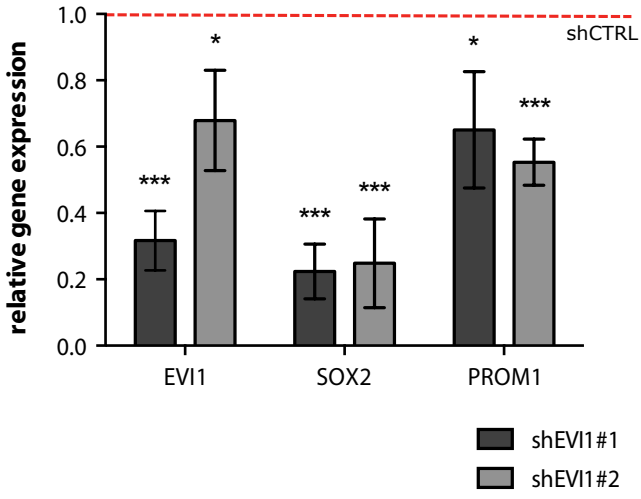

Supplementary Figure 2

a

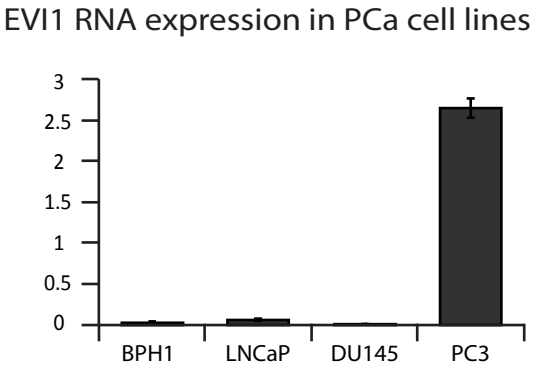

b

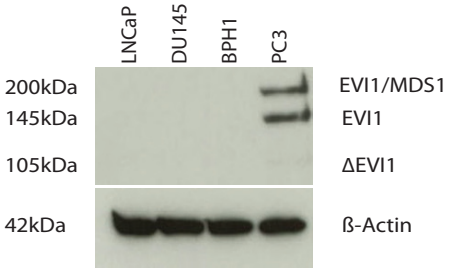

Supplementary Figure 3

a

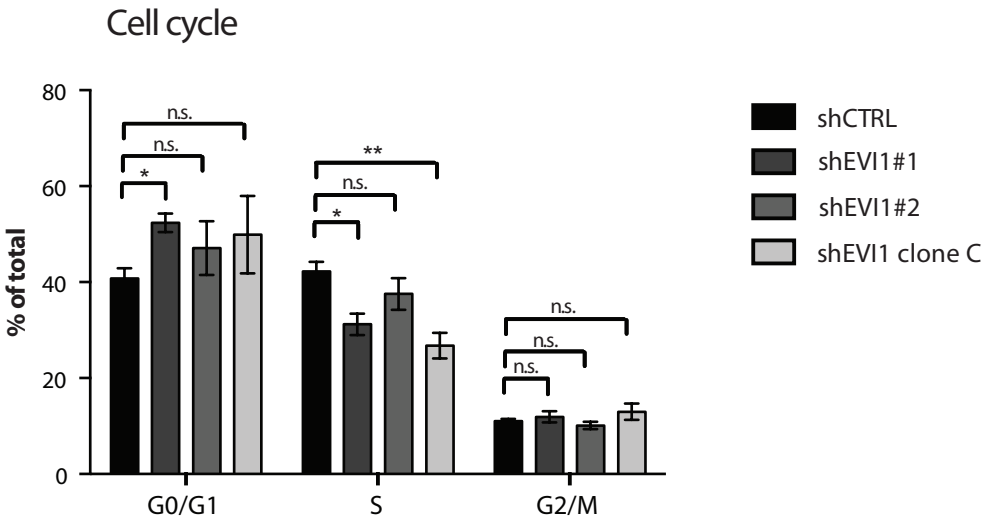

b

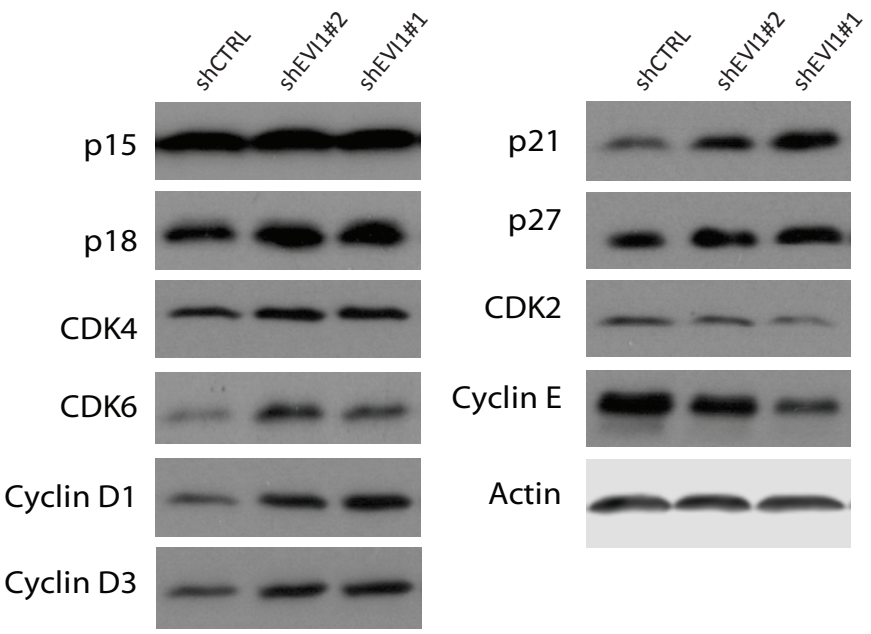

Supplementary Figure 4

a

Cell mobility array
Up-regulated

Gene Symbol	Fold Regulation	p-Value
PTEN	39.83	0.003279
ITGA4	21.95	0.034576
STAT3	18.89	0.000151
WIPF1	18.67	0.000084
CSF1	14.34	0.000077
PAK1	5.31	0.000471
ITGB2	4.99	0.000967
EGF	4.08	0.023085
RHOB	4.06	0.000808
PLAUR	3.91	0.009075
MYLK	3.80	0.001309
MYH10	3.75	0.000001
MYL9	3.70	0.000011
PTK2B	3.03	0.003410
PAK4	2.78	0.002142
VEGFA	2.75	0.000162
ARHGEF7	2.33	0.011418
CRK	2.31	0.003377
BAIAP2	2.16	0.000917
IGF1R	2.07	0.009893

Down-regulated

Gene Symbol	Fold Regulation	p-Value
MMP14	-41.35	0.000296
DPP4	-35.66	0.000000
ITGB3	-9.37	0.000067
SRC	-5.62	0.000547
RAC2	-5.27	0.000005
PLCG1	-4.40	0.000016
RASA1	-3.93	0.000352
VCL	-2.28	0.003769
RHOC	-2.27	0.001263
ACTN1	-2.18	0.000046
CDC42	-2.06	0.009924

b

Tumor metastasis array
Up-regulated

Gene Symbol	Fold Regulation	p-Value
CD82	37.95	0.000005
CTNNA1	36.13	0.000000
FLT4	33.82	0.000009
PTEN	27.83	0.000124
MCAM	15.34	0.000027
TP53	14.93	0.000247
MTSS1	14.25	0.000066
KRAS	9.22	0.000005
CXCR4	6.14	0.000113
ITGA7	5.82	0.000179
KISS1R	4.79	0.003463
CTSL	4.29	0.000043
KISS1	4.19	0.037403
PLAUR	4.01	0.000367
MMP11	3.62	0.000050
COL4A2	3.23	0.000037
CDKN2A	2.88	0.000000
NR4A3	2.80	0.000366
VEGFA	2.69	0.000181
CST7	2.39	0.011732
SMAD2	2.28	0.002418
CTSK	2.14	0.024971

Down-regulated

Gene Symbol	Fold Regulation	p-Value
IL1B	-426.38	0.000000
CDH11	-155.27	0.000044
FN1	-48.76	0.000005
EPHB2	-20.80	0.000160
ITGB3	-8.79	0.000000
CDH1	-6.21	0.011771
MMP10	-4.95	0.010969
FAT1	-4.90	0.000776
SRC	-4.42	0.003105
MMP13	-4.41	0.000709
SERPINE1	-4.14	0.000004

c

Up-regulated

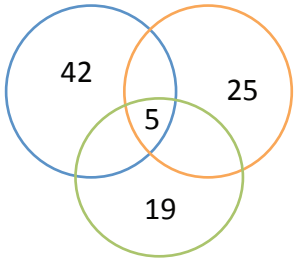

CRK
ITGB2
CD82
KISS1
MTSS1

Down-regulated

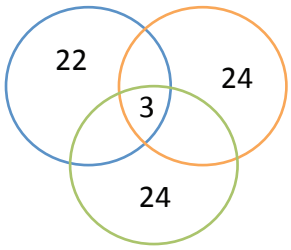

IL1B
ITGB3
EPHB2

Supplementary Figure 5

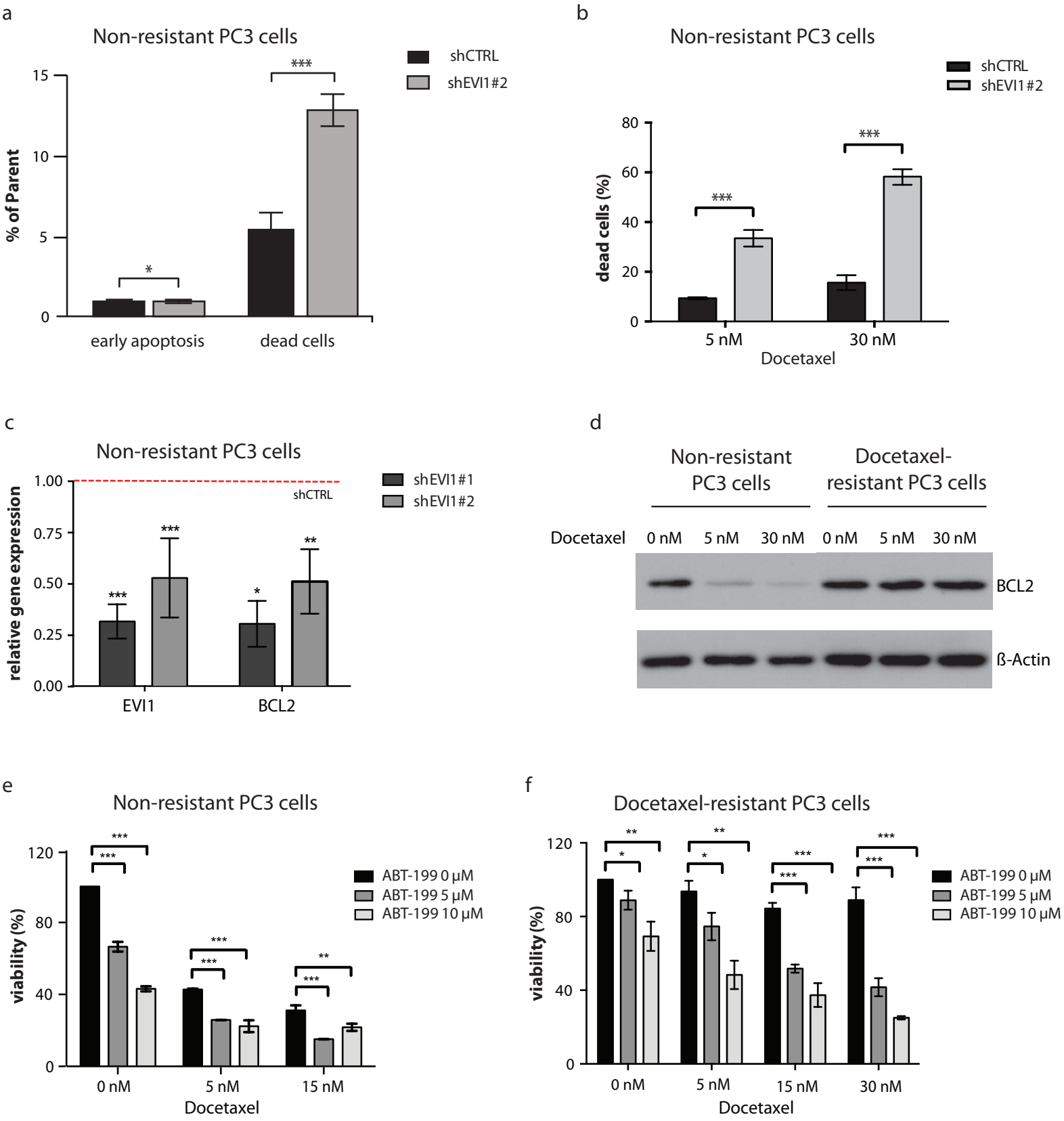

Paper V

In Vitro Tumorigenic Assay: The Tumor Spheres Assay.

Wang H, Paczulla AM, Konantz M, Lengerke C.

Methods Mol Biol. 2018;1692:77-87.

Chapter 7

In Vitro Tumorigenic Assay: The Tumor Spheres Assay

Hui Wang, Anna M. Paczulla, Martina Konantz, and Claudia Lengerke

Abstract

Cancer stem cells (CSCs) are a subpopulation of cells within cancer tissues that are thought to mediate tumor initiation. CSCs are furthermore considered the cause of tumor progression and recurrence after conventional therapies, based on their enhanced therapy resistance properties. A method commonly used to assess CSC potential in vitro is the so-called tumor spheres assay in which cells are plated under non-adherent culture conditions in serum-free medium supplemented with growth factors. Tumor spheres assays have been used in cancer research as an intermediate in vitro cell culture model to be explored before performing more laborious in vivo tumor xenograft assays.

Key words Cancer stem cell, Tumor spheres assay, In vitro

1 Introduction

Years of research indicate pronounced cellular heterogeneity within individual tumor samples, with only a subpopulation of tumor cells—the CSCs—being able to both self-renew and differentiate giving rise to more differentiated tumor cell types. Given this definition, putative CSC populations need to be analyzed in functional assays. In the past two decades, the identification of CSCs able to establish tumors following experimental implantation in immunosuppressed murine hosts [1] (versus non-tumorigenic non-CSC tumor cells derived from the same sample) brought CSCs to the spotlight in cancer research.

The tumor spheres assay has been developed as an in vitro surrogate method to study CSC potential, next to the more time-consuming and laborious in vivo tumorigenicity assays. When cultured under certain conditions (with low nutrients but specific growth factor exposure) and in a suspension environment, CSCs can survive and clonally expand building so-called tumor spheres, whereas non-CSCs undergo programmed cell death presumably due to anchorage loss to substrates from the surrounding extracellular matrix [2]. Of note, while tumor spheres are enriched for

Gianpaolo Papaccio and Vincenzo Desiderio (eds.), *Cancer Stem Cells: Methods and Protocols*, Methods in Molecular Biology, vol. 1692, DOI 10.1007/978-1-4939-7401-6_7, © Springer Science+Business Media LLC 2018

CSCs, these also contain more differentiated tumor cells that emerge from CSCs. Tumor spheres assays are reported to enrich CSCs from bulk cells in various types of cancers and are here widely used to analyze self-renewal.

Spheres assays allowing quantification and characterization of floating spherical aggregates were first developed in the neural system, where healthy neural stem cells were demonstrated to undergo clonal expansion and form neurospheres on a single-cell basis under specific culture conditions [3, 4]. Shortly after, free-floating sphere cultures were reported to identify brain tumor CSCs [5]. Dontu and colleagues later adapted and confirmed the suitability of this assay for the evaluation of stem cells in healthy and malignant breast tissues [6, 7]. Human mammary epithelial cells plated in different numbers in serum-free medium supplemented with epidermal growth factor (EGF), basic fibroblast growth factor (bFGF), B-27, and heparin were cultured under non-adherent conditions for 7–14 days before sphere formation was scored microscopically. Following this protocol with some adjustments in cell numbers, growth medium, and supplements, several groups have explored in vitro stem cell potential from several cancer types such as breast [8, 9], brain [10], ovarian [11, 12], pancreas [13], colon [14], and prostate carcinoma [15].

Traditionally, spheres assays are performed by plating multiple cells per well, and thus, as we and others have shown, are easily influenced by cell density [12]. Single cell-based sphere formation assays are an attractive alternative to identify CSCs. Figure 1 shows schematic experimental steps for single cell-based spheres assays.

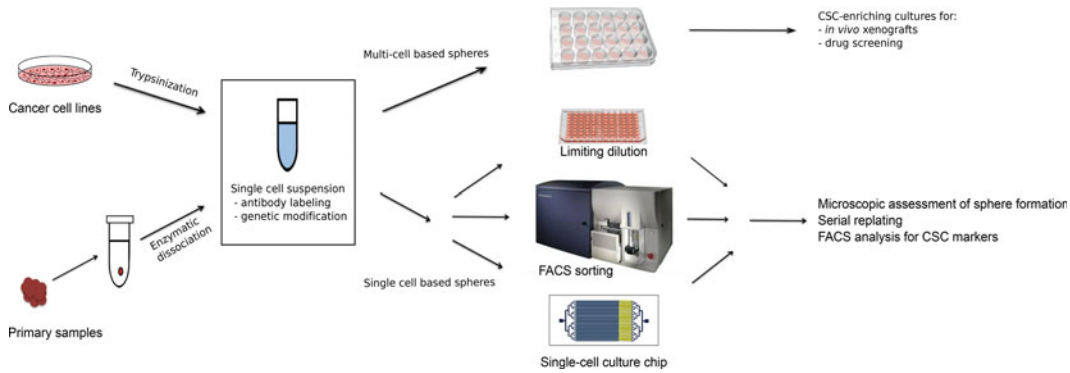

Fig. 1 Workflow of tumor spheres assay. After cell preparation (stem cell marker positive) tumor cells are sorted by FACS into individual wells of a 96-well plate in spheres medium; alternatively, suitable cell populations are plated into individual wells or through a single-cell chip. For multi cell-based spheres assays, 100–1000 cells are placed into one well. Plating efficiency is assessed by microscopy performed after sorting or plating. Spheres were scored by microscopy after 1–2 weeks, then dissociated into single cells and if applicable analyzed for surface expression of CSC markers via flow cytometry. At this stage, collected cells can be also replated into secondary spheres assays or used for other assays

Performing in vitro single cell-based spheres assays, however, is technically more challenging than the traditional multi cell-based assays.

2 Materials

2.1 Preparation of Primary Tumor Single-Cell Suspensions (Here for Example: Ovarian Tumor Tissue)

1. Washing solution: Phosphate-buffered saline (PBS), 2% Penicillin/streptomycin.
2. Digestion solution: Collagenase (Biochrom, CI-22) 2 mg/ml in RPMI (NO FBS) or other medium according to tumor origin.
3. Trypan blue.

2.2 Preparation of Cancer Cell Line Single-Cell Suspensions

1. Phosphate-buffered saline (PBS).
2. 0.05% Trypsin-EDTA.
3. Basic Medium: cell culture medium (according to the origin of tumor, e.g., for ovarian cancer cell lines normally RPMI is used) supplemented with FBS 10% and 2% penicillin/streptomycin.

2.3 Preparation of Spheres Culture Medium (see Table 1)

Spheres culture medium was prepared as shown in Table 1.

2.4 Equipment

1. Ultra-low attachment plates (6, 24, 48, 96, or 384 wells, Corning).
2. Petri dishes.
3. 25 ml, 10 ml, 5 ml serological pipettes.
4. Surgery tools (scalpels, scissors).
5. Cell strainer (40 and 70 μm).
6. 37 °C water bath.
7. Incubator (37 °C and 5% CO_2).
8. Microscope.
9. Fluorescence Activated Cell Sorter (FACS).
10. Centrifuge.

3 Methods

3.1 Medium Preparation

For conventional 2D cell cultures and generation of single-cell suspensions from cell lines a medium is generated according to the protocol of ATCC. The same medium is used, where applicable,

Table 1
Spheres culture medium for different sources of cells (basic medium + supplements)

Human cancer cell source	Basic medium	Supplements
Ovarian carcinoma cell lines (OVCAR-3, Caov-3) and primary cells [11, 12]	MEGM	20 ng/ml rEGF, 20 ng/ml bFGF, B-27, 4 μg/ml heparin, hydrocortisone, insulin (SingleQuot kit)
Breast carcinoma cell lines (MCF7, T47D) and primary cells [8]	DMEM	30% F12, 20 ng/ml rEGF, 20 ng/ml bFGF, 2% B-27, 1% penicillin/streptomycin, 1% L-glutamine
Colon carcinoma cell lines (Colo205) and primary cells [14]	DMEM/F12	20 ng/ml rEGF, 10 ng/ml bFGF, 2% B-27, 10 ng/ml LIF, 2 mM L-glutamine
Lung carcinoma, primary cells (lung) [16]	DMEM/F12	50 μg/ml insulin, 20 μg/ml rEGF, 10 μg/ml bFGF, 0.4% BSA, 100 mg/ml apo-transferrin, 10 mg/ml putrescine, 0.03 mM sodium selenite, 2 mM progesterone, 0.6% glucose, 5 mM HEPES, 0.1% sodium bicarbonate,
Glioblastoma, primary cells [10]	Stem cell media	20 ng/ml rEGF, 20 ng/ml bFGF, 2% B-27, Neurobasal A, 1% penicillin/streptomycin, non-essential amino acids, sodium pyruvate, vitamin A,
Pancreas carcinoma, primary cells [13]	DMEM/F12	3% FBS, 20 ng/ml rEGF, 20 ng/ml bFGF, 2% B-27, 10 ng/ml LIF, 1% N2 supplement, 1% penicillin/streptomycin, non-essential amino acids, 100 μM Beta-mercaptoethanol
Prostate carcinoma cell lines (PC3) [15]	DMEM/F12	20 ng/ml rEGF, 20 ng/ml bFGF, B-27, 4 μg/ml heparin, insulin (SingleQuot kit)

for 2D cultures and generation of single-cell suspensions from primary tumor specimens. For tumor spheres assays/cultures, the tumor spheres medium is generated by the addition of specific supplements to basic medium as indicated in Table 1 (*see* **Note 1**). Carry out all the procedures in a sterile hood to minimize chances of culture contaminations.

3.2 Preparation of Single-Cell Suspensions from Primary Tumor Samples (Here for Example: Ovarian Carcinoma Tissue)

1. Wash fresh tumor samples washing solution.
2. Place tumor samples in a petri dish.
3. Cut the tumor samples into small pieces using autoclaved scissors and mince completely using a scalpel.
4. Digest tumor pieces enzymatically with a digestion solution and incubate at 37 °C for 3 h, mix occasionally.
5. Mix digested tumor samples sequentially with a 25 ml, 10 ml, and finally 5 ml pipette to separate the cells.
6. Filter the digested sample through a 70 μm cell strainer cap filter twice.

7. Centrifuge cells at 1500 × *g* at room temperature (15–25 °C) for 7 min, wash once with PBS, and resuspend the pellet in the spheres medium.

3.3 Preparation of Single-Cell Suspensions from Cell Lines

1. Aspirate media from flask, wash cells once with PBS, and trypsinize cells for 3 min.
2. Inactivate trypsin by using basic medium (see above, containing FBS and penicillin/streptomycin), centrifuge cells at 1500 × *g* at room temperature (15–25 °C) for 5 min, and resuspend the pellet in the spheres medium.
3. Use a 40 μm cell strainer cap filter to obtain single-cell suspension.

3.4 Plating Multi-Cell Tumor Spheres Assays

For multi cell-based spheres assays, adjust cells to a proper concentration in the spheres medium, e.g., plate 100 cells per well in a 100 μl spheres medium in a 96-well plate. For this, test different concentrations side by side to identify the concentration window introducing minimal bias [12].

For a methylcellulose-based spheres assay, prepare first a twofold concentrated spheres medium and 2% methylcellulose (Sigma-Aldrich, M-0387). Resuspend cells in a 1/2 volume (e.g., for 96-well plate is 50 μl, for 24-well plate is 250 μl) with twofold concentrated medium, mix the cells in a 1:1 ratio in 2% methylcellulose, and plate in each well (*see* **Notes 2** and **3**).

3.5 Plating Single-Cell Tumor Spheres Assays

Adjust cell number to 1000 cells per 100 μl, dilute every sample 1:2 to access one cell per 100 μl, and plate 100 μl per well in ultra low-attachment 96-well plates.

3.5.1 Limiting Dilution

3.5.2 Single-Cell Sorting

1. Prepare an ultra low-attachment 96-well plate with a 100 μl spheres medium (Table 1). (Penicillin/streptomycin may be added to the medium at a concentration of 1:1000 to minimize the risk of putative contamination.)
2. Stain cells with stem cell markers (e.g., CD24, CD44, CD133, etc.) if required.
3. Sort (stem cell marker positive) cells (using, e.g., FACS Aria II, BD Biosciences) into each well of a medium-filled 96-well plate (*see* **Note 4**). Check sort success and respectively numbers of sorted cells in each well after sorting (Fig. 2 top).
4. Incubate cells under standard conditions at 37 °C and 5% CO_2.
5. After 10 days, total tumor spheres counts and, if applicable, fluorescence signal intensities are quantified on a fluorescence microscope (e.g., Olympus IX50 Osiris, Fig. 2 bottom) (*see* **Notes 5**–7).

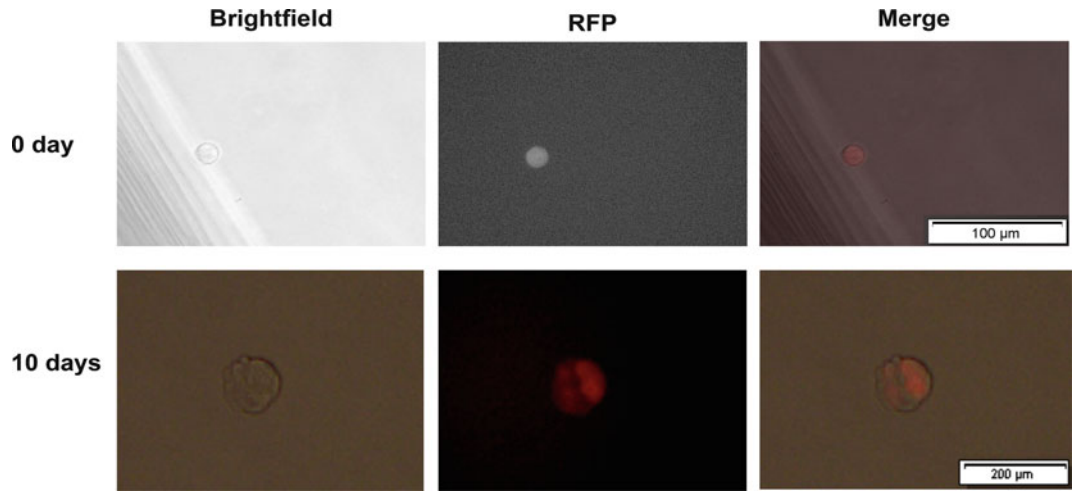

Fig. 2 Imaging of sorted single cells after plating and after 10 days of tumor spheres formation. Single fluorescence marked cells (here RFP+, ref. 12) are sorted into each well of a 96-well plate and analyzed for correct plating by using a (fluorescence) microscope. Tumor spheres are assessed by microscopy performed after 10 days (adapted from ref. 12)

6. Calculate spheres-forming capacity (*see* **Note 8**) in the 96-well plate according to the following formula:

$$\text{Tumor spheres efficiency}(\%) = (\text{number of spheres})/(\text{number of wells seeded}) \times 100$$

3.6 Serial Passaging of Spheres

1. Place the content of each well in an appropriate sterile tube and centrifuge at 1000 × *g* for 5 min at room temperature.
2. Remove the supernatant and resuspend the pellet in 200 µl of 0.05% Trypsin-EDTA.
3. In order to achieve optimal cell separation, incubate the cell suspension at 37 °C for 5–8 min on a soft shaker and then triturate gently using a 100 µl pipette tip.
4. Wash the cells by adding 500 µl sterile PBS and centrifuge at 1500 × *g* for 5 min.
5. Remove the supernatant and resuspend in the spheres medium. Use a 40 µm cell strainer cap filter to obtain a single-cell suspension.
6. Seed 1 cell per well manually into a new ultra low-attachment 96-well plate. For 100 cells per well, seed as described in Subheading 3.4 and count the number of cells after plating.
7. Assess spheres-forming efficiency in secondary, tertiary, and quaternary passages using the formula described above (Subheading 3.5.2, **step 6**).

4 Notes

1. The activity of the growth factors may decrease over time. Make new spheres medium after 7 days when stored at 4 °C. In addition, it is speculated that EGF and FGF may quickly degrade. In some protocols, these growth factors are added daily to the growing spheres. We tested daily EGF and FGF addition versus initial supplementation only in OVCAR-3 cells, but achieved similar results with both the methods [12]. Since individual cancer types might be differentially affected by EGF and FGF concentrations, we recommend upfront testing of the requirement for daily versus one-time growth factor supplementation for the specific tissues, if feasible.
2. Initial cell density can influence the numbers of scored spheres. In some cases, wells seeded with lower cell numbers paradoxically showed higher spheres numbers than those seeded with higher cell numbers (Fig. 3a left, Fig. 3b). We hypothesize that cell clumping and/or sphere fusion or disaggregation can occur, modifying sphere numbers and leading to inaccurate results especially in multi cell-based spheres assays. To reduce this bias, we propose to use addition of1% methylcellulose to the sphere culture to limit cell mobility. Indeed, methylcellulose addition improved accuracy of results that were more comparable to those obtained in single-cell assays [12]. Nevertheless, also in the presence of methylcellulose, sphere disaggregation or fusion might occur, latter for example at particularly high densities. Furthermore, semi-solid methylcellulose, collagen, or matrigel, which have been also previously used to limit cell mobility and aggregation, have limitations: not all cell types can form spheres in semi-solid medium, and medium exchange is challenging.

   Therefore, if multi-cell-based sphere assays are used, upfront investigation of the proper cell concentration will be performed [12] and supplementation with methylcellulose evaluated additionally.
3. Rapid movement of plates (e.g., when the medium is changed or spheres are analyzed under the microscope) should be avoided especially for multi-cell-based spheres assays since they can lead to aggregation or disruption of cells and respectively spheres.
4. Most accurate results are obtained with single-cell-based spheres. However, to reliably quantify rare CSCs, thousands of such single-cell suspension cultures are required. If the limiting dilution method is used without a robotic system, this method is labor intensive.

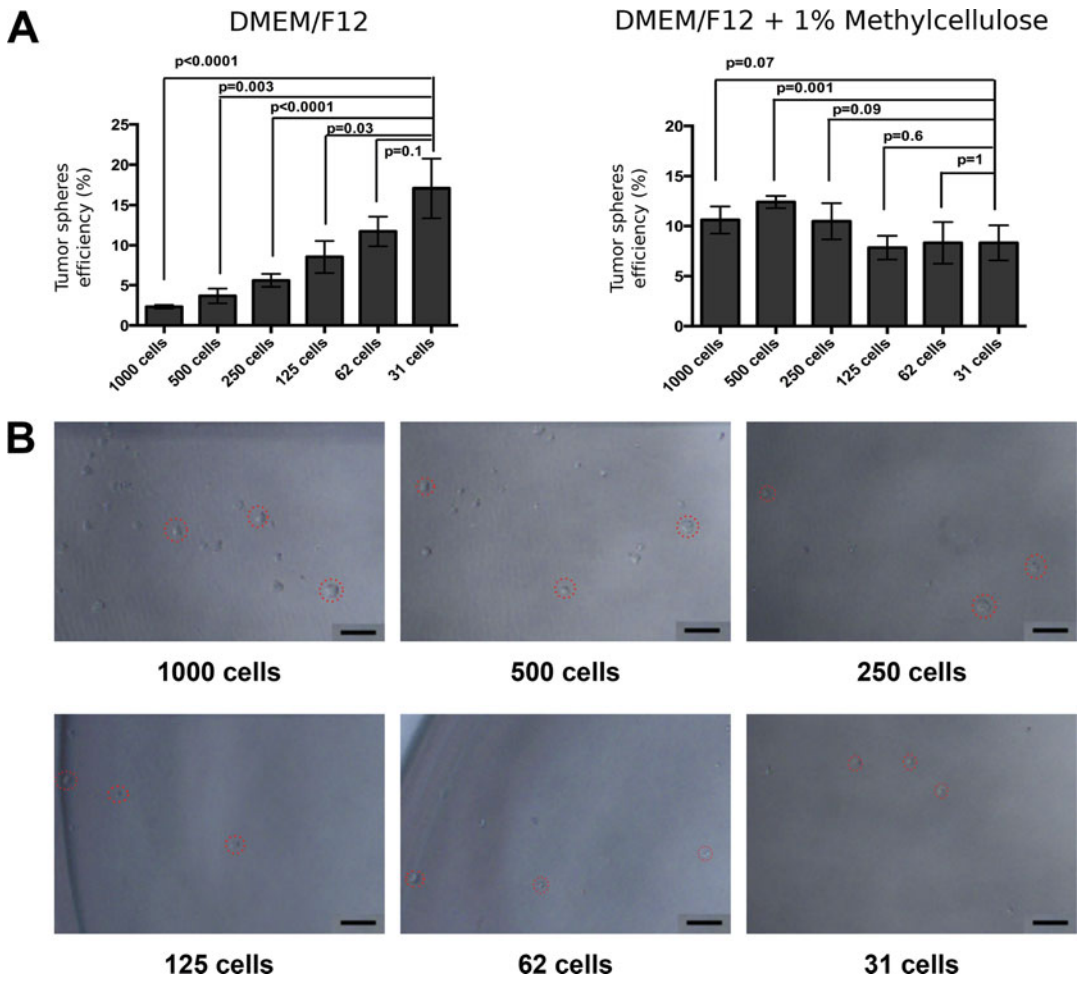

Fig. 3 Cell plating density strongly impacts sphere counts from ovarian carcinoma cell line (OVCAR-3) derived cells in the multi cell-based spheres assay performed in liquid but not in methylcellulose supplemented cultures. Use of different cell densities to analyze possible biases introduced by these variables. Therefore, cells plated at different densities in 200 μl of different spheres culture media (DMEM/F12 with all supplements as detailed in the protocol section, or DMEM/F12 with all supplements and containing 1% methylcellulose) and sphere formation is scored after 7 days (**a**). Shown in (**b**) are microscopy pictures of cells plated at different densities taken 1 day after plating in DMEM/F12 spheres culture medium without methylcellulose. Note the cell clusters emerging at high cellular density as opposed to single cells seen in low-density plates. Scale bar for pictures: 50 μm (adapted from ref. 12)

Fluorescence-activated cell sorting (FACS) can automate the single-cell dispensing process and achieve higher single-cell seeding rate; however, high shear stress during sorting can potentially affect cell viability and also influence results [17]. Moreover, single plated cells may display different growth properties in the absence of supportive signals provided by

neighboring cells, thus perhaps lowering sensitivity of this assay.

The microfluidic culture system is a newly established method for single-cell studies. Single-cell capture chips were developed for single-cell-derived sphere assays in combination with a non-adherent culture substrate [18].

5. Typically, a spheres assay would require 7–14 days of culture. For some tumor cell types, spheres formation might require longer time, especially if emerging from single cells. Thus, when establishing spheres assays with a new tumor type longer observation times should be included.
6. Tumor spheres from CSCs should reach a diameter of >50 μm to be scored as such.
7. The prolonged time for imaging over large areas limits the assay throughput and could potentially affect cell viability if no environmental chamber is used during image capture under the microscope.
8. Side-by-side analyses of tumor cells of the same source indicate that not every sphere-forming cell has in vivo tumorigenic properties upon transplantation in immunosuppressed mice [11]. The frequency of sphere initiating cells was higher than the frequency of tumor initiating cells measured in vivo [11], suggesting that either the tumor spheres assay may lead also to false positive results (e.g., due to co-recognition of more differentiated progenitor cells) or, alternatively, the in vivo assay may be inefficient and results in false negative results (perhaps due to technical reasons). Recently, our laboratory has performed further side-by-side investigations of in vivo tumorigenicity using zebrafish as an alternative animal model [19]. Indeed, this model, which allows highly sensitive detection of tumor formation via in vivo microscopy, revealed much higher frequencies of tumor initiating cells when compared to the murine model (Fig. 4). While the results obtained in zebrafish suggest that indeed murine xenotransplant studies might underestimate the frequency of CSC, this model has its own caveats (as reviewed in [19]) and requires further investigation. Of note, the zebrafish environment might be more supportive for the outgrowth of some xenotransplanted tumor types and less of others (e.g., of tumor cells that heavily rely on cytokines or growth factors that are perhaps not fully conserved cross-species between fish and human).

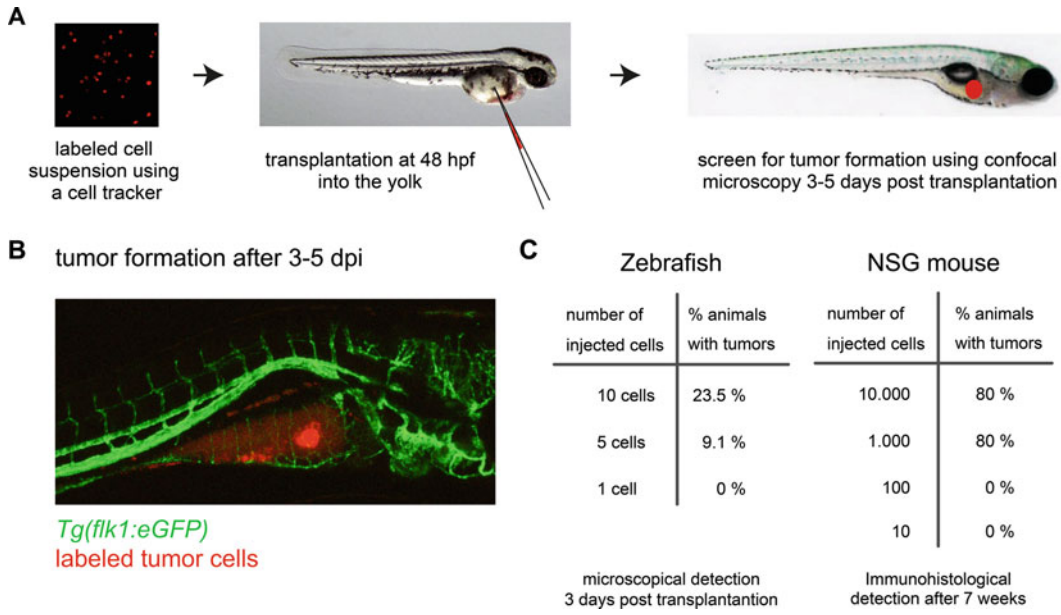

Fig. 4 Human OVCAR-3 cells harboring GFP as a selection marker were xenotransplanted at different numbers into zebrafish embryos or via subcutaneous injection into NSG mice. Note the low numbers of human cells (down to single cells) that can be transplanted and visualized by in vivo microscopy into the yolk of 48 hpf zebrafish embryos (**a**) and that tumor development can be scored—due to the transparency of the zebrafish—already 3 days post injection (**b**). Note that the zebrafish xenotransplant assays indicate a much higher frequency of tumor initiating cells as the murine assay (**c**)

Acknowledgment

This work was supported by grants from the Deutsche Forschungsgemeinschaft to C. Lengerke (Project C6, SFB773) and the Schweizer Nationalfonds to C. Lengerke (SNF 310030E_164200).

References

1. Hermann PC et al (2010) Cancer stem cells in solid tumors. Semin Cancer Biol 20(2):77–84
2. Kruyt FA, Schuringa JJ (2010) Apoptosis and cancer stem cells: implications for apoptosis targeted therapy. Biochem Pharmacol 80 (4):423–430
3. Reynolds BA, Weiss S (1992) Generation of neurons and astrocytes from isolated cells of the adult mammalian central nervous system. Science 255(5052):1707–1710
4. Uchida N et al (2000) Direct isolation of human central nervous system stem cells. Proc Natl Acad Sci U S A 97(26):14720–14725
5. Singh SK et al (2003) Identification of a cancer stem cell in human brain tumors. Cancer Res 63(18):5821–5828
6. Dontu G et al (2003) In vitro propagation and transcriptional profiling of human mammary stem/progenitor cells. Genes Dev 17 (10):1253–1270
7. Shaw FL et al (2012) A detailed mammosphere assay protocol for the quantification of breast stem cell activity. J Mammary Gland Biol Neoplasia 17(2):111–117
8. Leis O et al (2012) Sox2 expression in breast tumours and activation in breast cancer stem cells. Oncogene 31(11):1354–1365

9. Schaefer T et al (2015) Molecular and functional interactions between AKT and SOX2 in breast carcinoma. Oncotarget 6 (41):43540–43556
10. Higgins DM et al (2013) Brain tumor stem cell multipotency correlates with nanog expression and extent of passaging in human glioblastoma xenografts. Oncotarget 4(5):792–801
11. Bareiss PM et al (2013) SOX2 expression associates with stem cell state in human ovarian carcinoma. Cancer Res 73(17):5544–5555
12. Wang H, Paczulla A, Lengerke C (2015) Evaluation of stem cell properties in human ovarian carcinoma cells using multi and single cell-based spheres assays. J Vis Exp 95:e52259
13. Wang YJ et al (2013) Sphere-forming assays for assessment of benign and malignant pancreatic stem cells. Methods Mol Biol 980:281–290
14. Li YF et al (2012) Cultivation and identification of colon cancer stem cell-derived spheres from the Colo205 cell line. Braz J Med Biol Res 45(3):197–204
15. Queisser A et al (2016) Ecotropic viral integration site 1, a novel oncogene in prostate cancer. Oncogene 36(11):1573–1584
16. Eramo A et al (2008) Identification and expansion of the tumorigenic lung cancer stem cell population. Cell Death Differ 15(3):504–514
17. Shapiro E, Biezuner T, Linnarsson S (2013) Single-cell sequencing-based technologies will revolutionize whole-organism science. Nat Rev Genet 14(9):618–630
18. Cheng YH et al (2016) Scaling and automation of a high-throughput single-cell-derived tumor sphere assay chip. Lab Chip 16 (19):3708–3717
19. Konantz M et al (2012) Zebrafish xenografts as a tool for in vivo studies on human cancer. Ann N Y Acad Sci 1266:124–137

CURRICULUM VITAE

Personal Details:

Name:	Hui Wang
Nationality:	Chinese
Date of birth:	18. Feb. 1981
Address:	Dornacherstrasse 56, 4053 Basel, Switzerland
E-mail:	cecilia_wh218@hotmail.com

Education:

2013 – 2017	Ph.D. Universität Basel, Switzerland Department of Biomedicine, University Hospital of Basel (Relocation of the whole lab to University Hospital Basel continuation of Ph.D.) Supervisor: Prof. Dr. med. Claudia Lengerke Title of Ph.D. thesis: Characterization of Stem Cell Genes in Solid Tumors
2011 – 2013	Ph.D. Eberhard Karls Universität Tübingen, Germany Department of Hematology and Oncology, University Hospital of Tübingen Supervisor: Prof. Dr. med. Claudia Lengerke Title of Ph.D. thesis: Characterization of Stem Cell Genes in Solid Tumors
2005 – 2010	Diplom Eberhard Karls Universität Tübingen, Germany Major subject: Biochemistry Minor subject: Immunology and Pharmaceutical chemistry
2009 – 2010	Diploma thesis Eberhard Karls Universität Tübingen, Germany Interfaculty Institute of Biochemistry, Supervisor: Prof. Dr. Klaus Schulze-Osthoff Title of Diploma thesis: Molecular mechanism of Salinomycin's toxicity
2003 – 2005	Goethe Institut – Beijing, China German intensive course TestDaF
1999 – 2003	Bachelor Beijing University of Technology, China Chemistry
1996 – 1999	Beijing Bayi Middle School, China
1993 – 1996	Beijing No. 67 Middle School, China
1990 – 1993	Hongxing Primary School, Beijing, China
1987 – 1990	Zhangxiqiao Primary School, Shandong, China